MODE DIVISION MULTIPLEXING IN RADIO-OVER-FREE-SPACE-OPTICAL SYSTEM INCORPORATING ORTHOGONAL FREQUENCY DIVISION MULTIPLEXING AND PHOTONIC CRYSTAL FIBER EQUALIZATION

SUSHANK

DOCTOR OF PHILOSOPHY
UNIVERSITI UTARA MALAYSIA
2017

Awang Had Salleh
Graduate School
of Arts And Sciences

Universiti Utara Malaysia

PERAKUAN KERJA TESIS / DISERTASI
(Certification of thesis / dissertation)

Kami, yang bertandatangan, memperakukan bahawa
(We, the undersigned, certify that)

SUSHANK

calon untuk Ijazah PhD
(candidate for the degree of)

telah mengemukakan tesis / disertasi yang bertajuk:
(has presented his/her thesis / dissertation of the following title):

"MODE DIVISION MULTIPLEXING IN RADIO-OVER-FREE-SPACE-OPTICAL SYSTEM INCORPORATING ORTHOGONAL FREQUENCY DIVISION MULTIPLEXING AND PHOTONIC CRYSTAL FIBER EQUALIZATION"

seperti yang tercatat di muka surat tajuk dan kulit tesis / disertasi.
(as it appears on the title page and front cover of the thesis / dissertation).

Bahawa tesis/disertasi tersebut boleh diterima dari segi bentuk serta kandungan dan meliputi bidang ilmu dengan memuaskan, sebagaimana yang ditunjukkan oleh calon dalam ujian lisan yang diadakan pada : *08 Jun 2017.*
That the said thesis/dissertation is acceptable in form and content and displays a satisfactory knowledge of the field of study as demonstrated by the candidate through an oral examination held on: ***June 08, 2017.***

Pengerusi Viva: *(Chairman for VIVA)*	Prof. Dr. Norshuhada Shiratuddin	Tandatangan *(Signature)*
Pemeriksa Luar: *(External Examiner)*	Prof. Dr. Sulaiman Wadi Harun	Tandatangan *(Signature)*
Pemeriksa Dalam: *(Internal Examiner)*	Dr. Massudi Mahmuddin	Tandatangan *(Signature)*
Nama Penyelia/Penyelia-penyelia: *(Name of Supervisor/Supervisors)*	Assoc. Prof. Dr. Angela Amphawan	Tandatangan *(Signature)*

Tarikh:
(Date) *June 08, 2017*

Permission to Use

In presenting this thesis in fulfilment of the requirements for a postgraduate degree from Universiti Utara Malaysia, I agree that the Universiti Library may make it freely available for inspection. I further agree that permission for the copying of this thesis in any manner, in whole or in part, for scholarly purpose may be granted by my supervisor(s) or, in their absence, by the Dean of Awang Had Salleh Graduate School of Arts and Sciences. It is understood that any copying or publication or use of this thesis or parts thereof for financial gain shall not be allowed without my written permission. It is also understood that due recognition shall be given to me and to Universiti Utara Malaysia for any scholarly use which may be made of any material from my thesis.

Requests for permission to copy or to make other use of materials in this thesis, in whole or in part, should be addressed to:

Dean of Awang Had Salleh Graduate School of Arts and Sciences
UUM College of Arts and Sciences
Universiti Utara Malaysia
06010 UUM Sintok

Abstrak

Radio melalui optik ruang bebas (Ro-FSO) adalah teknologi revolusi yang digunakan untuk menyepadukan radio dan rangkaian optik tanpa menggunakan kabel gentian optik yang mahal. Teknologi Ro-FSO memainkan peranan penting dalam menyokong penyambungan jalur lebar di kawasan pedalaman dan kawasan terpencil di mana infrastruktur jalur lebar semasa tidak dapat digunakan disebabkan kesulitan geografi dan ekonomi. Walaupun kapasiti Ro-FSO boleh ditingkatkan dengan pemultipleksan pembahagi mod (MDM), jarak penghantaran dan kapasiti masih terbatas oleh kekaburan arah yang pelbagai dan kehilangan gandingan mod akibat gelora atmosfera seperti kabus ringan, kabus nipis dan kabus tebal. Tujuan utama projek ini adalah untuk mereka bentuk satu sistem pemultipleksan pembahagi mod (MDM) untuk Ro-FSO untuk komunikasi jarak jauh dan pendek. Pemultipleksan pembahagi frekuensi berortogon (OFDM) dicadangkan untuk komunikasi jarak jauh untuk mengurangkan kekaburan pelbagai arah dan gentian kristal fotonik (PCF) dicadangkan untuk komunikasi jarak dekat bagi mengurangkan kehilangan gandingan mod. Keputusan yang dilaporkan mengenai skema yang dicadangkan untuk komunikasi jarak jauh menunjukkan 47% peningkatan kuasa yang ketara akibat kekaburan yang mendalam melalui perambatan pelbagai arah dengan menggunakan OFDM dalam sistem MDM-Ro-FSO berbanding tanpa OFDM. Keputusan yang dilaporkan mengenai skema yang dicadangkan untuk komunikasi jarak dekat menunjukkan 90.6% peningkatan kuasa dalam mod dominan dengan menggunakan PCF di dalam MDM-Ro-FSO berbanding tanpa PCF. Keputusan yang dilaporkan dalam tesis ini menunjukkan peningkatan yang ketara dalam sistem Ro-FSO berbanding dengan sistem yang terdahulu dari segi kapasiti dan jarak penghantaran di bawah keadaan cuaca yang baik dan juga di bawah pelbagai peringkat kabus. Sumbangan tesis ini dijangka dapat menyediakan perkhidmatan jalur lebar yang lancar di kawasan terpencil.

Kata kunci: Komunikasi jarak dekat, Komunikasi jarak jauh, pemultipleksan pembahagi frekuensi berortogon (OFDM), gentian kristal fotonik (PCF)

Abstract

Radio over free space optics (Ro-FSO) is a revolutionary technology for seamlessly integrating radio and optical networks without expensive optical fiber cabling. Ro-FSO technology plays a crucial role in supporting broadband connectivity in rural and remote areas where current broadband infrastructure is not feasible due to geographical and economic inconvenience. Although the capacity of Ro-FSO can be increased by mode division multiplexing (MDM), the transmission distance and capacity is still limited by multipath fading and mode coupling losses due to atmospheric turbulences such as light fog, thin fog and heavy fog. The main intention of this thesis is to design MDM system for Ro-FSO for long and short haul communication. Orthogonal frequency division multiplexing (OFDM) is proposed for long haul communication to mitigate multipath fading and Photonic Crystal Fiber (PCF) is proposed for short haul communication to reduce mode coupling losses. The reported results of the proposed scheme for long haul communication show a significant 47% power improvement in deep fades from multipath propagation with the use of OFDM in MDM-Ro-FSO systems as compared to without OFDM. The results of the proposed scheme for short haul communication show 90.6% improvement in power in the dominant mode with the use of PCF in MDM-Ro-FSO as compared to without PCF. The reported results in the thesis show significant improvement in Ro-FSO systems as compared to previous systems in terms of capacity and transmission distance under clear weather conditions as well as under varying levels of fog. The contributions of this thesis are expected to provide seamless broadband services in remote areas.

Keywords: Short haul communication, Long haul communication, Orthogonal frequency division multiplexing (OFDM), Photonic crystal fiber (PCF)

Acknowledgement

With the graceful presence of the Almighty God, this research work is a culmination of sincere efforts, time, and a quest for knowledge where I have been accompanied and supported by many. At the very outset, I would like to offer my sincere gratitude to **School of Computing, Universiti Utara Malaysia** for giving me the opportunity to conduct this research work. I would like to express my special appreciation and thanks to my supervisor and mentor **Assoc. Prof. Dr. Angela Amphawan**, who encouraged me to take up this research work and allowed me to grow as a research scientist. You have been a tremendous support throughout my research work. Thank you so much for always being the helpful mentor and for guiding me in my research without any hassles.

I must say a huge Thank You to the current and past members **of InterNetworks Research Lab** whom I enjoyed working with; especially, **Prof. Suhaidi Hassan, Dr. Ahmad Suki Che Mohamed Arif, Dr. Mohd. Hasbullah Omar, Dr. Adib Habbal, Dr. Osman Ghazali, Dr. Massudi Mahmuddin** and other staff. Thank you for your incredible support and understanding.

I would also like to thank **Dr. Dipima Buragohain**, **Dr. Mawfaq Alzboon** and my friends from **D.P.P Proton** and **Tradewinds** for their valuable suggestions and guidance which profoundly helped me shape my research work.

Finally, my heartiest gratitude goes to my family – my pillar of strength, my father **Sh. Harmesh Lal**, my mother **Smt. Nirmala Devi**, and my sister **Neha Chaudhary** who always have trusted in me and my strength, and prayed for my success. I stand committed to dedicate myself for the enhancement and completion of this research work.

Table of Contents

List of Tables

List of Figures

List of Abbreviations

BER	-	Bit Error Rate
CD	-	Chromatic Dispersion
DSB	-	Double Side Band
DWDM	-	Dense Wavelength Division Multiplexing
EDFA	-	Erbium Doped Fiber Amplifier
EOS	-	European Optical Society
FSO	-	Free Space Optics
IEEE	-	Institute of Electrical and Electronics Engineers
IF	-	Intermediate Frequency
ITU	-	International Telecom Union
MDM	-	Mode Division Multiplexing
OFDM	-	Orthogonal Frequency Division Multiplexing
ONU	-	Optical Node Unit
OSA	-	Optical Society of America
OTSB	-	Optical Tandem Side Band
PON	-	Passive Optical Network
QAM	-	Quadrature Amplitude Modulation
QM	-	Quadrature Modulation
QPSK	-	Quadrature Phase Shift Key
RF	-	Radio Frequency
RoF	-	Radio over Fiber
Ro-FSO	-	Radio over Free Space Optics
SNR	-	Signal to Noise Ratio
SOA	-	Semiconductor Optical Amplifier
SSB	-	Single Side Band
THz	-	Terahertz
WDM	-	Wavelength Division Multiplexing

CHAPTER ONE
INTRODUCTION

Radio over free space optics (Ro-FSO) is one of the remarkable technologies for seamless integration of wireless and optical networks without using expensive optical fibers. The future of Ro-FSO technology aims to not only build a universal platform for distributing broadband services for wireless local area networks but also address the issue of scarcity of radio frequency spectrum and channel degradation by allocating frequency spectrum in a more flexible manner. Various atmospheric turbulences, particularly fog, can affect the transmission distance, bandwidth and capacity of Ro-FSO systems. On the other hand, Mode Division Multiplexing (MDM) plays a vital role in increasing the bandwidth of optical networks. The use of MDM may also increase the aggregate bandwidth of Ro-FSO systems. The main intention of this thesis is to design MDM scheme for Ro-FSO system to make it useful for distributing broadband services.

This chapter aims to place this research thesis into context by first providing an introduction to Ro-FSO in Section 1.1 followed by the research motivation in Section 1.2. This lays the foundation for the Problem Statement in Section 1.3, followed by Research Questions in Section 1.4 and Research Objectives in Section 1.5. The scope of this research is mentioned in Section 1.6 whereas the key contribution of this thesis is presented in Section 1.7. The organization of the rest of the thesis is presented in Section 1.8.

1.1 Ro-FSO Transmission Systems

Ro-FSO technology is promising for providing a ubiquitous platform for seamless integration of radio and optical networks without expensive optical fiber cabling. The last decade has experienced enormous growth in the development of optical

transmission systems in almost all parts of the world. The increasing demand for bandwidth due to proliferation of video and multifarious online services has inspired the generation of new optical techniques to accommodate the rise in number of subscribers. Due to the explosive growth of mobile subscribers and data surge, it is increasingly a challenge for the International Telecommunications Union (ITU) to allocate limited radio frequency (RF) spectrum among various wireless operators [1, 2]. Ro-FSO is a prospective technology for addressing the growth of mobile subscribers, enabling transmission of multiple RF signals via a high-speed optical carrier without expensive optical fiber cabling or licensing for RF solutions. In Ro-FSO, utilizing an optical carrier exploits a different segment of the electromagnetic spectrum for the mobile backbone, thus alleviating RF spectrum congestion issues in current wireless networks. Ro-FSO harnesses the merits of both radio-over-fiber (RoF) and free-space optical (FSO) technologies [3]. As with RoF, Ro-FSO allows expensive equipment responsible for processes such as RF up-down conversion, handoff, switching, coding and multiplexing to be centralized and shared among all base stations [4]. In addition, the ability of RoF technology to distribute the RF signals at large bandwidths, low attenuation losses and low power consumptions are some of the main benefits of RoF technology shared by Ro-FSO [5, 6]. These features assure compatibility with existing mobile cellular architectures. On the other hand, in contrast to RoF, FSO allows the transportation of data signals through the atmosphere instead of optical fiber, thus eliminating the need for exorbitant optical fiber installations and allowing for rapid adoption. The schematic scenario of Ro-FSO implementation is illustrated in Figure 1.1.

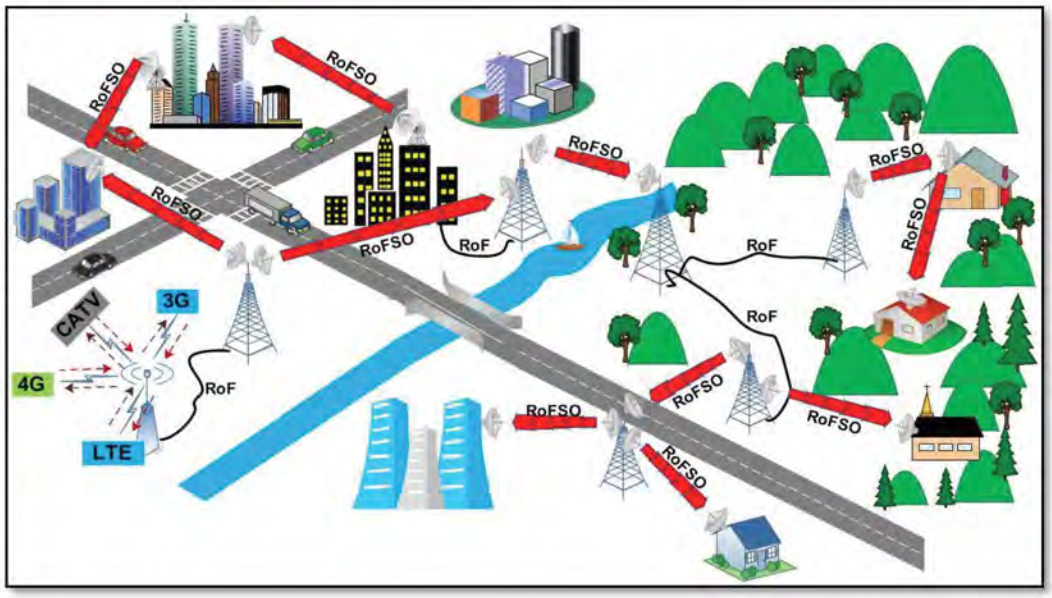

Figure 1.1. Scenario of Ro-FSO Implementation

To increase the capacity of Ro-FSO system, researchers have used polarization division multiplexing (PDM) scheme [3, 7-9] and wavelength division multiplexing (WDM) scheme [10-12]. However, these multiplexing schemes are still insufficient to cope with the demands of Ro-FSO systems. MDM scheme can fulfil the requirement of high bandwidth by transmitting various channels over single communication link with the use of different modes. Recently, many researchers have used MDM in optical networks to increase the capacity as well as bandwidth [13-17].

Hence, MDM-based Ro-FSO can become fascinating as an enabling ubiquitous platform for seamless integration with RF wireless networks to extend the achievable capacity of current wireless networks rapidly and cost effectively. Moreover, Ro-FSO, as a significant and cost-efficient technology used across the telecommunications sector, is appropriately applicable as a universal platform for enabling seamless convergence of fiber and free-space optical communication networks. Featured with rapid deployment, the technology supports high broadband transmission with high security [18, 19]. It is also capable of extending the reach of

the optical fiber backbone and can be used in disaster recovery situations. These features empower the Ro-FSO technology to extend broadband connectivity to even underserved areas while ensuring last mile access and serving as fiber back up. Therefore, Ro-FSO technology plays a crucial role in supporting broadband connectivity in rural and remote areas as well as in increasing opportunities for enterprises [20].

1.2 Research Motivation

The increasing number of subscribers in wireless radio networks over recent years has incurred a strain on its bandwidth [21]. Due to the limited availability of radio frequency (RF) spectrum, it has been a challenge for ITU to allocate the available spectrum among the mobile operators. The total number of mobile subscribers in 2015 reported by the ITU is 7.2 billion [22]. According to a survey by Ericsson, annual mobile data traffic saw an increase of 65% in 2015 which is assumed to grow ten times bigger by the end of 2021 [23]. Moreover, a growing number of connected devices, predictably 26 billion connected devices, are likely to develop through a wide range of applications and business models at lower modem costs by 2020 [23].

To cope with the bandwidth increase of current wireless radio networks, more users have been accommodated by reducing the cell size and operating in microwave/millimeter frequency band so that the spectral congestion is avoided in lower frequency bands [24]. This requires a large number of base stations to accommodate the service area which further increases the cost and system complexity.

FSO has thrived in application in high-speed wireless networks as it provides valuable features that are vital to transfer the traffic to the fortitude of optical fiber [25-27]. In addition, FSO uses point-to-point laser signals for negligible interception which

makes transmission secure [28]. Other merits of FSO include high capacity, low power consumption, light weight, small sizes and low implementation costs [29-32]. The integration of RoF with FSO alleviates the last mile problem of high data networks [12, 33-37] and reduces costs for wireless operators [38, 39]. Significant research in Ro-FSO has focused on experimental measurements [3, 12, 40] and statistical modeling [10, 37, 41, 42] under various atmospheric turbulence and scintillation effects in Ro-FSO systems.

To improve channel performance in free space optical communications, researchers have found innovative methods for multiplexing several data streams for increasing channel diversity and for reducing signal degradation. Multiplexing of data in the wavelength [12, 43, 44], time [45-47], polarization [48, 49], intensity [50-52], phase and code [53, 54] dimensions have been rigorously explored. Nevertheless, mode is still an un-capitalized dimension which may be valuable for Ro-FSO communication systems. In optical communications, Eigen modes are used in mode division multiplexing (MDM) to propagate various channels on different modes generated by various mechanisms including spatial light modulators [55-58], optical signal processing [59, 60], few mode fiber [61-63], photonic crystal fibers (PCF) [64-66] and modal decomposition methods [67, 68].

Although, MDM in Ro-FSO systems can be used to increase transmission capacity, atmospheric turbulence due to fog degrades the signal quality and leads to deep fading of the radio subcarriers [69, 70].

Few Mode Raman Amplifiers, Few Mode Erbium Doped Amplifiers and multi core erbium doped amplifiers have been used for mitigating mode coupling losses in optical fiber communications but these have drawback of expensive cost and complexity. Solid-core photonic crystals fibers (SC-PCF), which were previously used in optical fiber communications for dispersion compensation [71, 72] and have

advantage of excellent birefringence and dispersion properties [73] but have not been used in MDM Ro-FSO systems. For the first time in the literature, it is proposed that SC-PCF be adapted for mode coupling mitigation in MDM Ro-FSO systems. Thus, the SC-PCF will be designed to convert a pure Gaussian beam into the desired mode for launching into a MDM-Ro-FSO channel and to filter noisy modes at the receiver due to the fog-attributed atmospheric turbulence.

On the other hand, orthogonal frequency division multiplexing (OFDM) is an established technique in wireless communications for alleviating frequency-selective fading and narrow-band interference, having been approved for several digital communication standards including IEEE 802.11 local area network and IEEE 802.16 wireless broadband [74-76]. OFDM outperforms other fading mitigation technique's such as code division multiple access (CDMA), frequency division multiple access (FDMA) and time division multiple access (TDMA) for higher data rate applications [77]. In this thesis, to alleviate the effects of fog in MDM Ro-FSO systems, OFDM is proposed for addressing the effects of multipath fading of radio subcarriers and PCF based equalization scheme is proposed for addressing mode coupling losses.

1.3 Problem Statement

Current broadband infrastructure contains expensive licensing and optical fiber infrastructure, which is not applicable for some rural and underserved areas [78] due to geographical and economic inconvenience [79]. Ro-FSO communication can replace current broadband infrastructure by transporting optical data signals through atmosphere without any expensive optical fiber.

Although MDM Ro-FSO increases the number of channels and aggregate capacity, the transmission distance and capacity is still constrained by multipath fading and mode coupling [62, 80-82] due to atmospheric turbulences as shown in previous

works (Table 2.3). The use of OFDM in Ro-FSO system can reduce multipath fading [83-86]. On the other hand, mode coupling may be compensated by the use of an equalization scheme [87-89]. Thus, the concise problem statement for this thesis is the subcarrier multipath fading and mode coupling losses due to atmospheric turbulences, particularly fog, in Ro-FSO confines the transmission distance and capacity.

1.4 Research Questions

The research aims to solve the following questions:

1. How would an MDM scheme be designed to mitigate radio subcarrier multipath fading due to fog in Ro-FSO for long-haul communication?

2. How would a power equalization scheme be designed to filter noisy modes due to fog in Ro-FSO to reduce the broadening of the channel impulse response for short-haul communication?

3. What is the performance of MDM Ro-FSO in conjunction with OFDM and power equalization?

1.5 Research Objectives

The broad objective of this research is to design a MDM scheme in conjunction with OFDM and PCF equalization for Ro-FSO transmission systems. Specific objectives are elucidated as follows:

1. To design an OFDM-integrated MDM scheme for mitigating radio subcarrier multipath fading in Ro-FSO for long-haul communications.

2. To design a PCF-integrated MDM equalization scheme for optimizing mode distribution in Ro-FSO for short-haul communications.

3. To evaluate the performance of OFDM-MDM and PCF-MDM schemes in Ro-FSO by using the key metrics of mode spectrum, constellations, signal to noise ratio (SNR), bit error rate (BER), eye diagrams and received power.

1.6 Research Scope

This research focuses on the design of OFDM-MDM and PCF-MDM schemes for Ro-FSO transmission systems to mitigate atmospheric turbulences as well as to increase the bandwidth for long haul and short haul communication. The main scope of this research is highlighted by a circle, as shown in Figure 1.2. In this thesis, long-haul communication is considered to be more than the distance of 40 km, whereas short-haul distance is considered to be less than 5 km.

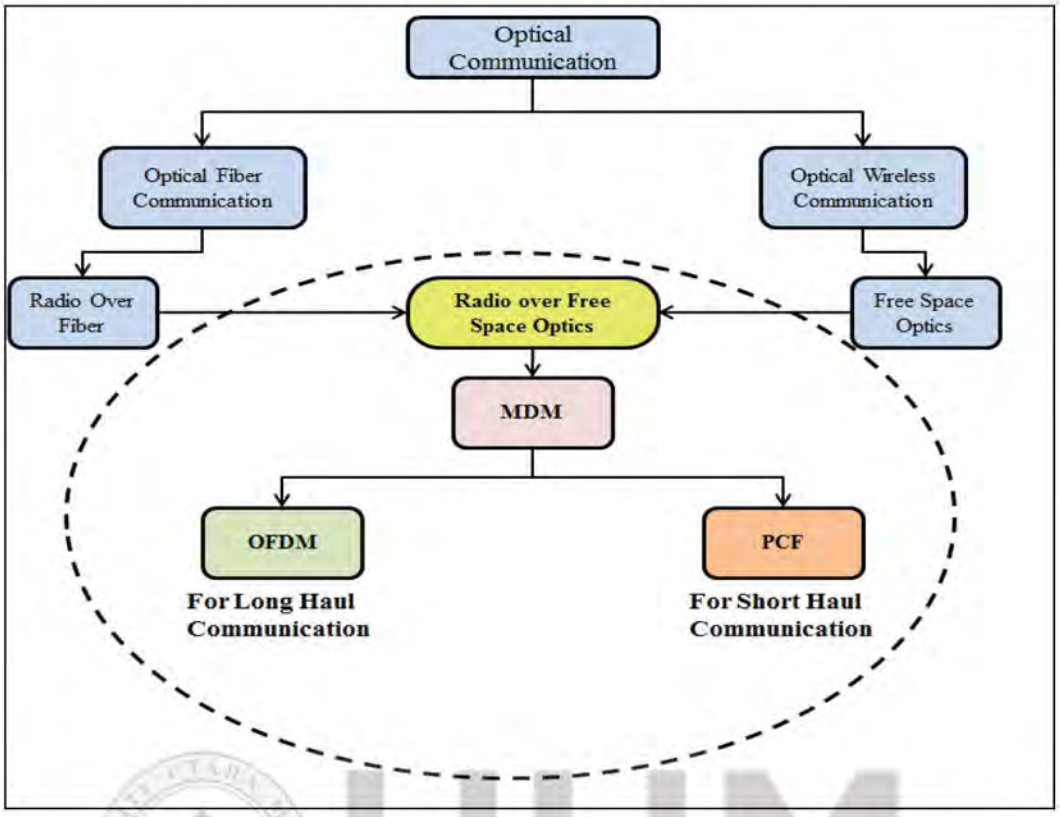

Figure 1.2. Research Scope

1.7 Research Organization

This thesis is organized in six chapters, where the following is a summary of key chapter highlights:

Chapter One covers the introduction of Ro-FSO, motivation of the research, problem statement, research questions, research objectives, scope of the research and research contributions.

Chapter Two provides an extensive literature review outlining an overview of optical communications, current progress in radio-over-fiber technology, current developments in MDM free-space optical systems, recent advances in MDM Ro-FSO transmission systems and challenges in MDM Ro-FSO systems. Mitigation and bandwidth enhancement techniques for MDM Ro-FSO systems are also addressed.

Chapter Three is focused on the research methodology used for achieving the research objectives.

Chapter Four is focused on the design, simulations and evaluation of the proposed MDM-OFDM-Ro-FSO transmission system.

Chapter Five is focused on the design, simulations and evaluation of the proposed MDM-PCF-Ro-FSO transmission system.

Chapter Six covers the overall conclusion of this theses as well as future scope of this research.

CHAPTER TWO
LITERATURE REVIEW

This chapter explores technologies and recent developments related to the proposed research on MDM-Ro-FSO system. The chapter provides an overview of optical communication systems and essential enabling technologies for achieving high capacity systems. Ro-FSO technology inherits features from both FSO communication systems and RoF communication systems, as illustrated in Figure 2.1. Considering that both RoF and FSO systems have advantages over one another, it is vital to analyze current developments in both RoF and FSO systems. Section 2.2 reviews the main principles of RoF and provides an insight into recent developments in RoF systems. Section 2.3 examines the principles of FSO and compares various implementations of FSO systems. Section 2.4 describes primary research in Ro-FSO systems leading to the development of a new Ro-FSO system. Section 2.5 describes the various challenges in Ro-FSO systems, Section 2.6 describes the principle of MDM, Section 2.7 describes the principle of OFDM followed by Section 2.8 which describes the principle of PCF.

2.1 Overview of Optical and Radio Communication Systems

Over the last decade, optical communication system has advanced in terms of capacity, connectivity, and architecture. Recent key enablers for multi-terabits optical communication systems are high-speed modulators [90, 91] and high-speed photodetectors [92, 93], optical amplifiers [94, 95], and silicon photonics [96]. On the electromagnetic spectrum, there are two windows typically used for modern broadband communication. The first window span covers the operating range from

100 KHz to 300 GHz or long wave radio to millimeter range, which has been widely used in our daily life such as television broadcasting, cellular networks, local area networks, and metropolitan area network. The second window span covers the frequency range from 300 GHz to 300 THz which lies in the infrared region of the electromagnetic spectrum [97].

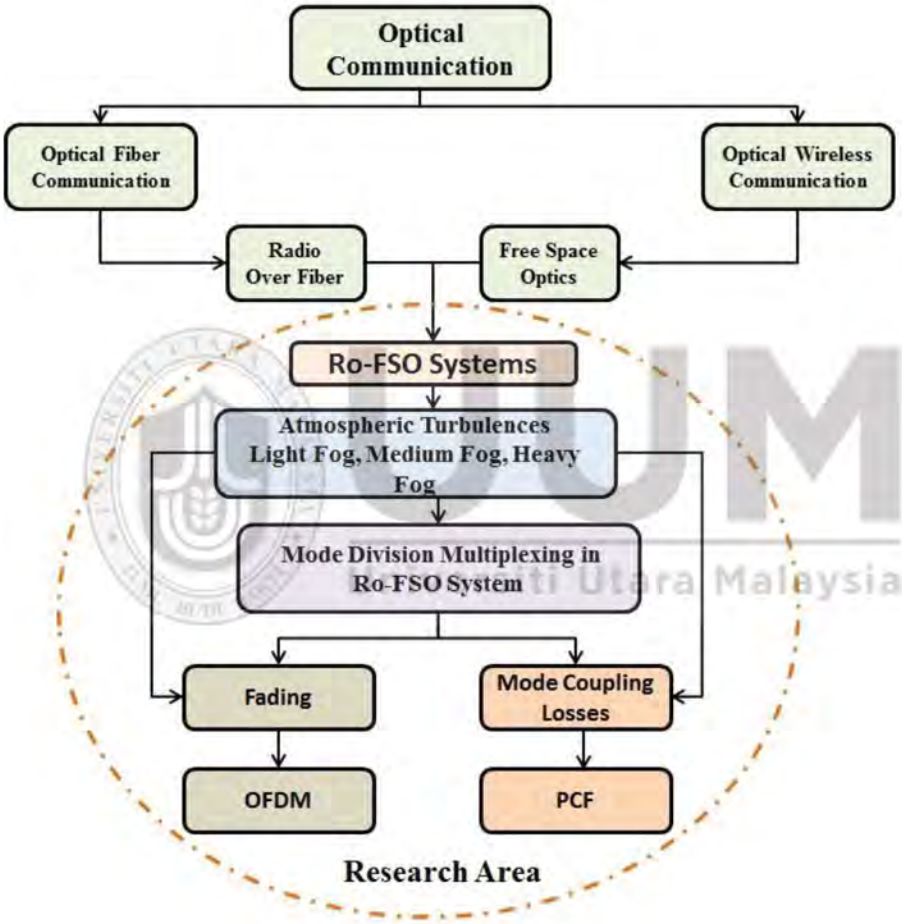

Figure 2.1. Research Area

Due to the shortage of available spectrum in RF microwave range, most of the data rates are eclipsed below gigabit per second [98, 99]. Data bandwidth increase to 2.5 exabytes has brought up the scarcity issue of radio frequency (RF) spectrum among wireless operators resulting in intense bandwidth competition among them [1, 100]. RoF can transport radio signals over optical fiber for integrating wireless networks

with optical networks. However, fiber cable installation is expensive. On the other hand, Ro-FSO can provide an appropriate solution to this scarcity issue as it transmits RF signals through high-speed optical carrier and does not require any expensive optical fiber cabling [4-7]. Ro-FSO can also be used in electromagnetic spectrum for improving congestion issues in wireless networks. Moreover, it can be used in various processes including handoff, RF up-down conversion, switching, coding and multiplexing through centralized or shared base stations [8-9].

In distinction, due to massive bandwidth over several terahertzes (THz) in the second window, optical systems can provide an astounding capacity of 100 Gbps and beyond [101-105]. Earlier, optical fiber was used as introductory formation for the long-haul communication systems, but now optical fiber communication systems are extensively used in almost all metro networks. Optical systems are used as medium of transmission at a very high speed since mid of 1990s. Low cost, high bandwidth, immunity to electromagnetic radiations, and no cross talk are some of the benefits of optical systems [106]. The increasing demand for high bandwidth due to the advent of real-time multimedia services in the early 21st century spurred on various multiplexing schemes in the fifth generation optical systems, used individually or in combination with one another, comprising wavelength division multiplexing (WDM) [107-111], OFDM [112-116], intensity multiplexing [117], polarization multiplexing [118-120], subcarrier multiplexing (SCM) [116, 121-123], and code division multiple access schemes [124-126]. In addition, multi-level modulation schemes such as quadrature phase shifting keying (QPSK) [127-129], quadrature amplitude modulation (QAM) [130-133], and binary phase shift key (BPSK) [6, 134, 135], as well as coherent detection [136-138] were employed to further increase data rates and improve spectral efficiency. Unfortunately, the achievable optical signal-to-noise ratio at the receiver is restricted by the nonlinear characteristics of silica optical fiber [139].

Furthermore, higher order modulation formats are usually less tolerant to the nonlinearity due to power variation [106]. In view of the limits imposed by optical fiber nonlinearity and current multiplexing schemes, MDM is emerging as a potential technology for breaking through the bandwidth-distance product and spectral-efficiency barriers. In MDM, laser beams of specific mode or mode groups are used to transmit distinct data signals in a multimode fiber, resulting in different parts of the spectrum utilized for each channel [140]. By controlling the incident field, the impulse response of each channel may be optimized [141, 142]. Further, MDM-based network systems can increase transmission capacity by using solid-core photonic fibers (SC-PCFs) through selective excitation [65, 143]. SC-PCF is a mode-filtering device that includes a solid core at the center with a modal profile, periodic air holes, and a large numerical aperture that enables strong guidance [36]. SC-PCF can assemble the launch beam into an MDM-Ro-FSO network which further enhances its impulse response and bandwidth.

Current work aims to transfer the principles of MDM, OFDM, SC-PCF, and multi-level modulation formats used in optical fiber communications to the Ro-FSO domain for improving spectral efficiency and mitigating channel noise. This chapter extensively discusses the applications of MDM, OFDM, and multi-level modulation formats in RoF, FSO, and Ro-FSO systems as well as in the design of an MDM scheme for Ro-FSO.

2.2 Radio over Fiber (RoF)

Radio over fiber is very attractive solution of merging radio networks with optical networks by transporting radio signals over optical fiber. Section 2.2.1 discusses about principles of RoF and Section 2.2.2 discusses about recent work of RoF.

2.2.1 Principles of RoF

To fulfill the demand of subscribers for broadband or other multimedia services, cellular networks need to accommodate more users by reducing the cell size and to operate in microwave/millimeter frequency band so that spectral congestion is avoided in lower frequency bands. This requires large number of base stations (BSs) to accommodate the service area which increases the cost and system complexity. BS is thus considered as the success factor in the market [144]. Further, it led to the enhancement of system architecture that involves various functions such as handover, signal routing and processing, and frequency allocation at the central control station (CS). This type of centralized configuration can locate sensitive equipment in safe environments while sharing the component expenses among the BSs [145]. CS can be alternatively linked with BSs through an optical fiber network due to its low loss, no electromagnetic interference (EMI) and broad bandwidth [146].

In order to minimize cost, radio signals over fiber can be transmitted by connecting to a CS through simple optical-to-electrical conversion and radiation at remote antennas. Cost reduction can happen in two ways: a) BS remote antenna or radio distribution point can perform simple functions in small size and low cost, and b) CS-based resources can be shared among BS antennas [147]. This technique is known as Radio over Fiber (RoF) where radio frequency (RF) subcarrier is modulated onto an optical carrier to distribute via fiber network.

The simplest technique of distributing the radio signal over fiber is direct transmission of radio signal without any conversion known as RF over an optical fiber as shown in Figure 2.2. The RF links, for distributing RF signals over fibers, were started 24 years ago. The first commercial RF link for transportation of Cable television (CATV) signal (analog) was available in 1990 [148]. RoF technology has been the driver for sharing the expensive equipment responsible for processes such as coding and

decoding, multiplexing and de-multiplexing, and frequency up-down conversion from the centralized station to all base stations.

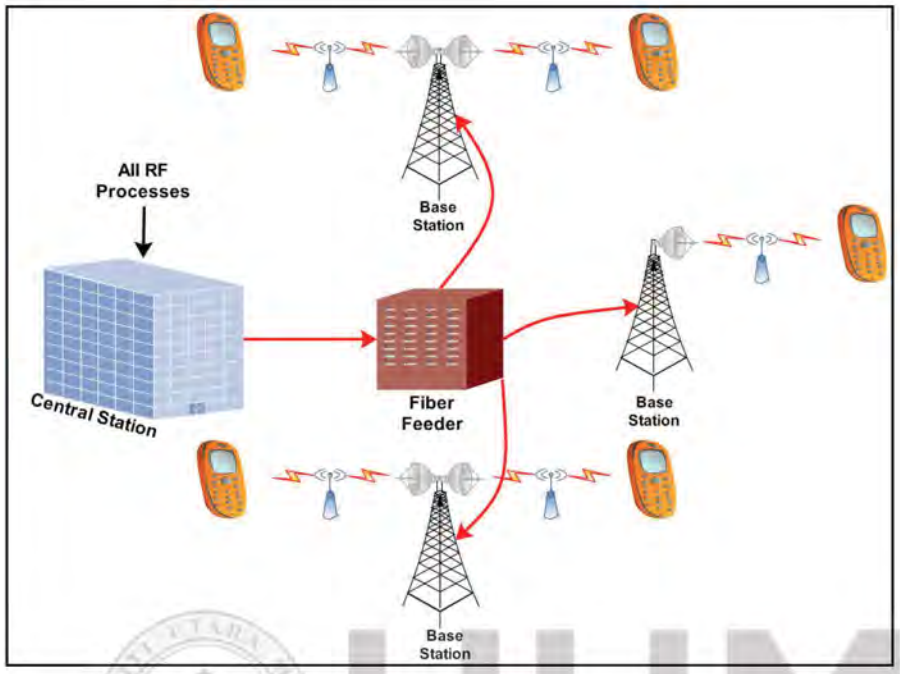

Figure 2.2. RoF Architecture

This effectively reduces cost and system complexity. The main benefits of RoF technology include its ability to distribute the RF signals at larger bandwidth, low attenuation losses, immunity to radio frequency interference, low power consumption, and ease of deployment [149]. The system configuration is arranged in such a manner that all the expensive processes including handoff, switching, RF up/down conversion, coding and multiplexing are carried out at central station and shared equally with all base stations by using fiber feeder network [150].

The main benefits of RoF technology are listed below.

- **Low Attenuation:** RoF transmits information in the form of light signals over optical fibers with low attenuation [151, 152]. Unlike expensive coaxial transmission cables, single-mode optical fibers in the market offer 0.2 dB/km

and 0.5 dB/km for operating wavelength of 1550 nm and 1350 nm respectively.

- **High Bandwidth:** Optical fibers offer tremendous bandwidth and high transmission capacity for three windows of 850 nm, 1350 nm, and 1550 nm along with more than 50 THz of bandwidth by a single-mode fiber. High bandwidth can also help mitigate difficult or impossible signal processes in electronic system [153].
- **Electromagnetic Interference (EMI) Immunity:** Optical fibers offer electromagnetic interference immunity through signal transmission in the form of light, which results in radio signal transportation as well as secure and private immunity [154].
- **Low Power Consumption:** RoF technique can be used in most of the complex and expensive processes such as signal processing, handoff, RF up-conversion, down-conversion, switching, coding, multiplexing, etc. mainly for its low power consumption at the central station shared among all base stations.
- **Multiple Service Capability:** RoF systems feature enhanced transmission capacity due to wavelength division multiplexing (WDM) [155] and subcarrier division multiplexing (SCM) [156] which transmit large number of radio signals over single optical fiber with increased economic benefits.

2.2.2 Recent Work in RoF

In 2009 [157], 1.25 Gbps with 8 GHz was transported over 23 km single mode fiber (SMF) by employing subcarrier multiplexing scheme incorporating WDM and semiconductor optical amplifier (SOA) techniques. The authors experimentally demonstrated a bidirectional RoF link which supports transmission of 8 channels in

uplink as well as downlink with acceptable bit error rate (BER). In 2010 [158], the performance of OFDM is investigated for 13.87 Gbps transmission at 60 GHz over 3 km SMF fiber and 3m wireless link by utilizing QPSK. The power penalty is reported as less than 3 dB without any need of compensation scheme.

In an experimental work [159], 28 Gbps-60 GHz data is transported over a 25 km link by employing 16 QAM-OFDM schemes. Moreover, three RoF systems are investigated by employing frequency doubling, sextupling, and optical conversion techniques. The constellations are measured for each RoF system illustrating that optical conversion scheme performs better as it supports 28 Gbps data rate as compared to frequency doubling and sextupling schemes which are limited to 13.8 Gbps at 30 GHz and 20.73 Gbps data rate respectively. In 2011 [160], 40 Gbps data at 75 GHz is transported over 30 mm wireless link with the aid of horn antenna by using optical single side band (OSSB) scheme. In this experiment, polarization-based 16 QAM scheme is compared by combining two optical QPSK signals before the optical modulator, which results in the ease of controlling the bias voltage of modulator. The results are reported in terms of BER and constellations which show that 16 QAM performs better with less BER as compared to QPSK signal.

In an another experiment [161], 2 X 2 multiple-input-multiple-output (MIMO) scheme is employed to transmit 50 Gbps-60 GHz data over a 1 km fiber link and 30 mm wireless link by comparing QPSK, 8 QAM and 16 QAM modulation techniques. 16 QAM achieved the highest data transmission of 50 Gbps with acceptable SNR and precise constellations as compared to QPSK and 8 QAM which support the data rate of 28 Gbps and 42 Gbps respectively. In an another simulation work [162], a bidirectional RoF link is established over the optical span of 30 km which supports data transmission of 10 Gbps-60 GHz in downstream and 2.5 Gbps-60 GHz in upstream. The results are reported in terms of constellations and BER, elucidating that

proposed system is efficient for bidirectional transmission by adopting 16 QAM modulation format.

In 2013 [163], 51 Gbps-60 GHz is transported over a 1 km optical link and 4 m wireless link using MIMO-OFDM. In this experiment, the performance of QPSK, 8 QAM, 16 QAM, 32 QAM, and 64 QAM modulations are investigated and results are reported in terms of BER and constellations. The measured constellations and BER revealed that data transmission of 28 Gbps and 42 Gbps is achieved by QPSK and 8 QAM modulation formats respectively with acceptable BER. 32 QAM and 64 QAM systems failed to transmit the 70 Gbps data whereas 16 QAM successfully transmits the data rate of 51 Gbps with high spectral efficiency of 8b/s/Hz.

In 2014 [164], authors have demonstrated transmission of 22 Gbps -100 GHz over fiber link having span of 150 km and 3 m wireless by employing direct detection OFDM scheme. In this experiment, QPSK and pilot aided phase noise suppression (PANP) techniques are utilized to overcome the effect of chromatic dispersion (CD) in the fiber link. The results are reported in terms of SNR and constellations which showed that by adopting QPSK and PANP techniques, BER and CD is improved, resulting in high data transmission up to longer distances.

Similarly, in another simulation work [165], a full duplex 40 Gbps-60 GHz RoF link is employed over the optical span of 30 km by incorporating 16 QAM. In this work, homodyne/heterodyne coherent detection is used to receive the optical signals at the receiver side. In 2015 [166], 25 Gbps-60 GHz data is transmitted over 22 km fiber with 2 m wireless link by adopting OFDM scheme and pre-compensation scheme.

Without 2 m wireless link, transmission link prolongs to 50 km of fiber with acceptable forward error correction limit. In another experiment [167], 40 Gbps-60 GHz radio data is transmitted over 150 km fiber by using OFDM and 4 QAM modulation. Optical heterodyne method is used to generate 60 GHz millimeter signal.

In 2016 [168], authors have demonstrated transmission of 4.46 Gbps OQAM radio signals over 2 km 3-core fiber with wireless link of 0.4 m by using OFDM technique. In another experiment [169], 40 Gbps-60 GHz radio signal is transported over long haul 150 km optical fiber by using QPSK and OFDM scheme. The authors have used EDFA and dispersion compensated fiber as post compensation technique. In another experiment [170], authors have demonstrated transmission of 5 Gbps, 3.75 Gbps and 2.5 Gbps radio signals over 1 km few mode fiber (FMF) with 10 cm wireless link by using 16 QAM-OFDM, 8 QAM-OFDM and 4 QAM-OFDM scheme respectively in conjunction with MDM scheme. LP 00 and LP 01 modes are used for MDM scheme.

In another experiment [171], authors have demonstrated proof of concept of transmission of 4G LTE signal and 35.4 GHz radio signal over 40km fiber by using OFDM and 256 QAM scheme. Table 2.1 compares the key works in RoF systems based on OFDM, SCM and multi-level modulation formats.

RoF technology is a relevant name in the wireless market for its immense support of ever-growing data traffic volumes. It uses optical fibers for distributing radio signals among different locations. However, it is difficult to install optical fibers in areas such as mountains, metropolitan cities, etc. Free space optics (FSO) can be used as an appropriate alternative in places where fiber installation is not feasible practically, since it uses atmosphere instead of optical fibers for data transmission. From the table it shows that, OFDM, QPSK and QAM are used widely as modulation format in RoF system.

Table 2.1 *Key works in RoF*

Journals/ Conferences Year	Experimental Setup/ Simulation	Experimental Procedure	Data Rate	Advantages	Disadvantages
OSA/2009 [157]	Experimental WDM-SOA-RoF (Bidirectional Set Up)	Subcarrier Multiplexing + 8 channels	1.25 Gbps	Can apply to WDM-PON to extend the capacity.	Limited to 23 km
OSA/2010 [158]	Experiment: OFDM-QPSK-RoF (60 GHz)	13.85 Gbps is mixed with radio carrier of 25 GHz.	13.85 Gbps	Tuning of Relative intensity is easy.	Limited to 3 km.
OSA/2010 [159]	Experiment 16 QAM-OFDM-SOA-60 GHz RoF, TSSB Modulation	(TSSB), sextupling, and All optical conversion schemes	13.74 Gbps-30 GHz, 20.73 Gbps-10GHz, 28 Gbps	High data Rate	Limited to 25 km
IEICE /2011 [172]	Experiment 20Gbps-75-110 GHz-QPSK-	Dual Parallel MZM/FBG/EDFA Amplifier	20Gbps/75 GHz	Feasibility of hybrid RF Wireless/Optical link	Demonstrated only in Free space up-to 100- mm.
OSA/2011 [141]	Experiment 1 Gbps/PON-RoF	DSB, Optical Carrier Suppression, SSB	1 Gbps-60GHz	Long connectivity upto 100 km	Data Rate is low

Table 2.1 Continued

OSA/2012 [173]	Experiment 16 QAM	2 x 2 MIMO Scheme	27.5 Gbps-60 GHz	25 km Fiber Link + 3 m Wireless with high data rate	Indoor Environment
OSA/ 2012 [161]	Experiment 50 Gbps-OFDM-RoF-60 GHz	2 x 2 MIMO Scheme, QPSK/8 QAM/16 QAM	50 Gbps-60 Ghz	4 m Wireless Link with very High speed	Optical link is 1 km
IEEE/ 2013 [163]	Experiment/51 Gbps/60 GHZ RoF	16 QAM/OFDM /MIMO	51 Gbps /60 GHz	Highest data rate	1 km Optical link and 4 m wireless
OSA/ 2014 [174]	Experiment/ 30 Gbps full duplex	QPSK/EDFA Amplifier	15 Gbps QPSK	Less Complex and cheaper	Link is limited 3 m wireless
OSA/ 2014 [164]	Experiment/ 22 Gbps-100 GHz	DD OFDM with Pre and Post Compensation Techniques	22 Gbps	Link connectivity is 150 km fiber	Complex

Table 2.1 Continued

Elsevier /2014 [165]	Simulation/ 40 Gbps-RoF Bidirectional	16 QAM	40 Gbps	Hybrid optical and wireless	Link is limited to 30 km
IEEE/ 2015 [166]	Experiment/ 20 Gbps-60 GHz	OFDM	20 Gbps	Hybrid optical and wireless	Wireless link is limited.
Taylor/ 2015 [167]	Experiment/ 40 Gbps-60 GHz	4 QAM-OFDM	40 Gbps-60 GHz	Optical heterodyne method is used	Link is limited to 150km
OSA/2016 [168]	Experiment/ 4.46 Gbps	OQAM-OFDM-3 Core Fiber	4.46 Gbps	Less Complex and cheaper	Link is limited to 3km only
Nucleus/ 2016 [169]	Simulation/ 40 Gbps-60 GHz	QPSK-OFDM	40 Gbps	Long haul link of 150 km	Complex

Table 2.1 continued.

IEEE/ 2016 [170]	Experiment	16-8-4 QAM-MDM-OFDM	5Gbps 3.7Gbps 2.5Gbps	Hybrid Optical + Wireless Link	Link is limited to 2 km fiber with 20 cm
IEEE/ 2016 [171]	Experiment	256 QAM-OFDM	4G LTE-35.4 GHz	Less Complex	Link is limited to 40 km

2.3 Free Space Optics (FSO)

Free Space Optics (FSO) is one of the pioneer technologies to realize the future of broadband networks. The transportation of signals by using the atmosphere as a medium instead of fiber is referred to as FSO. Section 2.3.1 discusses principles of FSO whereas Section 2.3.2 discusses the related work of FSO.

2.3.1 Principles of FSO

The FSO has the combined characteristics of the most prevailing communication technologies, i.e., fiber optics and wireless access. FSO has the same working mechanism as fiber optics, the only difference being that FSO utilizes the atmosphere for transmission of signals instead of guided medium as in fiber optics. The transmitting lens projects the light signal in the atmosphere towards the receiving lens, which further connects to high sensitivity receiver via optical fiber. FSO has become a very intriguing technology to researchers as an alternative for replacing existing wireless networks due to its ability to cope with high speed networks. In addition, due to its imperceptible interference by employing point-to-point laser signals, it provides secure transmission as compared to the optical fibers. The deployment of FSO in urban areas is schematically illustrated in Figure 2.3.

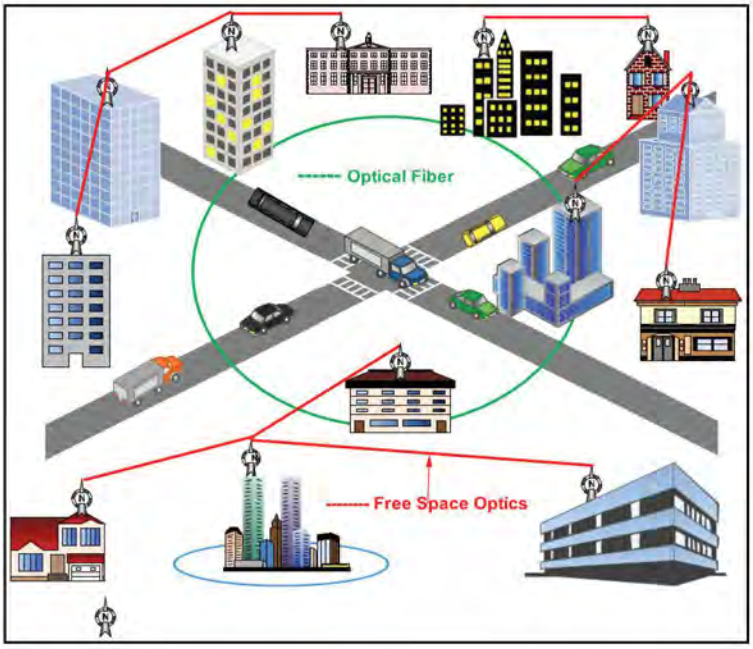

Figure 2.3. Deployment of FSO

The main advantage of FSO is that contrary to radio frequency communications, no license is required for transmission in FSO. Moreover, low power consumption, high capacity, small sizes, light weight, and low price are other credits of FSO implementation [174, 175].

2.3.2 Recent Work in FSO

In 2010 [176], 112 Gbps data was transported over 2 km FSO link by incorporating a polarized- multiplexed QPSK scheme. In this work, four channels of 7 Gbps each are multiplexed with two Mach-Zehnder modulators (MZM) which are further polarized-multiplexed to realize transmission of112 Gbps data under the effect of low, moderate and high scintillations. The results are reported in terms of constellations and BER which state that 5-12 dB improvement with twice the data rate is noted in polarization multiplexing as compared to without polarization multiplexing.

In 2011 [177], the effect of scintillation was investigated over FSO link of 1 km by utilizing a non-return-to-zero (NRZ) modulation scheme. In this work, attenuations

are theoretically calculated for different scintillations (low, medium, and high) and verified by the simulations. In another experiment [178], the effect of tropical climate is investigated by implementing the FSO link having span of 5 km between two points in Malaysia. In this work, FSO link is implemented practically between Ex Engineering, IIUM and Batu Caves, Malaysia under tropical climate and the effect of rain, scintillations, geometrical attenuations, molecular attenuations, and haze are investigated.

In 2012 [179], the author experimentally verified the FSO link for indoor applications by comparing on-off keying (OOK)-NRZ, OOK-return-to-zero (RZ) and pulse position modulation (PPM) schemes. The FSO link having a span of 5.5 m under effect of fog is tested in the laboratory in terms of Q factor, eye diagram by transmitting 1 Gbps, 100 Mbps and 1 Mbps data, highlighting that PPM scheme is the best as compared to OOK-RZ and OOK-NRZ modulation schemes. In another experiment [180], MDM, polarization multiplexing and orbital angular multiplexing (OAM) are employed to transmit 1.37 Tbps and 2.65 Tbps of data over FSO link without consideration of atmospheric turbulences. This experiment is focused on utilization of modes for carrying the data over FSO link by utilizing 16 QAM scheme. The authors successfully demonstrated the transmission of four mode division multiplexed OAM beams having 171.2 Gbps data each (171.2 X 4) and then polarized multiplexed with 2 states, thereby achieving a total capacity of 1.37 Tbps (171.2 X 4 X 2).

In 2013 [181], 40 Gbps using QPSK modulation was transported over a FSO link by incorporating OAM multiplexing under atmospheric turbulences for indoor applications. In this experiment, the effects of strong, weak, and moderate turbulence is investigated over FSO link in laboratory. In another work [182], 1 Gbps and 2 Gbps of data are transported over FSO link of 1 km by employing QAM modulation under

the effect of atmospheric turbulences. Scintillations, geometrical attenuations, and atmospheric attenuations are considered as atmospheric turbulences in this work. In 2014 [183], 2.5 Gbps data was transported over a FSO link having a span of 8 km by employing NRZ modulation. In that work, no atmospheric turbulences are considered as clear weather is assumed.

In 2014 [184], authors have demonstrated simulative transmission of 1 Tbps data over 5km FSO link by using coherent OFDM scheme. They have also compared the performance of optical double side band (ODSB) and Optical Single Side Band (OSSB) modulation. The results are reported in terms of SNR and total received power which shows that OSSB performs better as compared to ODSB. In another simulative work [185], authors have transmitted of 2.5 Gbps and 5 Gbps over 5 km FSO link by using coherent OFDM scheme. Moreover, authors have also evaluated the performance of system under various atmospheric turbulence which shows that under the influence of low fog, the FSO link prolongs to 2.2 km and 2 km, under the influence of mild fog, the FSO link prolongs to 1.3 km and 1 km, under the influence of dense fog, the FSO link prolongs to 0.6 km and 0.5 km for the transmission of 2 Gbps and 5 Gbps respectively.

In 2015 [186], authors have demonstrated transmission of BPSK and 4 QAM radio signal over 5 km FSO link by using time division multiplexed (TDM) and OFDM scheme. The reported results show that OFDM performs better as compared to TDM scheme. In another simulative work [187], the authors have demonstrated transmission of 20 Gbps data over FSO link by using OFDM and semiconductor amplifier (SOA). The FSO link prolongs to 260 km under clear weather conditions whereas under influence of heavy fog, FSO link prolongs to 4 km.

Table 2.2 *Key works in FSO*

Journal/ Conferences/ Year	Experimental Setup/ Simulation	Experimental Procedure	Data Rate	Advantages	Disadvantages
OSA/2010 [177]	Experiment	Polarized Multiplexed QPSK Scheme	112 Gbps	Scintillations Included	Link is limited to 2 km Only
IEEE/2011 [178]	Simulation	NRZ Scheme	Not Mentioned	Attenuations are calculated for Different Scintillations	Link is tested for only 1 km
IEEE/2011 [179]	Practical Implementation/ Malaysia weather	The effect of Scintillation/Rain and Fog is evaluated	Not Mentioned	No data is modulated only optical beam is evaluated	Link is tested for 1 Km and 5 Km
IEEE/2012 [194]	Experimental, OOK- NRZ, 4-PAM and BPSK,	Under Fog.	10 Mbits	4 PAM is superior as compared to others	Low Date rate, High Power required 10 dB, 5.5 m only
OSA/2012 [195]	Theoretical, OOK and PPM technique	Fog, Haze, Rain and Snow, Path Loss Model	1 Gbps, 1 Mbps, 10 Mbps, 100 Mbps	Data rate is low	1 km link only

Table 2.2 Continued

IEEE/ 2012 [180]	Experimental, Ethernet FSO link, OOK-NRZ, OOK-RZ and PPM, Fog Analysis	Indoor Application, Lab test	Ethernet 10 Base T link is transported	Useful for Indoor link	FSO link is 5.5 m under Fog.
Nature/ 2012 [181]	MDM+ Polarization (X and Y), Orbital Angular Multiplexing	16 QAM, 4 data each on 4 OAM with 2 polarization states	42.8X4X4X2 =1.37 Tbits 42.8x4x8x2= 2.65 Tbits	The capacity can be increased	Turbulences are not considered
OSA/ 2013 [182]	Experiment/ Atmospheric Turbulences on Free Space Optics/40 Gbps	40 Gbps QPSK+ EDFA+ OAM Multiplexing	40 Gbps	Scintillations are Considered	Indoor Application
OSA/ 2013 [196]	Experiment/2.5 Gbps/WDM-Fiber Feeder+ FSO	OOK-NRZ-WDM-FSO	2.5 Gbps	Scintillations are considered, For Remote Nodes	Fiber Link= 20km, FSO link-2km
Elsevier/2013 [51]	Simulation/OFDM -FSO	4 QAM Scheme-OFDM	2.5Gbps/5 Gbps	Atmospheric turbulences are considered.	Under Heavy fog, Link is limited to 355 m

Table 2.2 Continued

IEEE/ 2013 [197]	Experiment/Fog and Smoke Analysis	Optical Beam is evaluated under Fog Chamber	N-A	Fog conditions and Smoke are evaluated	Length of chamber is 2.5 m
OSA/ 2013 [198]	Experiment/New modulation Format-PQP, DPSK, QPSK	PQP is advance version of PPM.	100 Gbps	PQP modulation has better performance as compared to another ones	High power optical Amplifier is required
OSA/ 2013 [183]	Theoretical/QAM-FSO	QAM Scheme is employed, considered	1 Gbps and 2 Gbps	Atmospheric Turbulences as well as APD shot noise characteristics are also considered	Link is limited to 1 Km
Elsevier/2014 [184]	Simulation/NRZ	NRZ Scheme is employed	2.5 Gbps	No scintillations/atmospheric turbulences.	Link is limited to 8 km.
IEEE /2015 [187]	Experiment	TDM and OFDM	BPSK and OAM radio signal	Comparison of TDM and OFDM	Complex

Table 2.2 Continued

IEEE/ 2015 [115]	Simulation	OFDM and SOA	20Gbps	Atmospheric Turbulences are considered	High cost
Springer/ 2016 [189]	Simulation	QAM, OFDM and Square Root	10Gbps	Atmospheric Turbulences are considered	Link is limited to 1.8km
Elsevier/2016 [190]	Experiment	CoiPM and OFDM	Not Mentioned	COiPM is better as compared to ID-OFDM	Complex
Hindawi/ 2016 [191]	Simulation	DWDM and RZ encoding	40Gbps	Less complex	Link is limited to 4km
Elsevier/2017 [192]	Experiment	SSWDM and WDM scheme	1 Gbps	Practically Implemented and turbulences are included.	Link is limited to 1km under heavy rain
JOOC/ 2017 [193]	Simulation	NRZ	Not Mentioned	Less Complex	Link is limited to 1km

In 2016 [188], authors have demonstrated simulative transmission of 10 Gbps data over 1.8 km by using QAM, OFDM and square root module schemes. The reported results show improvement of SNR with the use of square root modulator. In another work [189], the authors have proposed consecutive polarization modulation (CoiPM) to transmit OFDM signal over FSO channel with turbulences. The reported result shows significance improvement in SNR in case of CoiPM-OFDM system as compared to intermediate detection (IM –OFDM) system. In another work [190], the authors have reported 40 Gbps data over 4 km FSO link by using dense wavelength division multiplexing (DWDM) and return to zero (RZ) scheme. Recently in 2017 [191], the authors have demonstrated transmission of 1 Gbps data over FSO link in Changsha city, China under the influence of heavy rain by adopting spectrum slicing WDM scheme. The reported results show improvement of BER in case of spectrum slicing WDM as compared to ordinary OFDM. In another work [192], comparison of 1550 nm, 850 nm, 650 nm and 532 nm is done to transmit data over 1 km FSO link under atmospheric turbulences. The reported results show that transmission at 1550nm is best as compared to other wavelengths.

Table 2.2 analyzes the key works in FSO based on OFDM, SCM and multi-level modulation formats. Thus, FSO provides an appropriate solution for all future broadband networks that can transmit high-speed and secure data. It uses point-to-point laser signals with lower errors. Other benefits of using FSO are: high-end capacity, low power consumption, free license, light weight, small size and low price. However, it cannot transmit radio signals unless RoF technology is combined with FSO. This combination of FSO and RoF has given way to another revolutionary technology known as radio over free space optics or Ro-FSO. From the Table 2.2, it shows that OFDM, QAM and QPSK are widely used as modulation formats in FSO.

2.4 Radio over Free Space (Ro-FSO)

The ever-increasing demand of the bandwidth required for the future pervasive wireless networks has led to the researchers to develop new approaches to fulfill the data rate and bandwidth needs by the explosive growth of the subscribers. Radio over free space (Ro-FSO) is one of the emerging technologies which utilize the features of both RoF and FSO technologies. FSO is viable for transporting radio signals modulated by an optical carrier through a free-space link. This is referred to as Ro-FSO systems.

Section 2.4.1 discusses principles of Ro-FSO, Section 2.4.2 discusses the main applications of Ro-FSO whereas Section 2.4.3 reports on key work of Ro-FSO.

2.4.1 Principles of Ro-FSO

A Ro-FSO system utilizes the assets of both RoF and FSO technologies which makes it most beneficial for future wireless networks. In wireless networks, users require instant and efficient connection to access various services at any time from any location at a low cost. The advantages of FSO in terms of free licensing and high speed makes FSO a compelling candidate for future wireless networks.

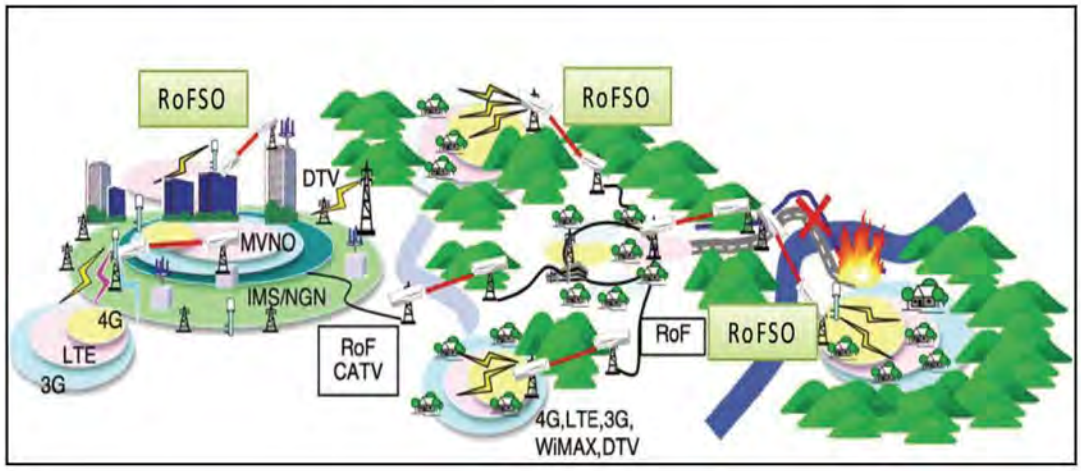

Figure 2.4. Ro-FSO Architecture [193]

In some geographical areas where current wireless radio technology are inaccessible such as in-building, hilly terrains and underground, FSO technology may be integrated with radio technology to promote more rapid deployment of a more ubiquitous wireless service and cellular architecture [3].

Ro-FSO system is one of the emerging technologies to realize the future broadband wireless systems which can transmit multiple RF signals over free space optical (FSO) networks as shown in Figure 2.4. Ro-FSO can be efficiently used as a substitute wireless technology especially in those areas where the formation of optical fiber is not attainable. Ro-FSO can also be used in rural areas with low populations where it may not be cost-effective to establish radio infrastructures.

2.4.2 Applications of Ro-FSO System

The Ro-FSO system provides global platform to transmit wireless signals in a ubiquitous network environment. Following are some applications of Ro-FSO systems:

- **Telephone network extensions through Ro-FSO:** Ro-FSO systems can be used to extend the telephone network connectivity especially in rural areas
- **Enterprise:** Ro-FSO system can be used to connect various networking topologies such as Local Area Network (LAN) to LAN connectivity, intra campus networking, Wide area Network (WAN) to WAN etc.
- **Cable Television Transmission:** Ro-FSO system can be employed to transmit the digital cable television signals at very high speed.
- **Dense wavelength Division Multiplexing (DWDM) services:** Ro-FSO systems can be used to provide optical connectivity in various applications including DWDM services.

- **Last Mile Connectivity Applications:** Ro-FSO systems can be employed to solve the last mile connectivity especially in those areas where it is impossible to install the optical fibers.
- **Mobile Wireless:** Ro-FSO system can be used as mobile wireless driver for today and future generation networks, including applications for base transceiver station, temporary service and WLAN "hotspot" connectivity.

2.4.3 Recent work in Ro-FSO

The last decade has experienced a lot of research in the era of Ro-FSO networks. In 2009 [194], Ro-FSO link is practically implemented in Tokyo which supports the transmission of 3G cellular, WLAN 11g/a, ISDB-T signals over link of 1 Km by considering clear weather conditions. In this experiment, 14 Mbps data is achieved as throughput in the FSO link under clear day by considering high scintillations with 16 QAM scheme. In 2010 [40], WDM scheme and EDFA is employed to transmit ISDB T, WCDMA, 802.11G and 802.11A digital signals over Ro-FSO link. This link was useful for useful for transmitting Mobile WCDMA, Digital TV Broadcasting and Wireless LAN Service as 12 Mbps is achieved as throughput.

In another experiment [11], the authors have investigated QPSK, 16 QAM and 64 QAM schemes to transmit radio carrier of 473 MHz which is suitable for indoor application. In this work, Gamma Gamma distribution model is used to analyze the scintillation for indoor applications. In another experiment [195], 4 channels having 12.5 Gbps data each with 0.80 nm channel spacing are transported over 5.6 Km fiber link and 2.2 m wireless link for indoor applications. The scintillations are not considered in that work. In another work [196], 20 Gbps-93 GHz data is transported over optical fiber link of 25 Km and wireless link of 20 cm by using ON-OFF key. In this work, horn antenna is used to transmit the 20 Gbps-93 GHz signal wirelessly by

considering it for indoor application without any scintillation effect. In another experimental demonstration [172], 20 Gbps-75GHz-100 GHz are transported over fee space link of 30 mm by adopting QPSK scheme. Horn antenna is used for transmitting the data in free space for indoor application without considering scintillations. Erbium Doped Amplifier (EDFA) is used as post compensation scheme in that work.

In 2012 [197], QAM and Fast Fourier Technique (FFT) is employed to transmit the 1 Gbps data over a free space link of 50 cm by using Light Emitting Diode (LED) for indoor applications. In another experiment [198], polarization multiplexing, 2X2 MIMO and QPSK scheme is employed to transmit 40 Gbps-40 GHz signal over optical fiber having long span of 400 km and wireless link of 100 cm for indoor application. The results are reported in terms of constellations and SNR which clearly stated the feasibility of transmission of high data with acceptable BER. Similarly in another experiment [199], 16 QAM-OFDM scheme is employed to transmit 42.7 Gbps -75 GHz-110 GHz data over optical fiber having span of 22 km and free space wireless link of 0.58 m without consideration of scintillations. To transmit the radio signal, Heterodyne up conversion and down conversion technique is used in that experiment work.

In 2013 [200], 1.25 M-bits and 2.5 M-bits data are transported over free space link of 2.5 m by using NRZ and Manchester modulation scheme with the aid of LED. In 2014 [201], the author's has investigated BPSK, QPSK, 16-QAM, and 64-QAM schemes to transmit the radio signal over free space link of 2 km using dual diversity reception with two diversity combining scheme by considering clear weather conditions.

In 2015 [10], authors have successful demonstrated transmission of 40 Gbps radio data over 1.5 km FSO link by employing OFDM and WDM scheme. In this

experiment, laser cavity in conjunction with add/drop filter was used to generate sixteen mode-locked optical carriers. In another experiment [202], LTE signals are transported over 1.6 m FSO link by using PDM and 64 QAM modulation technique. Moreover, the link was also tested under atmospheric turbulences. In another numerical work [203], OFDM is used to implement Ro-FSO link under weak turbulences. Phase shift Key (PSK) and QAM is used as modulation scheme. In this work, authors have presented mathematical analysis of PSK/QAM OFDM-Ro-FSO transmission system characterized by M-turbulences. In another simulative work [19], authors have transmitted global system for mobile communication (GSM) signal at 900 MHz with data rate of 270.8 kbps over different FSO models. A comparison of output signal spectrum through log normal, exponential and gamma channel model for weak, strong and saturation regime is presented in this work. The results are reported in terms of output spectrum which shows that log normal channels prolong to only weak turbulences whereas gamma-gamma channel model prolongs to weak as well as strong turbulences.

In 2016 [3], authors have demonstrated successful transmission of LTE signals over 5 km fiber with 2 m FSO link under strong turbulences by using PDM, OFDM and 64 QAM scheme. The results are reported in terms of error vector magnitude, SNR and constellations which show that the FSO link can prolongs to 100 m if turbulences are weak. In another work [204], the authors have derived a close form of mathematical expression for estimation of BER of proposed Ro-FSO system by using OFDM with QAM format. In this work, negative exponential distribution is used for atmospheric turbulences whereas non-linear BAC is used for optical fiber part. In another experiment work [205], 60 Mbps mobile signals are transported over 3 m FSO link to provide WiFi signals. Table 2.3 shows main key work on Ro-FSO systems in last 6 year.

Table 2.3 *Key work in area of Ro-FSO System*

Journal/ conferences Year	Experimental Setup/ Simulation	Experimental Procedure	Data Rate	Advantages	Disadvantages
IEEE/ 2009 [200]	Practically Implemented Tokyo/ 3G cellular, WLAN 11g/a, ISDB-T are transported over FSO	3 Radio channels are transported, EDFA and circulator are used.	16 Mbps	Scintillations are considered.	Only under clear weather conditions, link is limited to 1 km
IEEE 2010 [212]	Experimental/ ISDB T + WCDMA+802.11G+802.11A are transported over FSO	WDM Scheme is employed +EDFA	12 Mbps Throughput	Useful for Mobile WCDMA, Digital TV Broadcasting + Wireless LAN Service	Atmospheric Turbulences are not considered
IEEE 2010 [11]	Theoretical/QPSK/16 QAM/64QAM	Gamma Gamma Distribution is used for Scintillations	Radio Carrier 473 MHz	Scintillations are considered	Only for Indoor Application.
OSA/ 2011 [201]	Experimental/WDM-Indoor Application	0.80 nm spacing	50 Gbps	Indoor Applications is good	5.6km + 2.43 m only
IEEE/ 2011 [202]	Experiment/20Gbps/On-OFF Key/	EDFA Amplification, OOK Modulation	20 Gbps-93 GHz	Indoor Application	Optical Link is 25 km and wireless link is 20 cm

Table 2.3 Continued

IEICE/ 2011 [172]	Experiment/20Gbps-QPSK	Horn Antenna is used for wireless link	20Gbps-75-110 GHZ	Indoor Application	Wireless link is 30 mm, No scintillations are considered.
IEEE/ 2012 [203]	Experiment/White LED using Rate-Adaptive Discrete Multitone Modulation	QAM + FFT Technique	1 Gbps	Indoor Application	Wireless Link is limited to 10 cm to 50 cm
IEEE/ 2012 [75]	Experiment/PDM-QPSK	QPSK Technique + EDFA Amplifier + PDM	48 Gbps-48 GHz	400 km fiber link + 15 cm Wireless Link	Wireless Indoor Application
OSA/ 2012 [213]	Experiment/ WDM +VLC	Green Light + Red Light	500 Mbps + 500 Mbps	10 m Link, Indoor Applications	Scintillation is not considered.
PIER/ 2012 [205]	Experiment/16 QAM OFDM, 75-110 GHz	Heterodyne Up conversion and technique	8.9 Gbps+26.7Gbps+42.7 Gbps	22.8 km + 0.58m wireless	Scintillations are not considered.

Table 2.3 Continued

IEEE/ 2013 [206]	Experiment/LED	NRZ and Manchester Modulation	1.25 Mbps +2.5 Mbps	Indoor Application , Mitigate the Optical background noises	2.5 m only
IEEE/ 2014 [207]	Theoretical /OFDM-FSO	BPSK, QPSK, 16-QAM, 64-QAM.	N.M	Scintillations are considered	Link is limited to 2 km.
IEEE/ 2015/ [10]	Experiment	OFDM, WDM	40Gbps	Laser Cavity is used.	Link is limited to 2 km.
OSA/ 2015 [208]	Experiment	PDM, 64QAM	LTE Signals	Less Complex	Link is limited to 1.6 m.
IEEE/ 2015 [209]	Mathematical	PSK, QAM,OFDM	Not Mention.	M Turbulences are considered	Link rate is not mention.
IEEE 2016 [210]	Mathematical	OFDM, QAM	Not Mentioned	Closed form is derived for BER estimation	Link rate is not mentioned
OSA 2016 [211]	Experimental	Integrated WIFI	60 Mbps	Mobile signals are transported through FSO	Link is limited to 3 m

In order to optimize the features of RoF and FSO technologies, Ro-FSO systems incorporate high bandwidth of optical networks and mobility of wireless networks while transmitting RF signals over high-speed optical carrier without expensive RF licensing or cabling [4-7]. Ro-FSO can be utilized for different segments of electromagnetic spectrum. It can also be used for mitigating RF spectrum congestion issues in current wireless networks. Table 2.3 shows that OFDM, QAM and QPSK are widely used as modulation format whereas WDM is used widely as multiplexing scheme in Ro-FSO systems.

Apart from these benefits, there are some challenges which should be considered while designing Ro-FSO systems.

2.5 Challenges in Ro-FSO Systems

Ro-FSO technology may pave the way towards a universal platform to seamlessly integrate radio and optical networks while using no expensive optical fiber cables. Nonetheless, Ro-FSO guarantees high speed data rates but there are some challenges also such as scintillations, atmospheric turbulences like fog, rain, snow, etc. which need to be alleviated in order to improve the signal-to-noise ratio of the Ro-FSO link. These atmospheric turbulences are described as follows:

(a) **Fog Attenuation**: The atmospheric fog attenuation is persisted by the Beer–Lambert law which states that the attenuation due to fog and haze in the optical signal at a distance R is given by the following relation:

$$A_{fog} = \frac{3.912}{v(km)}\left(\frac{\lambda}{\lambda_o}\right)^{-q} \tag{2.1}$$

Where v defines the visibility in km, λ defines the wavelength of transmitting signals, λ_o defines the visibility reference at wavelength at in nm and q defines the

size distribution coefficient of scattering. Kim and Kruze [206] propose a different model for the calculation of value q which is stated below:

Table 2.4

Kim and Kruse Model

Kim Model	Kruze model
1.6 if V > 50 **km** 1.3 if 6 **km** < V < **km** 0.16V + 0.34 if 1 **km** < V < 1 **km** V − 0.5 if 0.5 **km** < V < 1 **km**	1.6 if V > 50 **km** 1.3 if 6 km < V < **km** 0.585 $V^{\frac{1}{3}}$ if V < 0.5 **km**

(b) **Rain Attenuation**: Rain is also an important parameter to be considered while designing an FSO link. The equation [207] for specific rain attenuation is described by the following relation:

$$\alpha_{rain} = 1.076 \times R^{0.67} \tag{2.2}$$

where R defines the rate of rainfall in mm/hr.

(c) **Snow Attenuation**: The equation for snow attenuation is given by the following relation [181]:

$$\lambda_{snow} = \alpha \times S^{\beta} \tag{2.3}$$

Table 2.5

Values of β & α

Type of Snow	β	α
Dry Snow	0.000102λ + 5.50	1.38
Wet Snow	0.0000542λ + 3.79	0.72

where S describes the rate of snowfall in mm/hr and α & b are given according to ITU recommendations [208] as shown in Table 2.5.

(d) **Scintillation Effect**: Scintillations are also a dominant factor in FSO both in terrestrial communication as well as in space communication as the optical signal is fluctuated by the transient dips caused due to change in refractive index of the medium. Atmospheric scintillation is given by the following equation [209]:

$$A_{scin} = 2 * \sqrt{23.17(\frac{2\pi}{\lambda}10^6)^{7/6} * C_n^2 * l_6^{11}} \quad (2.4)$$

where λ is the wavelength in nm, l is the range in meter and c_n^2 is the refractive index parameter.

Ro-FSO uses the FSO as medium for transmitting radio signals from one place to another. The last decade has witnessed development of various multiplexing schemes such as wavelength [210], phase [160] and intensity [211] by the researchers for improving the bandwidth of FSO and Ro-FSO systems. However these multiplexing schemes are still insufficient to fulfil the demand of high speed data to large number of users. In last few years, researchers have demonstrated mode division multiplexing (MDM) for FSO systems to increase capacity and bandwidth. As an optical multiplexing technology, MDM uses spatial modes as information channels for carrying independent data streams. MDM has potentials for enhancing FSO transmission data rates proportional to the total number of modes used. Despite the use of multifarious MDM techniques in increasing the capacity of optical communications and free- space optical systems, it is still an unchartered domain in Ro-FSO based on Table 2.1, Table 2.2 and Table 2.3.

2.6 Mode Division Multiplexing (MDM)

MDM is a revolutionary technology used to increase the capacity of optical transmission systems. Section 2.5.1 discussed the principles of MDM and Section 2.5.2 discusses the key wok of MDM.

2.6.1 Principles of MDM

The concept of MDM is based upon transmission of channels on different fiber modes as shown in Figure 2.5. At transmission side, all channels are combined together with the aid of mode combiner and then transported over transmission channel. At the receiver side, a mode splitter or mode selector is used to select particular modes.

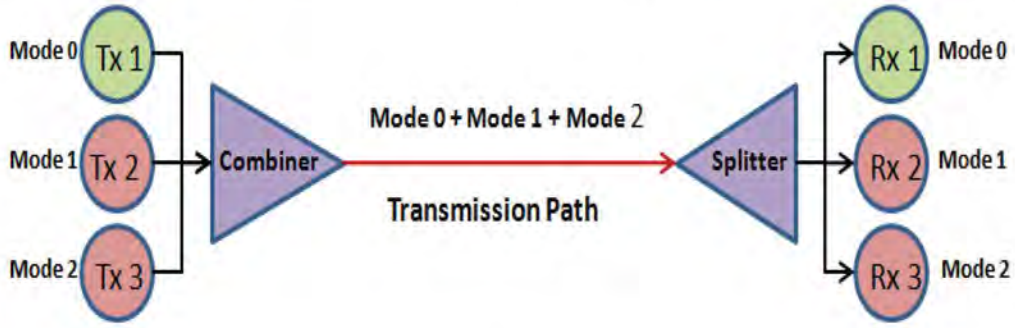

Figure 2.5. Mode Division Multiplexing

Modes are of various types such as Laguerre-Gaussian (LG), Hermite Gaussian (HG), Eigen modes, Donut modes and others can be generated with the aid of spatial lasers [184], spatial modulators [57-60] and fiber gratings [53]. LG modes (00, 01) and Donut modes (0, 1) excited by spatial laser are shown in Figure 2.6.

The LG mode is described mathematically [212] as

$$\psi_{m,n}(r,\varphi)=\left(\frac{2r^2}{w_o^2}\right)^{\left|\frac{n}{2}\right|}L_m^n\left(\frac{2r^2}{w_o^2}\right)\exp\left(\frac{r^2}{w_o^2}\right)\exp\left(j\frac{\pi r^2}{\lambda R_o^2}\right)\begin{Bmatrix}Sin(|n|\varphi), n\geq 0\\ Cos(|n|\varphi), n\geq 0\end{Bmatrix} \quad (2.5)$$

where m and n represents the X and Y index that describe the azimuthal and radial indexes, respectively. R is the radius of curvature, w_0 is the spot size and $L_{n,m}$ is the Laguerre Polynomial.

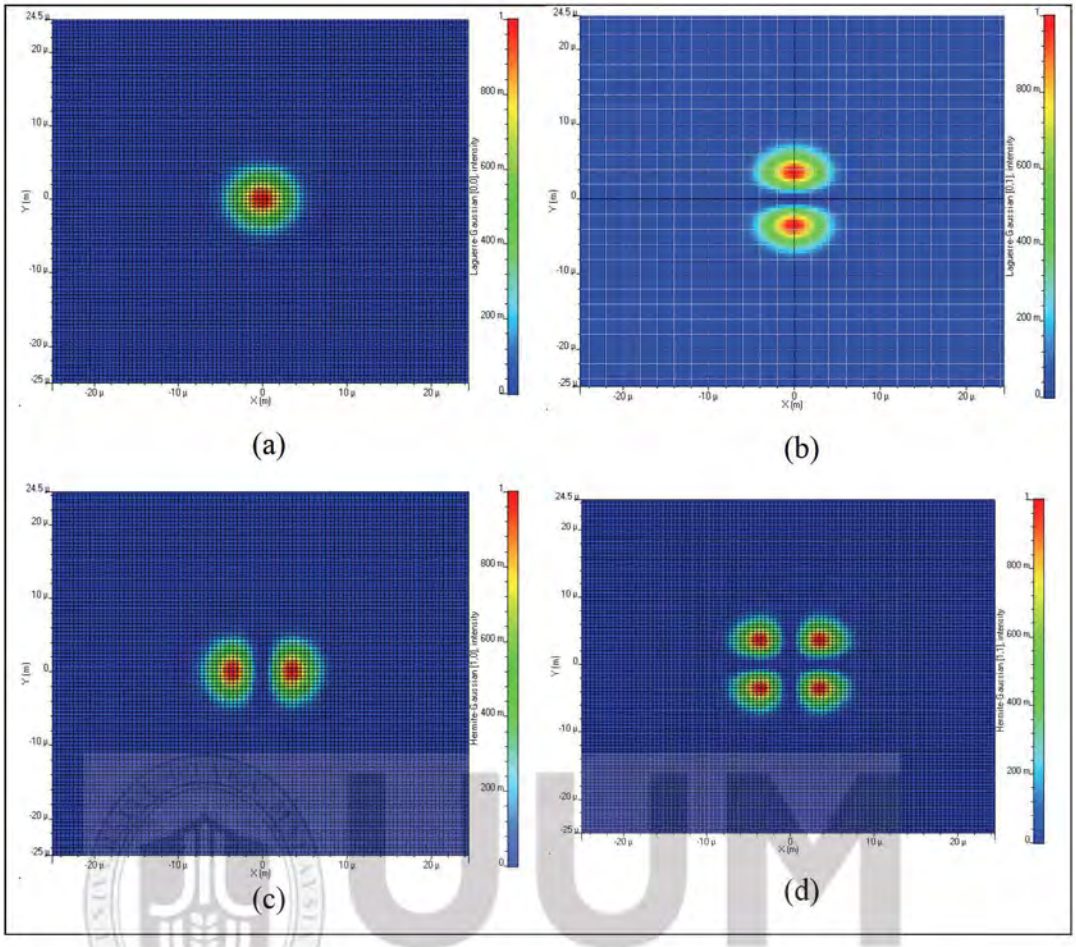

Figure 2.6. Excited Modes (a) LG 00 (b) LG 01 (c) HG 10 and (d) HG 11

Similarly, The HG mode is described mathematically as [213]

$$\varphi_{m,n}(r,\phi) = H_m(\frac{\sqrt{2}x}{w_o x})\exp(\frac{-x^2}{{w_o}^2 x})\exp(j\frac{\pi x^2}{\lambda R_o x})H_n(\frac{\sqrt{2}y}{w_o y})\exp(\frac{-y^2}{{w_o}^2 y})\exp(j\frac{\pi y^2}{\lambda R_o y}) \quad (2.6)$$

2.6.2 Recent work in MDM

MDM has been used widely both in optical fiber as well as free space optical systems. In 2013 [214], 100 Tbps data is transported over 1 m FSO link by incorporating MDM of 24 orbital angular momentum (OAM) modes (OAM $\pm$4, $\pm$7, $\pm$10, $\pm$13, $\pm$16, $\pm$19 on X and Y polarization state) and wavelength division multiplexing (WDM) scheme. In another experiment [215], the utilization of OAM, WDM and polarization division multiplexing (PDM) is reported to transmit 100.8 Tbps high speed data over

1 m FSO link. In 2014 [216], images are transported over 3 km FSO link in city of Vienna by employing multiplexing of OAM modes (OAM $\pm$ 1, $\pm$1 rotated, $\pm$4 and $\pm$ 15).

Optical fiber communication systems have implemented MDM by using spatial light modulators [56-58], optical signal processing [55, 59, 217, 218], few mode fiber [61, 63], photonic crystal fibers [64] and modal decomposition methods [219, 220]. Despite the use of multifarious MDM techniques in increasing the capacity of optical communications and free- space optical systems, it is still an unchartered domain in Ro-FSO. However in 2014 [9], author has reported transmission of 32 Gbps millimeter signal over FSO link of 2.5 m by using MDM of 4 OAM modes (-3, -1, +3 and +1) on each X and Y polarization.

In 2015 [221], orbital angular multiplexing (OAM) of two OAM modes $l = +1$ and $l = +3$ is used to transmit 80 Gbps data over free space link. In another work [222], 4 collocated OAM beams are used to carry 400 Gbps high speed data over 120 m FSO link. In 2016 [223], 400 Gbps data is transmitted over 120 meters FSO link by using 4 OAM beams $l = \pm 1$ and $l = \pm 3$. In another work [224], two OAM beams $l = \pm 3$ are used to transmit 40 Gbps 16 QAM data over 260 m FSO link.

Another experiment [225] reported the transportation of 200 Gbps data over 1 meter FSO link by using two Laguerre–Gaussian (LG) beams with different radial indexes $\zeta = 0, \rho = 0$ and $\zeta = 0, \rho = 1$, where the azimuthal index ζ is related to OAM and the radial index ρ is related to radial nodes. The experiment also reported an estimated OAM-carrying LG beam while the OAM beams were used with different ζ. LG modes can develop orthogonal and modal sets.

Table 2.6

Key work of MDM in FSO

Journal/ Year	Experimental/ Simulation	Mode generation at transmitter	Type of Modes	Data rate	No of Channels	Distance Achieved
OSA/2013 [222]	Experiment	Spatial Light Modulators	OAM (4, 7, 10, 13, 16, 19)	100 Tbps	24	1 m
OSA/2014 [224]	Practically Implemented	Spatial Light Modulators	OAM 1, 1 rotated, 4 and 15	Images	16	3 km
Nature/ 2014 [9]	Experiment	Spatial Light Modulators	OAM modes (-3, -1, +3 and +1)	32 Gbps	4	2.5 m
OSA/2015 [229]	Experiment		OAM modes l=+1 and l=+3	80 Gbps	2	1 m
OSA/2015 [230]	Experiment	Spatial Light Modulators	OAM modes l= 1 and l= 3	400 Gbps	4	120 m
OSA/2016 [232]	Experiment	Spatial Light Modulators	OAM modes l=+3, -3	40 Gbps	2	260 m
OSA/2016 [233]	Experiment	Spatial Light Modulators	LG beams	200 Gbps	2	1 m

LG modes with higher values of ρ can include OAM whereas OAM beams with higher values of ρ can also be used for multiplexing [226]. Although, MDM can be adapted in Ro-FSO to increase transmission capacity, atmospheric turbulence due to fog degrades the signal quality and leads to deep fading of the radio subcarriers [69, 70]. Moreover, MDM can also lead to increased mode coupling effects in Ro-FSO which causes degradation of signal quality such as channel impulse response, BER and SNR [74, 80]. The use of equalization scheme can compensate for mode coupling [87-89]. The equalization is used to compensate mode coupling effects introduced in transmission channel.

To solve the problem of fading in proposed MDM-based Ro-FSO system, OFDM can be used whereas to alleviate mode coupling effects, equalization by means of photonic crystal fiber is proposed.

2.7 Orthogonal Frequency Division Multiplexing (OFDM)

OFDM is a prominent ways to decrease the multipath fading effect during transmission of signal through free space medium. It was first introduced by Chang in a seminal paper in 1966 [183]. Section 2.6.1 discusses about principles of OFDM and Section 2.6.2 presents the key work of OFDM.

2.7.1 Principles of OFDM

The concept of dividing the data into parallel orthogonal sub carriers is known as OFDM technique. The frequency selective fading and narrow band interference can be minimized with increased robustness provided by OFDM. At the transmitter side, as shown in Figure 2.7, the input data is mapped into sub-carrier amplitude and phase represented by complex In Phase and Quadrature Phase (IQ) vector with the aid of sub carrier modulation scheme.

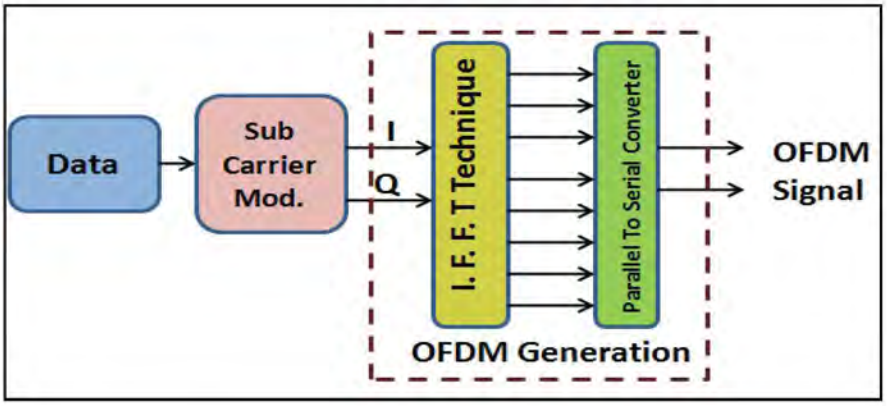

Figure 2.7. Generation of OFDM signal at transmission side

As for example, in case of 4 QAM subcarrier modulation scheme, it maps one bit for each symbol, each combination of one bit of data corresponds to unique IQ vector, represented by dot as shown in Figure 2.8.

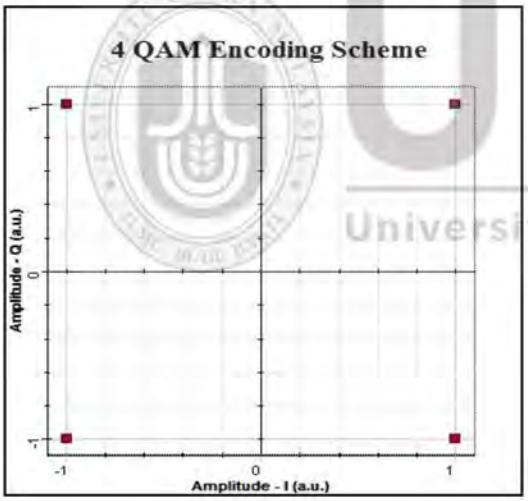

Figure 2.8. 4 QAM Encoding

This IQ vector is fed to Inverse Fast Fourier Technique (IFFT) block which converts this signal from frequency domain to time domain. The output of IFFT block is fed to parallel-to-serial convertor which converts signal into serial form as IQ signal.

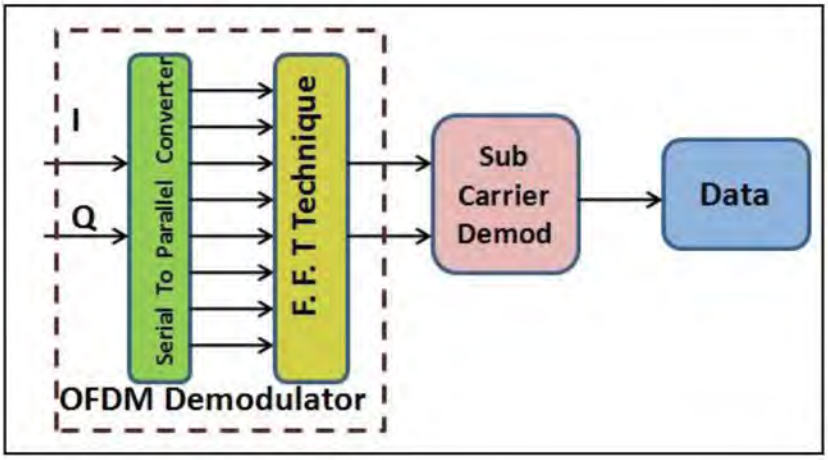

Figure 2.9. OFDM Detection

At the reception side shown in Figure 2.9, OFDM baseband IQ signal is fed to serial-to-parallel converter and then fed to Fast Fourier technique (FFT) for conversion of time domain to frequency domain. The output of FFT block is fed to the sub-carrier demodulator to recover original data from IQ signal.

2.7.2 Recent work in OFDM

In 2013 [227], the authors have used OFDM to reduce the effect of multipath fading in FSO system. In this simulative work, 5 Gbps and 2 Gbps data are transmitted over 10 km FSO link by adopting OFDM and optical double side band (ODSB) scheme under clear weather conditions. Further, the impacts of atmospheric turbulences, particularly different conditions of Fog, are also investigated. In 2014 [228], the authors have transmitted 10 Gbps data over 17.5 m FSO link by adopting OFDM and WDM schemes. In this experiment, 16 QAM modulation format is used. In another experiment [229], 10 Gbauds/s data is transmitted over turbulent FSO link by adopting coherent OFDM scheme. In this work, multilevel differential phase shift key (MDPSK) modulation format is used. The authors have compared frequency domain (FD) and time domain (TD) MDPSK modulation formats for non-equalization

coherent OFDM systems for FSO. The reported results show that FD-MDPSK has a high spectral efficiency with low complex hardware requirement as compared to TD-MDPSK.

In 2015 [186], the authors have compared OFDM and TDM scheme by transmitting 10 Gbps data over 5 km FSO link under the influence of turbulent weather. The reported results show that OFDM performs better as compared to TDM in order to reduce the effect of multipath fading in FSO systems. Another experimental work [230] used OFDM to gain high spectral efficiency while transmitting 1.45 Gbps data over 4.8 m FSO link under water. In this work, 64 QAM modulation format is used. In another work [231], the authors have reported the highest and longest transmission for visible light communication by using OFDM scheme. In this experiment, 750 Mbits data is transmitted over 2 m FSO link by using 64 QAM modulation format.

In 2016 [232], the author has transmitted 10 Gbps data over 500 m FSO link under the influence of different atmospheric conditions by adopting OFDM scheme. In this simulation work, 16 PSK is used as modulation format. In another work, the authors have compared the OFDM and TDM schemes for FSO system. In this work [233], 1 Gbps data is transmitted over 3.2 km FSO channel under the impact of strong turbulences by using OFDM and TDM schemes. The reported results show that an improvement of 17.9 dB is noticed in signal to noise ratio (SNR) by using OFDM scheme as compared to TDM scheme. In another work [234], 4 Gbps data is transmitted over 1.3 km FSO link under the influence of heavy rainfall by using OFDM scheme. The Table 2.7 shows key work of OFDM in FSO systems.

Table 2.7

Key Work of OFDM in FSO

Year/Journal	Experiment/Simulation	Data Rate	FSO Range	Modulation Format
2013/IEEE [227]	Simulation	5 Gbps	10 km	OFDM-ODSSB
2014/OSA [228]	Experiment	10 Gbps	17.5 m	OFDM-16 QAM
2014/IEEE [229]	Experiment	10 Gbaud/s	Not Mentioned	Coherent OFDM-FD-MDPSK and OFDM-TD-MDPSK
2015/IEEE [186]	Simulation	10 Gbps	5 km	OFDM
2015/OSA [230]	Experiment	1.45 Gbps	4.8 m	OFDM-64 QAM
2015/OSA [231]	Experiment	750 Mbps	2 m	OFDM-64 QAM
2016/Optics and Photonic Journal [232]	Simulation	10 Gbps	500 m	OFDM-16 PSK
2016/Elsevier [233]	Simulation	1 Gbps	3.2 km	OFDM and TDM
2016/Degrueter [234]	Simulation	4 Gbps	1.3 km	OFDM

OFDM is an established technique in wireless communications for alleviating frequency-selective fading and narrow-band interference, which has been approved for several digital communication standards including IEEE 802.11 local area network and IEEE 802.16 wireless broadband [74-76]. The optical communication community has shown profound interest in orthogonal frequency-division multiplexing (OFDM) in the last year. Tables 2.2 and 2.6 show the significant use of

OFDM in FSO systems for multipath fading effects under the influence of atmospheric turbulences. OFDM performs better as compared to other fading mitigation techniques such as CDMA, TDMA and FDMA, especially for high data rate applications [235].

Thus, OFDM can also be used in Ro-FSO system to mitigate multipath fading introduced by atmospheric turbulences in MDM. Chapter 4 of this thesis is focused on the design of MDM-OFDM-Ro-FSO system.

2.8 Photonic Crystal Fiber (PCF)

Based on photonic crystal properties, photonic-crystal fiber (PCF) is a recent inclusion in optical fiber. PCF has garnered significant attention with its developmental research in the last decade mainly due to its efficiency as compared to existing optical fibers. PCF is a mode-filtering device which can launch a beam into multimode fiber (MMF) for improving channel impulse response and bandwidth. Its power coupling can be managed by changing the number of rings, distance ratio between the holes and the size of the holes. PCF can be utilized for achieving zero dispersion wavelengths [236] by changing the ratio of the hole diameter and pitch. Section 2.7.1 discusses the principle of PCF and Section 2.7.2 discusses the key work of PCF.

2.8.1 Principle of PCF

PCF mainly controls three physical parameters as shown in Figure 2.10 – core diameter ρ (diameter of the ring formed by the innermost air holes), diameter of the air holes (cladding), and pitch Λ (distance between the center of the air holes). These parameters, when combined with the refractive index of the material and type of lattice, can supple PCF fabrication and manage its properties [237].

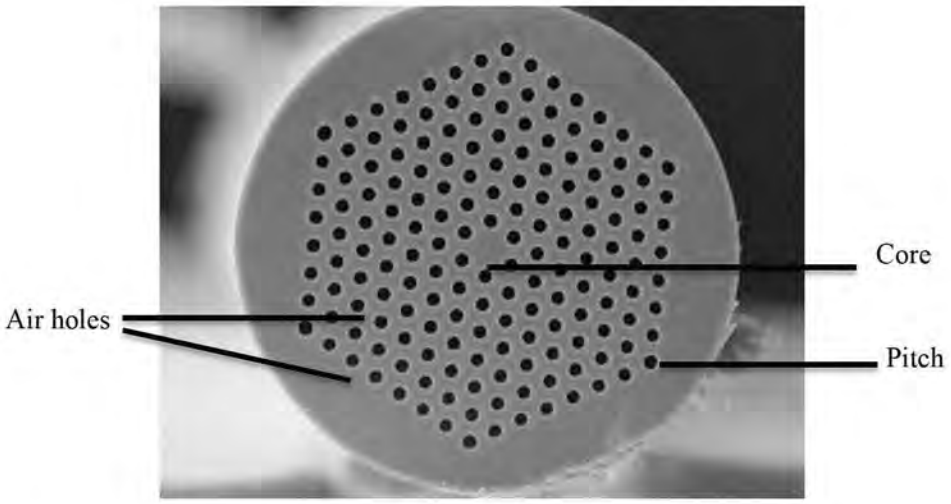

Figure 2.10. Diagram of typical solid core photonic crystal fiber [237]

Philip Russell first proposed the idea of trapping light in a hollow channel with photonic bandgap in 1991 [238]. PCF was first fabricated and reported in 1996. PCF has attracted considerable attention with its interesting properties, which provide a suitable platform for linear and nonlinear optics research. Different types of PCFs have been developed so far for different applications. An important feature of PCF is its flexibility in design and control over their optical properties that conventional fibers do not possess. In general, a PCF consists of a periodic array of hollow channels which are typically arranged in a hexagonal symmetry [239]. A lattice defect in the center forms the fiber core where light is confined and guided along the fiber axis. The guiding mechanism difference along with the nature of the defect makes PCFs widely classified into two categories: index-guiding PCF and hollow-core PCF. In an index-guiding PCF, the air-hole array reduces the effective refractive index of the cladding so that light can be confined in the silica core by means of a modified total internal reflection (TIR), similar to the guidance principle in a conventional step-index fiber [240, 241]. The index-guiding PCF offers greatly enhanced design freedom compared to standard optical fibers and has been shown to possess numerous

novel properties, such as endless single-mode operation and zero-dispersion wavelength in the visible wavelength region. In contrast, a hollow-core PCF guides light in different ways which cannot be explained with total internal reflection since light is guided in the low index region (air) and the effective refractive index is around 1 [241]. Solid-core photonic fibers (SC-PCF) can be used for decreasing mode-coupling losses of MDM-based systems through selective excitation [64]. In order to launch the MDM-Ro-FSO system, SC-PCF can convert a pure Gaussian beam into the desired mode while filtering the loud modes to enhance channel impulse response and bandwidth. A mode converter can be used for adiabatic transition between two optical modes. PCF can be designed and simulated as a mode converter from the Gaussian pulse to different LP modes. This will be achieved by changing the structure of each PCF connected to each concurrent Spatial VCSEL. Recently, various researchers have investigated the use of PCF in MDM-based systems [143, 242-246].

2.8.2 Related Work in PCF

In 2013 [64], authors have demonstrated solid core PCF for excitation of LP 01 modes in multimode fiber. In this work, 40 Gbps data is transported over 15 cm PCF and 1200 m MMF. The reported results show that with the use of PCF in transmission link, the power coupling coefficient improves which results in reduction of mode coupling losses. In another work [247], the authors have proposed PCF for dispersion compensation in optical fiber communication system. The proposed PCF is based on modified octagonal structure which can be useful for wavelengths ranging from 1460 nm to 1625 nm. The reported results show that the proposed broadband dispersion compensating M-OPCF can be designed to offer high negative dispersion coefficients ranging from -400 to -725 ps/nm/km over S and L bands along with RDS similar to a

conventional single-mode fiber. In another experiment [248], the authors have demonstrated error-free transmission of 25 Gbps over 1 km MMF by using photonic crystal implanted in voltage control semiconductor laser.

In 2014 [237], the authors have demonstrated modified hybrid PCF which can be useful for dispersion compensation in broadband applications covering the S, C and L bands communication bands. In this work, the proposed PCF can obtain large negative dispersion which is useful for compensation of dispersion introduced in optical transmission link. Another work [249] has shown the use of hybrid PCF for 40 Gbps optical fiber communication system to alleviate dispersion from transmission channel. The proposed hybrid PCF can be used as a dispersion compensation technique in optical fiber communication system. With its high negative dispersion coefficient of -10054 ps/nm/km, the proposed PCF can be considered pertinent for broadband dispersion compensation within E, S, C and L bands.

In 2015 [250], authors has shown 100 Gbps data transmitting over 1.15 km of low loss photonic band gap fiber and 1 km of solid core fiber. The reported results show that mode coupling to higher-order modes has resulted in minimal OSNR penalty associated with SCF and ~1-2 dB penalty associated with HC-PBGF. In another work [251], authors have shown zero dispersion PCF to minimize dispersion in optical fiber communication systems. The reported results show that the proposed PCF with its low confinement loss can be useful in sensor and communication applications. In 2016 [65], authors has shown dual core PCF for mode conversion (between LP 01 and LP 11 modes, and LP 01 and LP 21 modes). Authors from another work [143] have shown mode selective coupler based on dual core PCF for mode conversion between LP 01 and LP 11 modes. In 2017 [100], authors has reported polarization beam splitters based on dual core PCF with magnetic fluids in air holes.

Table 2.8

Key work of PCF

Year/ Journal	Experiment / Simulation	PCF type	Date Rate	Application	Medium
2013/ Taylor and Francis [64]	Simulation	Solid Core PCF	40 Gbps	Excitation of LP 01 mode	Optical Fiber
2013/ Elsevier [247]	Simulation	Modified Octagonal PCF	Not Mentioned	Dispersion Compensation	Optical Fiber
2013/ IEEE [248]	Experiment	Solid Core PCF	25 Gbps	PCF based VCSEL	Optical Fiber
2014/ Elsevier [237]	Simulation	Hybrid PCF	Not mentioned	Dispersion Compensation	Optical Fiber
2014/ Elsevier [249]	Simulation	Hybrid PCF	40 Gbps	Dispersion Compensation	Optical Fiber
2015/ OSA [250]	Simulation	Solid core Photonic bandgap fiber	100 Gbps	Dispersion Compensation	Optical Fiber
2015/ IEEE [251]	Simulation	Solid core PCF	Not mentioned	Dispersion Compensation	Optical Fiber
2016 /IEEE [65]	Simulation	Dual core PCF	Not Mentioned	Mode conversion	Optical Fiber
2016/ OSA [143]	Simulation	Spiral PCF	Not Mentioned	Dispersion compensation for X and Y polarization	Optical Fiber
2017 /IEEE [100]	Simulation	Dual core PCF	Not Mentioned	Dispersion compensation	Optical Fiber
2017/ Optik [252]	Simulation	Spiral PCF	Not Mentioned	Dispersion compensation	Optical Fiber

Another work [252] has shown spiral PCF by using an elliptical soft-glass rod in the core region to control dispersion properties. The proposed PCF features high negative dispersion ranging from -491.16 to -399.98 ps/nm/km for x and y polarizations which is useful for dispersion compensation in optical fiber communication systems. The Table 2.8 shows the adoption of PCF for dispersion compensation and mode conversion applications in optical fiber communication. Photonic crystal fibers (PCFs) are flexible for cross-section design along with properties in birefringence, dispersion, nonlinearity, and effective mode area. Moreover, PCFs perform remarkably when applied in fiber sensors, fiber lasers and nonlinear optics [73]. Thus, PCF can be adapted to MDM-based Ro-FSO system to minimize mode coupling losses due to atmospheric turbulences, particularly due to fog. Chapter 5 of this thesis is focused on the design of PCF for MDM-Ro-FSO system to mitigate the effect of mode coupling losses introduced by different severity levels of fog in the atmosphere.

2.9 Summary

This chapter provides an overview of optical communications, RoF, FSO, Ro-FSO transmission systems, MDM, OFDM and PCF. Current state-of-the-art multiplexing and modulation technologies for FSO, RoF and Ro-FSO systems in the MDM, subcarrier and intensity domains are presented. The surge of MDM experiments and simulations in the last five years demonstrate the importance of MDM in increasing the data capacity and improving the spectral efficiency in optical communications. While MDM has attracted significant attention in FSO and RoF systems, to date, there is valuable untapped potential in the application of MDM in Ro-FSO systems for mitigation of atmospheric turbulence, increasing channel diversity and enhancement of spectral efficiency. Notwithstanding the advantages, MDM in Ro-FSO suffers from fading of radio subcarriers and mode coupling losses. OFDM is aimed at mitigating

fading effects for long-haul communications whereas SC-PCF is proposed for mitigating mode coupling losses for short-haul communications. This gap presents a valuable niche area for this research.

CHAPTER THREE
RESEARCH METHODOLOGY

3.1 Research Framework

This chapter aims to address the methodology adapted to carry out this research. It explicates a research framework based on the Design Research Methodology (DRM) in order to explain the approaches and steps adopted to achieve the objectives of this research. DRM is an approach and a set of methods used collectively as a framework proposed by Luicienne Blessing and Amaresh Chakrabarty [253] to conduct effective and efficient design research. It is widely adopted by researchers for obtaining adequate and realistic research outcomes [254]. DRM can be divided into four different stages: 1) Research Clarification (RC), 2) Descriptive Study (DS), 3) Prescriptive Study (PS), and 4) Descriptive Study II (DS-II). The research framework for the current study is broadly categorized into four stages in relation to the four stages of DRM where the main methods and deliverables of each stage will be highlighted. Figure 3.1 describe the various stages in the research approach of the current study and the respective outcomes of each stage:

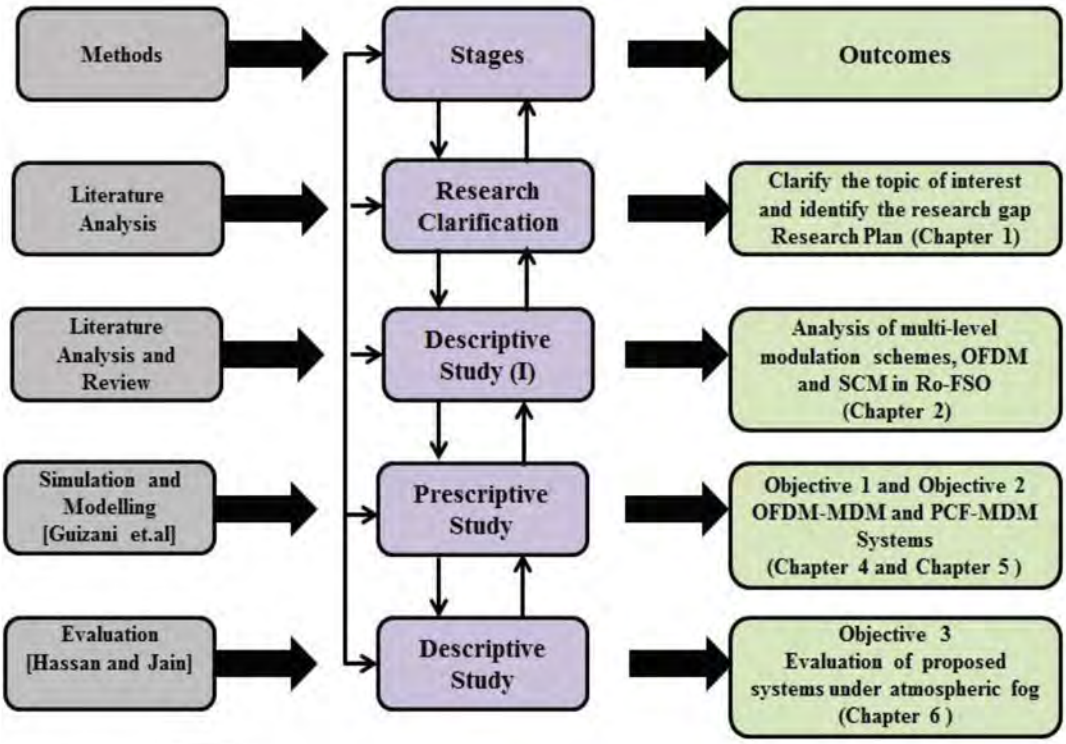

Figure 3.1. Research Approach

3.1.1 Stage 1: Research Clarification

This is the initial stage of the research which aims at providing a comprehensive understanding of the topic as well as deriving an overall research plan along with the following steps:

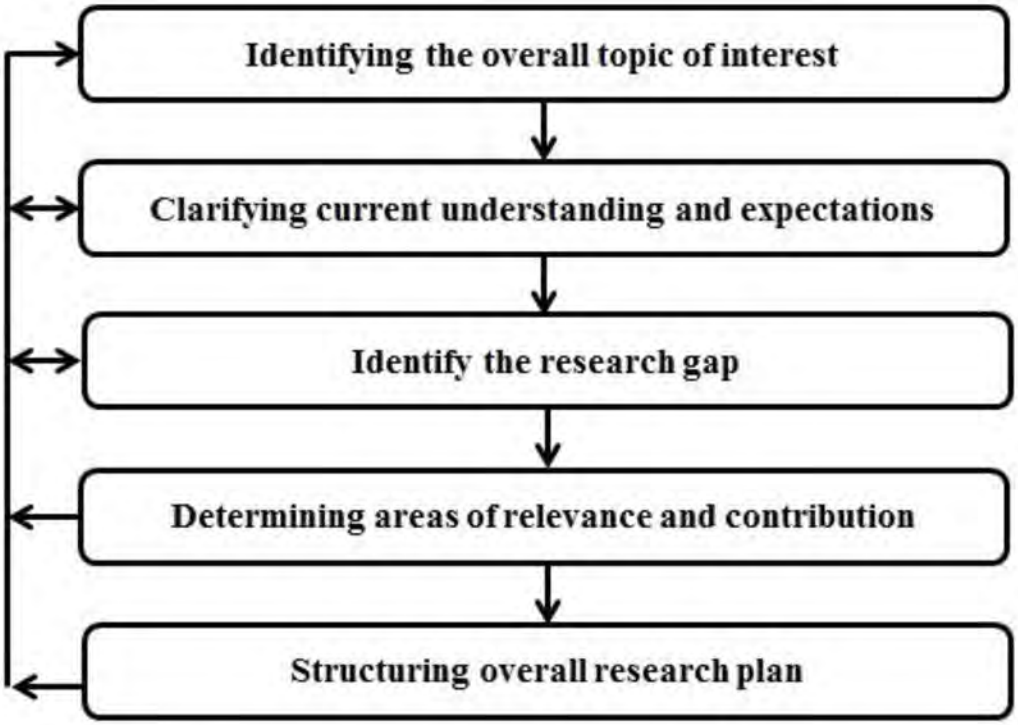

Figure 3.2. Research Clarification

Deliverables of this stage include the following:

- Research motivation
- Research problem
- Research questions
- Research objectives
- Research scope
- Areas of research contribution

3.1.2 Stage 2: Descriptive Study I (DS-I)

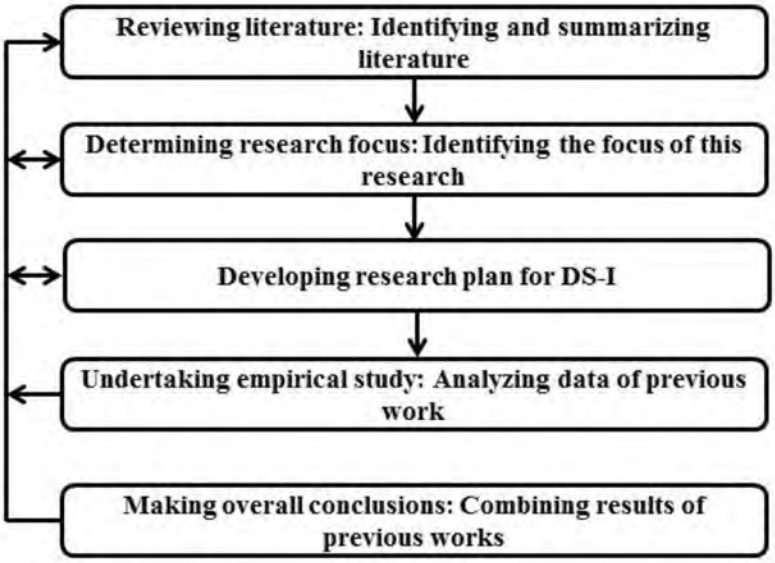

Figure 3.3. Main Steps in the Descriptive Study-I Stage

This stage aims at providing a critical review of the literature and empirical studies in the research area with a view to understand the existing solutions and directions along with the steps as shown in Figure. 3.3.

Outcomes of this stage include the following:

- Overview of RoF and FSO technologies.
- Critical review of previous works on RoF and FSO systems.
- Ro-FSO technology and its applications.
- Critical review of previous works on RoF and FSO systems.
- Analysis of multi-level modulation schemes, OFDM and SCM in Ro-FSO.
- Overview of MDM scheme.
- Overview of OFDM and PCF.

3.1.3 Stage 3 – Prescriptive Study (PS)

This stage aims at providing the design of the proposed mechanisms based on simulation and network modelling processes proposed by Guizani et al. [255]. The first part of this stage involves the design of an OFDM-MDM scheme for Ro-FSO long haul communication systems, based on the analysis of multi-level modulation schemes – OFDM and SCM.

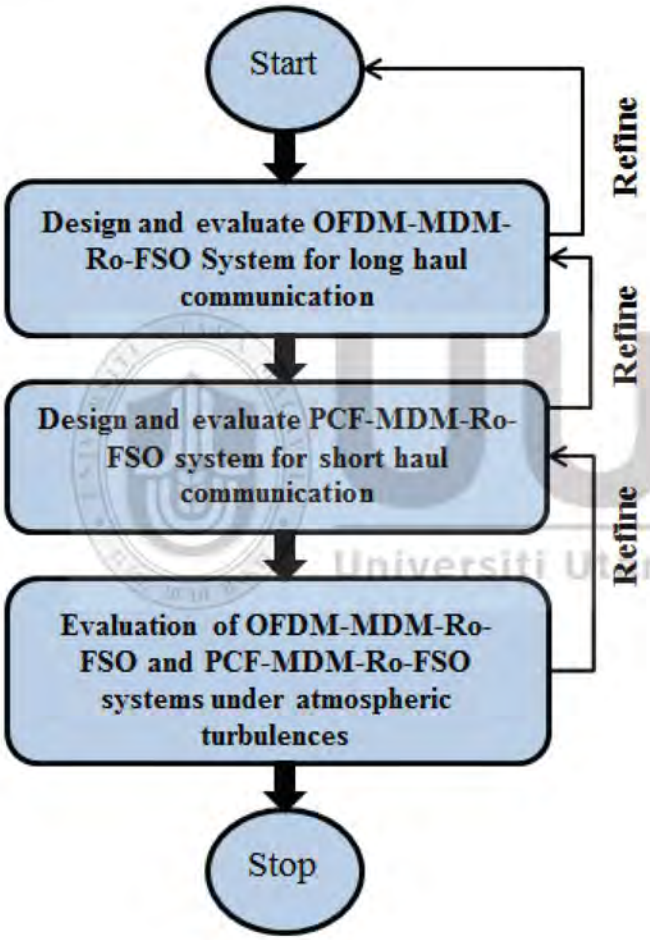

Figure 3.4. Main Steps in Prescriptive Study

This is followed by the evaluation of the performance of OFDM-MDM-Ro-FSO system under atmospheric turbulences, particularly different condition of fog. The second part of this stage involves the design of a PCF-MDM scheme for Ro-FSO short haul communication system. This is again followed by the evaluation of

performance of PCF-MDM-Ro-FSO system under atmospheric turbulences, particularly different condition of fog, as shown in Figure 3.4.

Deliverables of this stage include the following:

• Design and implementation of OFDM-MDM based Ro-FSO system for long haul communication (Chapters 4- Objective 1)

• Design PCF based equalization scheme for MDM-Ro-FSO system for short haul communication (Chapter 5-Objective 2)

• Validation of the proposed mechanisms and parameters (By comparing simulation results with previous works)

3.1.3.1 Approaches for designing and development of OFDM-MDM-Ro-FSO and PCF-MDM-Ro-FSO System

The designing and development process is an essential factor in any research in the field of communication system. It is crucial for the researcher to specify an approach for these processes. The prominent approaches for designing optical communication systems are: mathematical modeling, and simulation and real test beds [256] as summarized in Figure 3.5.

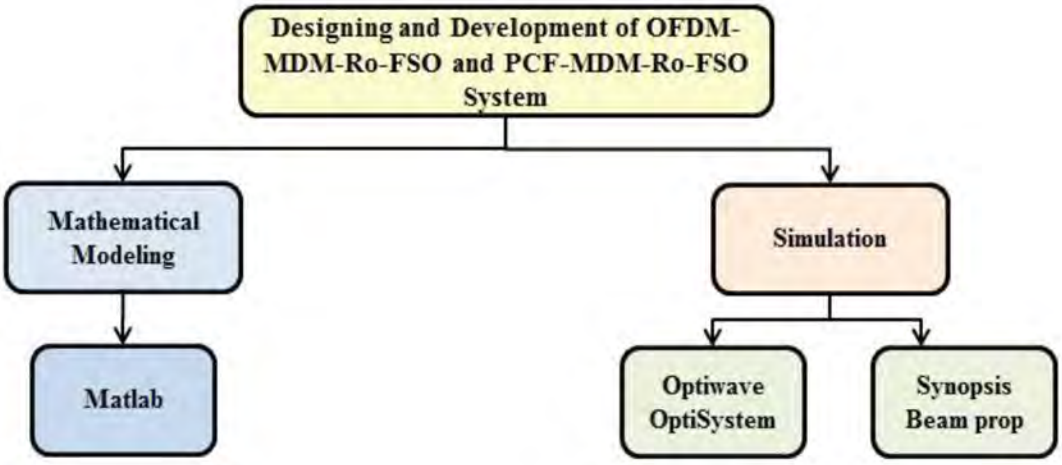

Figure 3.5. Design processes of OFDM-MDM-Ro-FSO and PCF-MDM-Ro-FSO System

The tools which are used for designing and development of OFDM-MDM-Ro-FSO and PCF-MDM-RO-FSO systems have been highlighted in Figure 3.5.

3.1.3.2 Mathematical Modeling

Mathematical modeling is an approach that is used to describe the changes in a system by means of a mathematical or analytical function with a set of equations. Analytical modeling is considered to be an appropriate model for dealing with simple systems but challenging for complicated systems which involve major simplifications and assumptions [257]. Mathematical modeling uses a set of solvable, derivable equation to model a system. Therefore, modeling a complex system is not advisable due to the lack of environmental interaction and circumstantial parameter settings which may significantly alter the outcomes. A Ro-FSO communications system is rather complex. Hence, too many simplifications and assumptions will affect the accuracy of the representation of the real communication system [258, 259].

3.1.3.3 Simulation

A simulation is an imitation of the real word, in particular, imitation of a real system or process which gives the ability to understand the things around us through creativity and imagination using simulators software [257]. With a view to evaluate real-world performance of a real system, simulations allow us to examine the system's behavior under different scenarios in order to find out and understand how the system design works best. Communication systems are complex to be modeled in a real world. Their modeling involves undertaking many assumptions, the best of which is to perform the "what if" technique. The best environment for its performance is simulation modeling. Through specific simulation, software system models can be designed, analyzed, and evaluated easily. Simulation enables modifications and

changes in certain parts of the system so that it can be re-corrected if there is a mistake or reevaluated as per the user's requirements. Simulation modeling has proven its credibility and used frequently in communications [259]. In this research, OptiSystem from Optiwave company and BeamPROP from Synopsis (previously R-Soft) company are used for design and development of the proposed MDM based Ro-FSO communications model.

3.1.3.4 OptiSystem Simulation

The complexity of an optical communications system is rapidly evolving. The configuration and examination of these optical communication systems, which typically incorporates nonlinear devices and non-Gaussian noise sources, are very intricate and greatly time-consuming. OptiSystem is powerful software from Optiwave Corporation [260] which is used to simulate optical communication systems at the physical layer. The latest version of this software is OptiSystem V-14 [261]. It is a stand-alone item that does not depend on other recreation structures but may integrate with Matlab and other software from the Optiwave Corporation.

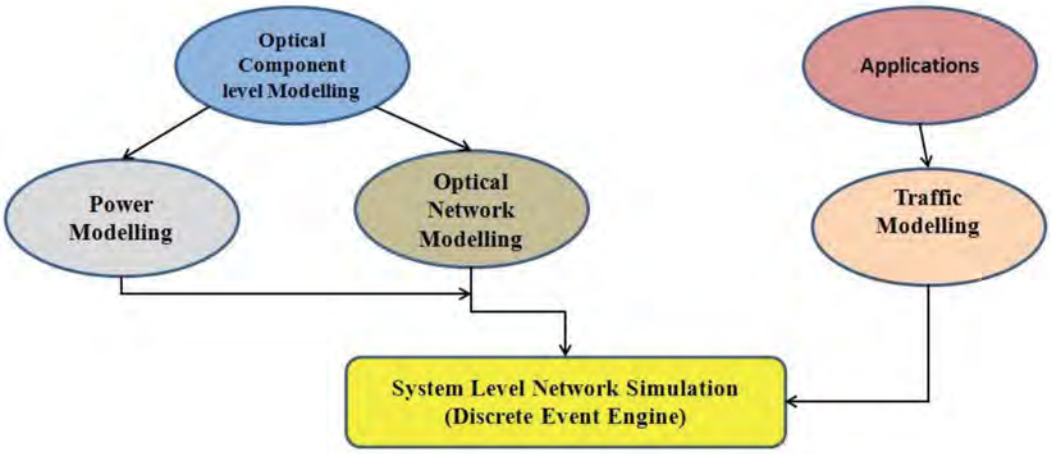

Figure 3.6. OptiSystem Methodology

OptiSystem has an extensive library of lasers, channels and photodetectors which may be individually customized. OptiSystem has a discrete event engine and offers a practical framework for performing different scenarios in an optical communication system as shown in Figure 3.6.

3.1.3.5 BeamPROP

BeamPROP™ [262] is a powerful and easy-to-use software system, provided by Synopsis company, developed to create designs in integrated and fiber optical waveguides. The beam propagation method (BPM) is a method used to simulate the passage of light via any wave-guiding medium. The software configures different simulations in order to develop waveguide devices. The graphical project layout of BeamPRO™ contains a number of toolbars and menu options, including waveguide primitives (the waveguide blocks), editing and manipulation tools, and special layout regions, which are used to design photonic devices. This software allows 3D geometry and material information representing photonic component, as for example a fiber device, to be described within one flexible and integrated tool. From this tool, the appropriate simulation methodology can then be selected and employed to readily analyze a wide variety of problems. This tool is used for designing and development of PCF.

3.1.4 Stage 4: Descriptive Study (DS)

This stage includes evaluation of proposed OFDM-MDM-Ro-FSO and PCF-MDM-Ro-FSO systems under the clear weather conditions as well as under the influence of different atmospheric conditions such as light fog, medium fog and heavy fog.

Deliverable of this stage includes the following:

- Evaluate the performance of OFDM-MDM-Ro-FSO system under clear weather conditions (Objective 1- Chapter 4).
- Evaluate the performance of OFDM-MDM-Ro-FSO system under different atmospheric fog conditions (Objective 3-Chapter 4).
- Evaluate the performance of PCF-MDM-Ro-FSO system under clear weather conditions (Objective 2-Chapter 5).
- Evaluate the performance of PCF-MDM-Ro-FSO system under clear weather conditions (Objective 3-Chapter 5).

3.1.4.1 Evaluation Metrics

In optical communications, selection of metrics plays a very important role in the evaluation of optical communication systems. In order to fulfill the objectives described in Chapter 1, the following metrics are selected based on their frequency of use and analysis adopted by many researchers as described in Table 2.1, Table 2.2 and Table 2.3.

1. **Signal to Noise Ratio (SNR):** SNR is defined as the ratio of signal power to the noise power. The higher the SNR, lower the noise power received at the output electrical signal. The minimum acceptable SNR for optical communication systems is 20 dB.
2. **Constellations**: In advanced modulation formats such as digital modulations like M-ary modulation scheme, constellations are used to determine the error received in the phase vector of output signal. Figure 3.7 shows the constellations of 4 QAM modulation format.

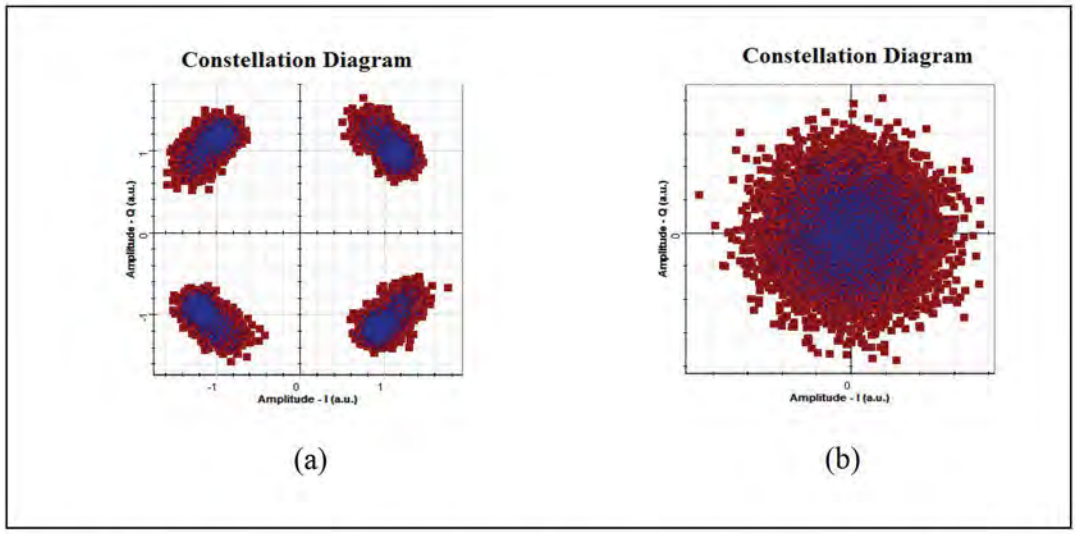

Figure 3.7. Constellations (a) Clear Constellation and (b) Distorted Constellation

3. **Total Received Power:** The total received power is defined as amount of power received at output of photo-detector. The higher the total received power, the higher the value of signal power and vice versa.
4. **Spatial Transverse Electric Field of Modes:** The spatial profile of modes deciphers information about the degradation of the modal profile and power coupling into other modes.
5. **Eye Diagrams:** Eye diagram is used for measuring the performance of optical communication networks. If receiving eye is open and clear, it means bit error rate is low whereas if receiving eye is distorted and closed, it means bit error rate is very high. In short, clear and open eye indicates good performance whereas distorted and closed eye indicates the bad performance of optical systems. Figure 3.8 represents the good eye as well as distorted eye.

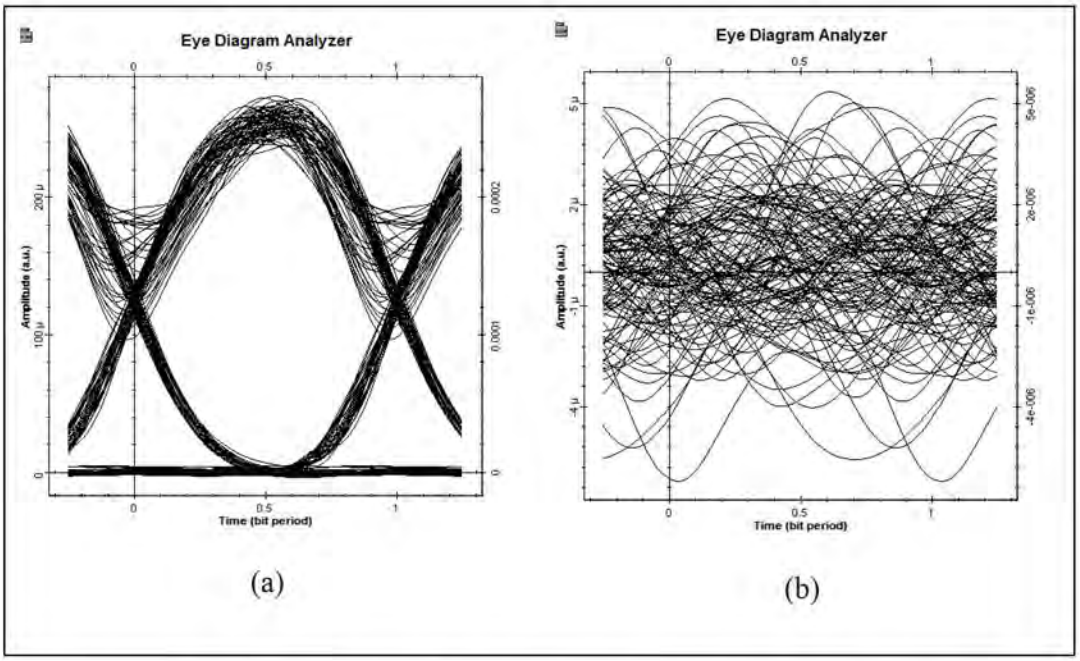

Figure 3.8. Eye Diagrams (a) Clear and open eye and (b) Distorted and closed eye

6. **Bit Error Rate:** Bit error rate (BER) is defined as error in number of received bits as compared to transmitted bits. More BER means more attenuation in transmission link whereas less BER means less attenuation in transmitted bits.
7. **Mode Spectrum:** Mode spectrum represents relative power in dominant mode.

3.2 Summary

This chapter is focused on determining an appropriate research methodology to ensure that all research objectives in Chapter 1 are successfully achieved. The extensive research methodology used for this research is divided into four stages. Stage 1 includes a comprehensive understanding of the topic pertaining to Ro-FSO systems in order to identify the problem statement. It attempts to derive an overall research plan. Stage 2 describes a critical review of the literature and empirical studies in the optical communication systems with a view to understand the existing solutions and directions of Ro-FSO systems. Stage 3 involves the design and development of

OFDM-MDM-Ro-FSO and PCF-MDM-Ro-FSO transmission systems. Stage 4 includes evaluation of performance of both systems, by using appropriate evaluation metrics, under clear weather as well as under the effect of different atmospheric fog conditions.

CHAPTER FOUR
OFDM-MDM-RO-FSO TRANSMISSION SYSTEM

This chapter reports on the design and implementation of MDM-OFDM in a Ro-FSO system long haul communication.

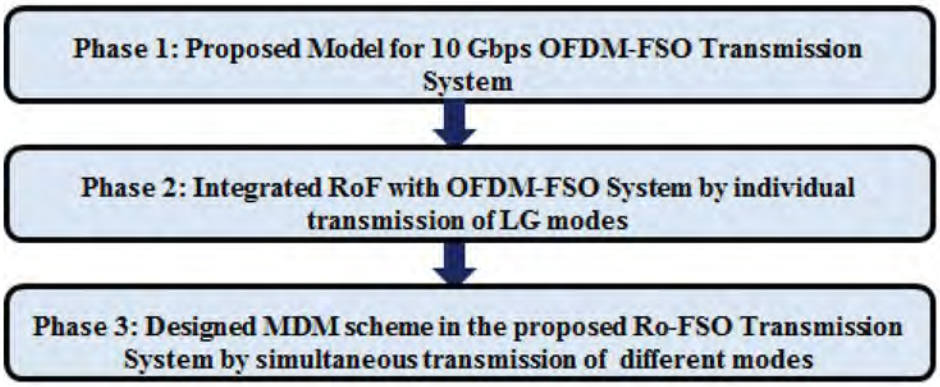

Figure 4.1. Phases of Ro-FSO Transmission System

The preliminary work on Ro-FSO is divided into three phases, as shown in Figure 4.1. Phase 1 presents a model for data transmission based on OFDM for an FSO link under atmospheric turbulences, detailed in Section 4.1. Phase 2 encapsulates the integration of a radio subcarrier on an optical carrier in an OFDM-FSO transmission system to realize a 20 Gbps-40 GHz Ro-FSO transmission system by transmitting individual LG modes, elucidated in Section 4.2. Finally, Phase 3 focuses on the design of MDM scheme for a Ro-FSO communication system by transmitting different modes simultaneously, elucidated in Section 4.3.

4.1 Phase 1: Proposed Model for 10 Gbps OFDM-FSO Transmission System

In this phase, 4-Quadrature amplitude modulation (QAM)-OFDM based FSO transmission system is proposed which is capable of transmitting 10 Gbps of data up to 180 km under clear weather conditions. Section 4.1.1 represents simulation setup whereas Section 4.1.2 represents the result and discussion.

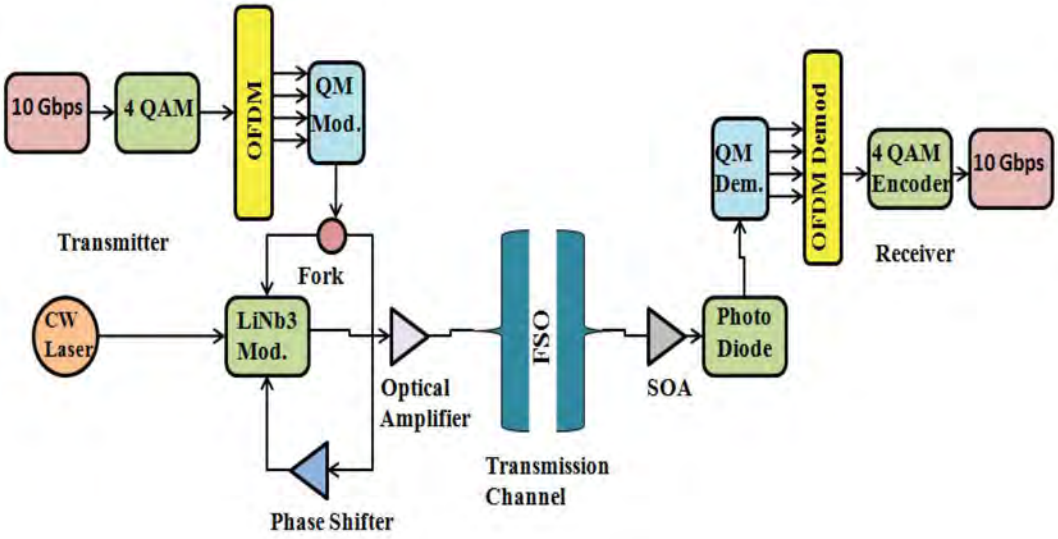

Figure 4. 2. Proposed Model for 10 Gbps FSO Transmission System

4.1.1 Simulation Setup

As shown in Figure 4.2, 4 QAM sequence generator uses 2 bits per symbol to encode 10 Gbps pseudorandom data. This encoded data is then fed to an OFDM modulator with 512 subcarriers, 1024 FFT points and 32 cyclic prefix. Quadrature modulator (QM) is used for further modulation at 7.5 GHz. The OFDM modulator has Inverse Fast Fourier Transform component (IFFT) which further includes a complex vector $X = [X_0, X_1, X_2 .... X_{N-1}]$ as input. The value of length of the vector is N, which refers to the size of the IFFT. The output of the IFFT is $x = [x_0, x_1, x_2 .... x_{N-1}]^T$. The model uses the definition of inverse discrete Fourier transform described mathematically as in [263]:

$$x_m = \frac{1}{\sqrt{N}} \sum_{k=0}^{N-1} X_k \exp(\frac{j2\pi km}{N}) \qquad \text{for } 0 \le m \le N-1 \tag{4.1}$$

where N is number of samples and k is the cycles of sinusoidal frequency.

The QM signal is optically modulated by Lithium Niobate ($LiNB_2$) using continuous wavelength laser with the power of 0 dBm. Optical single side band (OSSB) is generated by phase shift of 90^0 using phase shifter as shown in Figure 4.3.

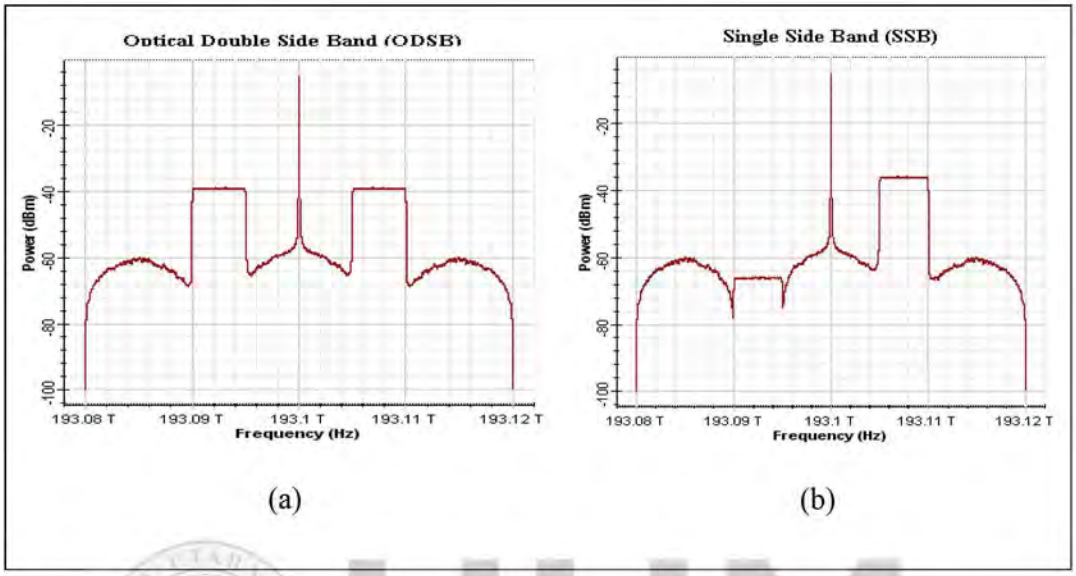

Figure 4.3. Bands generated after optical modulator (a) ODSB and (b) OSSB

The optical signal is transported over an FSO Channel having a span of 200 km by incorporating flat gain erbium doped fiber amplifier (EDFA) and semiconductor amplifier (SOA) as pre and post compensation techniques.

The link equation for FSO [264] is given by following:

$$P_{\text{Received}} = P_{Transmitted} \frac{d_R^2}{(d_T + \vartheta_R)^2} 10^{-\alpha R/10} \tag{4.2}$$

In the equation 4.2, d_R defines receiver aperture diameter, d_T is the transmitter aperture diameter, θ is the beam divergence, R is the range, and α is the atmospheric attenuation. At the reception side, an Avalanche photodiode (APD) is used to detect optical signal. This signal is then fed to QM demodulator, OFDM demodulator and 4 QAM decoder for recovering the original 10 Gbps signal. At the OFDM demodulator, a forward transform is performed by the FFT on the received and sampled data where the symbols denote the following [263]:

$$Y_k = \frac{1}{\sqrt{N}} \sum_{m=0}^{N-1} y_m \exp(\frac{-j2\pi km}{N}) \quad (4.3)$$

In the equation 4.3, $y = [y_0, y_1, y_2 .... y_{N-1}]^T$ refers to the sampled time domain vector at the input of the FFT demodulator and $Y = [Y_0, Y_1, Y_2 .... Y_{N-1}]^T$ represents the discrete frequency domain vector at the output. The performance of proposed system is evaluated under varied conditions of atmospheric fog.

4.1.2 Results and Discussion

Figure 4.4 shows the measured RF spectrum at photodetector with OFDM and without OFDM. It is noted that the effect of fading is reduced with the use of OFDM as compared to without the use of OFDM. RF power is measured as -50 dBm with the use of OFDM at FSO link of 40 km whereas it drops to -90 dBm without the use of OFDM.

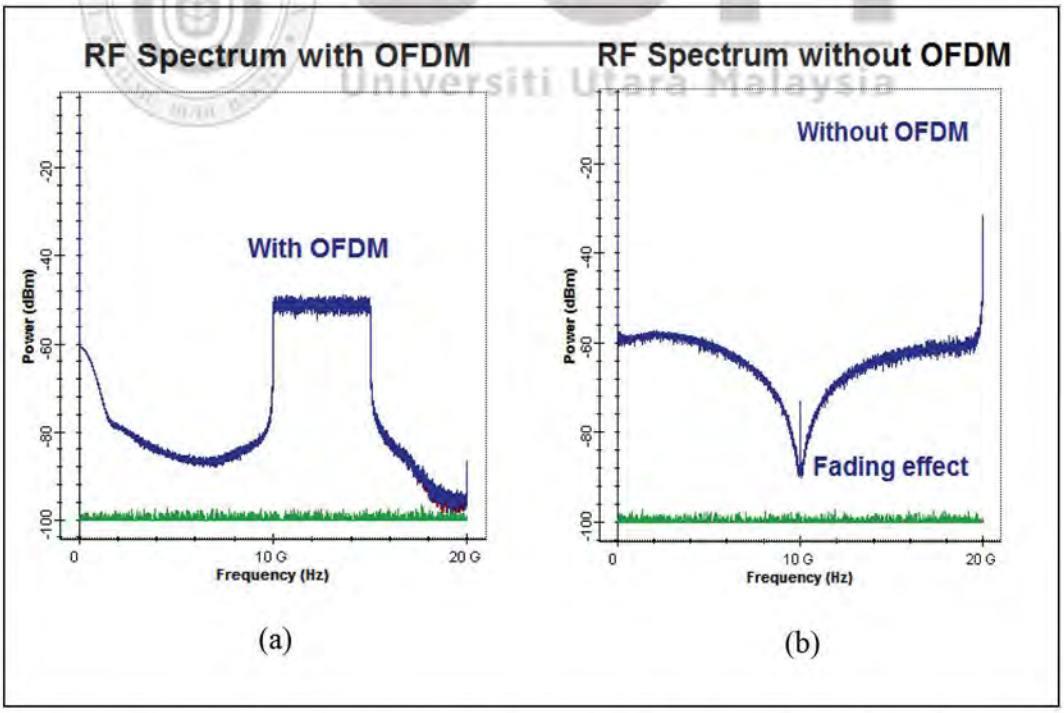

Figure 4.4. Measured RF Spectrum at 40 km FSO link (a) With OFDM and (b) Without OFDM

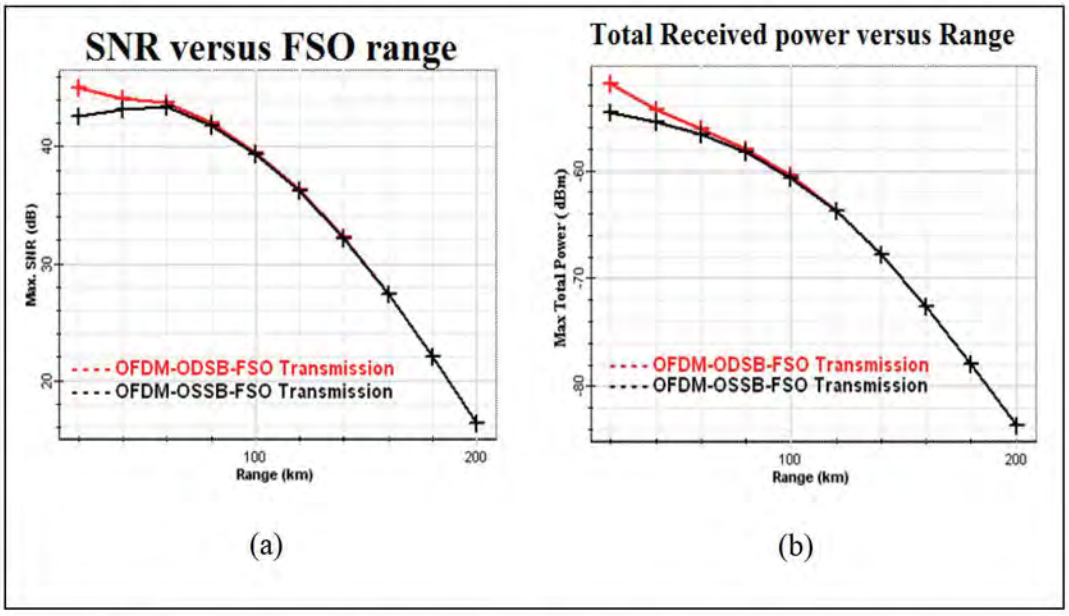

Figure 4.5. Measured (a) SNR versus Range and (b) Total Received Power versus Range under clear weather conditions

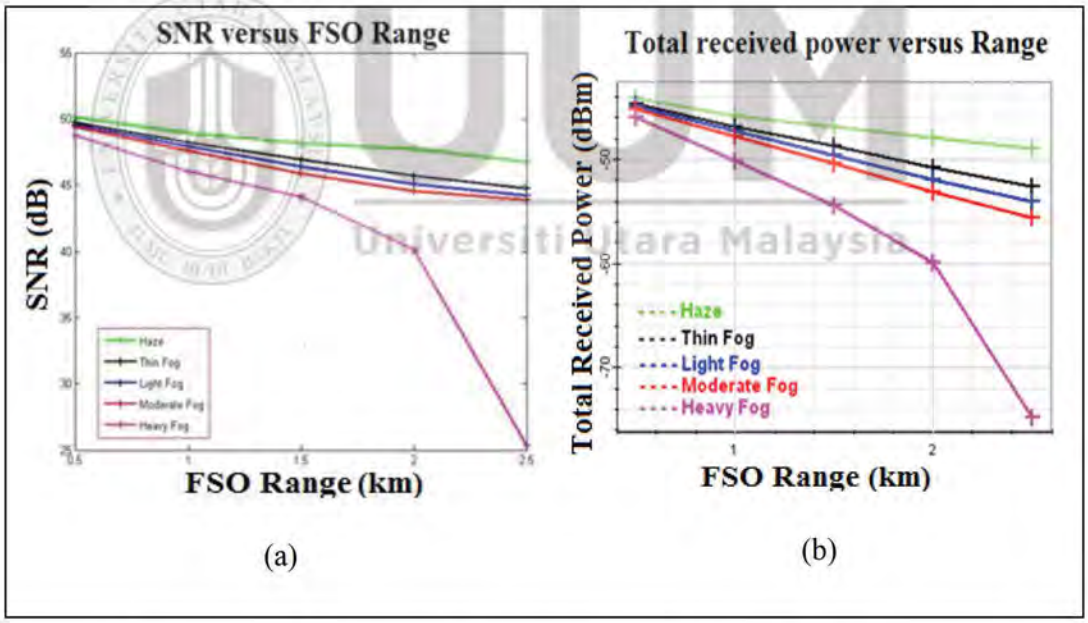

Figure 4.6. Measured Metrics (a) SNR versus Range and (b) Total Power versus Range under different atmospheric conditions.

The attenuation for clear weather condition is set to 0.14 dB/km [265, 266] . An improvement of 20 dB is noticed for ODSB modulation scheme as compared to OSSB modulation at FSO link of 40 km. After 60 km, both ODSB and OSSB modulations show similar behavior.

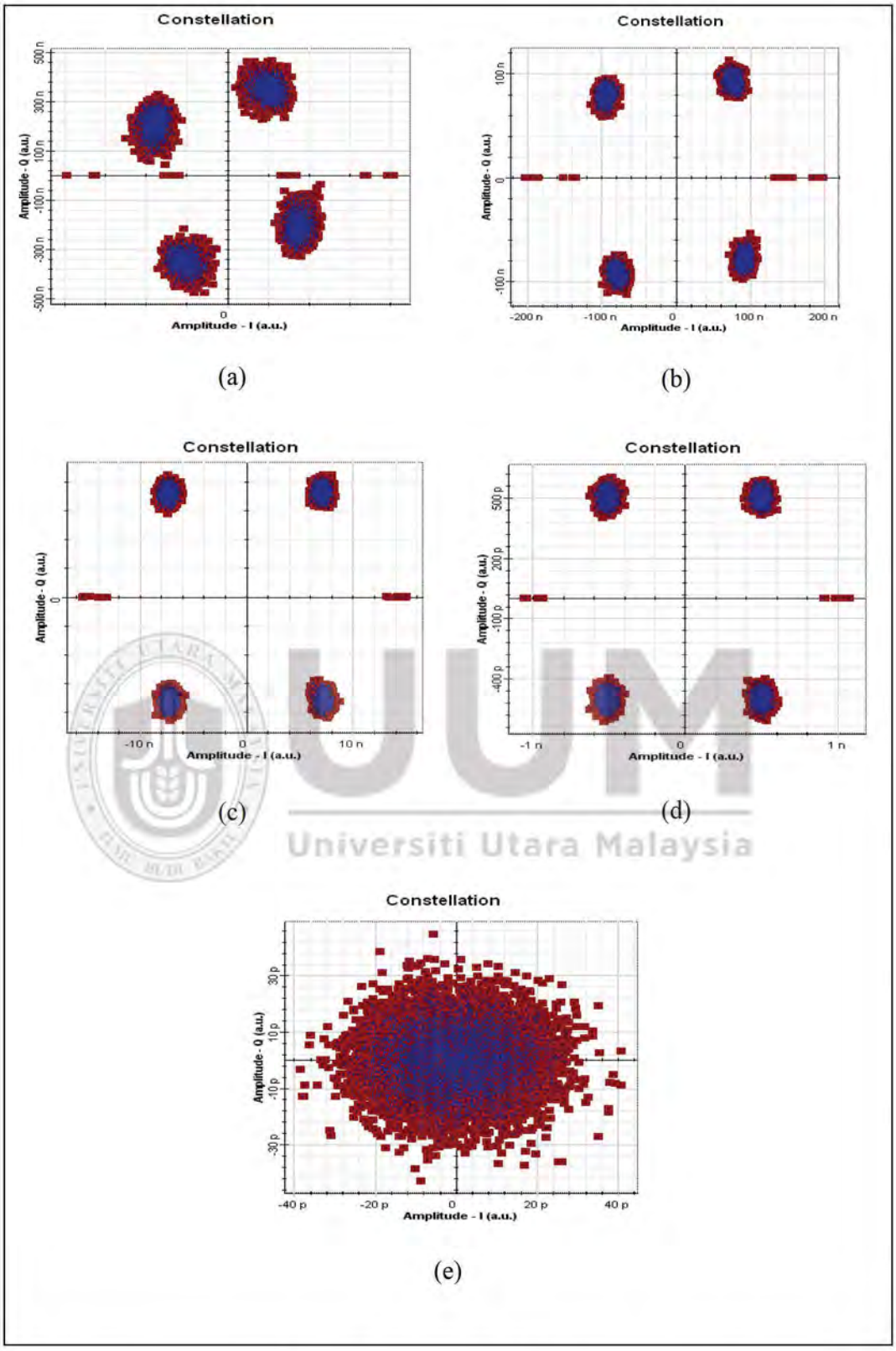

Figure 4.7. Constellation Diagram at FSO link of 3 km under different atmospheric conditions (a) Haze (b) Thin Fog (c) Light Fog (d) Moderate Fog and (e) Heavy Fog

Figure 4.6 shows SNR and total received power measured under different atmospheric weather conditions. In case of haze, attenuation for atmospheric turbulences is set to 4 dB/km. It is measured as 9 dB/km in case of thin fog, 13 dB/km in light fog, 16 dB/km in thick fog, and 22 dB/km in case of heavy fog [265, 266]. Similarly, constellations measured at receiver for different atmospheric turbulences is shown in Figure 4.7, which states that constellation becomes distorted when atmospheric conditions change from haze to heavy fog.

4.2 Phase 2: Integration with Radio Signal to Realize Ro-FSO Transmission System by Incorporating LG modes

In this phase, 40 GHz radio signal is added to 20 Gbps data and transported over FSO to realize Ro-FSO transmission system by incorporating Laguerre-Gaussian (LG) modes. Section 4.2.1 discusses simulation setup whereas Section 4.2.2 discusses results and discussion.

4.2.1 Simulation Setup

Figure 4.8 shows the simulation setup for the proposed Ro-FSO transmission system.

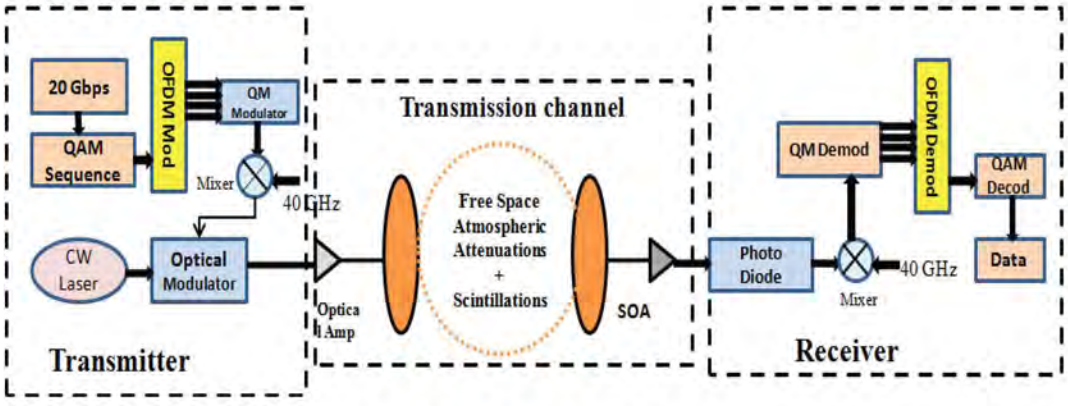

Figure 4.8. Ro-FSO Multimode Transmission System

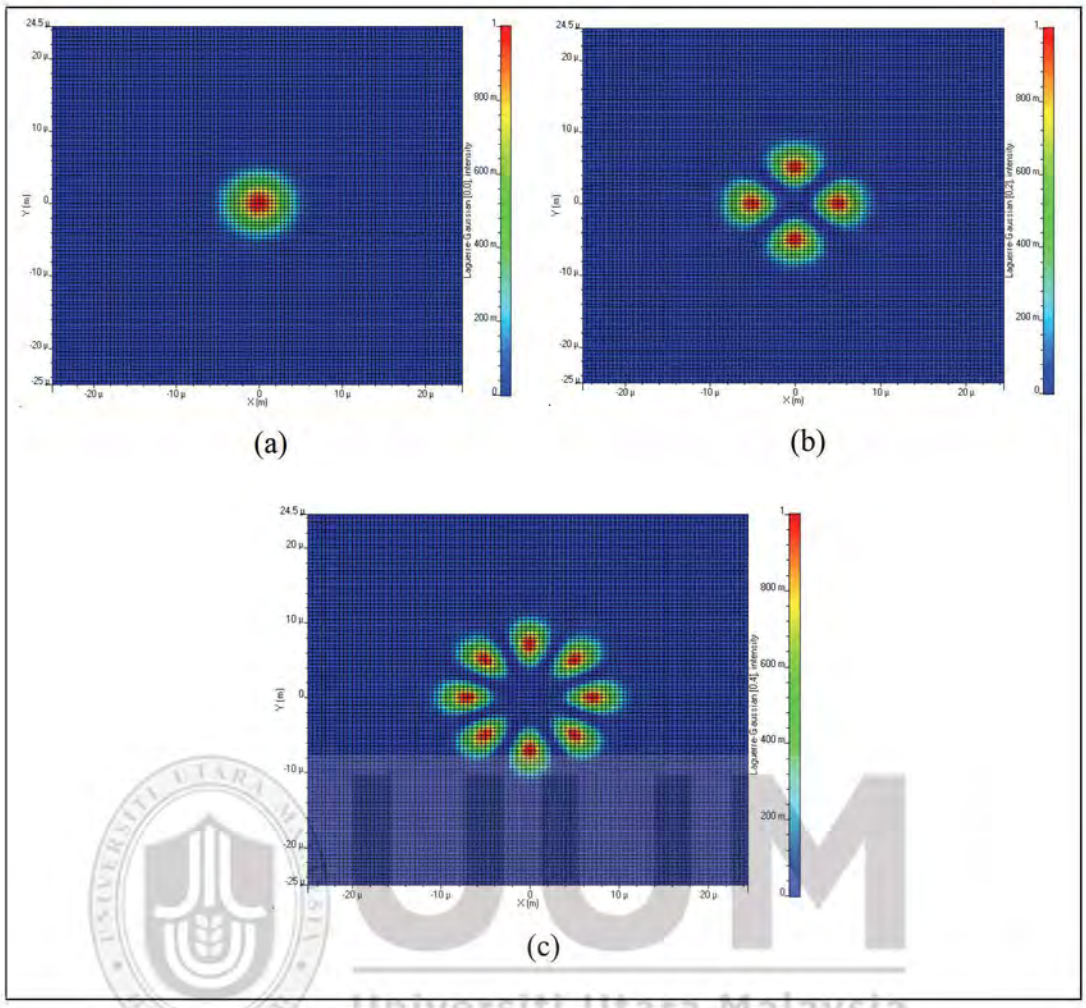

Figure 4.9. LG modes (a) LG 00 (b) LG 02 and (c) LG 04

A four-level QAM sequence generator is used to generate a 20 Gbps data stream with 2 bits per symbol which is further modulated using OFDM 512 sub-carriers and 1024 fast Fourier transform (FFT) points. These OFDM signals are again modulated at 7.5 GHz using a QM to overcome frequency-selective fading and establish a multiple-input-multiple-output system. A 40 GHz signal is modulated by the QM signal and then optically modulated by a Lithium Niobate (LiNb) modulator onto a Laguerre-Gaussian (LG) mode derived from a spatial continuous wave (CW) laser having a power of 0 dB. The transverse spatial profile of the LG mode generated using the spatial CW laser is shown in Figure 4.9. The LG mode are described mathematically [213] as

$$\psi_{m,n}(r,\varphi)=\left(\frac{2r^2}{w_o^2}\right)^{\frac{|n|}{2}} L_m^n\left(\frac{2r^2}{w_o^2}\right)\exp\left(\frac{r^2}{w_o^2}\right)\exp\left(j\frac{\pi r^2}{\lambda R_o^2}\right)\begin{Bmatrix} Sin(|n|\varphi), n\geq 0 \\ Cos(|n|\varphi), n\geq 0 \end{Bmatrix} \quad (4.4)$$

where m and n represents the X (describes the azimuthal index) and Y (describes the radial index) indexes. R refers to the radius of curvature, w_o is spot size and $L_{n,m}$ refers to the Laguerre Polynomial.

These optical signals on the LG mode are transmitted over an FSO link and received by the spatial avalanche photodiode (APD) photodetector. SOA is used for post amplification. A 40 GHz signal is again added after the photodiode for down conversion of signal. QM demodulator receives this electrical signal which is then fed to the OFDM modulator and QAM decoder for recovery of data.

4.2.2 Results and Discussion

The effective SNR and received power at receiver for LG modes LG00, LG 02 and LG 04 against FSO transmission link operating at 850 nm are measured in Figure 4.10 (a) and (b). It is clearly depicted from Figure 4.11 that LG 00 mode is less affected after transmission through the FSO link compared to LG 02 and LG 04.

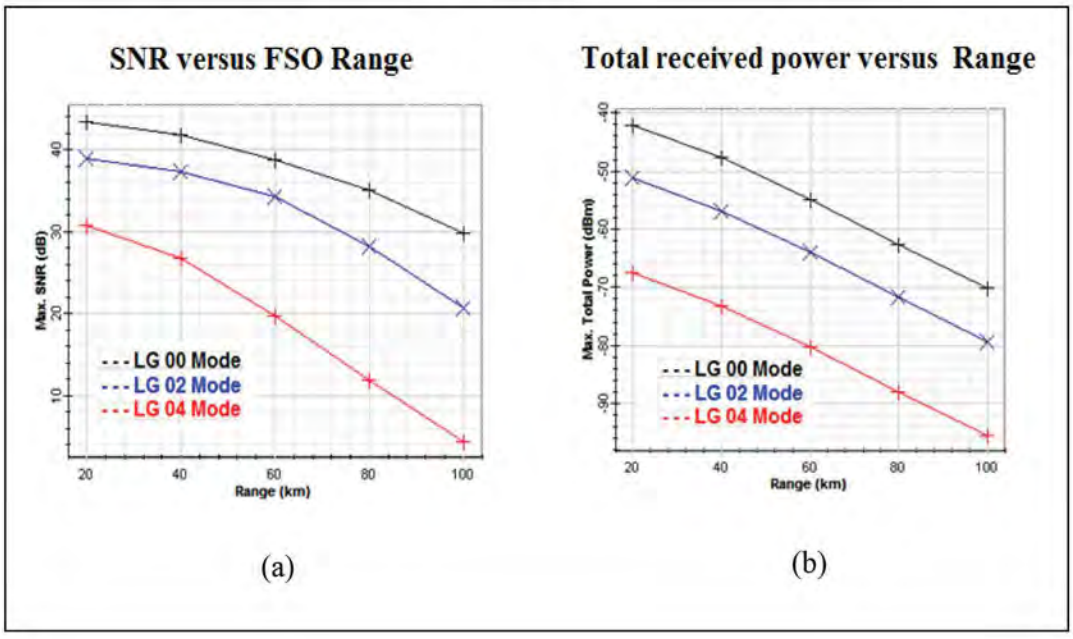

Figure 4.10. Transmission of signal through LG modes (a) SNR and (b) Total power

An improvement of 12.18 dB in SNR and -26 dBm in received power is noted in the case of transmission after 20 km over FSO link by using LG 00 mode as compared to the LG 04 mode. On the other hand, when compared to the LG 02 mode, an improvement of 4.51 dB in SNR and -9.14 dBm in received power is reported.

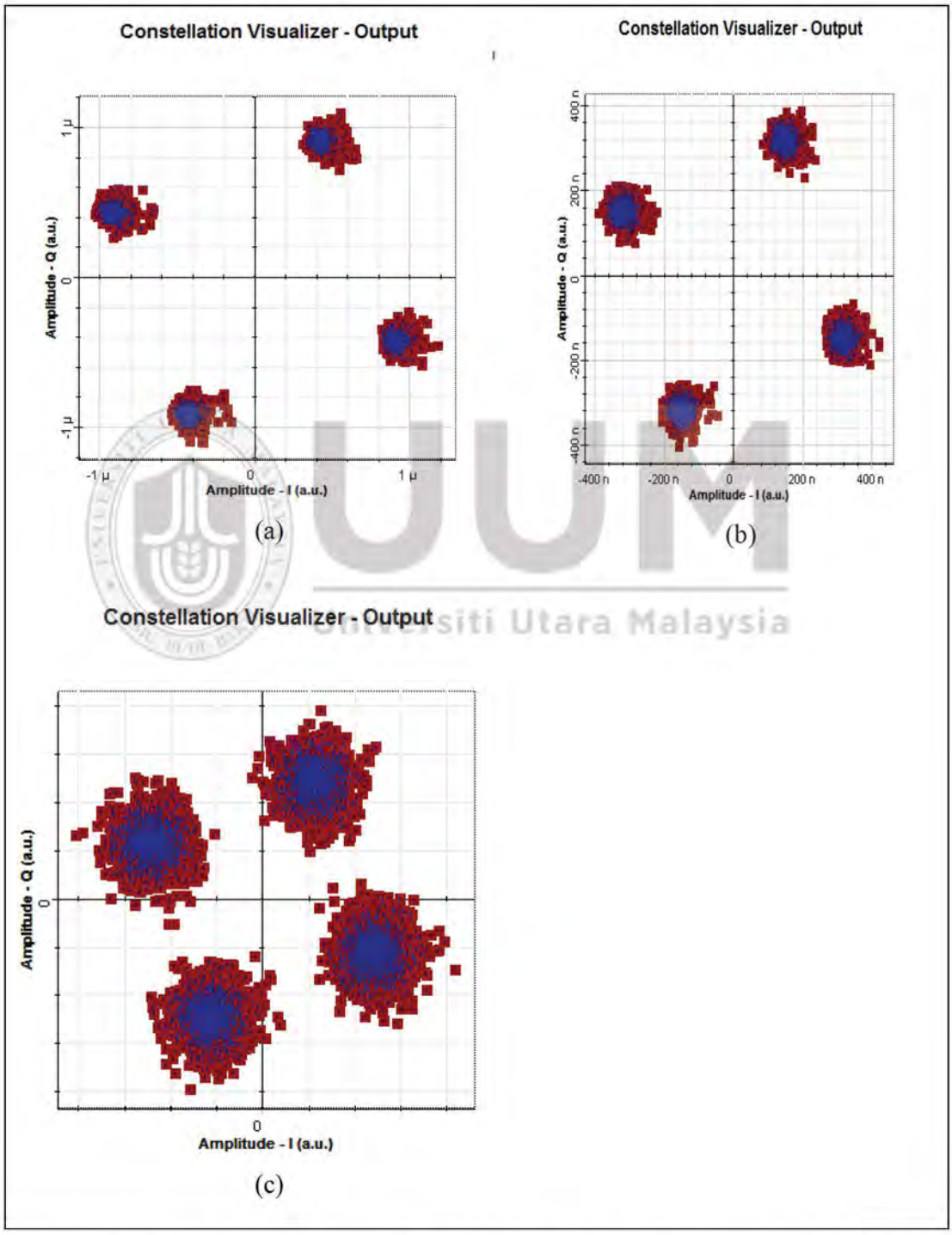

Figure 4.11. Constellation diagrams for FSO link of 100 km for (a) LG 00 (b) LG 02 (c) LG 04

Moreover, the proposed 20 Gbps-40GHz Ro-FSO transmission system prolongs the achievable distance to 100 km by using LG 00 mode as compared to LG 04 mode, which is extended to only 60 km with acceptable SNR and received power under clear weather conditions. The constellation diagrams for the LG modes after the transmission of 20 Gbps with 40 GHz radio signal through an FSO link of 100 km are shown in Figure 4.11. Figure 4.11 (a) indicates that the signal strength of transmitting signals for LG 00 mode is more precise with less noise power as compared to the signal strength of LG 02 and LG 04 modes, as shown in Figure 4.11 (b) and Figure 4.11 (c).

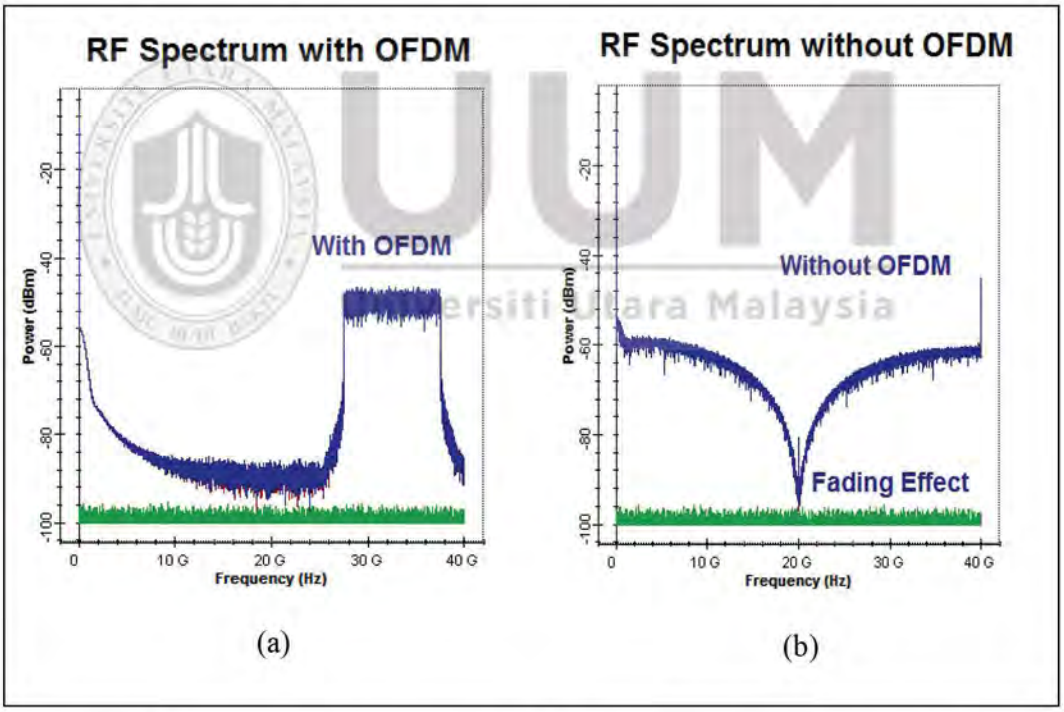

Figure 4.12. Measured RF Spectrum (a) With OFDM and (b) Without OFDM

Figure 4.12 shows the measured RF spectrum at photodetector with OFDM and without OFDM. It is noted that the effect of fading is reduced with the use of OFDM as compared to without the use of OFDM. RF power is measured as -45 dBm with the

use of OFDM at FSO link of 20 km whereas it drops to -100 dBm without the use of OFDM.

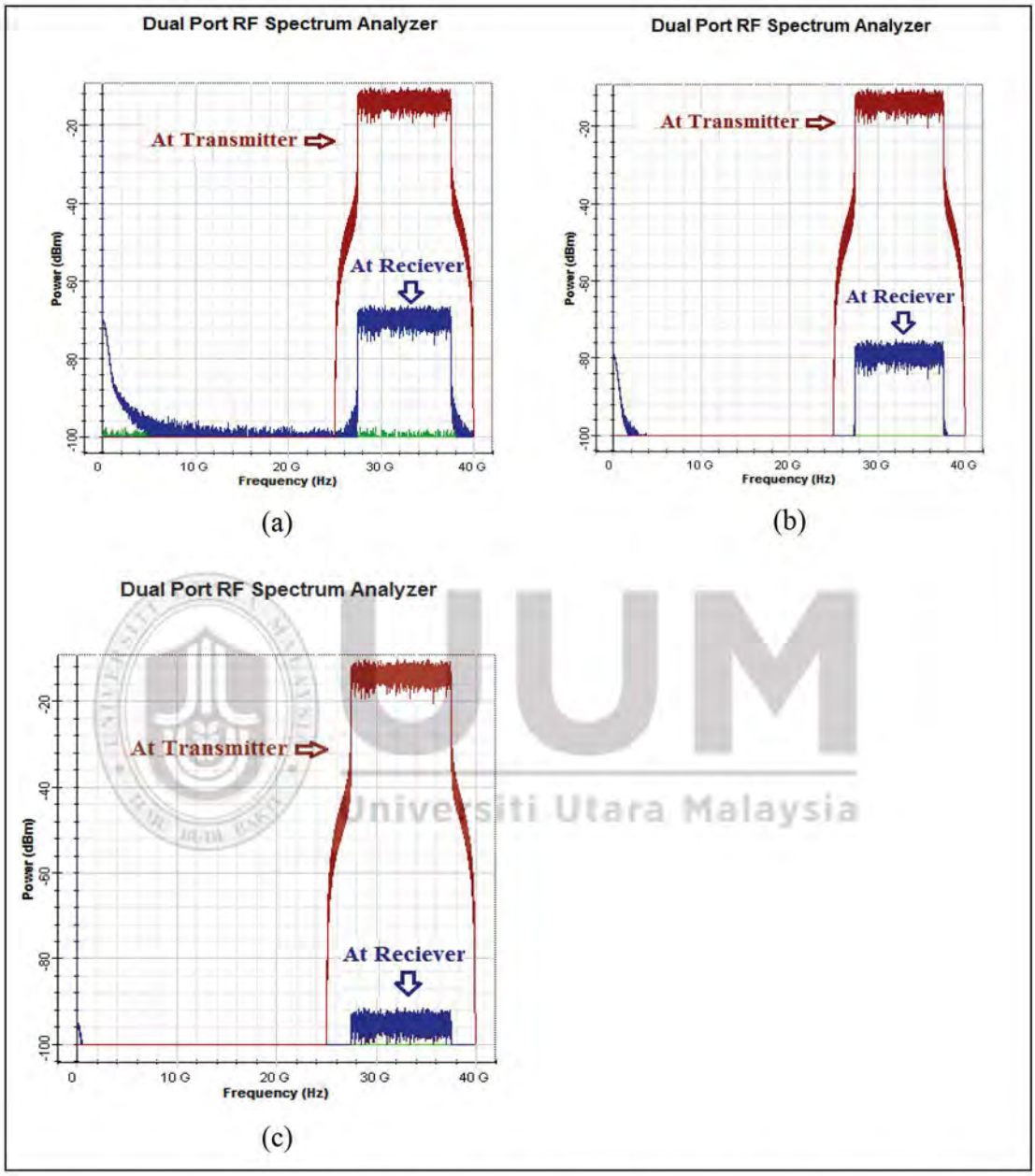

Figure 4.13. RF Spectrum for FSO link of 100 km for (a) LG 00 (b) LG 02 and (c) LG 04

Consequently, the RF spectrum of the transmitted signal as well as received signal of the proposed Ro-FSO system for LG modes is shown in Figure 4.13. The signal quality in the RF spectrum for LG 00 mode is enhanced as compared to LG 02 and LG 04 modes. As the LG modes are changed from LG 00 towards LG 04, the RF

spectrum is decreased due to escalation of noise during transmission through FSO link. Furthermore, the performance of the proposed Ro-FSO transmission system is evaluated under the effect of atmospheric turbulences in Figure 4.14.

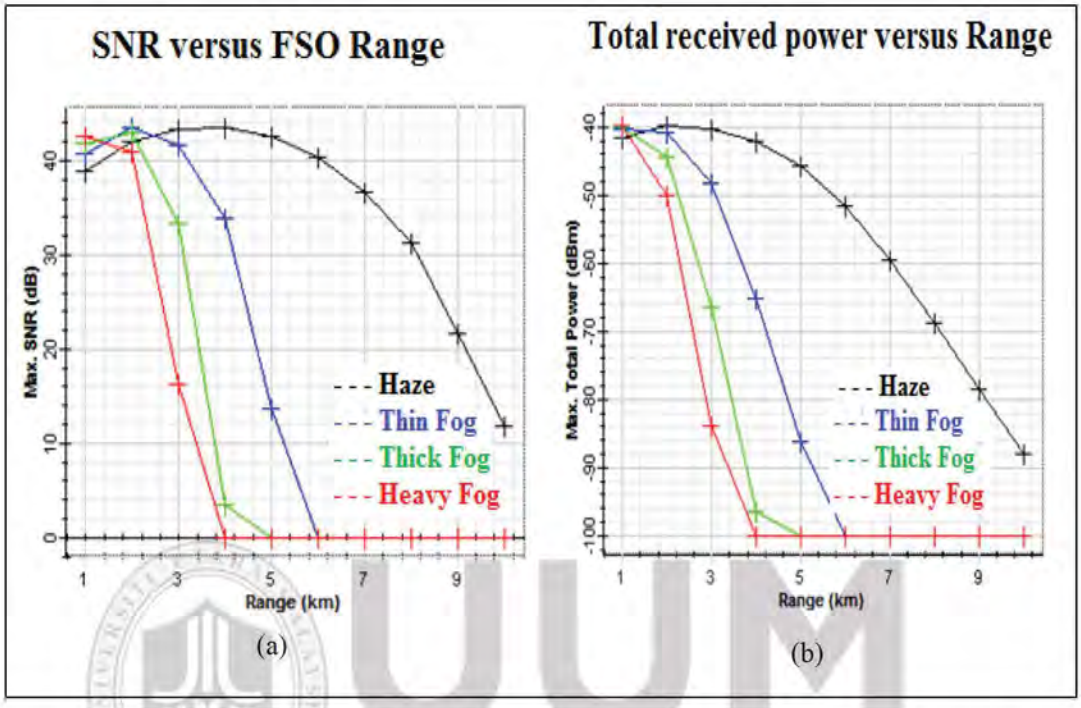

Figure 4.14. Ro-FSO system under atmospheric turbulences (a) SNR and (b) Total Power

It is reported that as the atmospheric conditions change from clear weather to turbulences, the connectivity of an FSO link decreases. The maximum achievable distances of acceptable SNR and received power are 9 km under the effect of haze, 4.9 km under thin fog, 3.4 km under thick fog, and 2.8 km under heavy fog.

In this phase, a new approach for high-speed OFDM-based Ro-FSO transmission system using LG modes for long-haul terrestrial applications is presented. For LG 00 mode and LG 02 mode, the maximum distance with acceptable BER and SNR is 100 km whereas for LG 04 mode, Channel is degraded as the maximum distance is only 60 km. Investigation of the effects of varying atmospheric turbulences reveals that the FSO link achieves a maximum distance of 9 km under haze, 4.9 km under thin fog, 3.4 km under thick fog, and 2.8 km under heavy fog respectively.

4.3 Phase 3 MDM Scheme for Ro-FSO transmission system

In this phase, MDM scheme is designed for Ro-FSO transmission system for three cases (a) LG modes (b) Hermite-Gaussian (HG) Modes (c) LG modes with vortex lens and HG mode. Section 4.3.1 discusses the simulation setup of MDM scheme by using LG modes, Section 4.3.2 discusses simulation setup of MDM scheme by using HG modes whereas Section 4.3.3 simulation setup of MDM scheme by using LG-HG modes with vortex lens.

4.3.1 Case 1: Simulation set up of MDM Scheme by using LG modes

Figure 4.15 displays a schematic diagram of the hybrid high speed Ro-FSO transmission system.

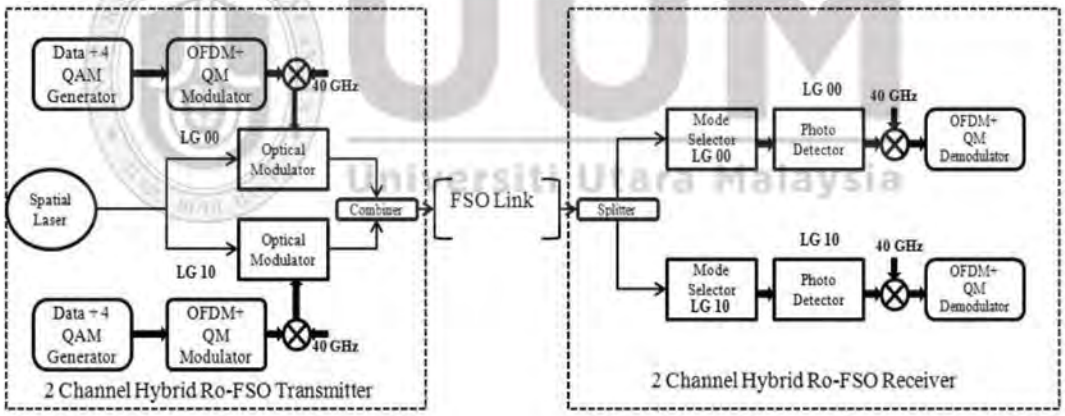

Figure 4.15. Proposed 2 ×20 Gbps Hybrid Ro-FSO Transmission System by incorporating LG modes

Two LG modes –LG 00 and LG 10 – are multiplexed through free-space. Ghatak [213] describes the transverse spatial profile of the LG mode in the source plane z = 0 as:

$$\psi_{m,n}(r,0,\vartheta)=\left(\frac{r}{w_o}\right)^m L_n^m\left(\frac{r^2}{w_o^{\,2}}\right)\exp(jm\vartheta) \tag{4.5}$$

where L_n^m refers to the associated Laguerre polynomial, n and m refer to the azimuthal and radial mode numbers respectively, $r = (x^2 + y^2)^{1/2}$ is the radius of curvature, $q = \tan^{-1}(y/x)$ and w_0 refers to the beam waist width of the fundamental Gaussian mode. A transmissive binary amplitude SLM, three lenses and a pinhole, based on [56] are used to experimentally generate the linearly polarized transverse electric field of the two LG modes. Figure 4.16 displays the construction of the mode transmitter. Encoding of a binary grating for the LG modes is achieved by a spatial light modulator through which an expanded collimated beam from the laser is directed. Its binary hologram is Fourier transformed by the first lens of focal length 300 mm.

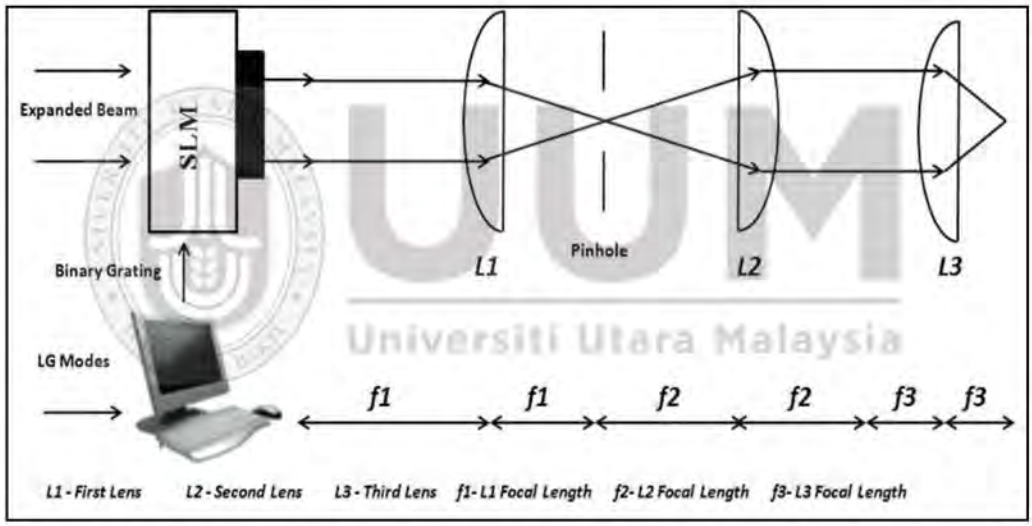

Figure 4.16. Generation of LG mode wavefront

The first diffraction order scaled by the second lens of focal length 100 mm and third lens of focal length 3 mm is retrieved by using a 0.2 mm pinhole. The modal fields are then concentrically combined while their amplitude and phase are measured and inserted into the OptiSystem™ software.

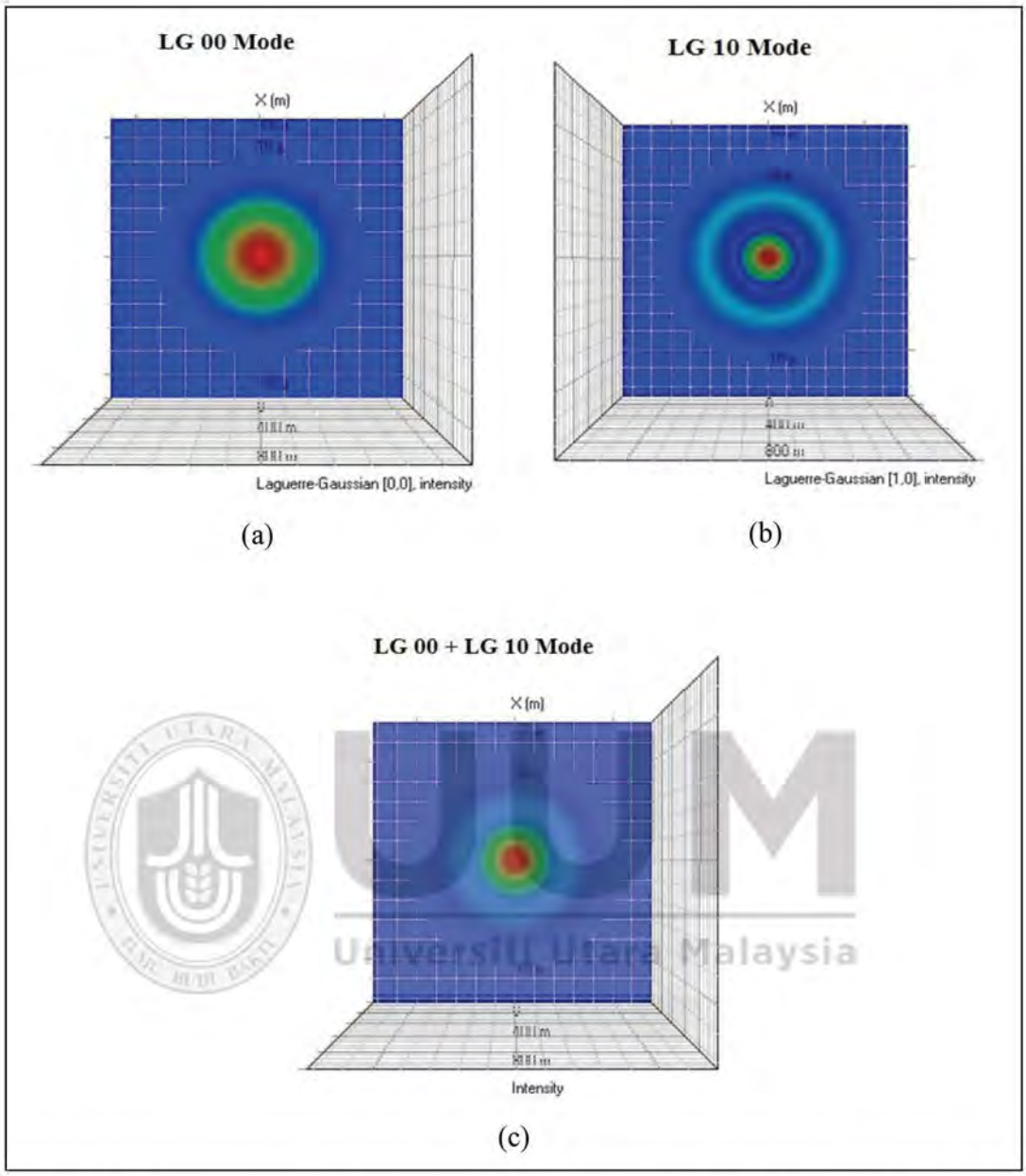

Figure 4.17. Excitation of LG modes (a) LG 00 (b) LG10 and (c) LG 00 + LG 10

Figure 4.17 (a) and 4.17 (b) display the electric field intensities of the two generated LG modes. Figure 4.17 (c) displays the electric field intensity of the combination of both modes. MATLAB and OptiSystem model the modulation and wave propagation A 4-level QAM is used to modulate two independent 40 GHz radio signals. This is followed by modulation by 512 OFDM subcarriers with a purpose to reduce the multipath fading effect incurred during the transmission through FSO link. The OFDM approach divides the data over a huge number of sub-carriers, which are

separated from each other at narrow frequencies. The OFDM signal is then modulated at 7.5 GHz by using QM.

This OFDM-QM modulated signal is further fed to a lithium niobate modulator in order to modulate the two experimental LG modes at 40 GHz with the assumption of preserving the modal stability of the two channels. The output from the two channels is transmitted over the FSO link. A Gamma-Gamma distribution is assumed under intensity scintillation [267, 268] to model atmospheric fading. The Rytov variance [267] for atmospheric scintillations is assumed. Kolmogorov theory is used to describe the atmospheric turbulence. The refractive index structure, $c_n^2 = 1\,X\,10^{-16}m^{-2/3}$ is considered for weak turbulence and $C_n^2 = 1\,X\,10^{-12}m^{-2/3}$ is considered for strong turbulence. The combined signal is then transported over the FSO link and post-amplified using a semiconductor optical amplifier (SOA). Fraunhoffer diffraction is considered for calculating the wavefield across the (x, y) receiving plane [269]:

$$U(x,y) = \frac{\exp(jkz)\exp(\frac{jk}{2z}(x^2+y^2))}{} (\int\int_{-\infty}^{\infty} U(\xi,n)\exp[-j\frac{2\pi}{\lambda z}(x\xi+yn)]d\xi dn \qquad (4.5)$$

where $U(\xi,\eta)$defines the wave field generated across the transmitting plane from the spatial light modulator, pinhole, and three lenses and z is the free-space distance. Simulation of de-multiplexing of the modes at the receiver happens in OptiSystem. A spatial photodetector is used for de-multiplexing where the LG 00 mode is extracted using an inner circular aperture of 5 cm and an outer ring aperture of 10 cm is used to extract the LG 10 mode. A 40 GHz is applied after the photodetector using a mixer in order to recover the SCM signal. Finally, the output signal after the mixer is fed to the OFDM and then the QM demodulator in order to recover the original data.

4.3.1.1 Results and Discussion

This section contains results from the simulation of the signal propagation through free-space. The two OFDM-Ro-FSO Channels are transported over the free-space link under clear weather conditions. Figure 4.18 (a) displays the value of SNR at the receiver for LG 00 Channel: it is 39.56 dB, 36.64 dB and 23.35 dB for an FSO link of 20 km, 60 km and 100 km respectively whereas for LG10, the SNR is 35.21 dB, 28.57 dB and 14.70 dB for an FSO link of 20 km, 60 km and 100 km respectively.

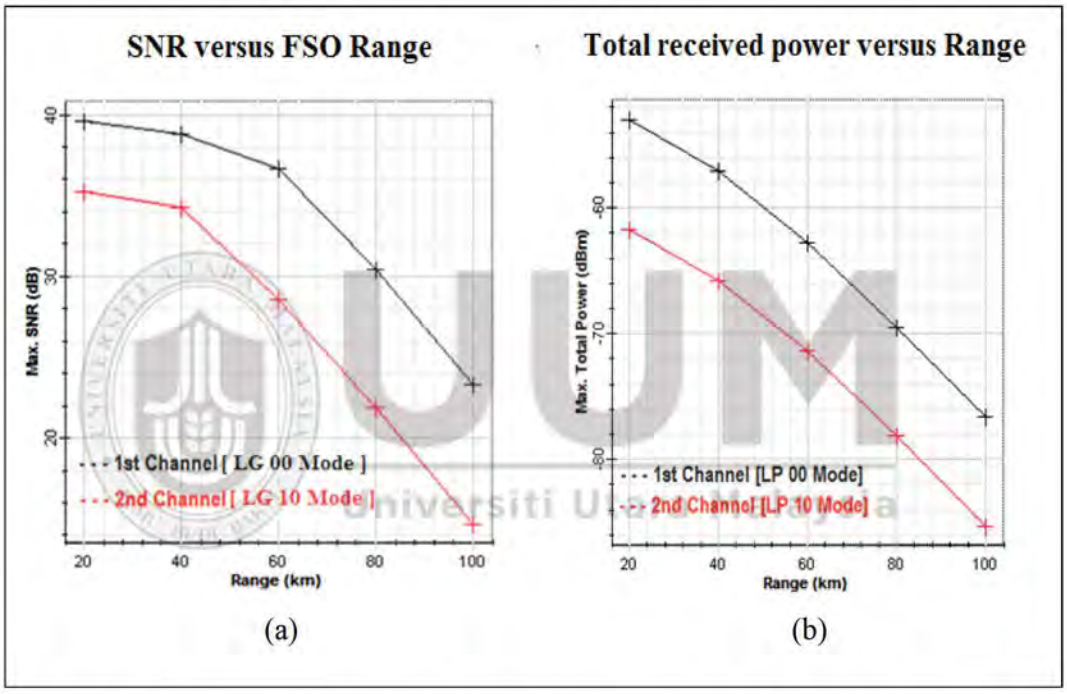

Figure 4.18. Transmission of LG 00 and LG 10 Channels (a) SNR and (b) Total Power

Figure 4.18 (b) displays that the total power received at the receiver for LG 00 mode is 53.12 dBm, -62.96 dBm and -76.65 dBm for an FSO link of 20 km, 60 km and 100 km respectively whereas for LG 10 mode, the total power is -61.67 dBm, -71.42 dBm and -85.62 dBm for an FSO link of 20 km, 60 km and 100 km respectively. This shows that under clear weather conditions the proposed Ro-FSO system will prolong to 90 km with the acceptable SNR and received power.

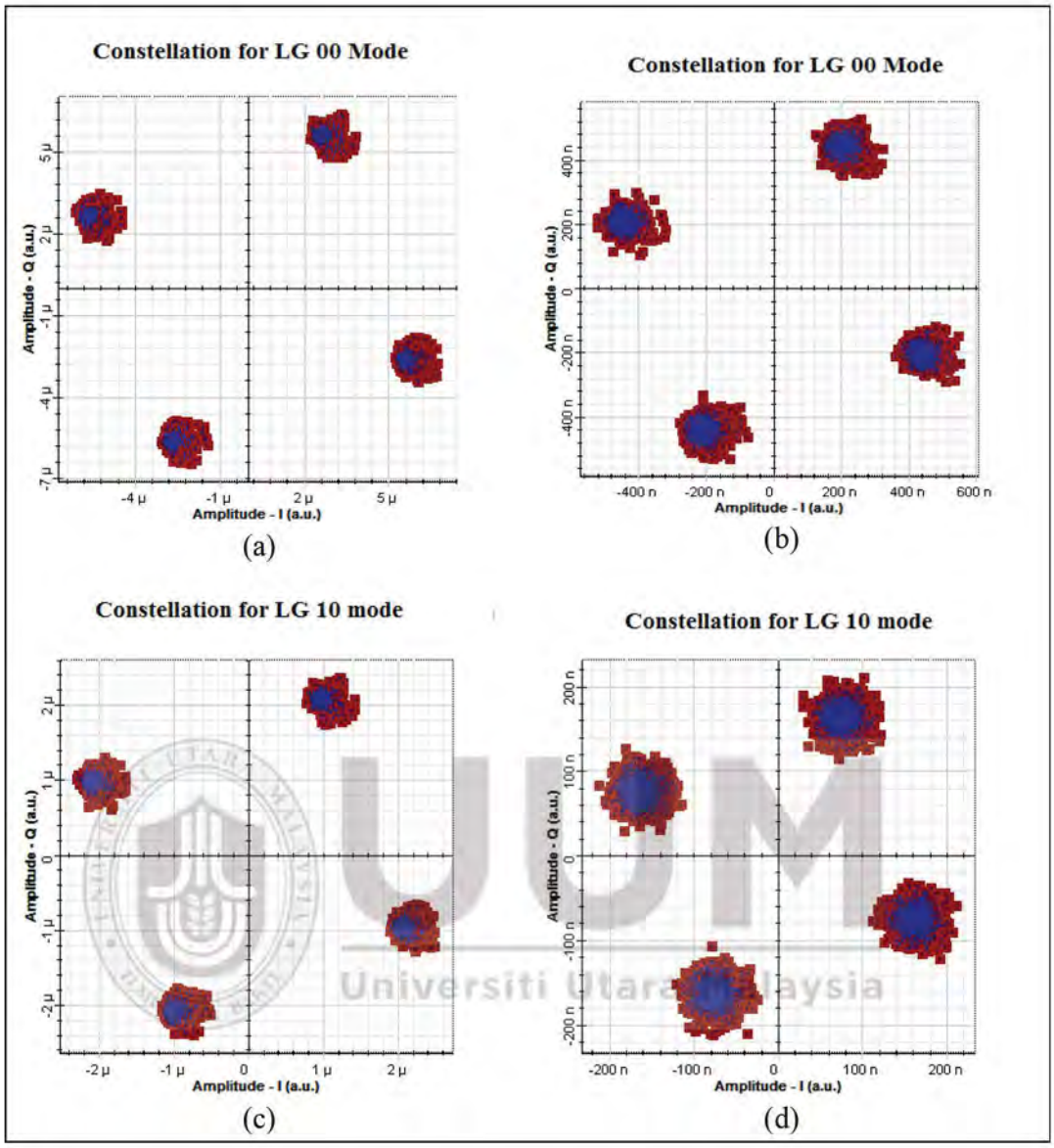

Figure 4.19. Constellations Diagram (a) LG 00 at 40 km (b) LG 00 at 100 km (c) LG 10 at 40 km and (d) LG 10 at 100 km

Figure 4.19 displays constellation diagrams of the proposed Ro-FSO transmission system under clear weather conditions which indicates that the constellation is more precise at 40 km for both Channels. However, as the link distance is increased up to a span of 100 km, the noise spectrum increases, thus distorting the constellation. The constellation for the LG 00 mode is clearer than the constellation for the LG 10 mode regardless of the distance. This happens as LG 00 collects more power than LG 10 due to higher shape distortion in LG 10 with distance.

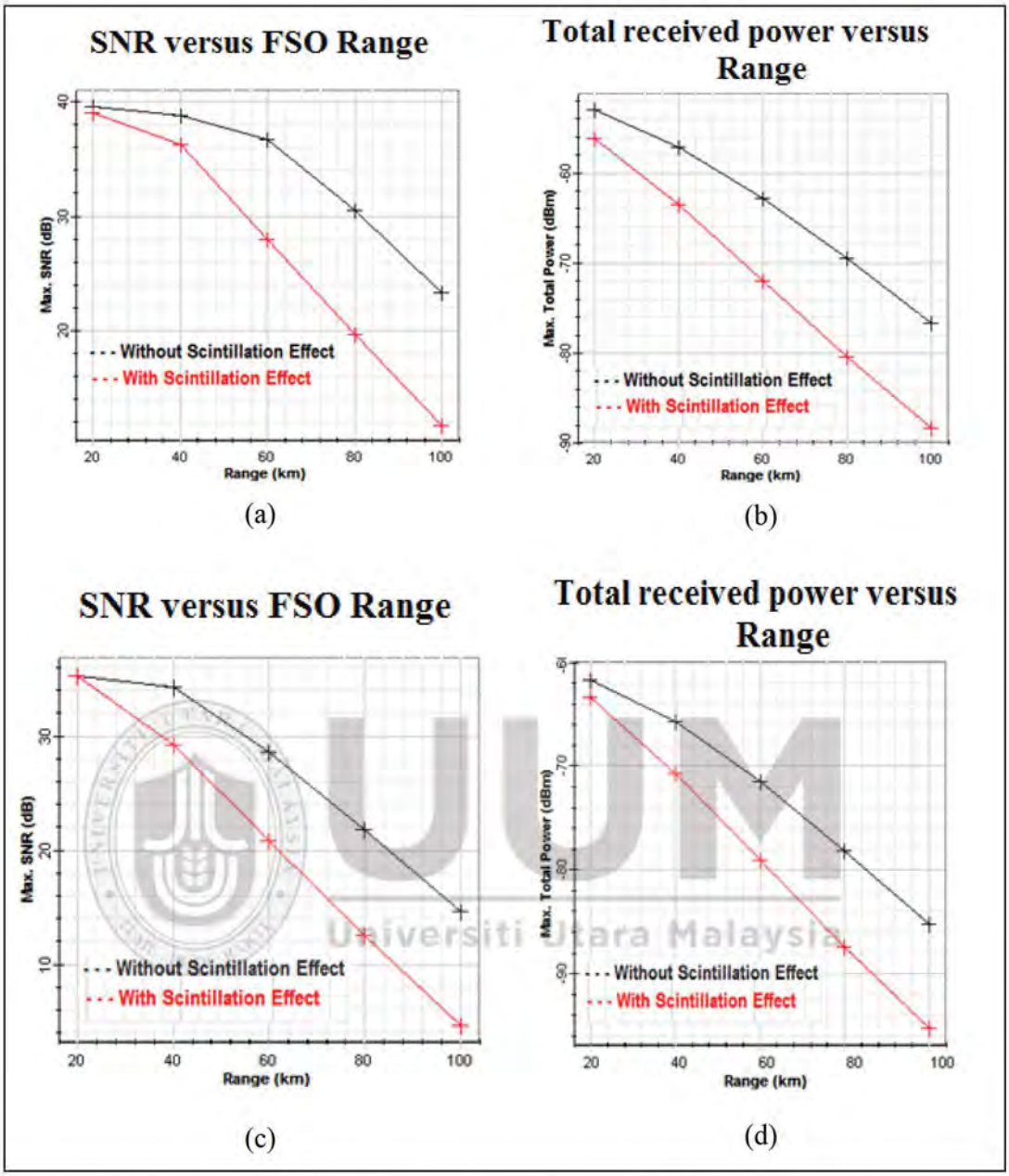

Figure 4.20. Under strong turbulences (a) SNR for LG 00 (b) Total Received Power for LG 00 (c) SNR for LG 10 and (d) Total Received Power for LG 10

Figure 4.20 calculates the effect of scintillations for the system. For a LG 00 Channel under high turbulences in the form of scintillations, degradations of 13.24 dB in SNR and -12.56 dBm in total received power are reported for a FSO length of 100 km. In case of the LG 10 Channel, degradations of 10.22 dB in SNR and -10.12 dBm in received power are reported at the same FSO length. This indicates that the proposed Ro-FSO system can extend up to 60 km under the effect of strong turbulences

together with acceptable SNR and received power.

4.3.2 Case 2 Simulation set up of MDM Scheme by using HG modes

The proposed OFDM-Ro-FSO transmission system with propagating HG modes is illustrated in Figure 4.21.

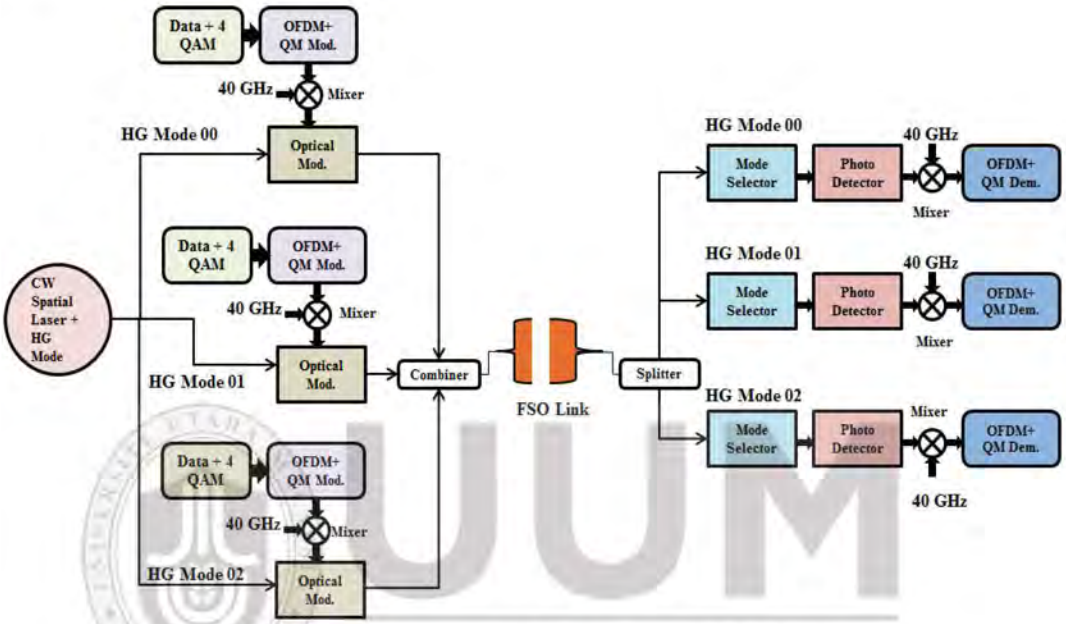

Figure 4.21. Proposed Ro-FSO Transmission System by incorporating HG Modes

Three independent 4 level quadrature modulation OFDM based Channels, each of carrying 20Gbps-40GHz signal are modulated over optical spatial carrier by modal multiplexing on three laser modes HG mode 00, HG mode 01 and HG mode 02 and are transmitted over FSO link of 50 km.

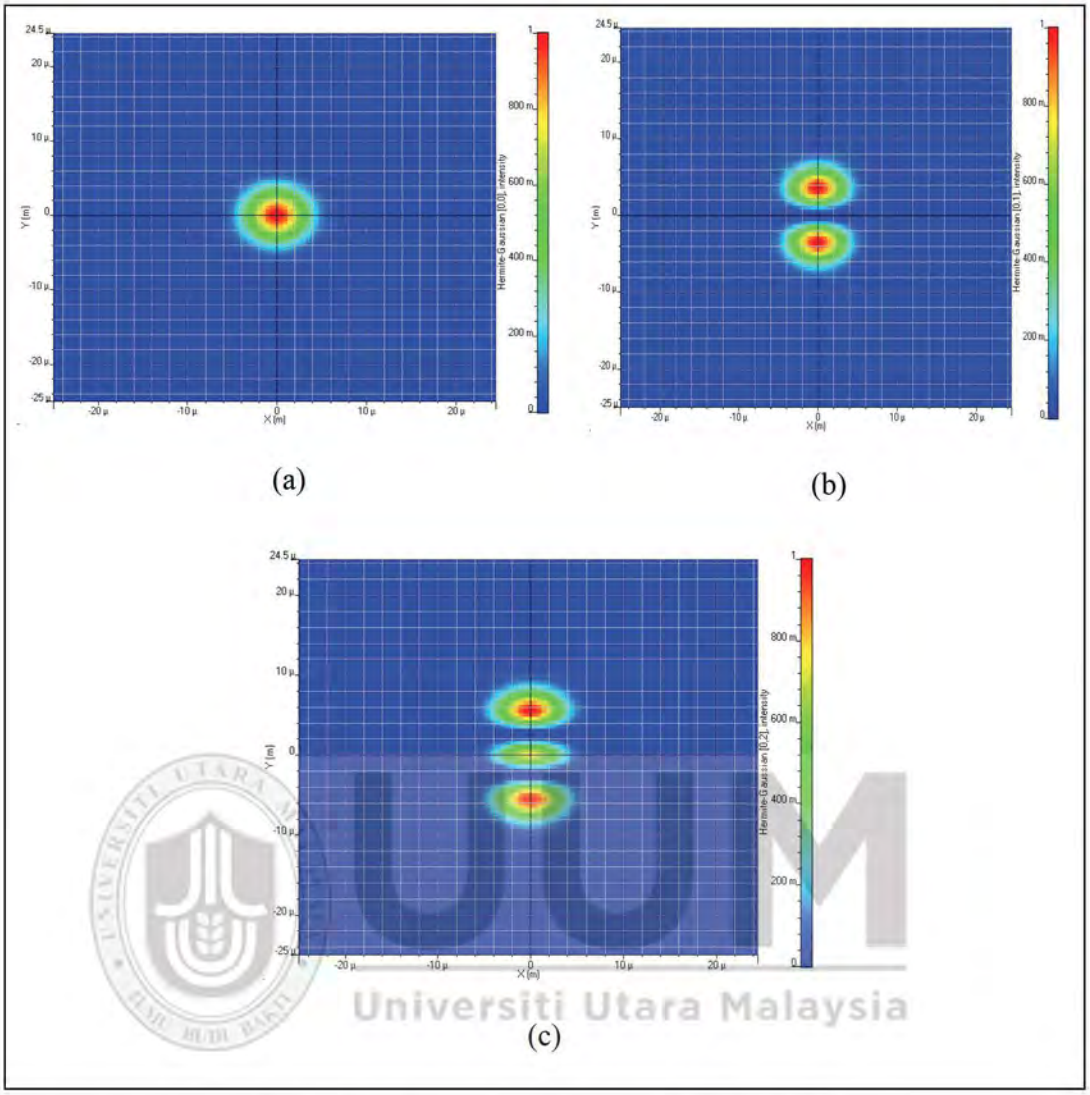

Figure 4.22. Excited HG Modes (a) HG 00 (b) HG 01 and (c) HG 02

The HG mode is mathematically described as [213]

$$\varphi_{m,n}(r,\phi) = H_m(\frac{\sqrt{2x}}{w_o x})\exp(\frac{-x^2}{{w_o}^2 x})\exp(j\frac{\pi x^2}{\lambda R_o x})H_n(\frac{\sqrt{2y}}{w_o y})\exp(\frac{-y^2}{{w_o}^2 y})\exp(j\frac{\pi y^2}{\lambda R_o y}) \quad (4.6)$$

In the equation 4.6, m and n represent the X and Y index that describe the mode dependencies for the X and Y-axis. R refers to radius of curvature and w_o is the spot size. H_m and H_n are the Hermite polynomials. A CW laser and HG mode generator is used to excite the HG modes as shown in the Figure 4.22. A 4 QAM sequence generator is used to generate the 20 Gbps of data by using 2 bits per symbol which is further modulated using OFDM 512 sub-carriers and 1024 FFT points. This OFDM

signals are again modulated at 7.5 GHz using QM modulator. A 40 GHz signal is mixed with this QM signal, further modulated by LiNb modulator driven by the CW source. These optical signals along with HG modes are transmitted over FSO link and received by the spatial APD photo-detector. At the reception side, a mode selector based on mean-squared error minimization is used to extract the required mode of particular wavelength from the optical signal. SOA is used as a post amplification technique. The FSO transmitter aperture and receiver apertures are set to 20 cm and 30 cm respectively. A 40 GHz signal is again added after photodiode for the down conversion of signal. This electrical signal is then fed to the QM demodulator followed by an OFDM modulator and QAM decoder for the recovery of data. The atmospheric turbulences are considered as ideal for clear weather conditions.

4.3.2.1 Results and Discussion

This section presents and discusses the results from simulation. Figure 4.23 reveals the SNR and total received power for proposed Ro-FSO transmission system under clear weather conditions. From the Figure 4.23 (a), the values of SNR for HG mode 00 is computed as 38.11 dB, 36.11 dB and 25.11 dB; for HG mode 01 as 31.12 dB, 17.22 dB and 11.16 dB and for HG mode 02 as 36.22 dB, 26.11 dB and 20.34 dB at the FSO link of 10 km, 40 km and 50 km respectively.

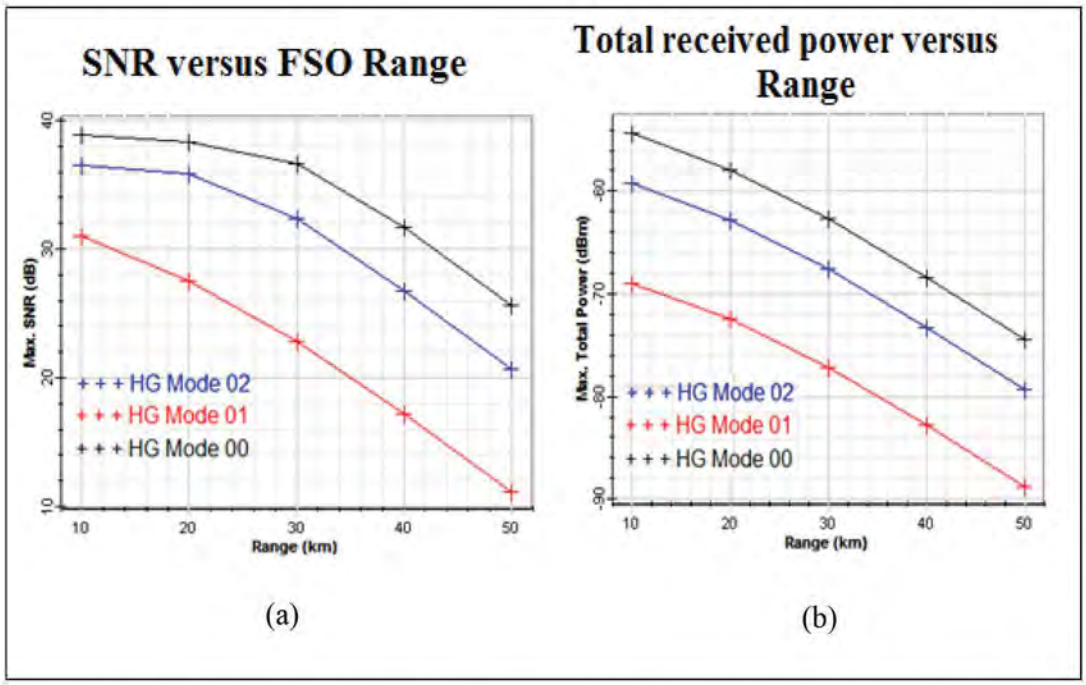

Figure 4.23. Evaluation of SNR and Total received Power under clear weather conditions

Consequently, the value of total received power for HG mode 00 is computed as -54.11 dBm, -68.54 dBm and -74.11 dBm; for HG mode 01 as -68.12 dBm, -82.11 dBm and -88.32 dBm; for HG mode 02 as -59.43 dBm, -73.11 dBm and -79.11 dBm at the transmission link of 20 km, 40 km and 50 km respectively. This indicates that under clear weather conditions, the excitation of HG mode 00 prolongs to FSO link to 50 km, HG mode 01 prolongs the FSO link to 25 km and HG mode 02 prolongs the FSO link to 40 km with acceptable SNR and total received power. It also indicates that HG mode 01 is more affected to fading as compared to HG mode 00 and HG mode 02. The constellations and RF spectrum at the receiver side measured at distance of 50 km under clear weather conditions are shown in Figure 4.24 and Figure 4.25. It is shown from Figure 4.24 (a), (b) and (c) the constellation diagram of HG mode 01 is more distorted as compared to HG mode 00 and HG mode 02.

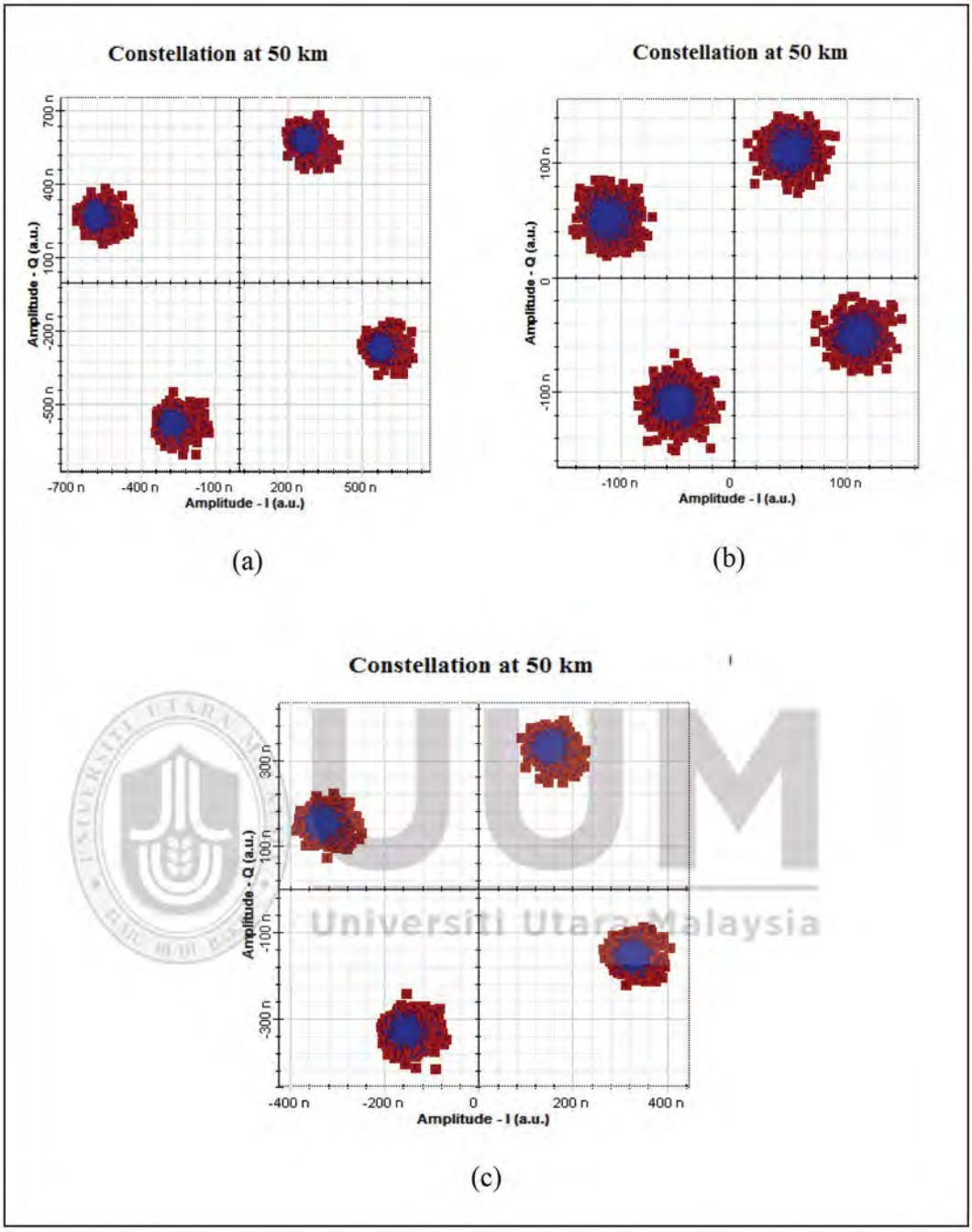

Figure 4.24. Constellation Measured at 50 km (a) HG mode 00 (b) HG mode 01 and (c) HG mode 02

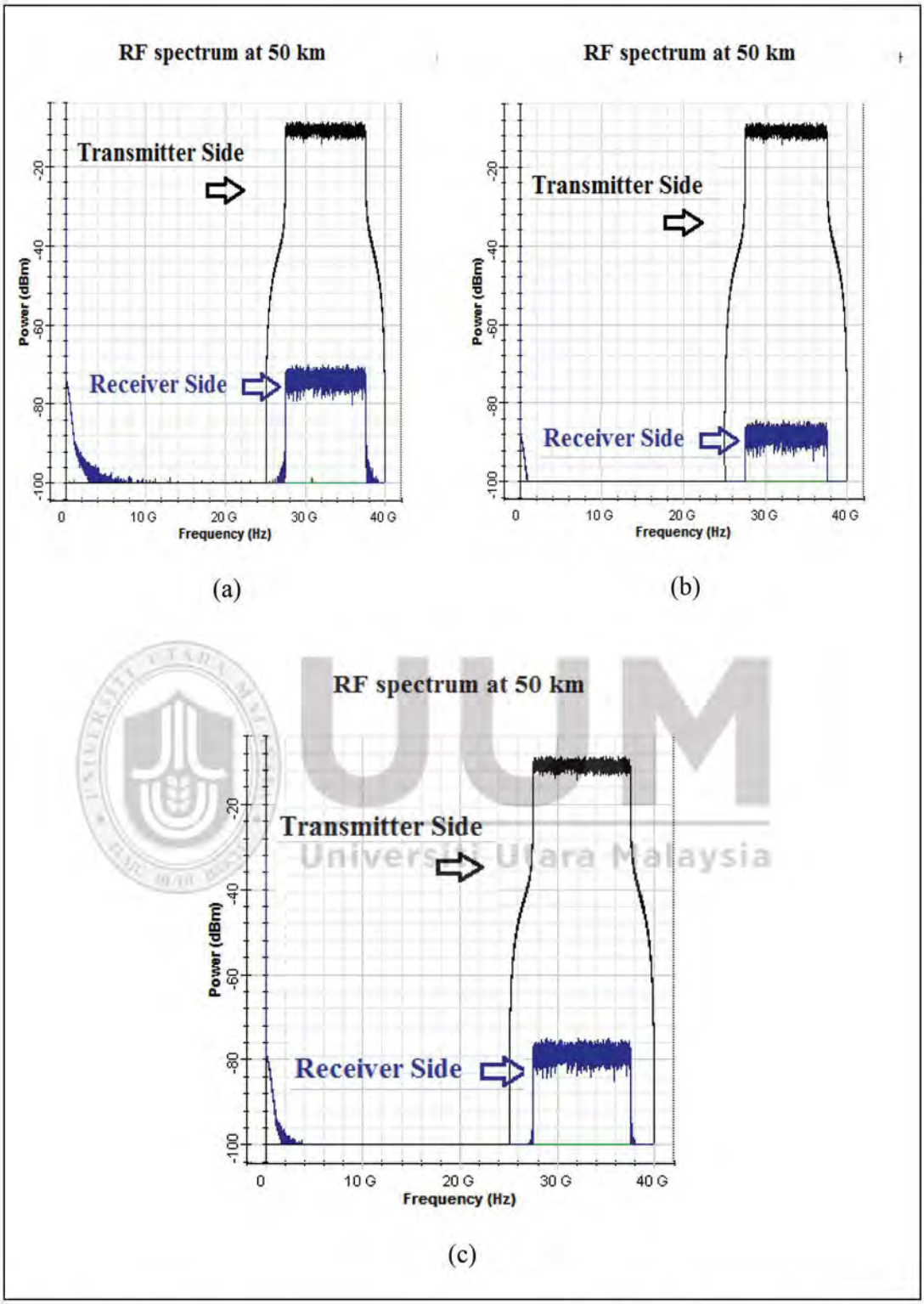

Figure 4.25. RF Spectrum measured at 50 km (a) HG 00 Mode (b) HG 01 Mode and (c) HG mode 02

Similarly, the RF spectrum measured at 50 km, reported in Figure 4.25 (a), (b) and (c), shows that the RF power of HG 01 mode is less as compared to HG mode 00 and HG mode 01 due to multipath fading.

Thus, In this work, mode division multiplexing is adopted to transmit 3 *X* 20Gbps-40 GHz OFDM-Ro-FSO transmission Channels using HG mode 00, HG mode 01 and HG mode 02 over FSO link of 50 km under clear weather conditions to realize the total transmission of 60 Gbps-120 GHz signal. From simulation results, it is concluded that HG mode 01 is more affected to severe multipath fading compared to HG mode 00 and HG mode 01. Under clear weather conditions, the HG mode 00 prolongs to 50 km as compared to the HG mode 01 and HG mode 02 which prolongs merely to 25 km and 40 km respectively with acceptable SNR and total received power.

4.3.3 Case 3 Simulation set up of MDM Scheme by using LG-HG modes with vortex lenses

Figure 4.26 shows the proposed MDM-Ro-FSO model with LG and HG modes designed in OptiSystem™. The model contains four independent OFDM subcarrier channels while each channel carries 20 Gbps data stream over a 40 GHz optical spatial carrier on four different laser modes: LG 02 mode with vortex lens m=2, LG 03 mode with vortex lens m=5, HG 11 mode, and HG 12 mode as shown in Figure 4.26. These modes are received from a continuous wave (CW) laser and multiplexed over free space, as shown in Figure 4.26.

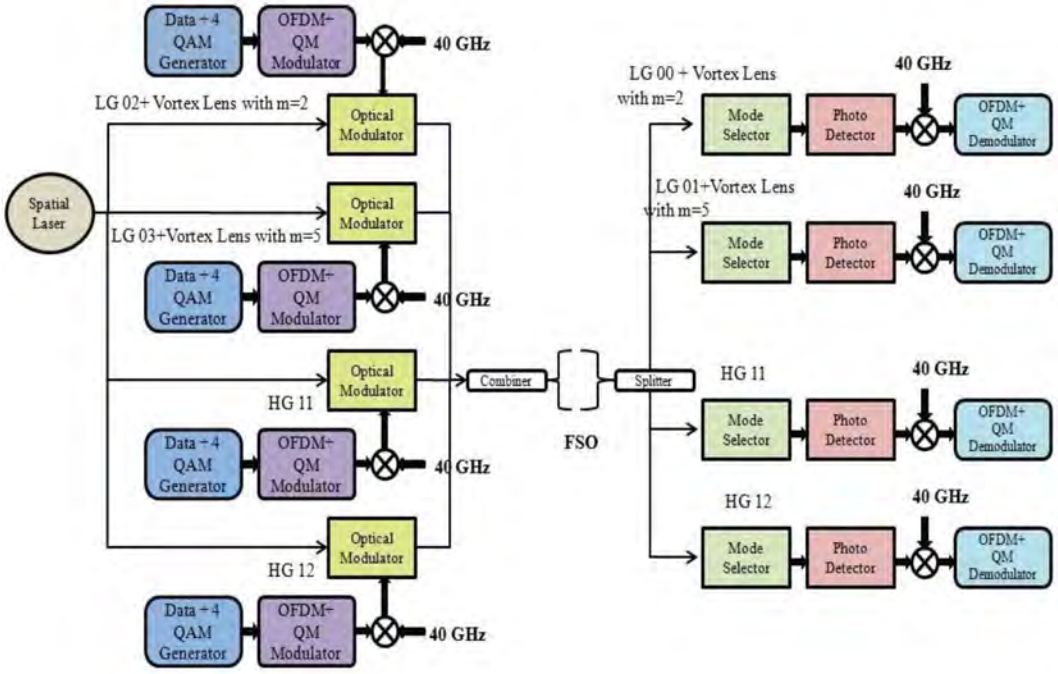

Figure 4.26. Proposed Model for Millimeter wave over free space optical channel

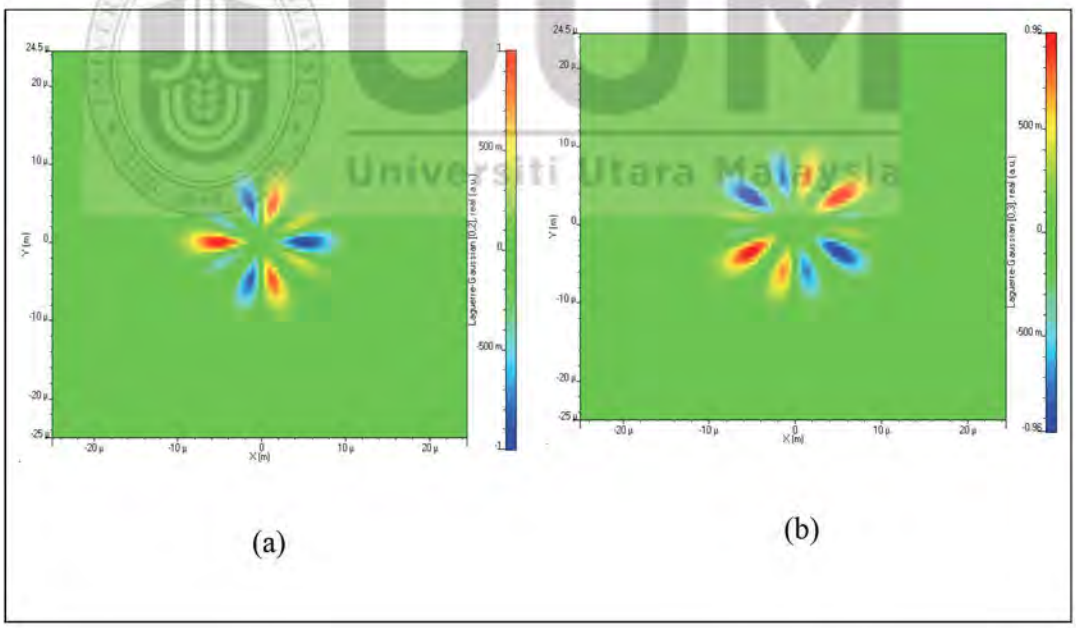

Figure 4.27 Excited Modes (a) LG 02 with vortex m=2 (b) LG 03 with vortex m=5 (c) HG 11 and (d) HG 12

Figure 4.27 continued.

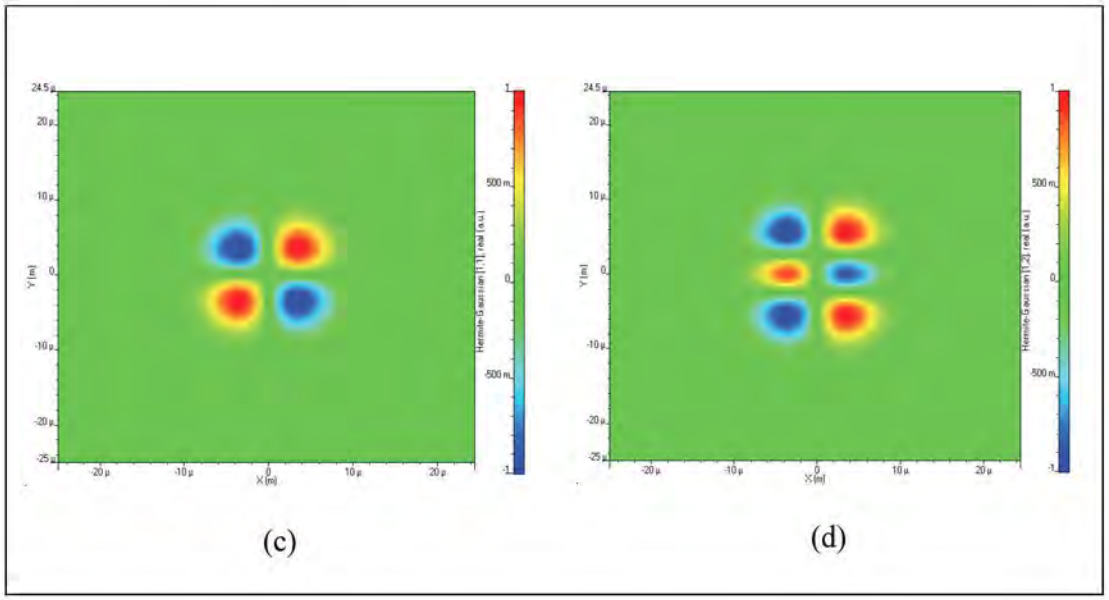

The vortex lens is used for applying phase to LG modes as shown in Figure 4.26. The following equation describes the applied phase [270]:

$$T(x,y) = \exp[-j\frac{\pi n(x^2+y^2)}{2\lambda f} + ma\tan(\frac{x}{y})] \quad (4.7)$$

where f=focal length, m is the vortex parameter, and n is the refractive index. The phase of exited modes generated with vortex lens is shown in Figure 4.27 (a) and (b). 1024 fast Fourier transform (FFT) points are used for generating and modulating four separate 20 Gbps four-level quadrature amplitude modulated (QAM) sequences on 512 OFDM sub-carriers. These sets of OFDM subcarriers are further modulated by using Quadrature modulation (QM) on a 7.5 GHz radio subcarrier. Multiplexing and transmission of these QM signals take place over a 50 km free-space channel. A spatial Avalanche photo-detector (APD) and a 40 GHz optical carrier are used to retrieve the four MDM signals. These MDM signals are mode-division de-multiplexed based on mean-squared error minimization of the spatial intensity distribution with an APD receiver aperture of 30 cm.

The value of attenuation for clear weather is considered as 0.14 dB/km; for thin fog, it is 9 dB/km; 15 dB/km for thick fog; and 22 dB/km for heavy fog [265, 266]. Post amplification process uses a semiconductor optical amplifier (SOA) with an injection current of 0.3A. A 7.5 GHz radio QM demodulator receives the retrieved electrical signal from the APD and initiates down-conversion. Further, an OFDM demodulator and QAM decoder receive the signal for recovering data.

4.3.3.1 Results and Discussion

Figure 4.28 shows signal-to-noise ratio (SNR) and total received power from the proposed Ro-FSO transmission system. The comparison of SNR and received power curves verifies that Channel 3 (HG mode 11) is the most dynamic, followed by Channel 1 (LG mode 02 with vortex m=2), Channel 4 (HG mode 12), and Channel 2 (LG mode 03 with vortex m=5). As shown in Figure 4.28 (a) and (b), the value of SNR for Channel 1 (LG mode 02 with vortex m=2) is measured as 35.11 dB, 33.99 dB and 32.45 dB respectively for a free-space link of 20 km, 40 km and 50 km respectively. For Channel 2 (LG mode 03 with vortex m=5), the SNR values are significantly lower, i.e. 29.11 dB, 27.23 dB and 26.11 dB respectively for a FSO link of 20 km, 40 km and 50 km respectively.

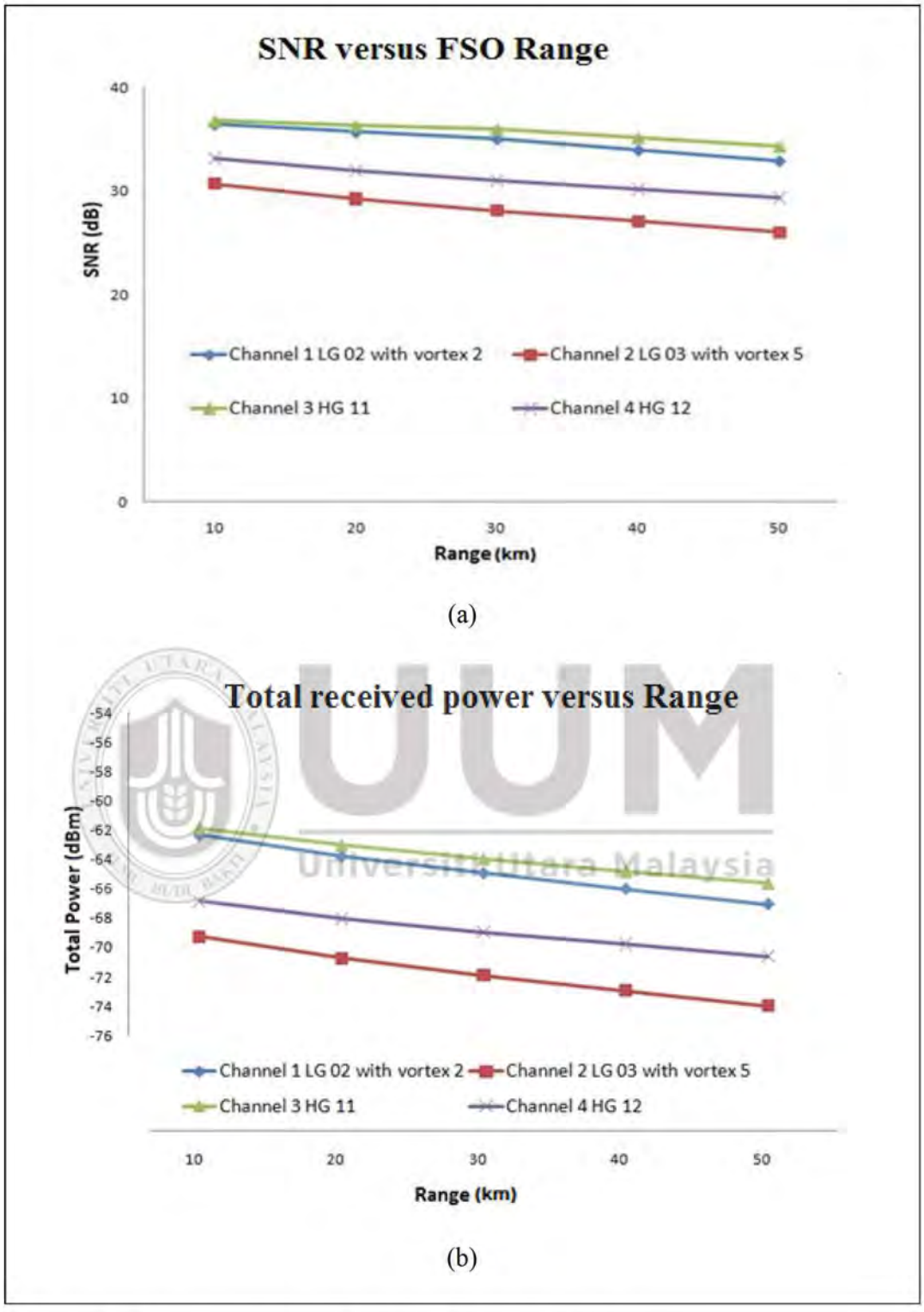

Figure 4.28. Evaluation of SNR and Total Received Power

For Channel 3 (HG 11 mode), the SNR values are higher than the SNR values for Channel 2 and are computed as 36.35 dB, 35.11 dB and 34.36 dB as compared to

Channel 4 (HG 12 mode) which shows SNR values of 31.11 dB, 30.44 dB and 29.11 dB for a free-space link of 20 km, 40 km and 50 km respectively. Consequently,

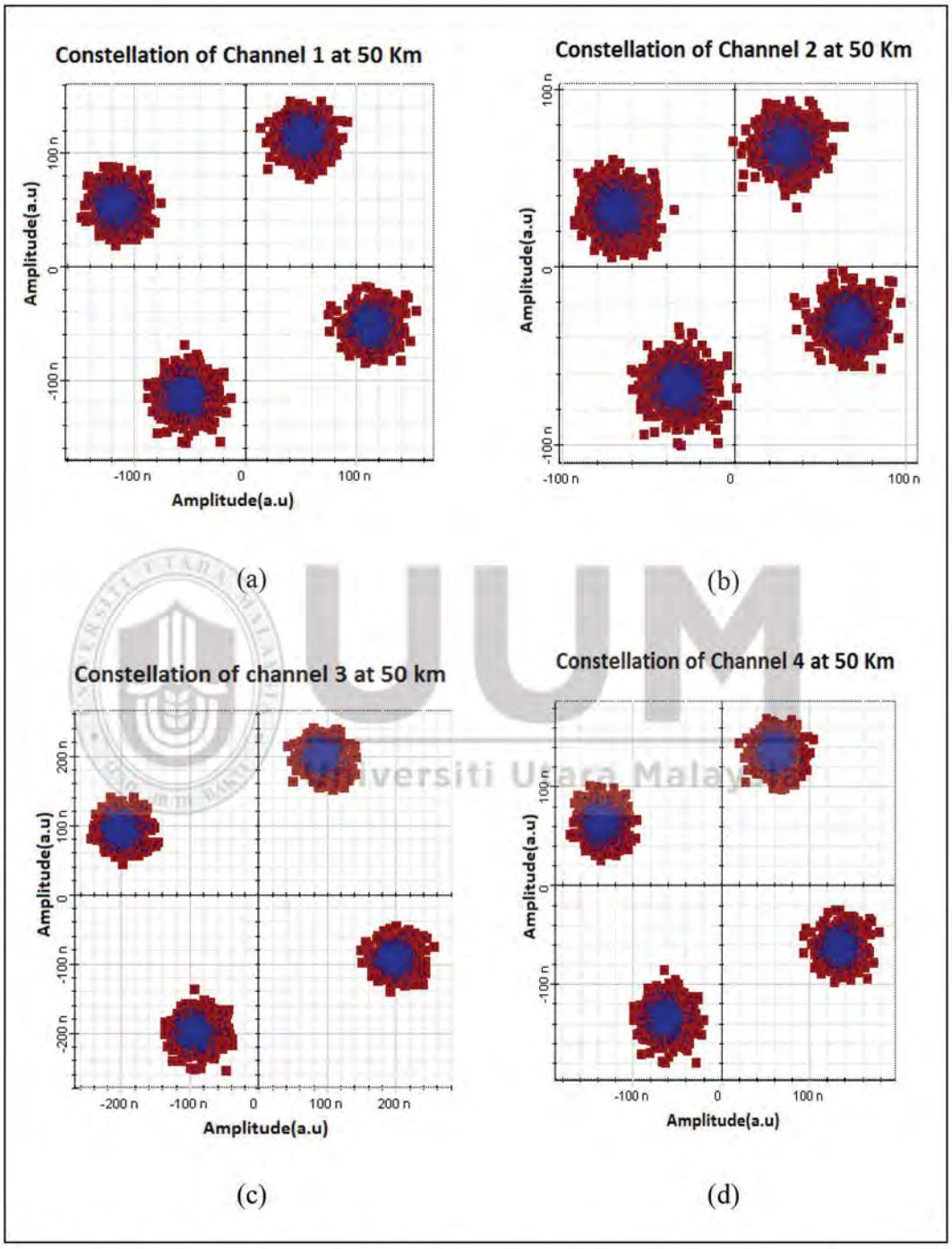

Figure 4.29. Measured Constellations at 50 Km (a) Channel 1 (b) Channel 2 (c) Channel 3 and (d) Channel 4

Figure 4.28 (b) shows that the values of total received power for Channel 1 is computed as -63.11 dBm, 66.34 dBm and -67.75 dBm; for Channel 2 as -70.76 dBm,

72.95 dBm and -73.98 dBm; for Channel 3 as -63.83 dBm, 64.93 dBm and -65.98 dBm; for Channel 4 as -68.54 dBm, 69.87 dBm and-70.86 dBm for a free-space link of 20 km, 40 km and 50 km respectively.

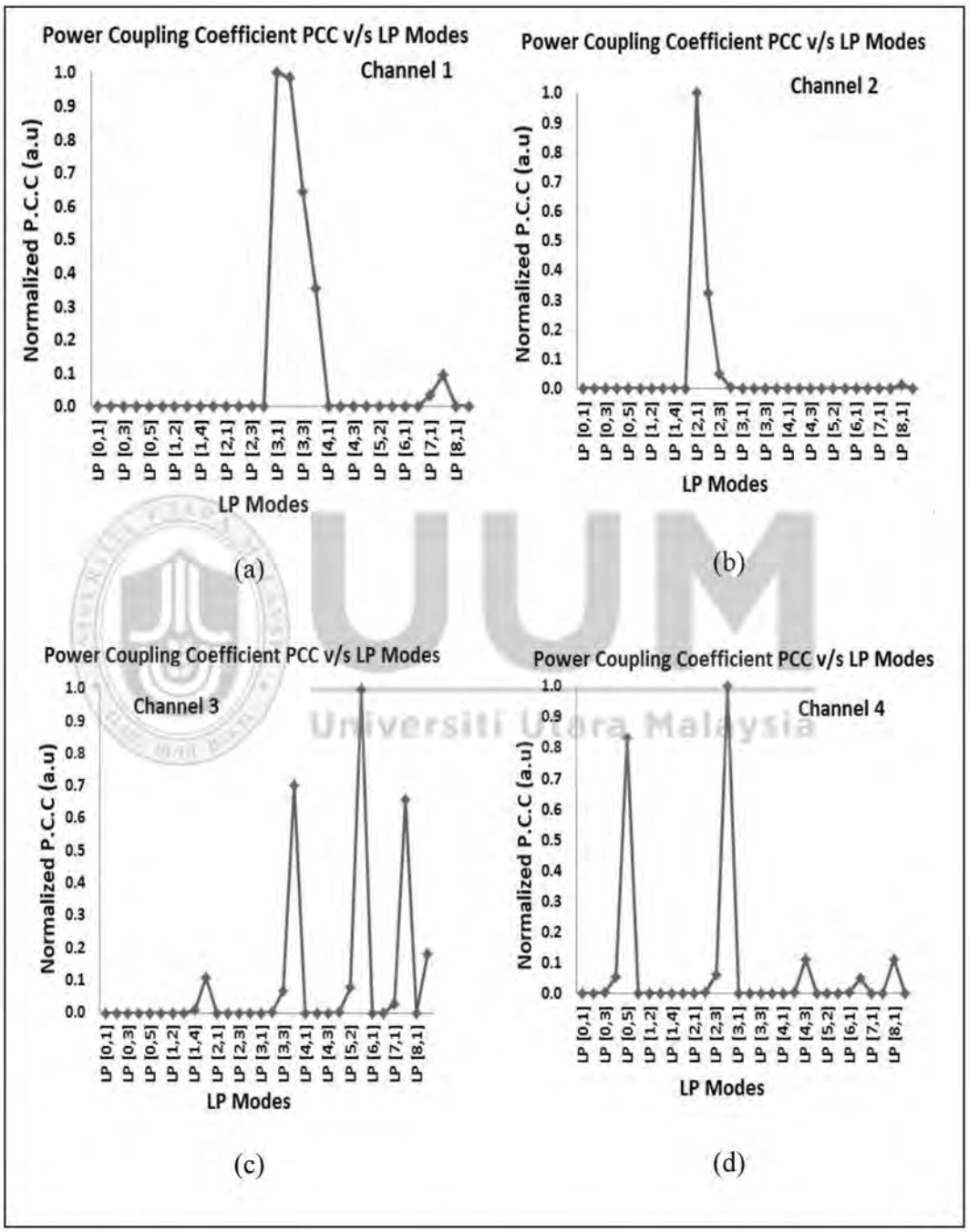

Figure 4.30. Measured PCC v/s Range (a) Channel 1 (b) Channel 2 (c) Channel 3 (d) Channel 4

This indicates that maximum achievable distance for channel 1, channel 2, channel 3 and channel 4 are 50 km with acceptable SNR and total received power. Figure 4.29

displays the measured constellations at a distance of 50 km, confirming that Channel 2 is more affected by multipath fading as compared to Channel 1, Channel 3, and Channel 4.

The results demonstrate that lower order HG modes are more robust to muti-path fading as compared to higher-order LG modes. This is due to the distortion of the transverse intensity profiles of higher order HG modes and higher-order LG modes with propagation distance. As propagation distance increases, the beam intensity gradually spills into the center of the beam for higher order HG modes and higher-order LG modes. This distorts signal constellations and reduces the SNR. In case of improved SNR and link distance, they are attained with HG modes as their spatial profiles are more intact with propagation distance. As shown in Figure 4.30, the computation of the modal decomposition at the receiver occurs by means of linearly polarized modes in descending order of power coupling coefficient. In case of Channel 1, the largest power coupling happens with mode LP 31 followed by LP 32, LP 33, LP 34 and LP 72; for Channel 2, the largest power coupling happens with LP 21 followed by LP 22, and LP 23; for Channel 3, the largest power coupling happens with LP 53 followed by LP 34, LP 72, LP 91, LP 15, LP 52 and LP 33; for Channel 4, the largest power coupling happens with LP 24 followed by LP 05, LP 81, LP 43, LP 23 and LP 62.

Figure 4.31 represents performance of proposed system under influence of atmospheric turbulences. When the clear weather changes to turbulent, the value of SNR for Channel 1 is computed as 35.11 dB, 32.23 dB and 24.68 dB under light fog; for thin fog it is computed as 34.43 dB, 28.32 dB and 0 dB and for heavy fog it is computed as 34.21 dB, 25.08 dB and 0 dB at FSO link of 1 km, 2 km and 4 km respectively.

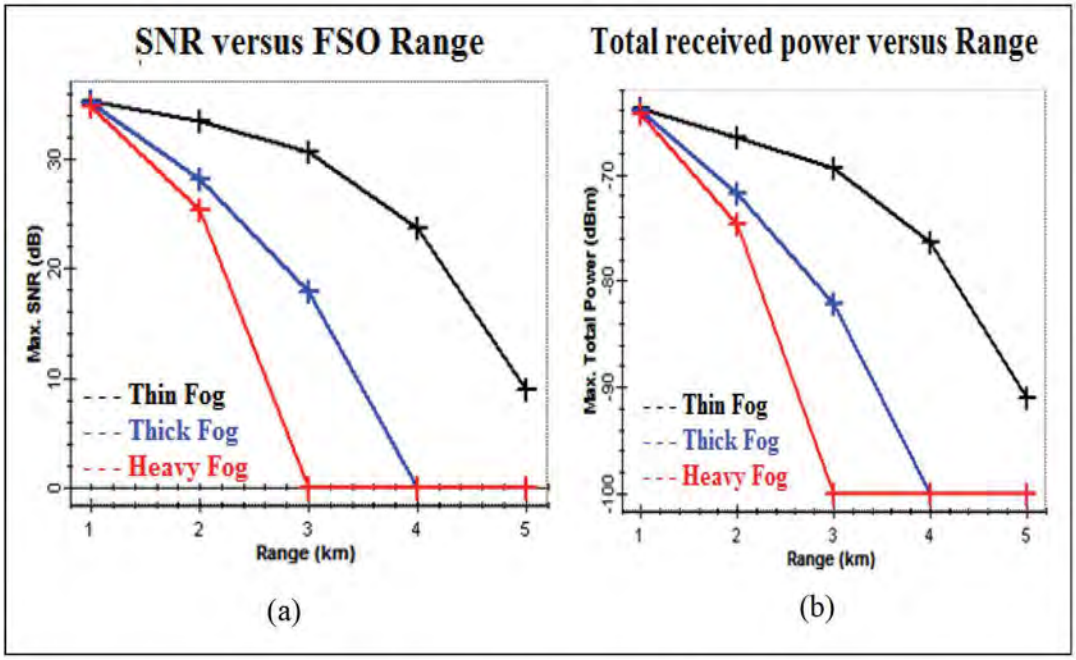

Figure 4.31. Measured SNR and Total Received Power under atmospheric turbulences

Similarly, the value of total received power for Channel 1 under light fog is noted as -63.32 dBm, -66.78 dBm and -76 dBm; for thin fog it is noted as -63.13 dBm, -71.43 dBm and -100 dBm and for heavy fog it is noted as -64.43 dBm, -74.41 dBm and -100 dBm at FSO link of 1 km, 2 km and 4 km respectively. This indicates that the FSO link prolongs to 50 km under clear weather conditions as the weather changes to thin fog, FSO link prolongs to 4 km whereas when weather changes to thick and heavy fog, the FSO prolongivity reduces to 3 km and 2 km respectively with acceptable SNR and total received power.

Ro-FSO technology provides a universal platform for seamless integration of radio and optical networks for distributing millimeter waves in WLANs without expensive optical fiber cabling. While inspecting the performance of simultaneous mode division multiplexing of four modes – LG 02 with vortex m=2, LG 03 mode with vortex m=5, HG 11 mode, and HG 12 mode – to transmit four radio OFDM Channels over FSO link of 50km, the study finds out that Channel 2 is more affected by multipath fading in comparison to other three Channels. Under clear weather

conditions, the maximum distance achievable by Channel 1, Channel 2, Channel 3 and Channel 4 are 50 km with acceptable SNR and total received power. As the atmosphere changes from clear weather to light fog, the FSO link prolongs to 4 km and when atmosphere is further changes from light fog to thin and heavy fog, the FSO link prolongs to 3 km and 2 km respectively with acceptable SNR and total received power.

4.4 Summary

In this chapter, MDM scheme is designed for hybrid OFDM-Ro-FSO transmission system. This chapter is divided into three phases.

Phase 1 is focused on the design of 10 Gbps-OFDM-FSO transmission system under the influence of atmospheric turbulences. The reported results indicate that under clear weather conditions, the FSO link prolongs to 180 km whereas under the influence of heavy fog, the FSO link prolongs to 2.5 km with acceptable SNR and total received power.

Phase 2 is focused on the integration of radio carrier of 40 GHz to 20 Gbps-OFDM-FSO transmission system under the influence of atmospheric turbulences. The LG modes are also investigated for transmission of Ro-FSO Channel. The reported results show that under clear weather conditions, in case of LG 00 and LG 02 modes, the FSO link prolongs to 100 km whereas in case of LG 04 mode, the FSO link prolongs to 60 km with acceptable SNR and total received power. When the atmosphere changes from clear weather to turbulent weather, the FSO link prolongs to 9 km under the influence of haze, 4.9 km under the influence of thin fog, 3.4 km under the influence of thick fog and 2.8 km under the influence of heavy fog with acceptable SNR and total received power.

Phase 3 is focused on the design of MDM scheme for OFDM-Ro-FSO transmission system. This phase is further divided into three cases:

Case 1 is focused on the adoption of LG modes for MDM scheme in OFDM-Ro-FSO systems. In this case, two Channels, each carrying 20 Gbps-40 GHz data, are transmitted by using MDM of LG 01 and LG 10 modes over FSO link. The reported results indicate that under clear weather conditions, the FSO link prolongs to 100 km whereas in case of atmospheric scintillations, the FSO link prolongs to 65 km with acceptable SNR and total received power.

Case 2 is focused on the adoption of HG modes for MDM scheme in OFDM-Ro-FSO transmission system. In this case, three Channels, each carrying 20 Gbps-40 GHz data, are transmitted by using MDM of HG 00, HG 01 and HG 02 modes over FSO link. The reported results show that under clear weather conditions, in case of HG 00 mode, the FSO link prolongs to 50 km whereas in case of HG 01 and HG 02 modes, the FSO link prolongs to merely 25 km with acceptable SNR and total received power.

Case 3 is focused on the adoption of LG modes with vortex lens and HG modes for MDM scheme in Ro-FSO transmission systems. In this case, four Channels, each carrying 20 Gbps-40 GHz data, are transmitted by using MDM of LG 02 with vortex lens m=2, LG 03 mode with vortex lens m=5, and HG 11 and HG 12 modes over FSO link. The reported results indicate that under clear weather conditions, the FSO link prolongs to 50 km; under the influence of thin fog, it prolongs to 4 km; under the influence of thick fog, it prolongs to 3 km whereas under the influence of heavy fog, FSO link prolongs to 2 km with acceptable SNR and total received power.

Thus, from the all the phases as shown in this chapter, it shows that an average significant 50% power improvement in deep fades from multi-path propagation with the use of OFDM in MDM-Ro-FSO systems as compared to without OFDM.

CHAPTER FIVE
PCF-MDM-RO-FSO TRANSMISSION SYSTEM

In the previous chapter, Orthogonal Frequency Division Multiplexing (OFDM) was introduced to design Radio over Free Space (Ro-FSO) transmission system in conjunction with mode division multiplexing (MDM) scheme. This chapter is focused on designing of Ro-FSO transmission system by using photonic crystal fibers (PCF) to mitigate mode coupling losses for short haul communication. This chapter is further divided into four cases as shown in Figure 5.1.

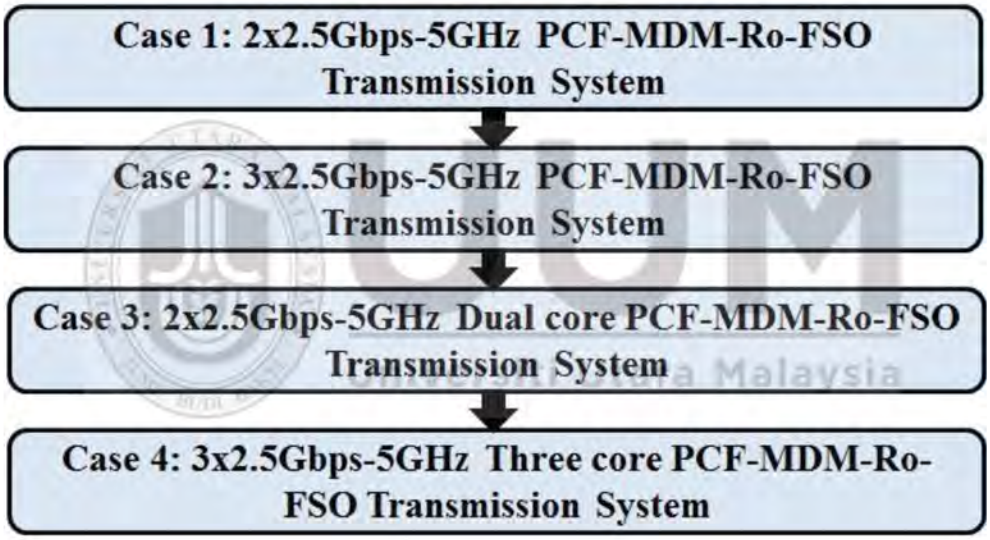

Figure 5.1. Cases of PCF-MDM-Ro-FSO Transmission System

Case 1 describes design of two channels Ro-FSO system by using two PCF's at transmitter side and two PCF's at receiver side, depicted in Section 5.1. Case 2 is focused on designing of three channels Ro-FSO system by using three PCF's at transmitter side and three PCF's at receiver side, illustrated in Section 5.2. Case 3 describes the transmission of two channels Ro-FSO system by using one dual core PCF at transmitter side and two single core PCF's at receiver side, illustrated in Section 5.3. Case 4 describes transmission of three channels Ro-FSO transmission

system by using one three core PCF at transmitter side and three single core PCF's at receiver side, illustrated in Section 5.4 followed by Section 5.5 which describes the summary of this chapter. Moreover, each phase is evaluated under the influence of atmospheric turbulences.

5.1 Case 1: 2 x 2.5Gbps-5GHz PCF-MDM-Ro-FSO Transmission System

In this case, two channels are transmitted by using two single core PCF's at transmitter side and received by using two single core PCF's at receiver side. Section 5.1.1 discusses the simulation setup whereas Section 5.1.2 discusses the results and discussion.

5.1.1 Simulation Setup

A schematic diagram of 2 x 2.5Gbps-5GHz proposed MDM-PCF-Ro-FSO transmission system, simulated in OptSim™ and BeamProp™ software, is illustrated in Figure 5.2. Two independent non return to zero (NRZ) encoded channels, excited from two different PCFs, are transmitted over 2 km free space link. Each channel carries 2.5Gbps-5GHz data modulated simultaneously by LiNB3 optical modulator. Two distinct modes LG 00 and LG 01 are excited from spatial laser. Channel 1 is operated on LG 00 mode in conjunction with PCF A whereas channel 2 is operated on LG 01 in conjunction with PCF B. Figure 5.3 represents internal core structures of PCF A and PCF B. Spatial laser is used to generate LG 00 and LG 01 modes, polarized in x-direction.

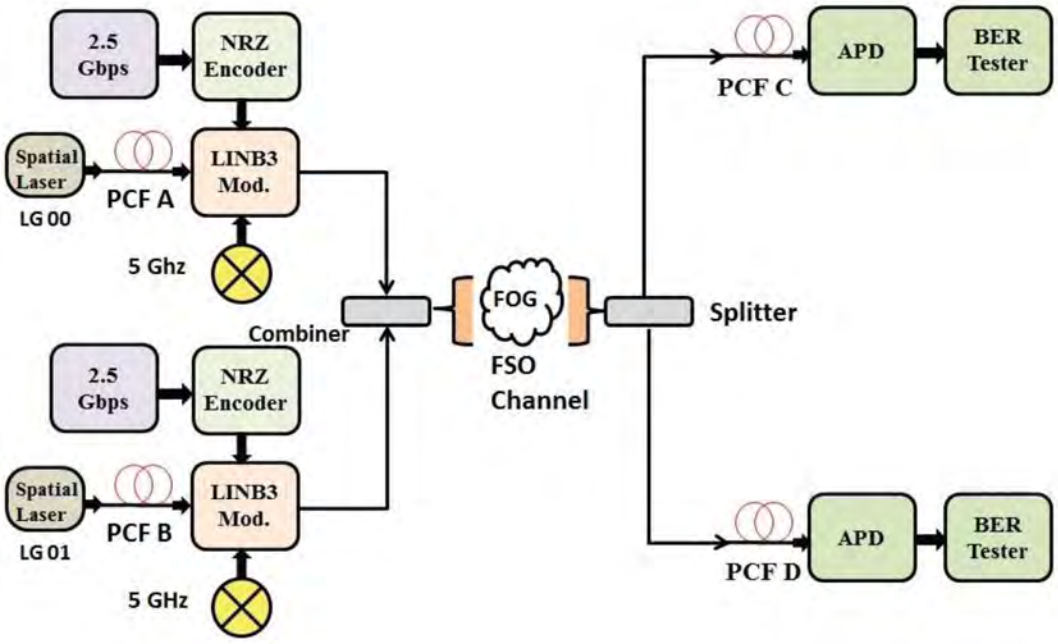

Figure 5.2. 2 x 2.5Gbps-5GHz MDM-PCF-Ro-FSO Transmission System

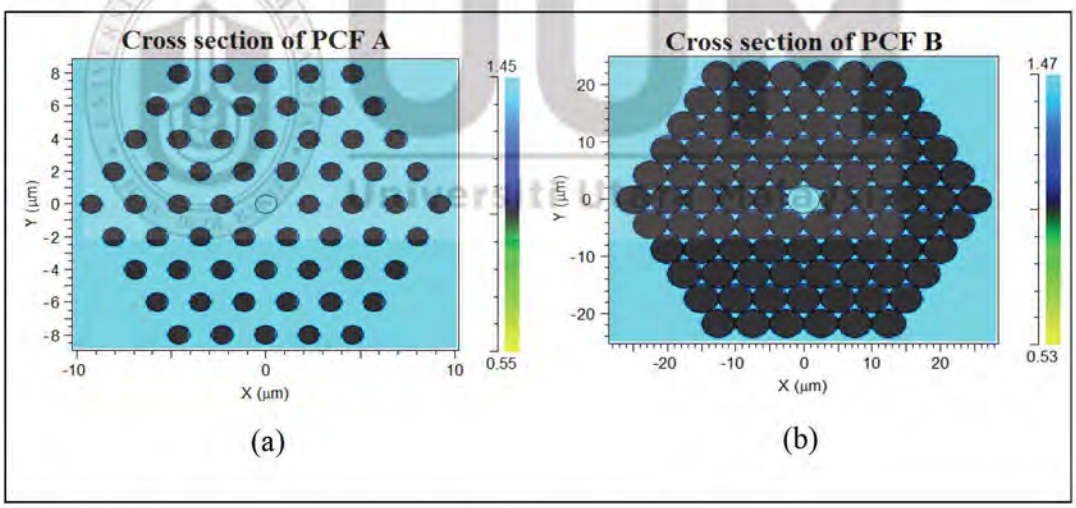

Figure 5.3. Structures of PCFs (a) PCF A and (b) PCF B

As shown in Figure 5.4 (c), when LG 00 is launched into PCF A, 93.1 % of power is computed in dominant mode at the output of PCF A with effective index of 1.45 whereas when LG 01 mode is launched into PCF B, 92.9 % of power is computed in dominant mode at output of PCF B with effective index of 1.47.

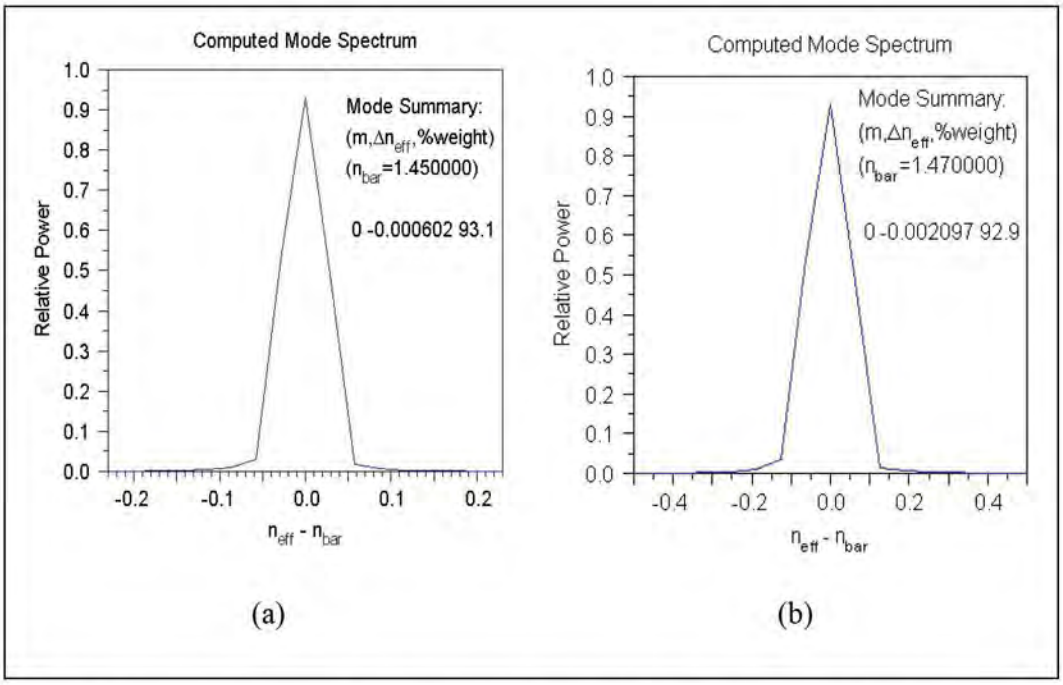

Figure 5.4. Computed Mode Spectrum (a) After PCF A and (b) After PCF B

Similarly, Figure 5.5 depicts the output modes from PCF A and PCF B. Coupling between mode groups is modelled based on an iterative method [271]:

$$\frac{\partial P_q}{\partial Z}+\frac{1}{v_g}\frac{\partial P_q}{\partial t}=-\alpha_q P_q+k_q d_q(P_{q+1}-P_q)-\gamma_{q-1}d_{q-1}(P_q-P_{q-1}) \tag{5.1}$$

Where q is the mode number, $P_q(z,t)$ is the average power signal, v_g is the group velocity, α_q is the power attenuation coefficient, d_q is the mode coupling coefficient between the mode groups q and $q+1$, k_q and γ_{q-1} are degeneracy factors. The other parameters of PCF A, PCF B at transmitter side and PCF C, PCF D at receiver side are illustrated in Table 5.1. The output of two channels is combined together and transmitted over FSO link having span of 2.5 km.

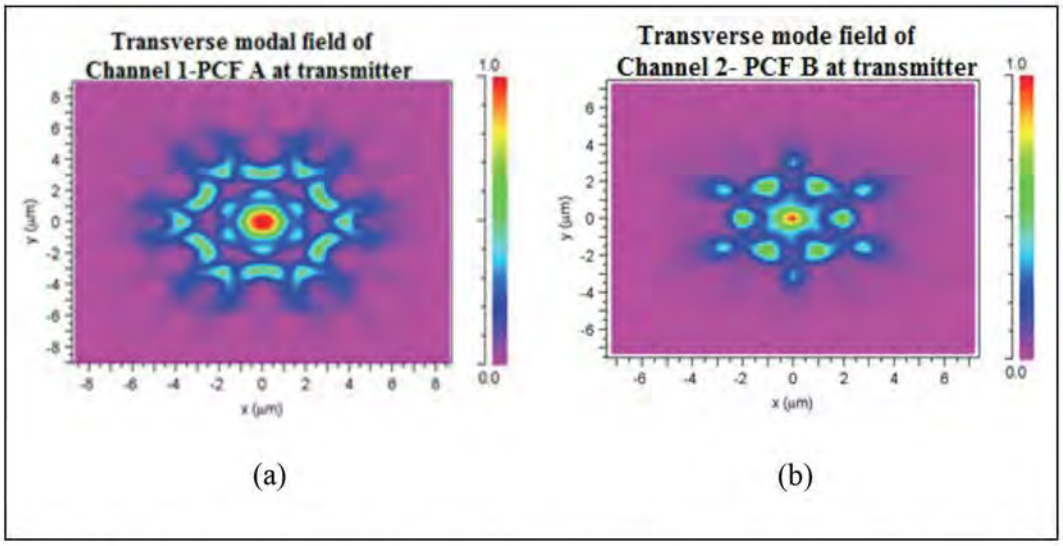

Figure 5.5. Transverse Mode Output at Transmitter Side (a) Channel 1- PCF A and (b) Channel 2- PCF B

Table 5.1

Parameters of PCFs at Transmitter Side

Parameters	**PCF A**	**PCF B**	**PCF C**	**PCF D**
No of Rings	4	5	4	5
Diameter of Air Holes, d (μ m)	1	2	1.6	2
Distance between air holes, g (μ m)	2.3	5	2.3	5
Ratio of Distance between Air holes to diameter of air holes, g/d	2.3	2.5	1.4375	2.5

In order to evaluate the performance of the proposed Ro-FSO system under atmospheric turbulences, the typical value of atmospheric attenuation with corresponding visibilities are assumed at 0.14 dB/km for clear weather conditions 9 dB/km for thin fog, 16 dB/km for thick fog and 22 dB/km for heavy fog [265, 266]. At the receiving side, splitter is used to split the optical beam into two PCFs C and D

to decompose the transmitted modes. The structures of PCF C and PCF D are slightly different and flipped with respect to PCF A and PCF B so that relevant mode is selected as shown in Figure 5.6.

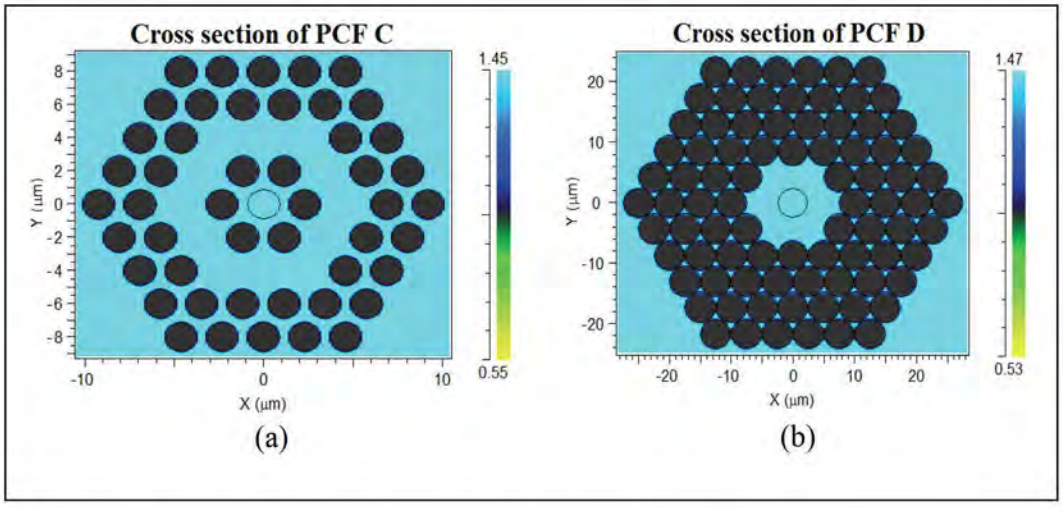

Figure 5.6. PCF Structures (a) PCF C and (b) PCF D

The effective index of PCF C is set at 1.45 in order to synchronize with PCF A whereas effective index of PCF D is set at 1.47 in order to synchronize with PCF B. After the PCFs, the optical beam is converted to electrical signal with the help of spatial photodetector followed by Bit error rate tester.

5.1.2 Results and Discussion

This section represents the results obtained from simulation setup of proposed MDM-PCF-Ro-FSO transmission system. Figure 5.7 represents the measured spectrum before the PCFs as well as after the PCFs at receiving side. It has been reported that 80% of optical power in dominant mode is achieved at output of PCF C with effective index of 1.45 whereas 85.1% of power in dominant mode is achieved at output of PCF D with effective index of 1.47 whereas without PCF only 25 % and 30 % of power is noted in dominant modes for both Channel and Channel 2 respectively.

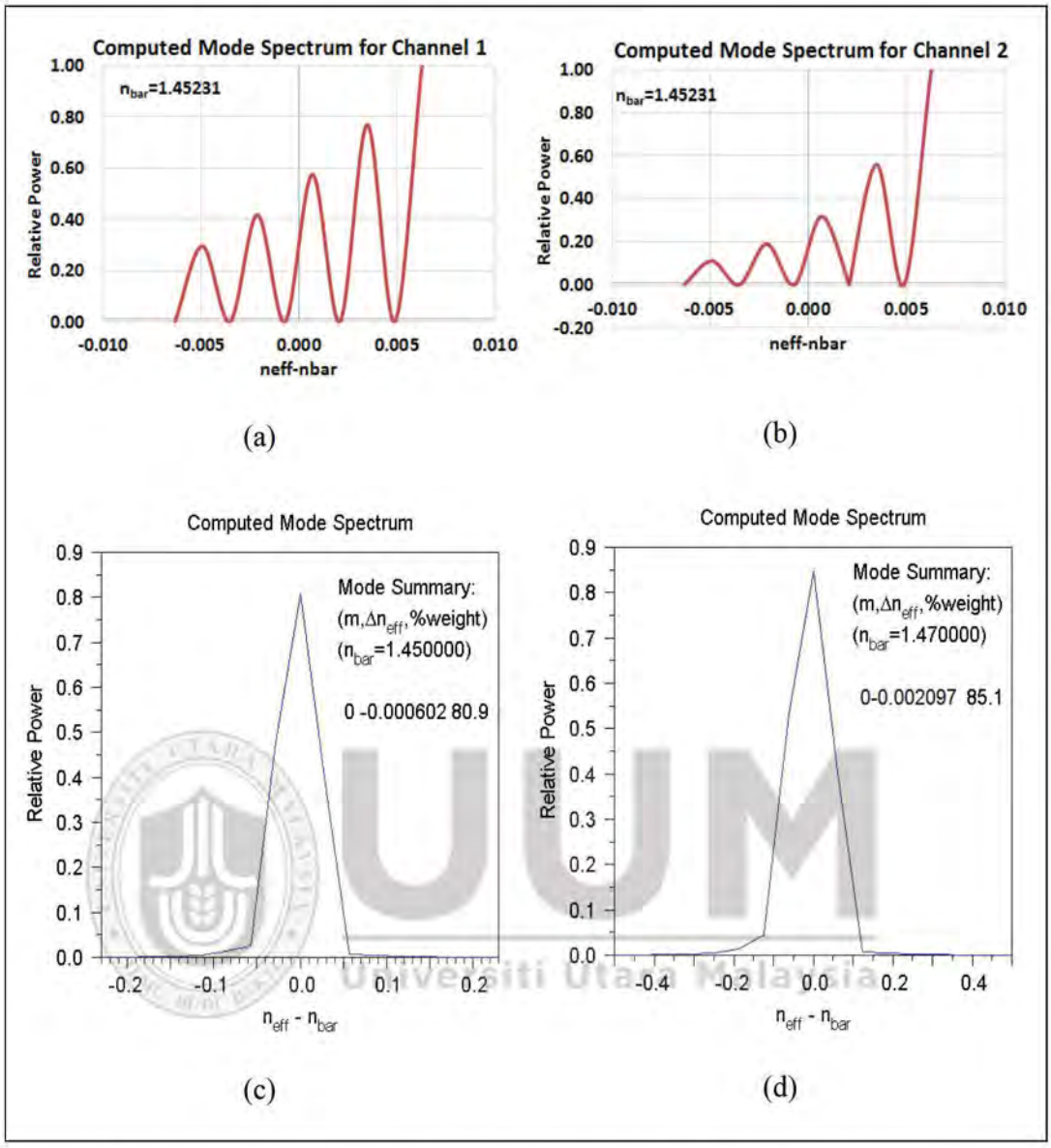

Figure 5.7. Computed Mode Spectrum at Receiver Side (a) after FSO channel 1 (b) after FSO channel 2 (c) after PCF C and (d) after PCF D

PCF C and PCF D are used to compensate mode coupling losses introduced in FSO transmission channel. Similarly, Figure 5.8 shows the measured BER of channel 1 and channel 2 with and without PCF conjunction. High improvement in BER is noted in case of PCF conjunction as compared to without PCF equalization.

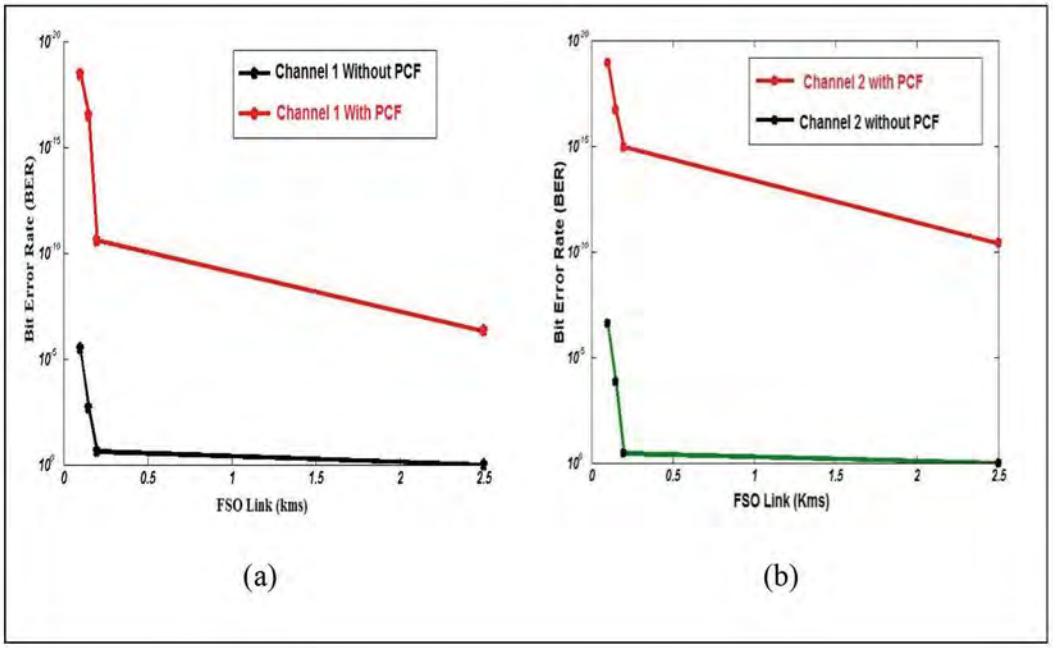

Figure 5.8. Measured BER (a) Channel 1 and (b) Channel 2

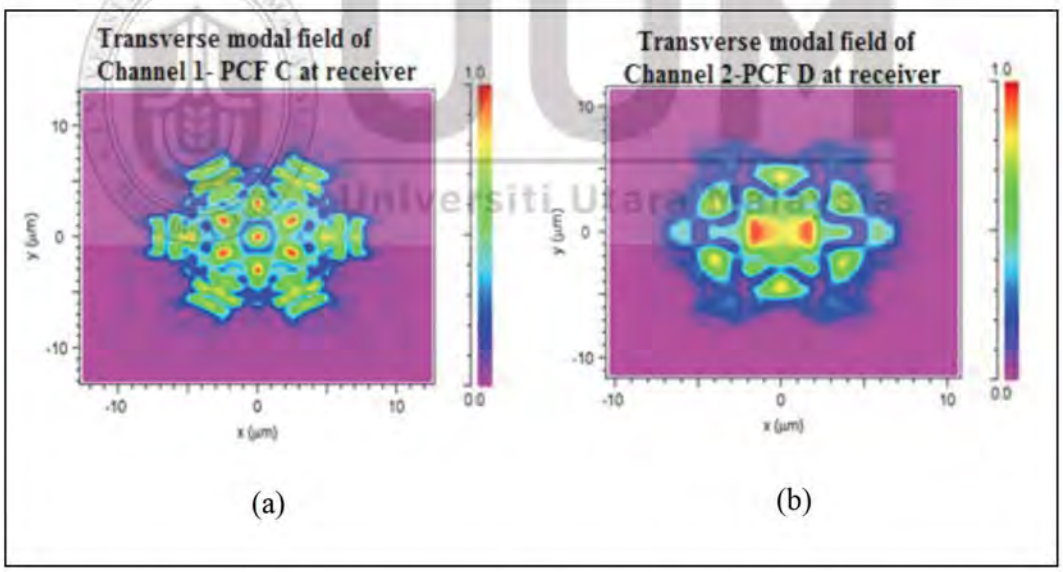

Figure 5.9. Received Modes at FSO link of 2 km (a) Channel 1- PCF C and (b) Channel 2-PCF D

The value of BER for Channel 1 with PCF equalization is computed as 3.6292×10^{-19}, 2.5599×10^{-11} and 5.0078×10^{-7} as compared to without PCF equalization for which it is noted as 3.3421×10^{-6}, 2.4526×10^{-1} and 1 at the FSO transmission link of 1000 m, 2000 m and 2500 m respectively.

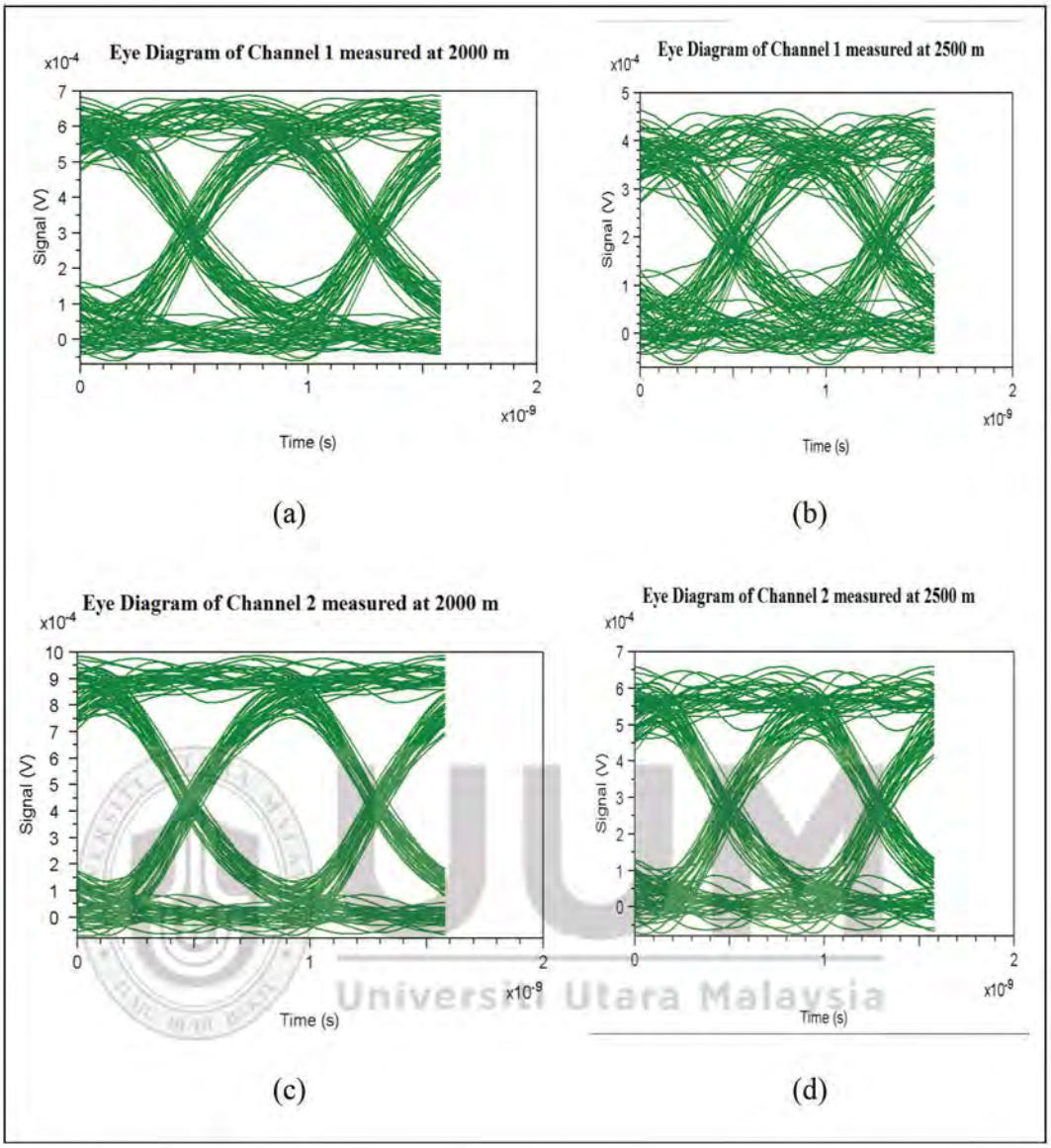

Figure 5.10. Measured Diagrams (a) Channel 1 at 2000 m (b) Channel 1 at 2500 m (c) Channel 2 at 2000 m and (d) Channel 2 at 2500 m

Consequently, the value of BER for Channel 2 with PCF equalization is computed as 1.1828×10^{-19}, 1.1695×10^{-15} and 4.0422×10^{-11} as compared to without PCF equalization for which it is noted as 2.4351×10^{-7}, 3.5434×10^{-1} and 1 at the FSO transmission link of 1000 m, 2000 m and 2500 m respectively. Figure 5.9 represents the received modes after PCF C and PCF D. The measured eye diagrams are shown in Figure 5.10 which indicates that with PCF equalization, the FSO link prolongs to 2.5 km with acceptable BER and eye diagrams.

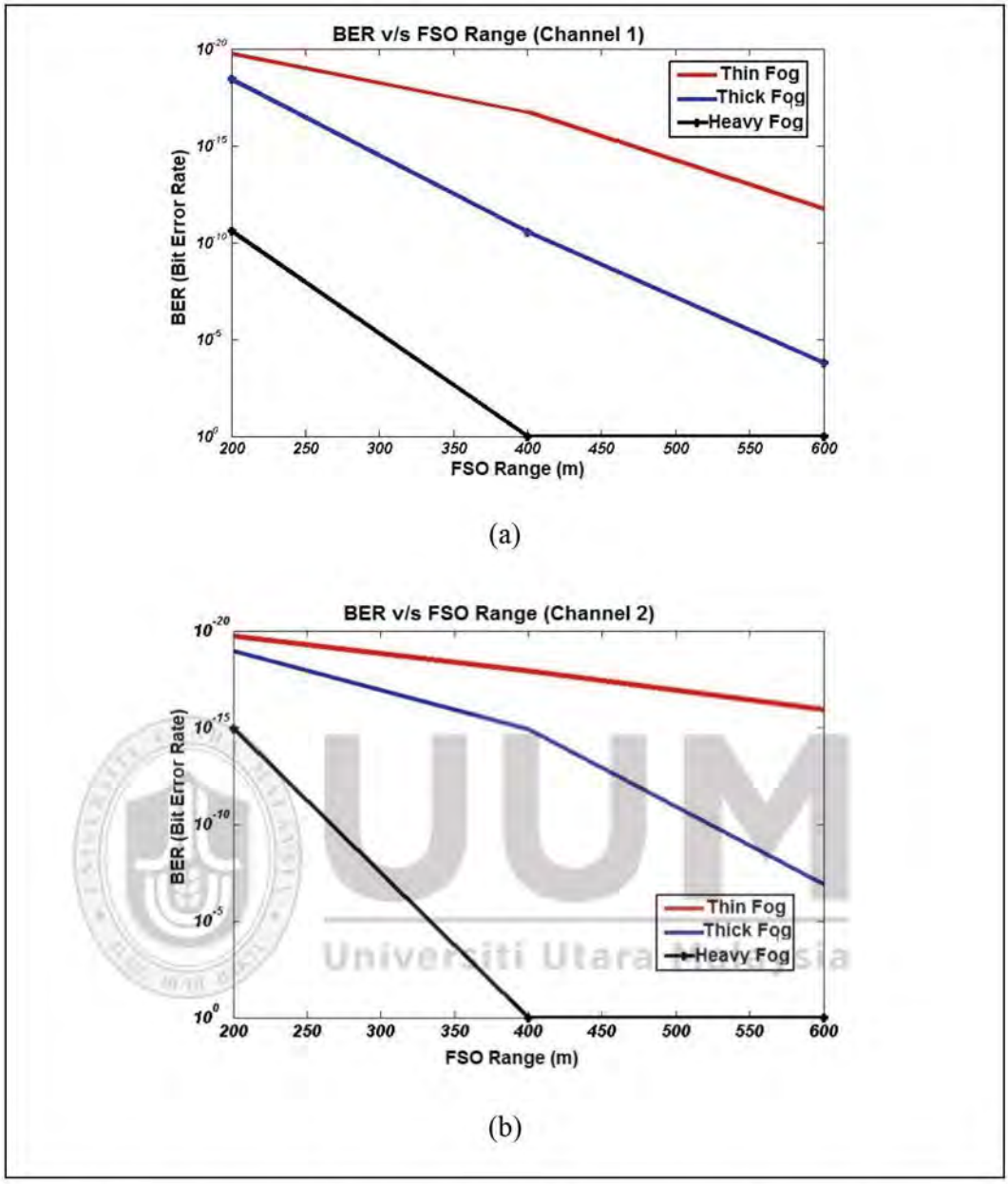

Figure 5.11. Evaluation of Proposed PCF-MDM Transmission System under atmospheric turbulences (a) Channel 1 and (b) Channel 2

Similarly, Figure 5.11 represents evaluation of proposed PCF-MDM transmission system under the influence of atmospheric turbulences. It indicates that under influence of thin fog the value of BER for Channel 1 is computed as 1.7157×10^{-20} and 1.9138×10^{-12} ; under thick fog it is 3.7344×10^{-19} and 1.6031×10^{-4} ; under heavy fog it is 2.5599×10^{-11} and 1 whereas for Channel 2, under influence of thin fog, it is computed as 1.8737×10^{-20} and 1.2229×10^{-16}; under thick fog it is 1.2026 x

10^{-19} and 1.2471 x 10^{-7}; under heavy fog it is 1.1695 x 10^{-15} and 1 at FSO transmission link of 200 m and 600 m. Thus under atmospheric turbulences, the FSO link for Channel 1 and Channel 2 prolongs to 600 m under thin fog, 400 m under thick fog and 200 m under heavy fog with acceptable BER.

In this work, two independent channels, each carrying 2.5 Gbps-5 GHz NRZ encoded data, operated on LG 01 in conjunction with PCF A and LG 02 in conjunction with PCF B are transmitted over FSO link having span of 2.5 km. The results are reported in terms of received spatial profiles of transmitted modes, mode spectrum at receiver side, BER and eye diagrams. It is concluded from the reported results that each channel is transmitted and received successfully over 2.5 km FSO link with acceptable BER and eye diagrams. The use of PCF both at transmitter side as well as receiver side shows significant improvement in data transmission. Under clear weather conditions, the FSO link for both channels prolongs to 2.5 km with acceptable BER whereas when atmospheric conditions are changes to thin Fog, it prolongs to 600 m; for thick Fog it prolongs to 400 m; for heavy fog it prolongs to 200 m with acceptable BER.

5.2 Case 2: 3 x 2.5Gbps-5GHz MDM-PCF-Ro-FSO Transmission System

In this case, three channels are transmitted by using three single core PCFs at transmitter side and received by using three single core PCF's at receiver side. Section 5.2.1 discusses the simulation setup whereas Section 5.2.2 discusses the results and discussion.

5.2.1 Simulation Setup

Figure 5.12 represents the schematic diagram of proposed MDM-PCF-Ro-FSO transmission system. The proposed system is modelled in OptSim™ and BeamProp™ software.

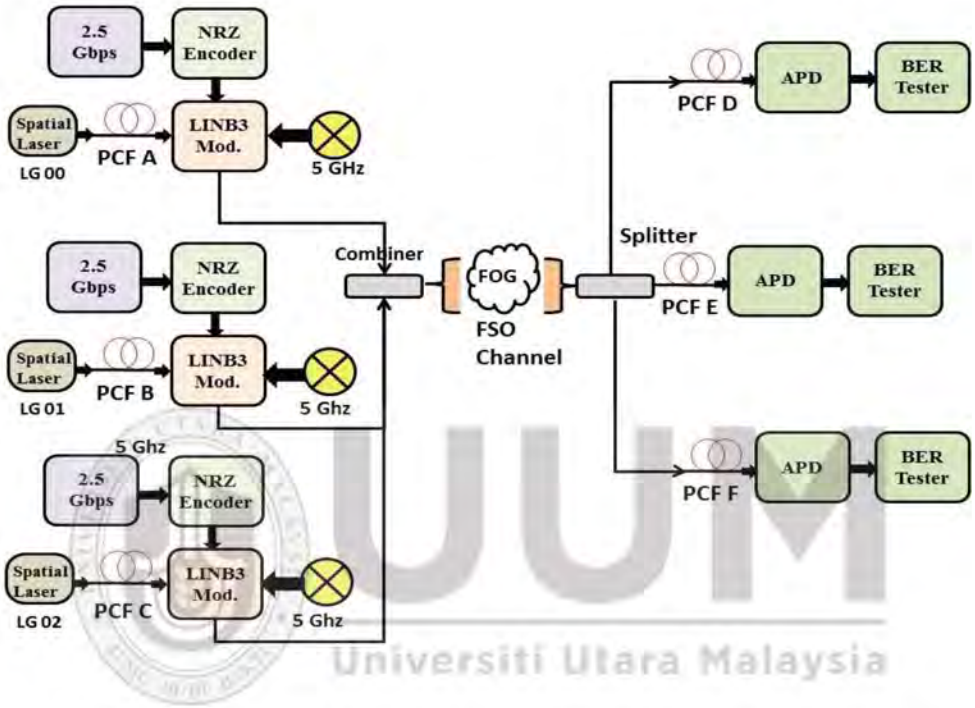

Figure 5.12. 3 x 2.5Gbps-5GHz MDM-PCF-Ro-FSO Transmission System

As shown in Figure 5.12, PCF A, PCF B and PCF C are used to transmit three channels carrying 2.5 Gbps-5 GHz data. Channel 1 is operated on LG 00 mode in conjunction with PCF A having effective index of 1.45, Channel 2 is operated on LG 01 mode in conjunction with PCF B having effective index of 1.47 whereas Channel 3 is operated on LG 02 mode in conjunction with PCF C having effective index of 1.47. LG 00, LG 01 and LG 02 modes are generated from spatial lasers.

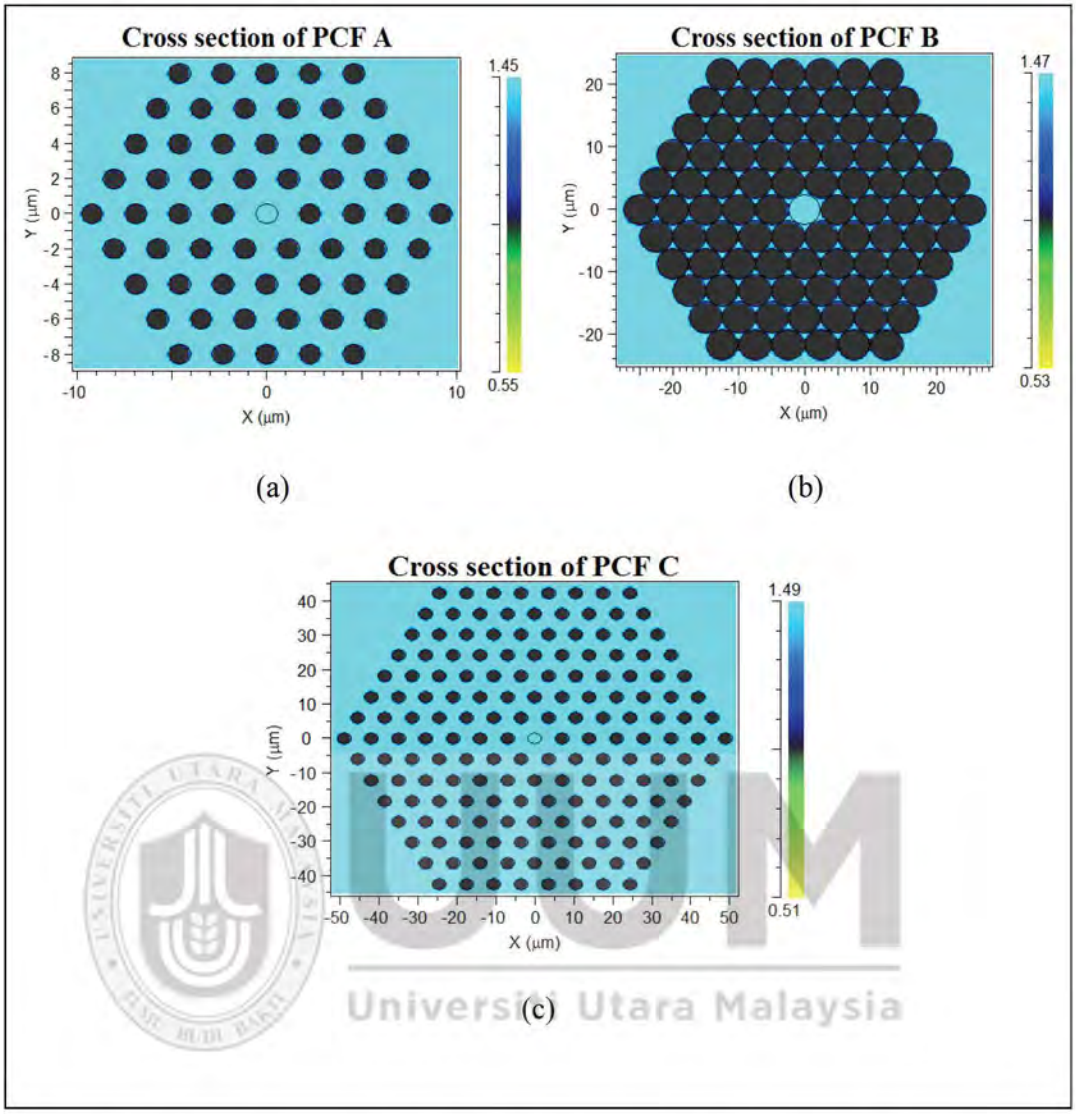

Figure 5.13. Core Structure of PCF at Transmitter Side (a) PCF A (b) PCF B and (c) PCF C

Figure 5.13 shows the core structure whereas Figure 5.14 represents the computed mode spectrum analysis of PCF A, PCF B and PCF C.

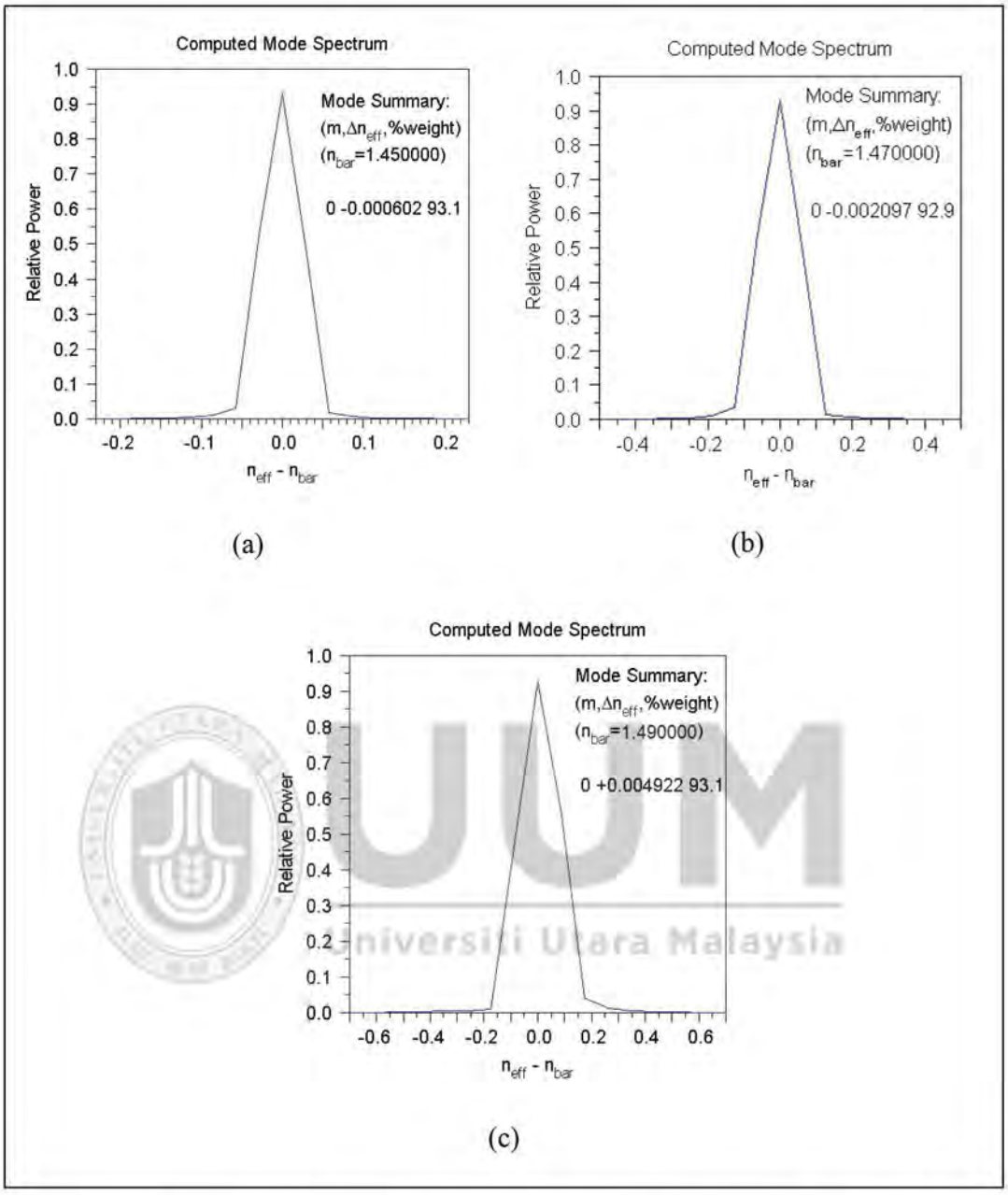

Figure 5.14. Computed Mode spectrum of PCF at Transmitter Side (a) PCF A (b) PCF B and (c) PCF C

As shown in Figure 5.14, when LG 00 mode is launched into PCF A, 93.1% of power is measured in dominating mode at its output; when LG 01 is launched into PCF B, 93% of power is measured in dominating mode at its output whereas when LG 02 is launched into PCF C, 92% of power is measured in dominating mode at its output.

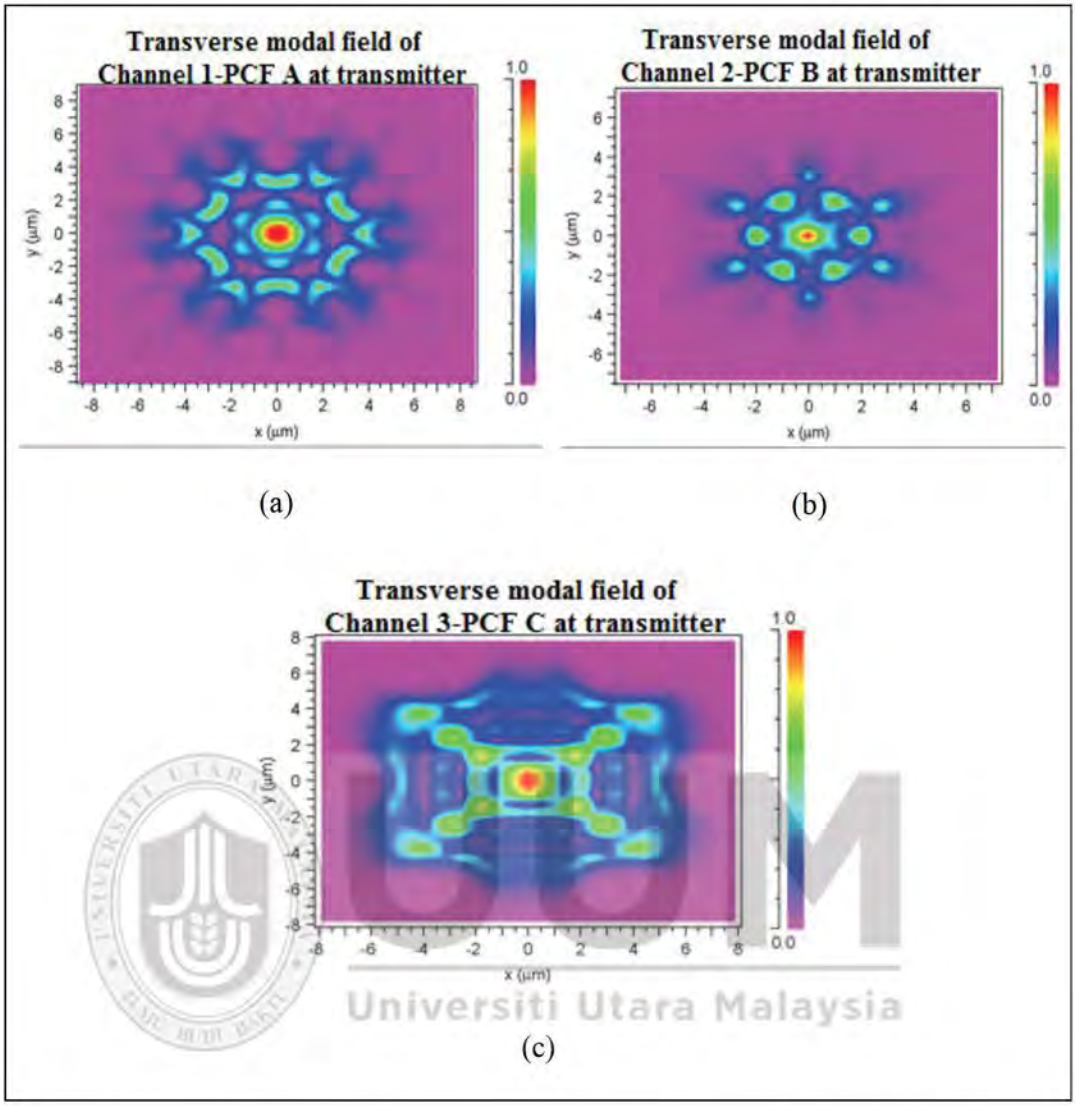

Figure 5.15. Spatial profiles of transverse modes at output (a) PCF A (b) PCF B and (c) PCF C

The output of all channels are combined together and transmitted over FSO link having a span of 2.5 km. The spatial profile of output modes from PCF A, PCF B and PCF C at transmitter side is shown in Figure 5.15.

At the receiver, splitter is used to split the signal into PCF D, PCF E and PCF F for decomposition of transmitted modes. The internal core structures of PCF D, PCF E and PCF F are slightly different and flipped from PCF A, PCF B and PCF C in order to select relevant mode with relevant effective indexes as shown in Figure 5.16.

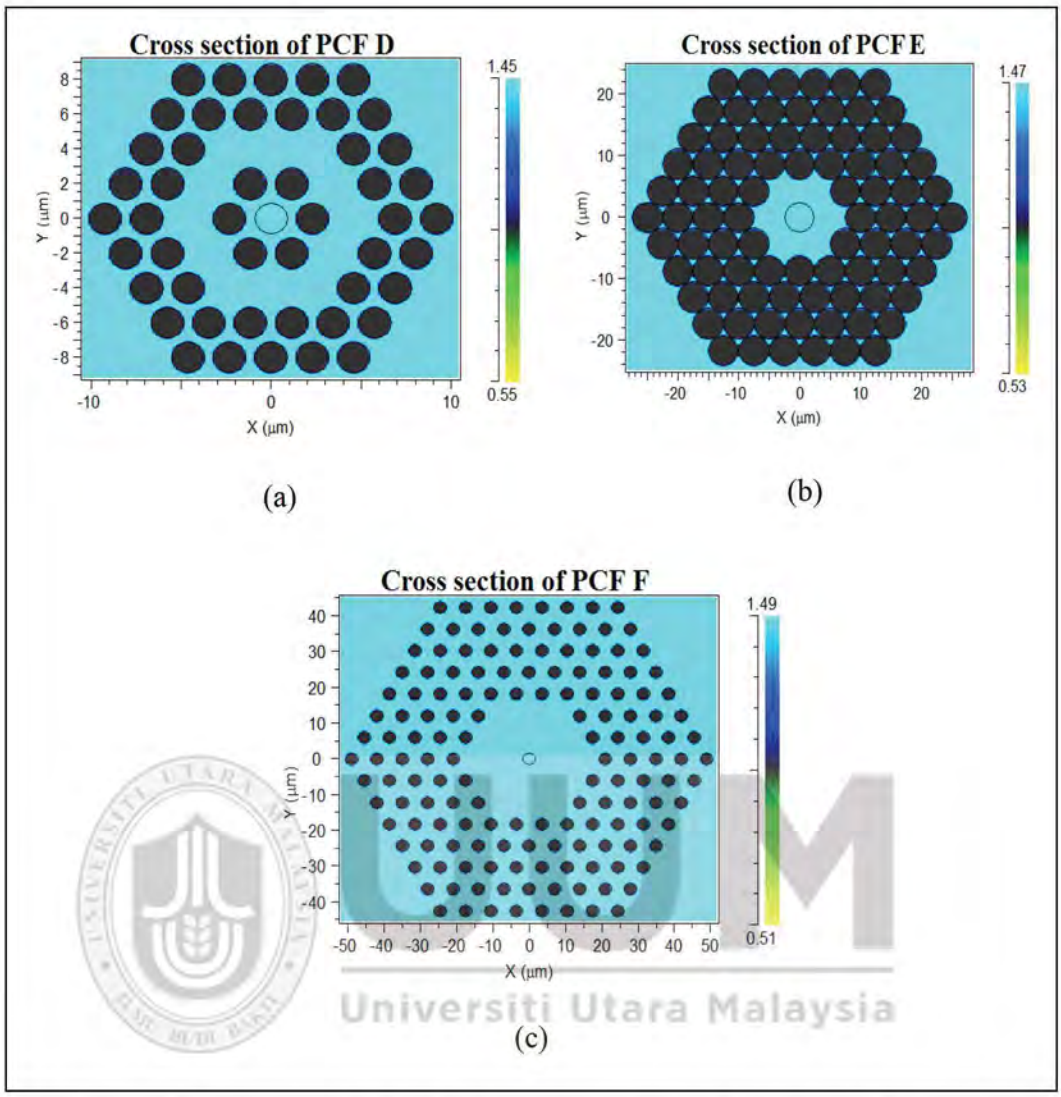

Figure 5.16. Core Structures of PCF at receiver side (a) PCF D (b) PCF E and (c) PCF F

Table 5.2

Parameters of SC-PCFs

Parameters	PCF A	PCF B	PCF C	PCF D	PCF E	PCF F
No of Rings	4	5	7	4	5	7
Diameter of Air Holes, d (μ m)	1	2	1	1.6	2	1
Distance between air holes, g (μ m)	2.3	5	7	2.3	5	7
Distance between Air holes/diameter of holes	2.3	2.5	7	1.4375	2.5	7

The other parameters of PCFs at transmitter as well as receiver are shown in Table 5.2

5.2.2 Results and Discussion

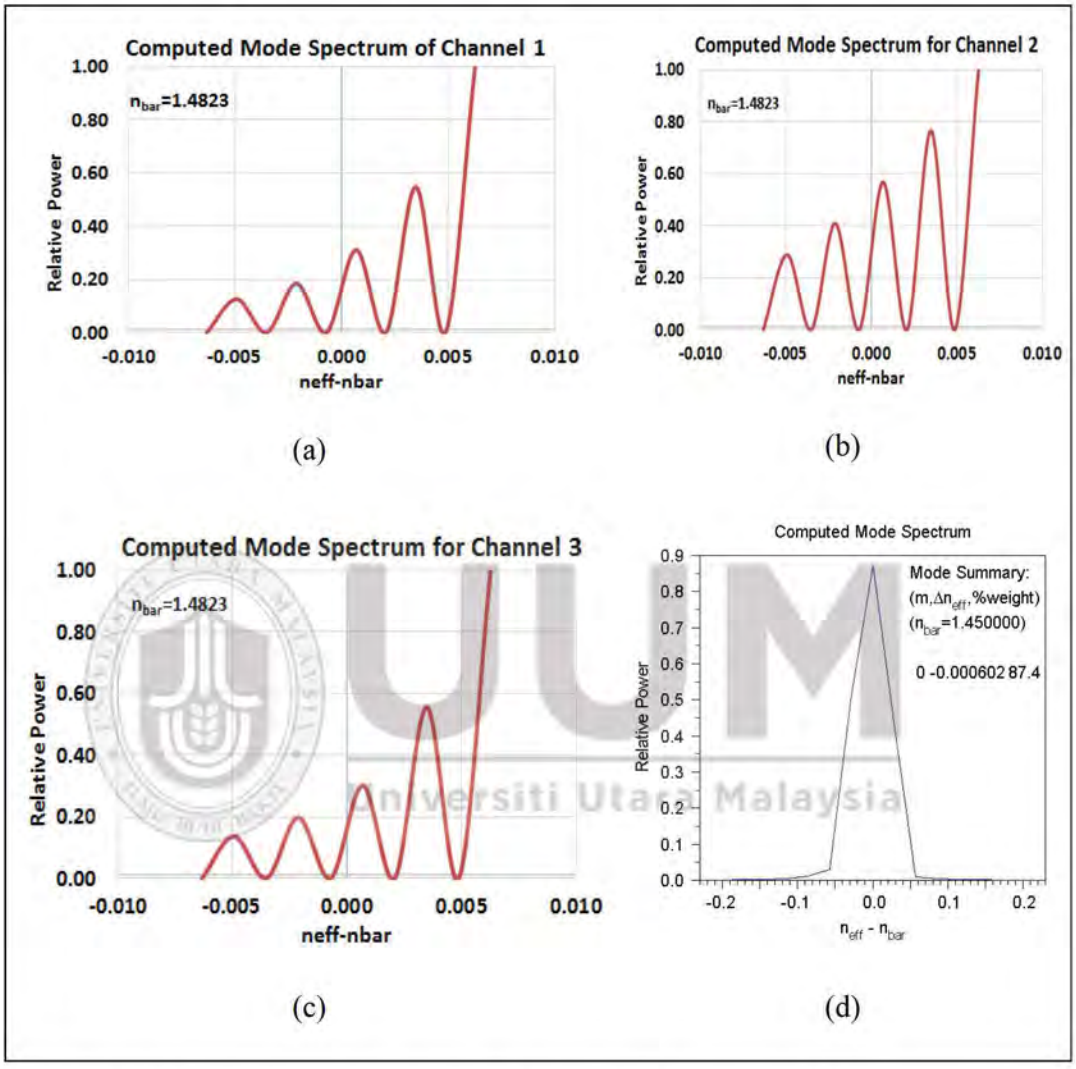

Figure 5.17. Computed mode spectrum at Receiver (a) Before PCF D (b) Before PCF E, (c) Before PCF F, (d) After PCF D, (e) After PCF E and (f) After PCF F

Figure 5.17 continued.

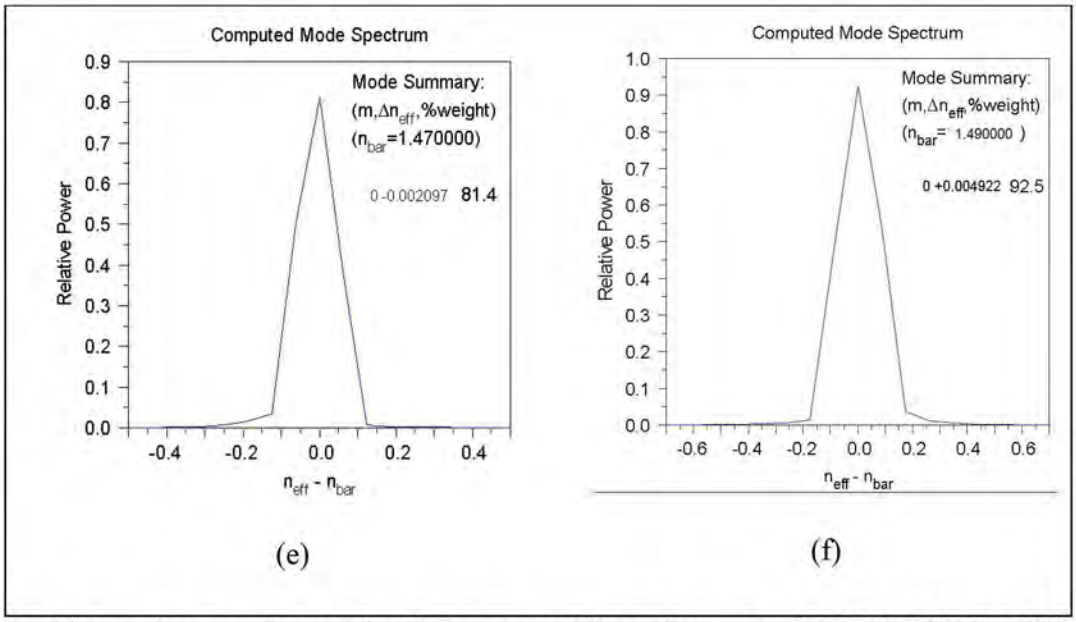

In this section, results obtained from modelling of proposed MDM-PCF-Ro-FSO transmission system is presented and discussed. It shows that 87.4% of power is received in dominant mode at output of PCF D with effective index of 1.45 as compared to 20 % of power in dominant mode before PCF D, 81.4% of power is achieved in dominant mode at output of PCF E with effective index of 1.47 as compared to 40 % in dominant mode before PCF E and 92.5% of power is received in

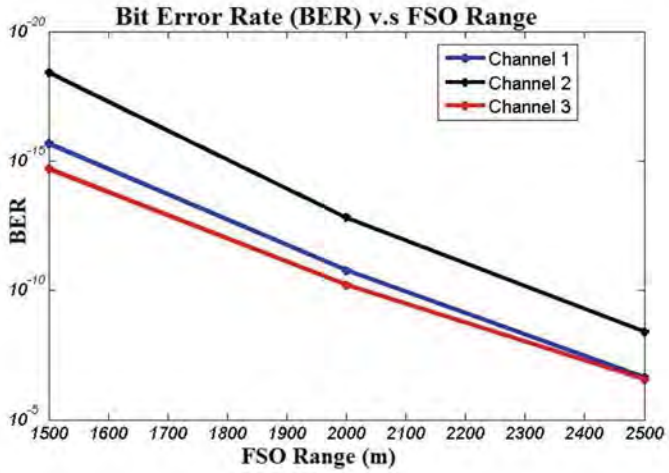

Figure 5.18. BER vs. FSO Range

dominant mode at output of PCF F with effective index of 1.49 as compared 20 % of power in dominant mode before PCF F. Figure 5.18 shows the measured BER against FSO range under clear weather conditions.

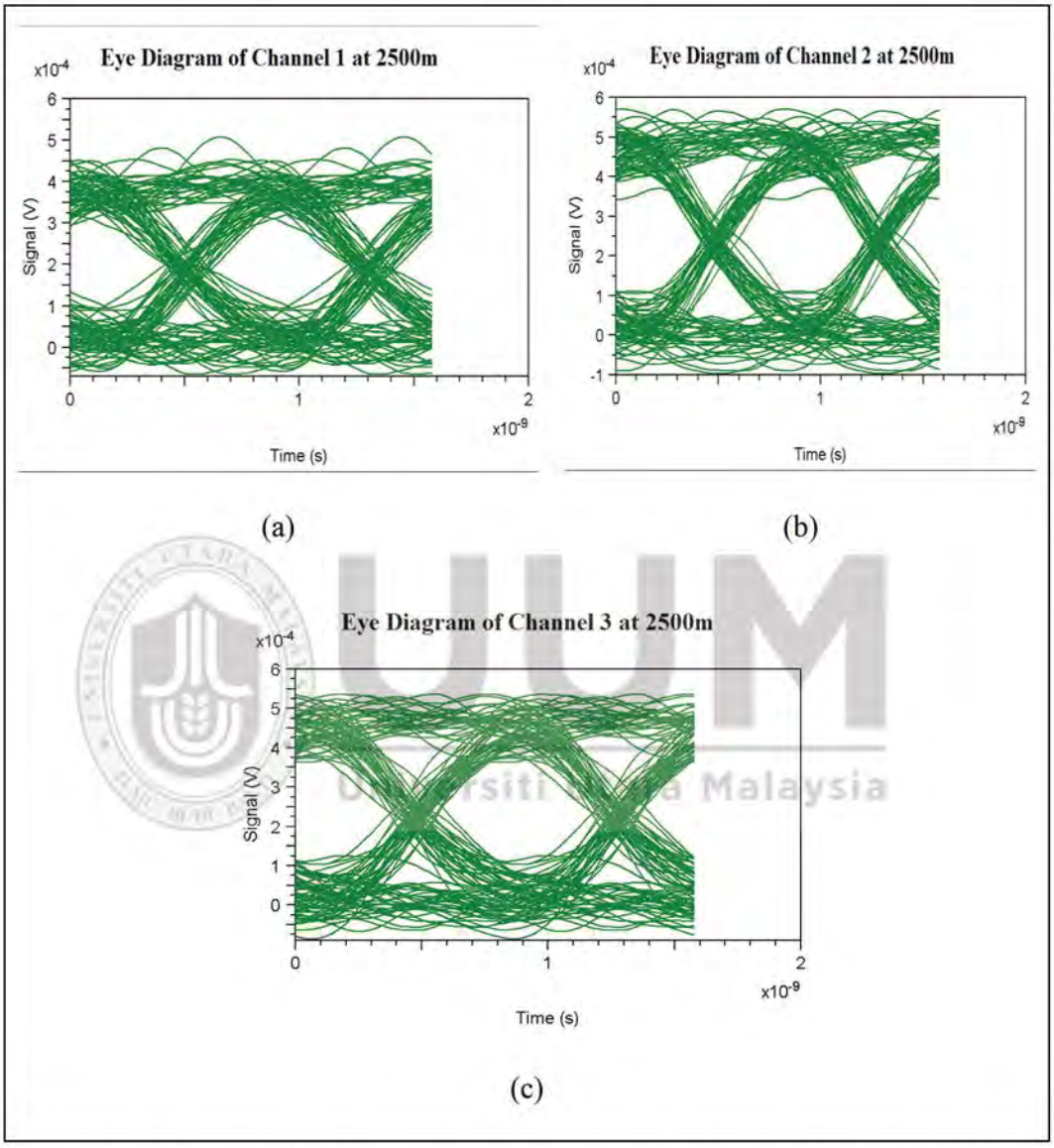

Figure 5.19. Measured Eye Diagrams at 2500 m FSO link (a) Channel 1 (b) Channel 2 and (c) Channel 3

The value of SNR for Channel 1 is computed as 2.1495×10^{-16}, 1.7159×10^{-11} and 2.2444×10^{-7}; for Channel 2 it is computed as 3.8812×10^{-19}, 1.5679×10^{-13} and 4.0713×10^{-9}; for Channel 3 it is computed as 2.0172×10^{-15}, 6.3333×10^{-11} and 2.8230×10^{-7} at FSO range of 1500m, 2000m and 2500m. The measured eye diagrams for Channel 1, Channel 2 and Channel 3 at 2500 m FSO transmission link in

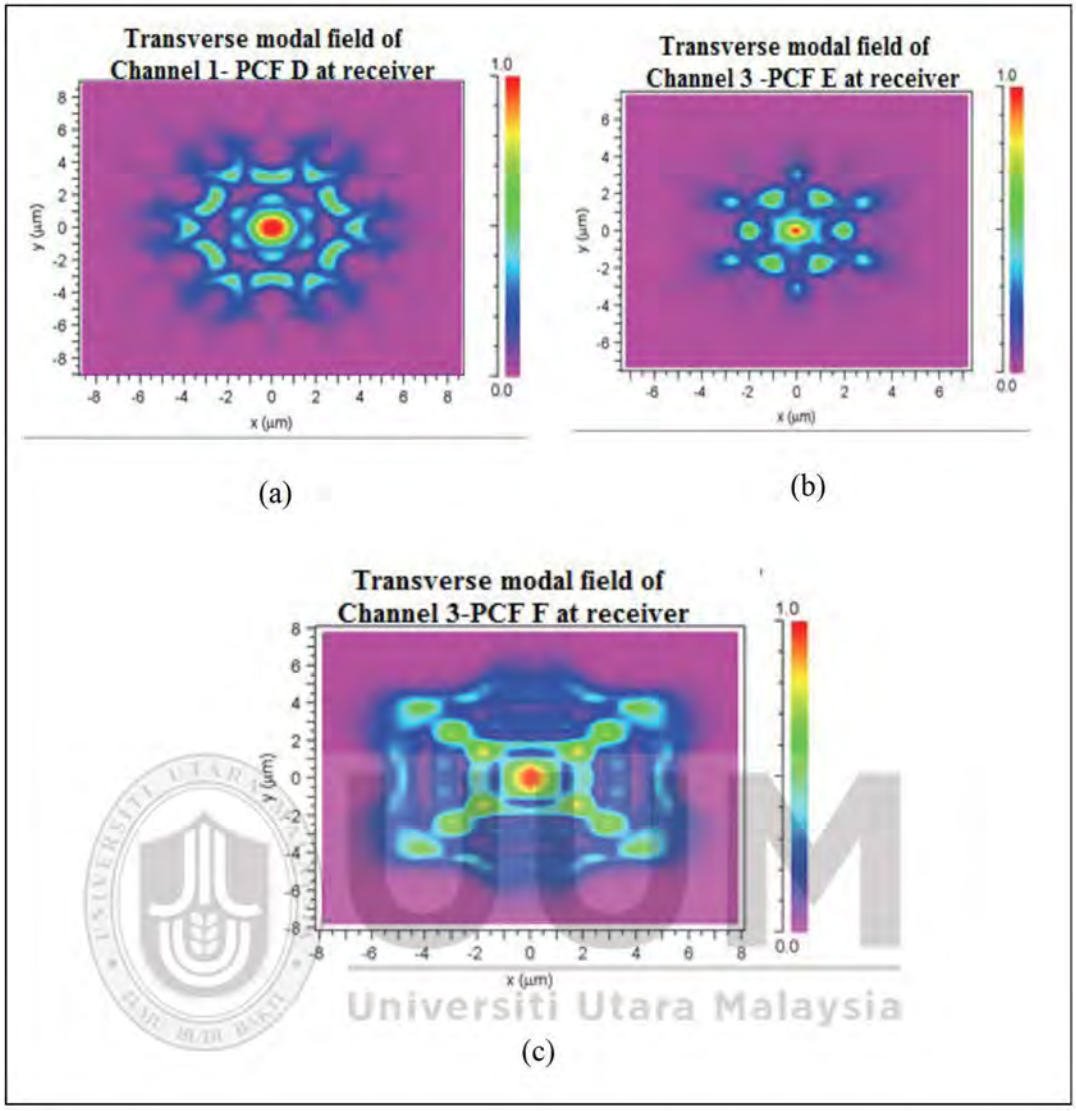

Figure 5.20. Measured Spatial Profiles at Receiver (a) PCF D (b) PCF E and (c) PCF F

Figure 5.19 shows that all channels are transmitted and received successfully under clear weather conditions. Figure 5.20 represents measured spatial profile of received modes for PCF D, PCF E and PCF F. The evaluation of proposed 3 x 2.5Gbps-5GHz MDM-PCF-Ro-FSO transmission system under atmospheric turbulences is shown in Figure 5.21. It indicates that under influence of thin fog the value of BER for Channel 1 is computed as 1.0693×10^{-20} and 1.6865×10^{-12}; under thick fog it is 3.7741×10^{-19} and 1.1525×10^{-3}; under heavy fog it is 1.7519×10^{-11} and 1 ; for Channel 2, under influence of thin fog it is computed as 1.1252×10^{-20} and 1.1186 x

10^{-14}; under thin fog it is 2.1573 x 10^{-22} and 1.7647 x 10^{-4}; under heavy fog it is 1.5679 x 10^{-13} and 1 whereas for Channel 3, under influence of thin fog it is computed as 2.5500 x 10^{-20} and 8.0043 x 10^{-12}, under thin fog, it is computed as 2.8995 x 10^{-18} and 7.8301 x 10^{-4}, under heavy fog, it is computed as 6.3333 x 10^{-11} and 1 at FSO

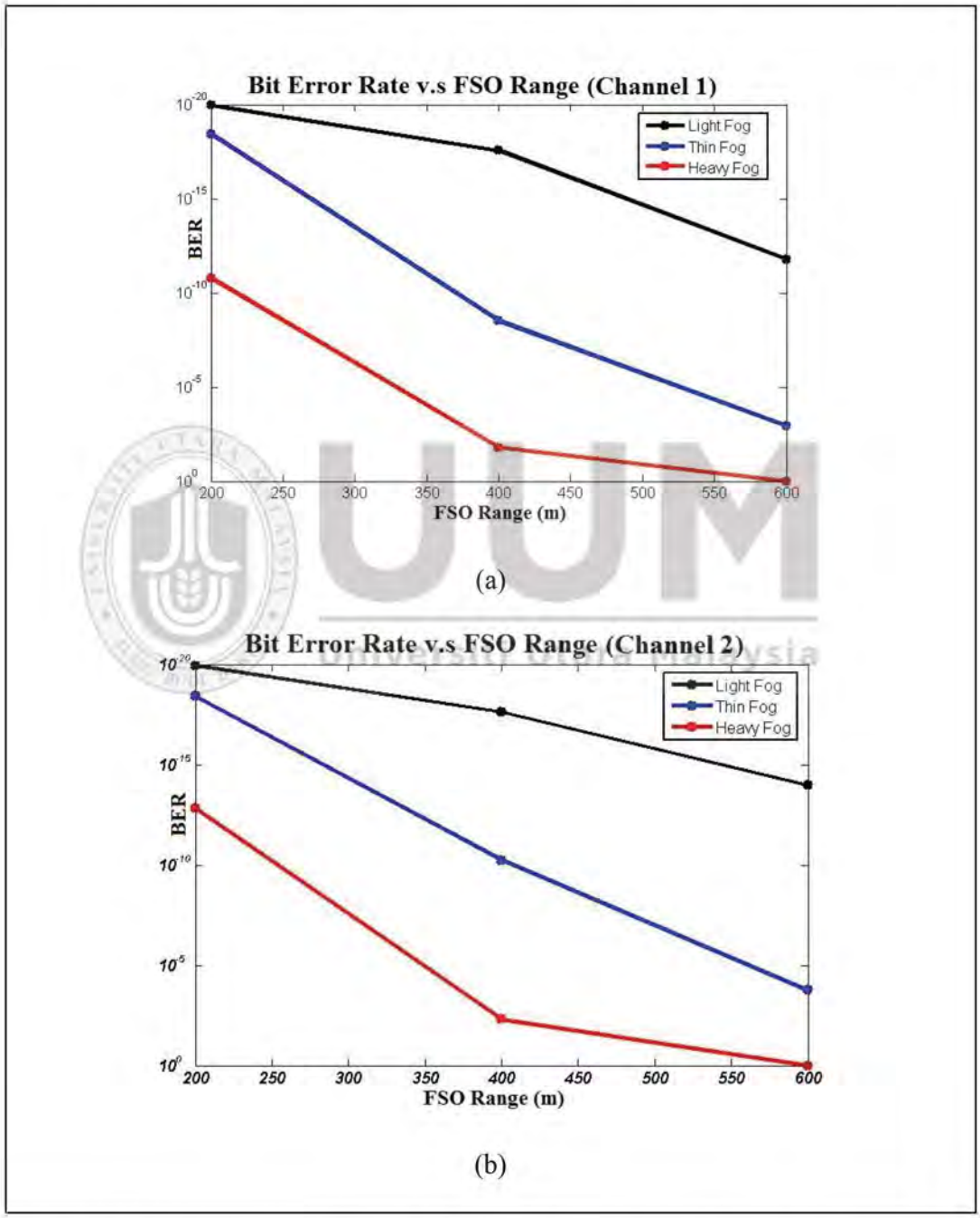

Figure 5.21. Evaluation of proposed MDM-PCF transmission system under atmospheric turbulences (a) Channel 1 (b) Channel 2 and (c) Channel 3

Figure 5.21 continued.

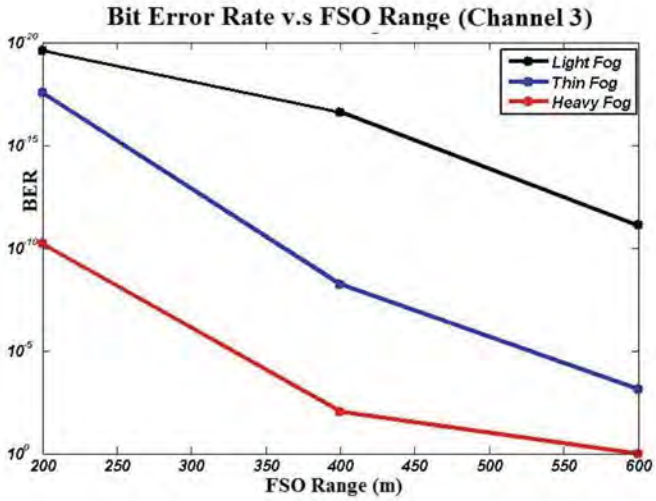

(c)

transmission link of 200 m and 600 m. It indicates that FSO link prolongs to 600 m under light fog, 400 m under thin fog whereas it prolongs to only 200 m under the influence of heavy fog.

In this work three independent channels, each carrying 2.5 Gbps-5 GHz data, are transmitted over 2.5 km FSO link by adopting MDM in conjunction with SC-PCF. Three PCFs are used to transmit three channels with different effective indexes whereas three PCFs are used to receive and separate channels with same effective indexes at receiver side. The results from modelling of proposed MDM-PCF-Ro-FSO transmission system show successful transmission of all channels with acceptable BER. It is reported that under clear weather conditions, FSO link prolongs to 2.5 km. When the atmosphere changes to light fog, FSO link prolongs to 600 m and when it changes to thin fog, the FSO link prolongs to 400 m whereas when atmosphere changes to heavy fog, FSO prolongs to only 200 m.

5.3 Case 3: Two Mode Dual core PCF-Ro-FSO Transmission System

In this case, two Ro-FSO channels are transported over FSO link by using one dual core PCF at transmitter side and received by using two single core PCF at receiver side. Section 5.3.1 discusses the simulation setup whereas Section 5.3.2 discusses the results and discussion.

5.3.1 Simulation Setup

Figure 5.22 below shows the proposed MDM-PCF-Ro-FSO system simulated in Opt-Sim™ and Beam-Prop™ software.

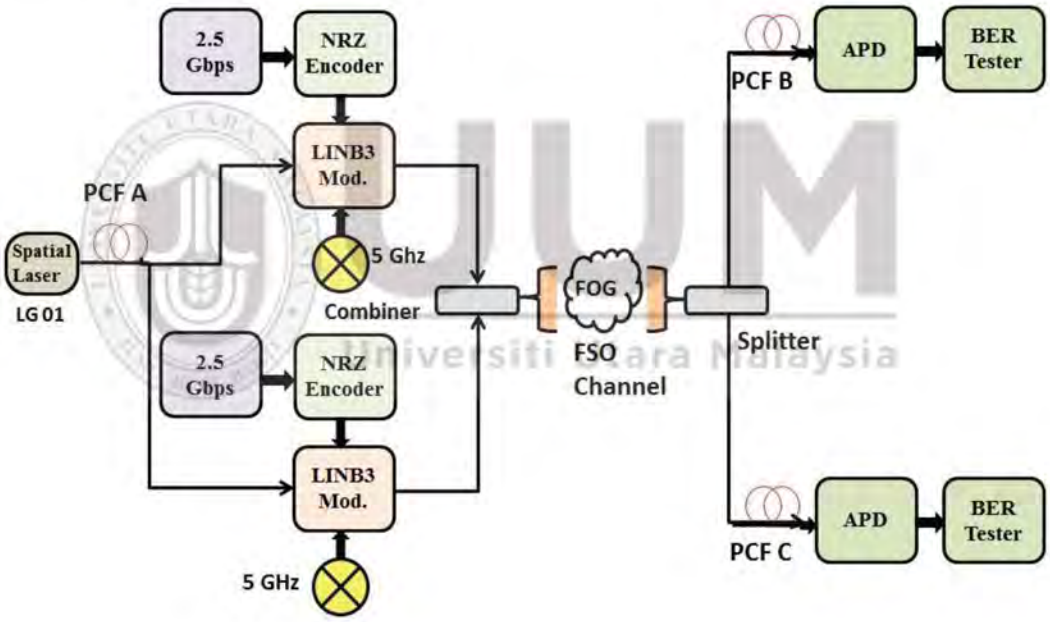

Figure 5.22. Two mode MDM-PCF-Ro-FSO Transmission System

The schematic diagram shows the transmission of two independent non return to zero (NRZ) encoded channels over 2 km free-space link using selective excitation from two different PCFs. LiNB3 optical modulator is used for modulating 2.5 Gbps-5 GHz in each of these channels.

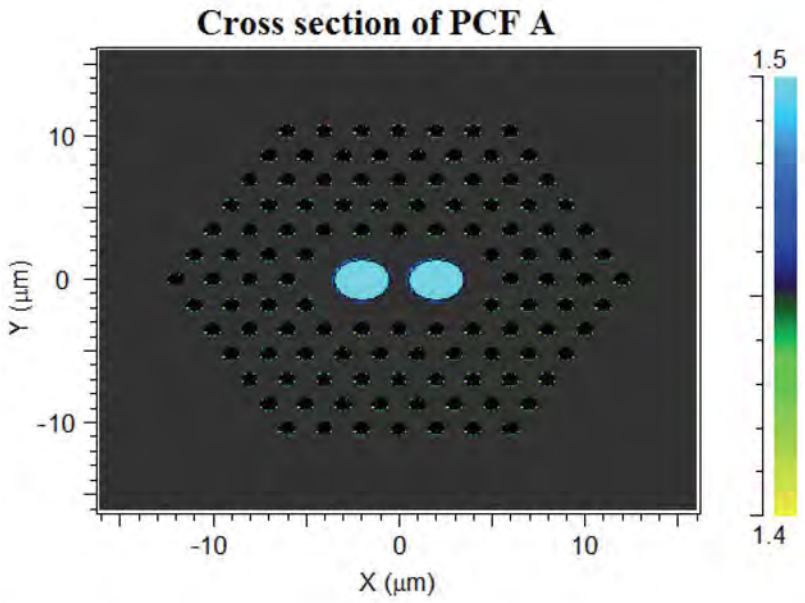

Figure 5.23. Structure of Dual Core PCF A

Spatial laser then excites LG 01 mode. Dual core PCF A is used to generate two distinct modes with effective index of 1.426796 and 1.476784. Figure 5.23 shows the internal structure of dual core PCF A.

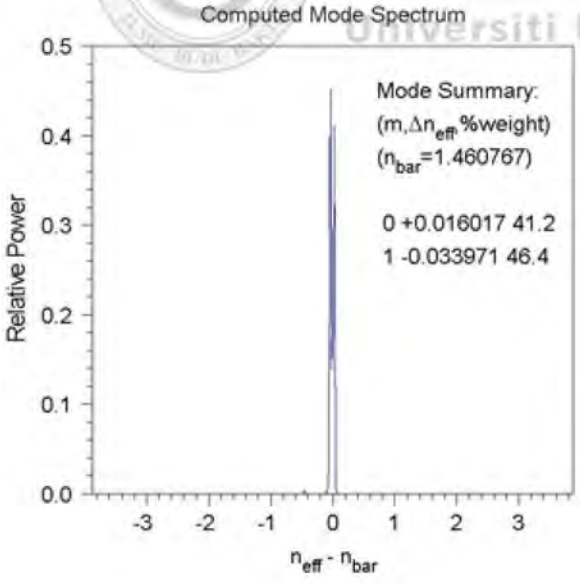

Figure 5.24. Computed Mode Spectrum of Dual Core PCF A

Figure 5.24 represents the computed mode spectrum at output of dual core PCF A which shows that with the launch of LG 01 into PCF A, the output power of PCF A is

computed as 46.4% with the effective index of 1.426796 and 41.2% with effective index of 1.476784 in dominant mode. The output of PCF A is fed to two channels, each carrying 2.5 Gbps-5 GHz data.

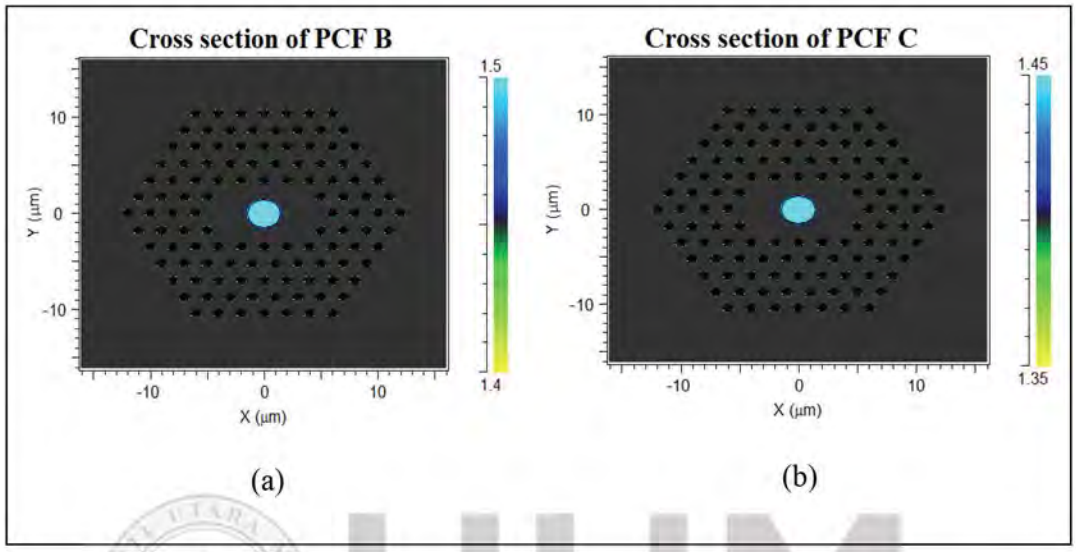

Figure 5.25. Internal Structure of PCFs at Receiver Side (a) PCF B and (b) PCF C

Table 5.3

Parameters of PCFs at Transmitter Side

Parameters	**PCF A**	**PCF B**	**PCF C**
No of Rings	7	7	7
Diameter of Air Holes, d (μm)	0.75	0.75	0.8
Distance between air holes, g (μm)	2	2	7
Ratio of Distance between Air holes to diameter of air holes, g/d	2.66	2.66	8.75
Background Index	1.45	1.45	1.44

At the receiving side, the optical beam is split into PCF B and PCF C using splitter for decomposing the transmitted modes. Figure 5.25 shows the structure of PCF B and PCF C. The other parameters of PCF A, PCF B and PCF C are described on Table 5.3. Further, spatial photodetector and Bit error rate tester are used for converting the optical beam into electrical signal.

5.3.2 Results and Discussion

This section represents the results obtained from simulation set up of proposed dual core PCF-Ro-FSO transmission system. Figure 5.26 represents the measured spectrum after the PCFs at receiving side. It has been reported that 96.7 % of optical power in dominating mode is achieved at output of PCF B with effective index of 1.426796 as compared to 30 % of power in dominating mode before PCF B where as 96.3 % of power in dominating mode is achieved at output of PCF C with effective index of 1.476784 as compared to 30% of power before PCF C. Figure 5.27 represents the received modes at receiver sides after FSO link of 2 km. PCF B and PCF C are used to compensate lost power and attenuation introduced in FSO transmission channel.

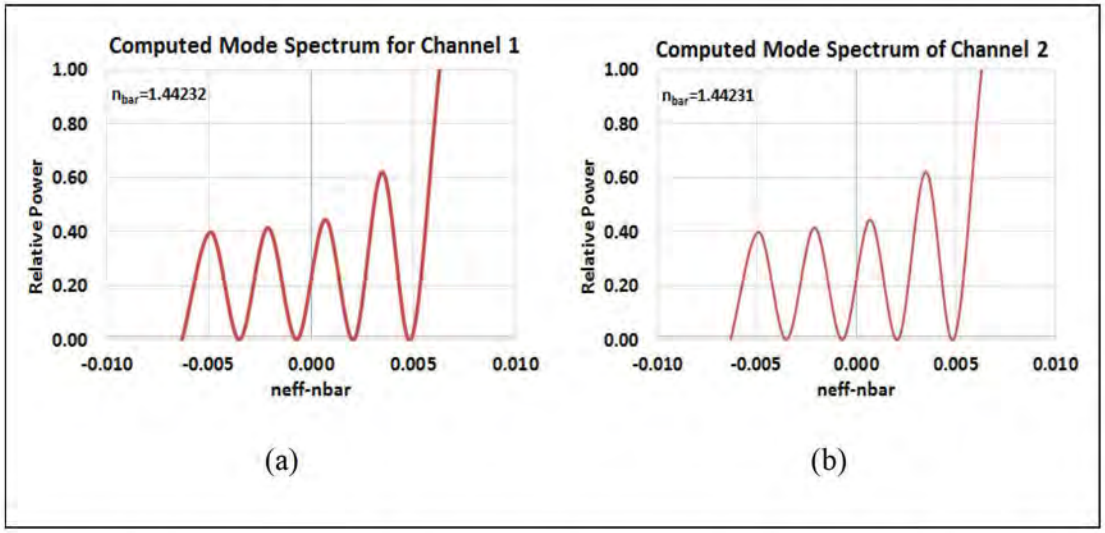

Figure 5.26. Computed Mode Spectrum at Receiver Side (a) Before PCF B (b) Before PCF C (c) After PCF B and (d) After PCF D

Figure 5.26 continued.

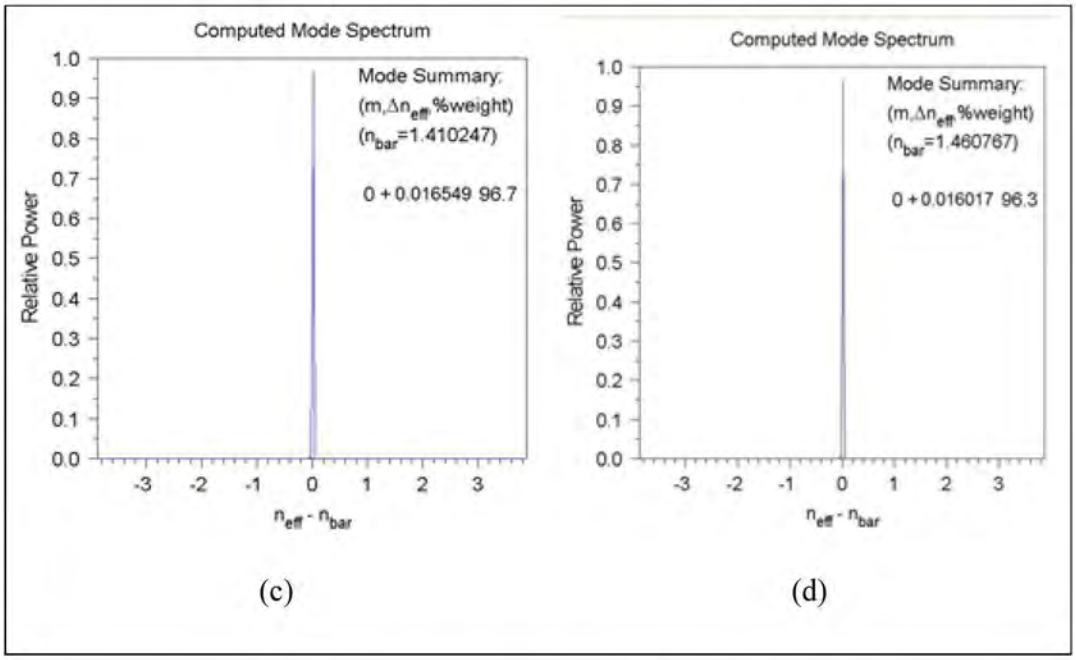

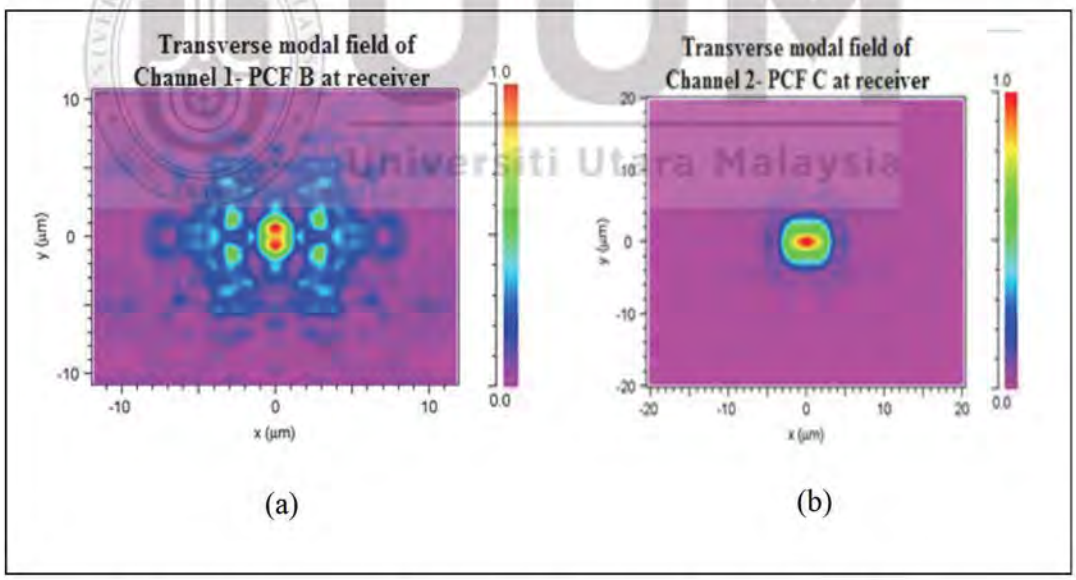

Figure 5.27. Received Modes at FSO link of 2 km (a) Channel 1- PCF B and (b) Channel 2-PCF C

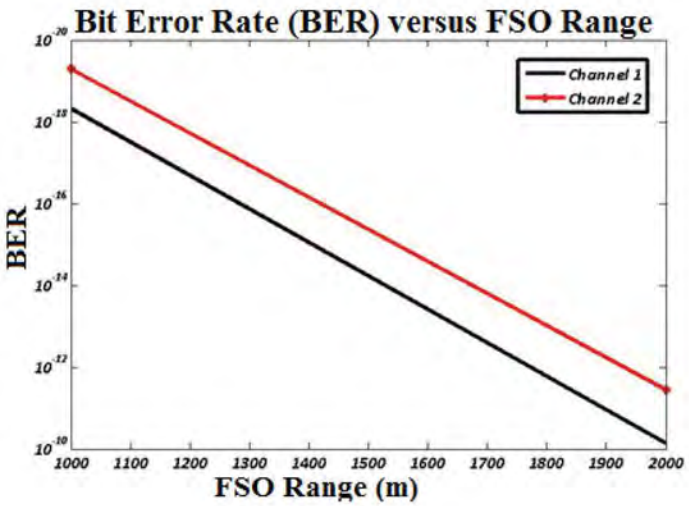

Figure 5.28. Measured BER under clear weather conditions

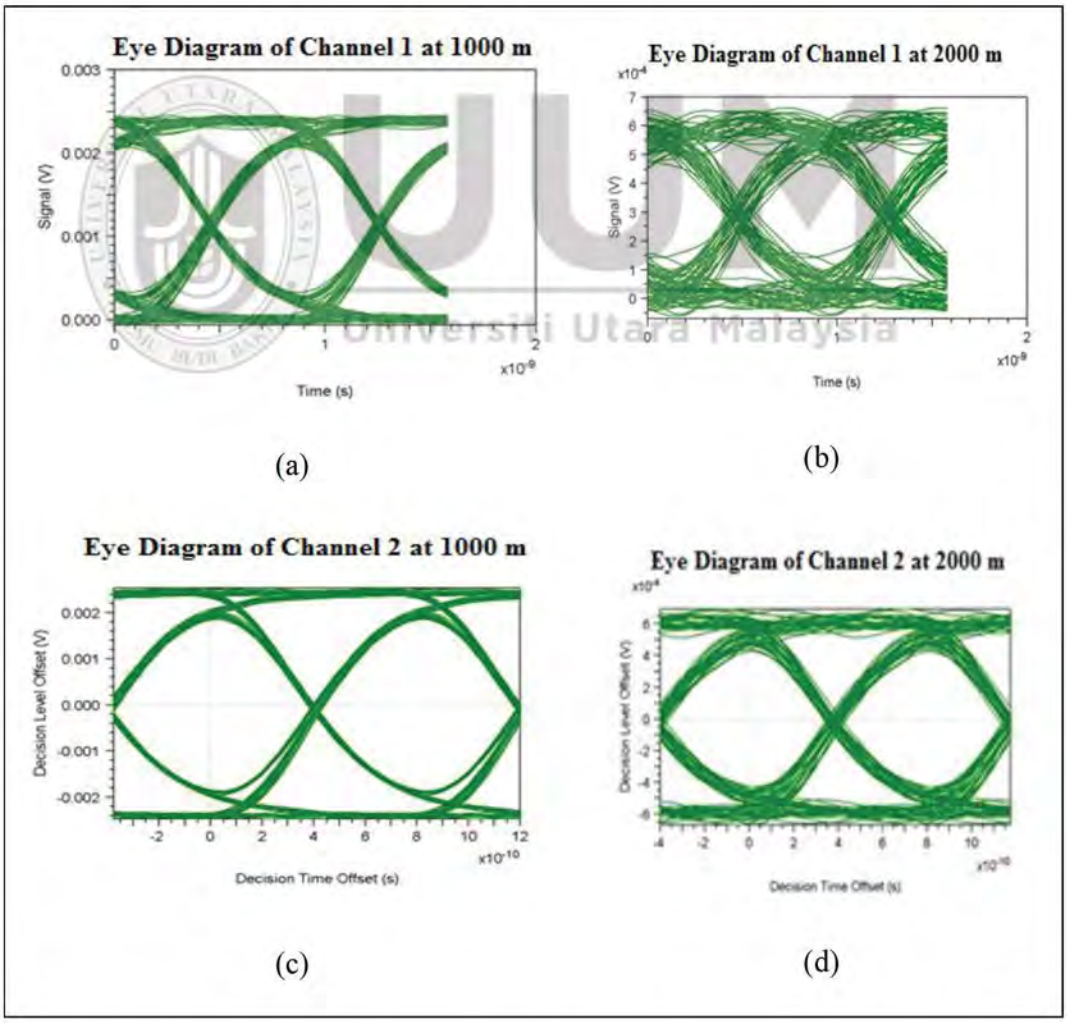

Figure 5.29. Measured Eye Diagrams under clear weather conditions (a) Channel 1 at 1000 m (b) Channel 1 at 2000 m (c) Channel 2 at 1000 m and (d) Channel 2 at 2000 m

It is noted that the value of BER for Channel 1 is computed as 4.7493 x 10^{-19} and 7.3630 x 10^{-11} as compared to the Channel 2 for which it is noted as 5.1704 x 10^{-20} and 3.5871 x 10^{-12} at the FSO transmission link of 1000 m and 2000 m respectively. The measured eye diagrams in Figure 5.29 clearly show that Channel 1 and Channel 2 transmit successfully over 2 km FSO link under clear weather conditions.

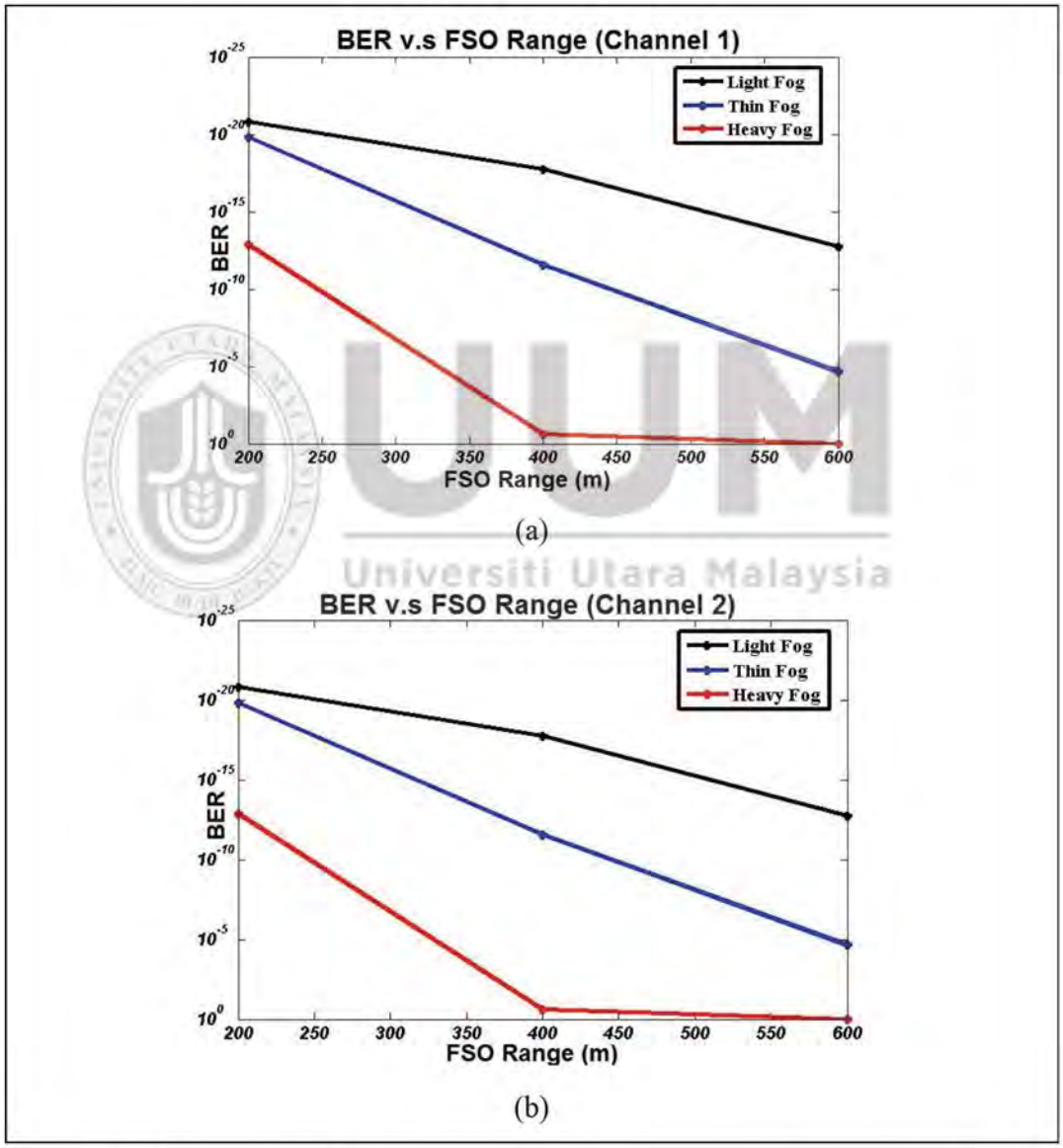

Figure.5.30. Measured BER under atmospheric turbulences (a) Channel 1 and (b) Channel 2

Figure 5.30 represents the measured BER at receiver side under the impact of atmospheric turbulences. It indicates that under influence of light fog the value of

BER for Channel 1 is computed as 1.5487×10^{-20} and 1.9578×10^{-12}; under thin fog it is 3.5687×10^{-19} and 1.3476×10^{-4}; under heavy fog it is 2.6748×10^{-12} and 1; for channel 2, under influence of light fog it is computed as 1.5634×10^{-21} and 1.9213×10^{-13}; under thick fog it is 1.5435×10^{-20} and 2.3181×10^{-5}; under heavy fog it is 1.4587×10^{-13} and 1 at FSO transmission link of 200 m and 600 m.

In this work, two independent channels, each carrying 2.5 Gbps-5 GHz NRZ encoded data, operated on LG 01 in conjunction with dual core PCF A, with effective indexes of 1.426796 and 1.476784, are transmitted over FSO link having span of 2 km. The results are reported in terms of received spatial profiles of transmitted modes, mode spectrum at receiver side, BER and eye diagrams. It is concluded from the reported results that each channel is transmitted and received successfully over 2 km FSO link with acceptable BER and eye diagrams. The use of dual core PCF at transmitter side as well as single core PCF at receiver side shows significant improvement in data transmission. Under clear weather conditions, the FSO link prolongs to 2 km with acceptable BER. When the atmosphere changes to light fog, FSO link prolongs to 600 m and when it changes to thin fog, the FSO link prolongs to 400 m whereas when atmosphere changes to heavy fog, FSO prolongs to only 200 m only with acceptable BER.

5.4 Case 4: Three Mode three core PCF-Ro-FSO Transmission System

In this case, three Ro-FSO channels are transmitted by using single three core PCF over 2 km FSO link and received successfully by three single core PCF's. Section 5.4.1 discusses simulation setup whereas Section 5.4.2 discusses the results and discussion.

5.4.1 Simulation Setup

Figure 5.31 below shows the proposed MDM-PCF-Ro-FSO system simulated in Opt-Sim™ and Beam-Prop™ software. The schematic diagram shows the transmission of three independent non return to zero (NRZ) encoded channels by using three core PCF over 2 km free-space link and received by using selective excitation from three different PCFs. LiNB3 optical modulator is used for modulating 2.5 Gbps-5 GHz in each of these channels. Spatial laser then excites LG 01 mode. Three core PCF A is used to generate three distinct modes with effective index of 1.50, 1.40 and 1.01.

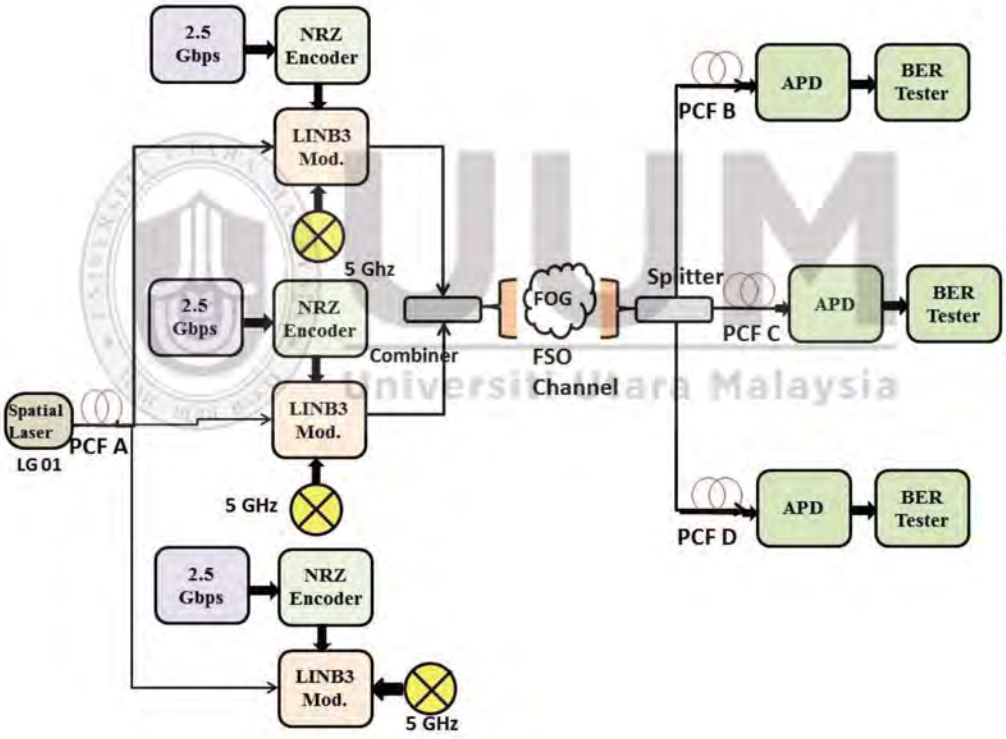

Figure 5.31. Three mode MDM-PCF-Ro-FSO Transmission System

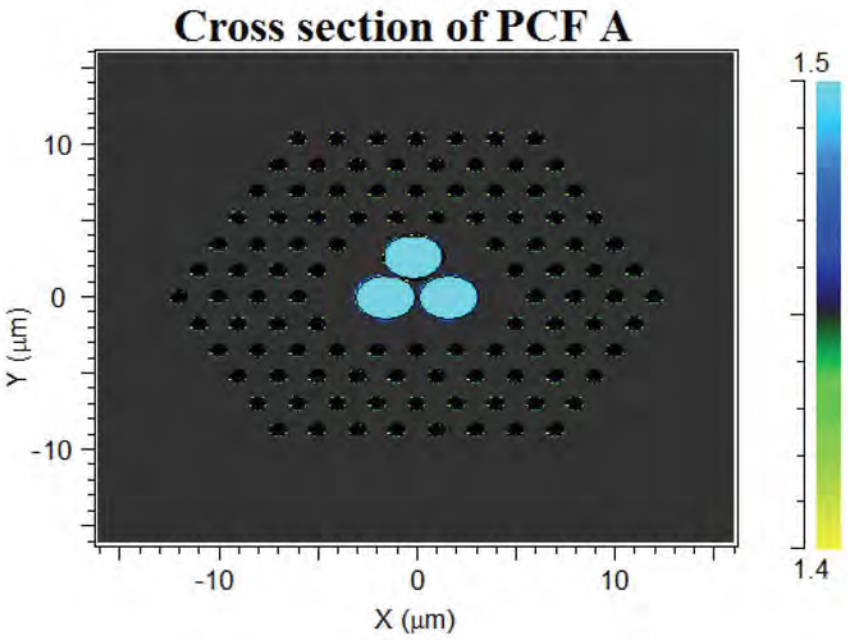

Figure 5.32. Structure of three core PCF A

Figure 5.31 shows the internal structure of dual core PCF A. The laser beam is coupled into 10 mm PCF structure. Figure 5.33 represents the computed mode spectrum at output of dual core PCF A which shows that with the launch of LG 01 into PCF A, the output power of PCF A is computed as 22 % in dominating mode with the effective index of 1.50, 33 % in dominating mode with effective index of 1.40 and 20 % in dominating mode with effective index of 1.01. The output of PCF A is fed to three channels, each carrying 2.5 Gbps-5 GHz data. The output of Channel 1, Channel 2 and Channel 3 is then combined and transmitted over 2 km FSO link.

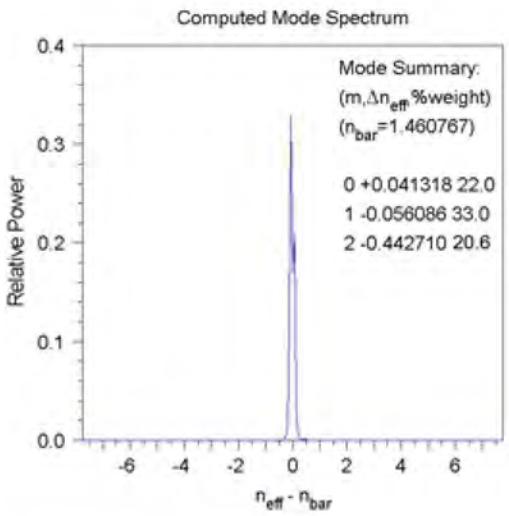

Figure 5.33. Computed Mode Spectrum of Three Core PCF A

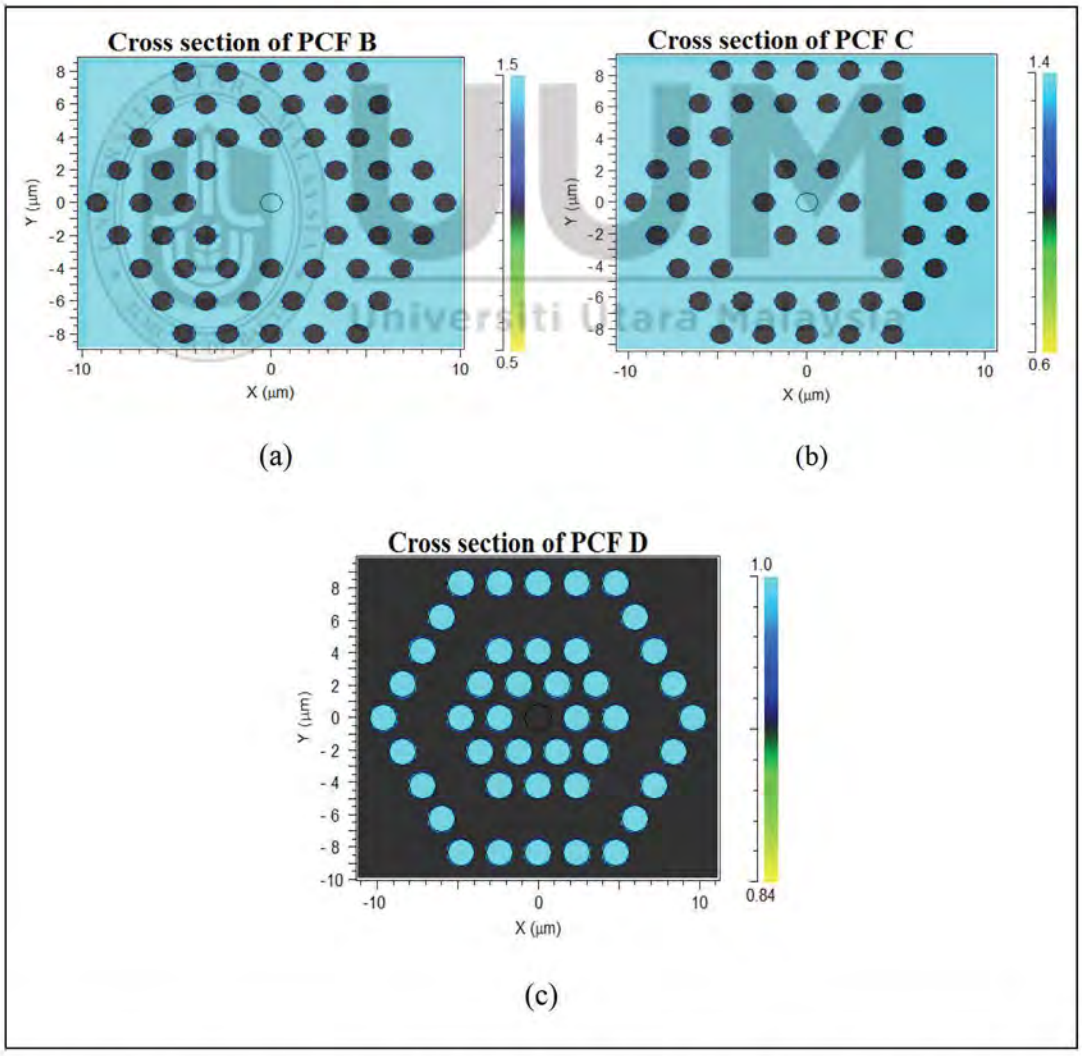

Figure 5.34. Internal Structure of PCFs at Receiver Side (a) PCF B (b) PCF C and (c) *PCF D*

At the receiving side, the optical beam is split into PCF B, PCF C and PCF D using splitter for decomposing the transmitted modes. Figure 5.34 shows the structure of PCF B PCF C and PCF D. The other parameters of PCF A, PCF B, PCF C and PCF D are described on Table 5.4. Further, spatial photodetector and Bit error rate tester are used for converting the optical beam into electrical signal.

Table 5.4

Parameters of PCFs at Transmitter Side

Parameters	**PCF A**	**PCF B**	**PCF C**	**PCF D**
No of Rings	7	4	4	4
Diameter of Air Holes, d (μ m)	0.75	1	1	1.14
Distance between air holes, g (μ m)	2	2.3	2.4	2.4
Ratio of Distance between Air holes to diameter of air holes, g/d	2.67	2.3	2.4	2.10

5.4.2 Results and Discussion

This section represents the results obtained from simulation set up of proposed three core PCF-Ro-FSO transmission system. Figure 5.35 represents the measured spectrum after the PCFs at receiving side. It has been reported that 88.4 % of optical power in dominating mode is achieved at output of PCF B with effective index of 1.50 as compared to 20 % in dominating mode before PCF B, 88.3 % of power is achieved in dominating mode at output of PCF C with effective index of 1.40 as compared to 20 % in dominating mode before PCF C whereas 85 % of power in dominating mode is achieved at output of PCF D with effective index of 1.01 as compared to 20 % in dominating mode before PCF D. Figure 5.36 represents the received modes at receiver sides after FSO link of 2 km. PCF B, PCF C and PCF D

are used to compensate lost power and attenuation introduced in FSO transmission channel.

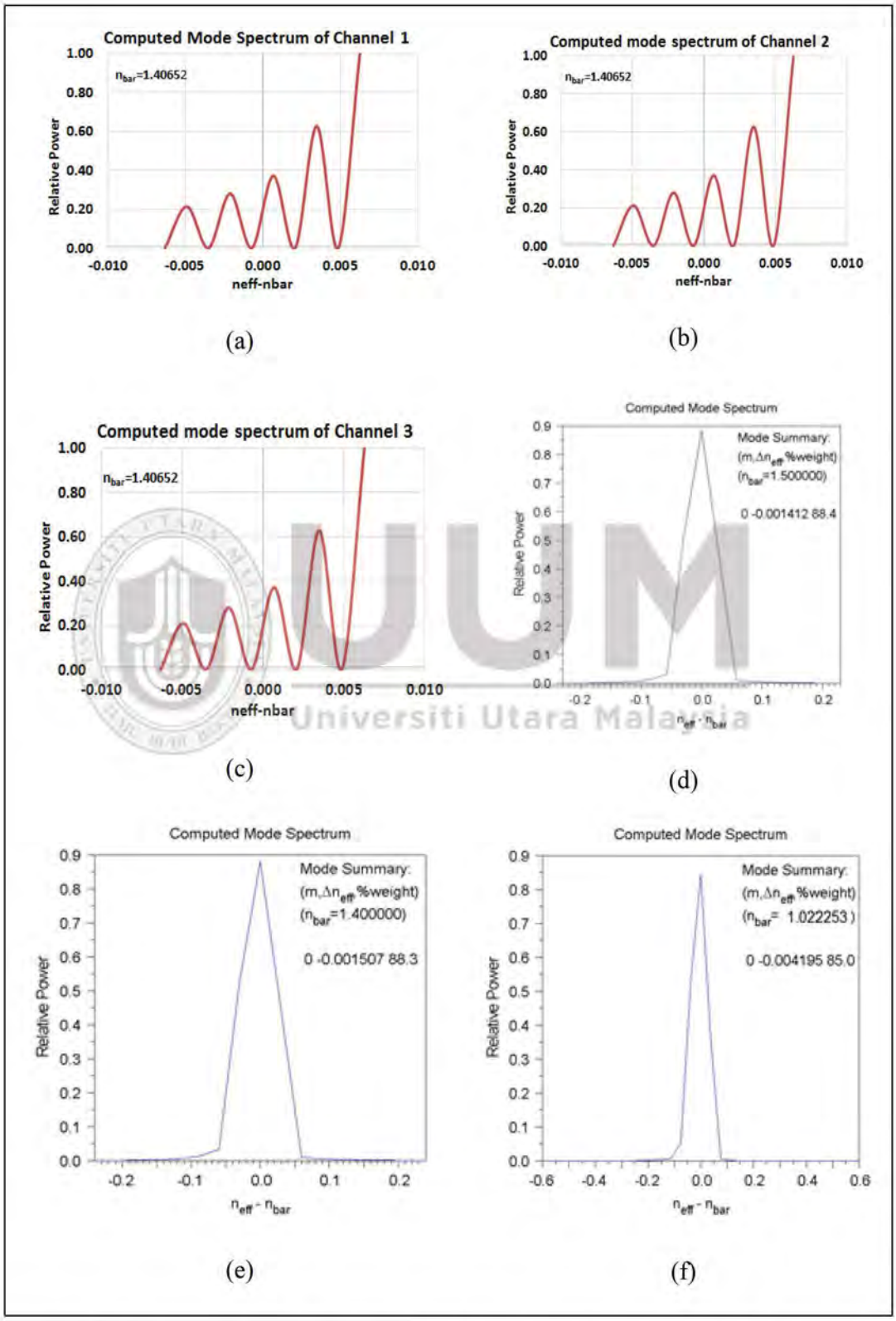

Figure 5.35. Computed Mode Spectrum at Receiver Side (a) Before PCF B (b) Before PCF C (c) Before PCF D (d) After PCF B (e) After PCF C and (f) After PCF D

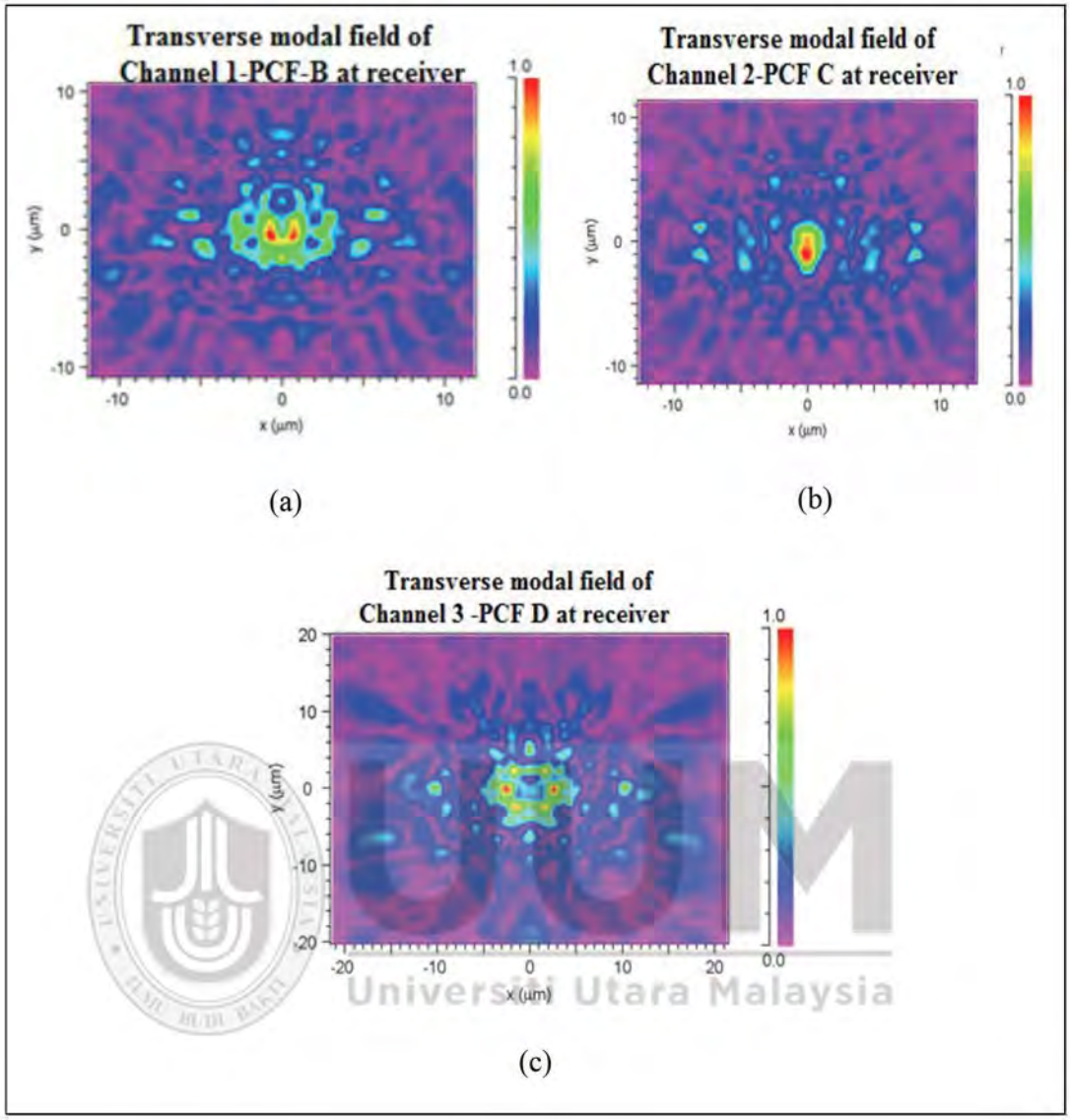

Figure 5.36. Received Modes at FSO link of 2 km (a) Channel 1- PCF B (b) Channel 2-PCF C and (c) Channel 3- PCF D

The value of BER for proposed three core PCF-Ro-FSO transmission system under clear weather conditions is measured in Figure 5.37. It is noted that the value of BER for Channel 1 is computed as 4.8855×10^{-19} and 6.4944×10^{-9}; for Channel 2 it is noted as 1.1720×10^{-21} and 1.62442×10^{-9} whereas for Channel 3 it is noted as $1.5195 \times 10^{-19}$and 3.1288×10^{-13} at the FSO transmission link of 1000 m and 2000 m respectively. The measured eye diagrams in Figure 5.38 clearly show that channel 1, channel 2 and channel 3 are transmitted successfully over 2 km FSO link under clear weather conditions.

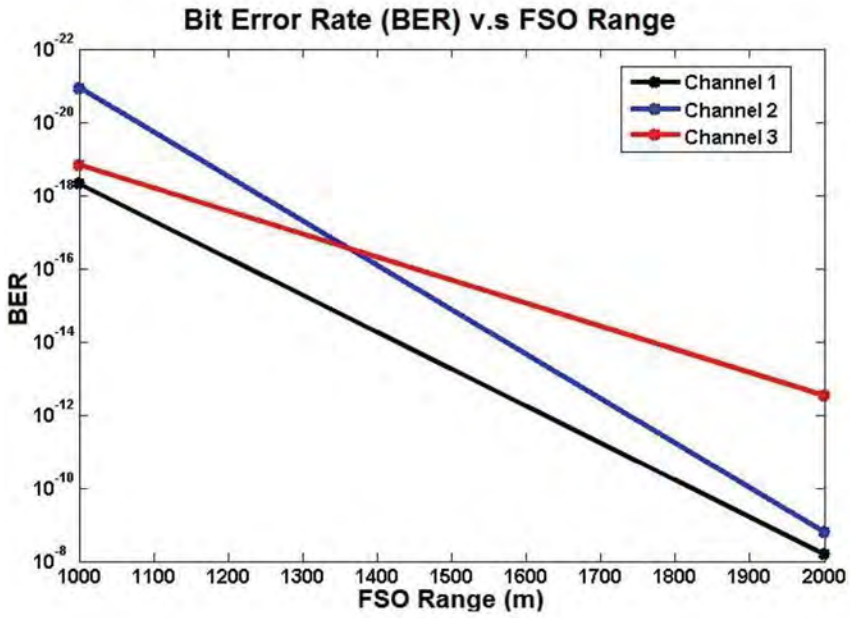

Figure 5.37. Measured BER under clear weather conditions

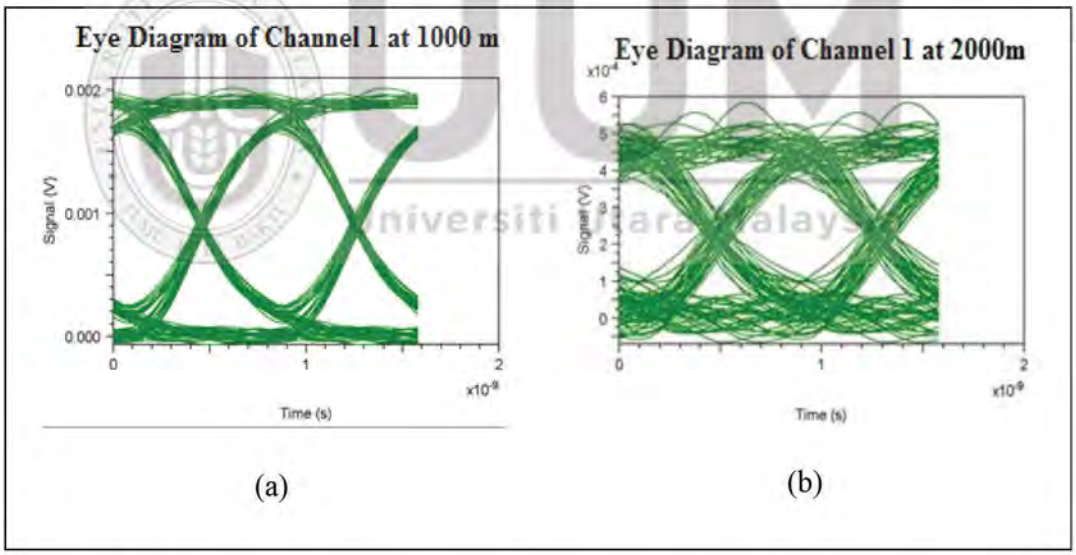

Figure 5.38. Measured Eye Diagrams under clear weather conditions (a) Channel 1 at 1000 m, (b) Channel 2 at 2000 m, (c) Channel 2 at 1000 m, (d) Channel 2 at 2000 m, (e) Channel 3 at 1000 m and (f) Channel 3 at 2000 m

Figure 5.38 continued.

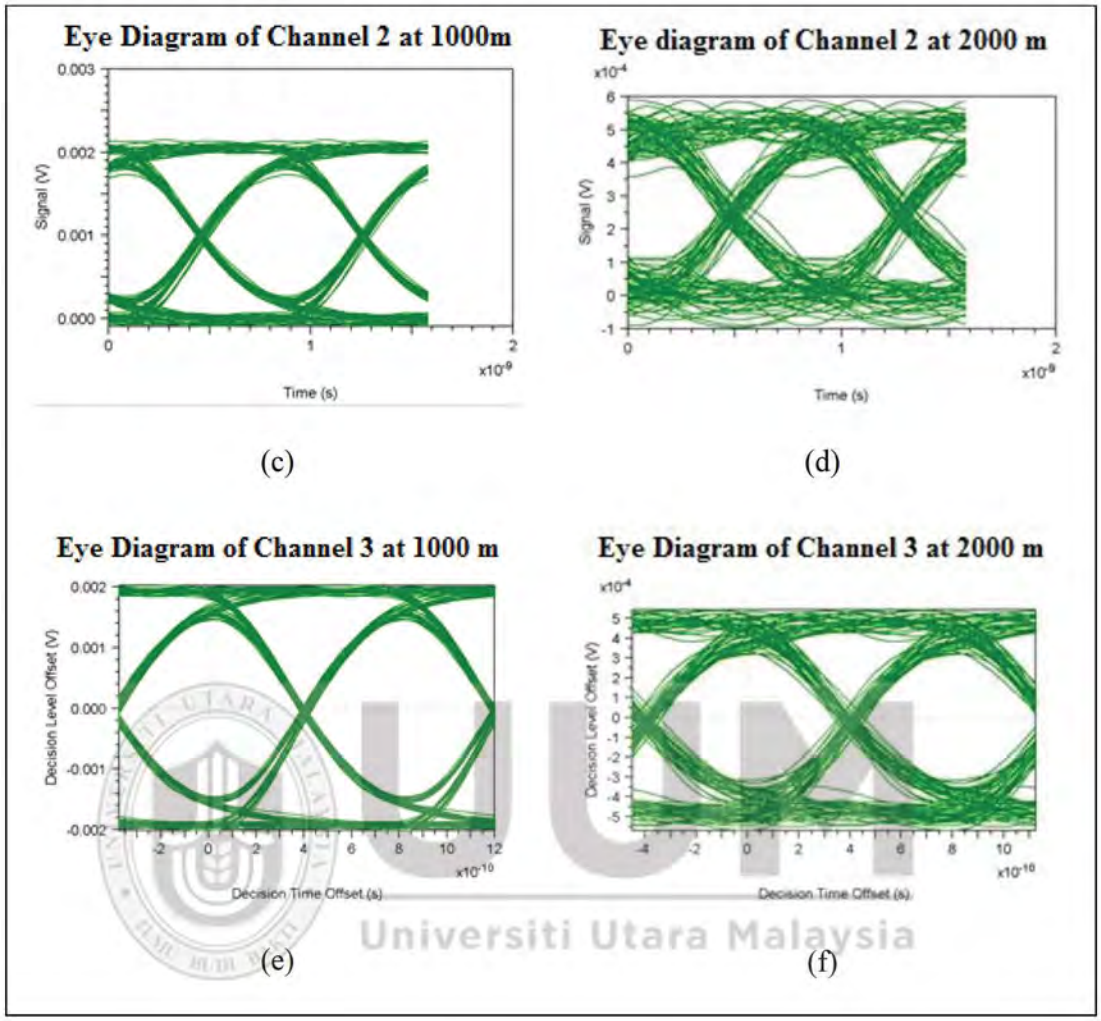

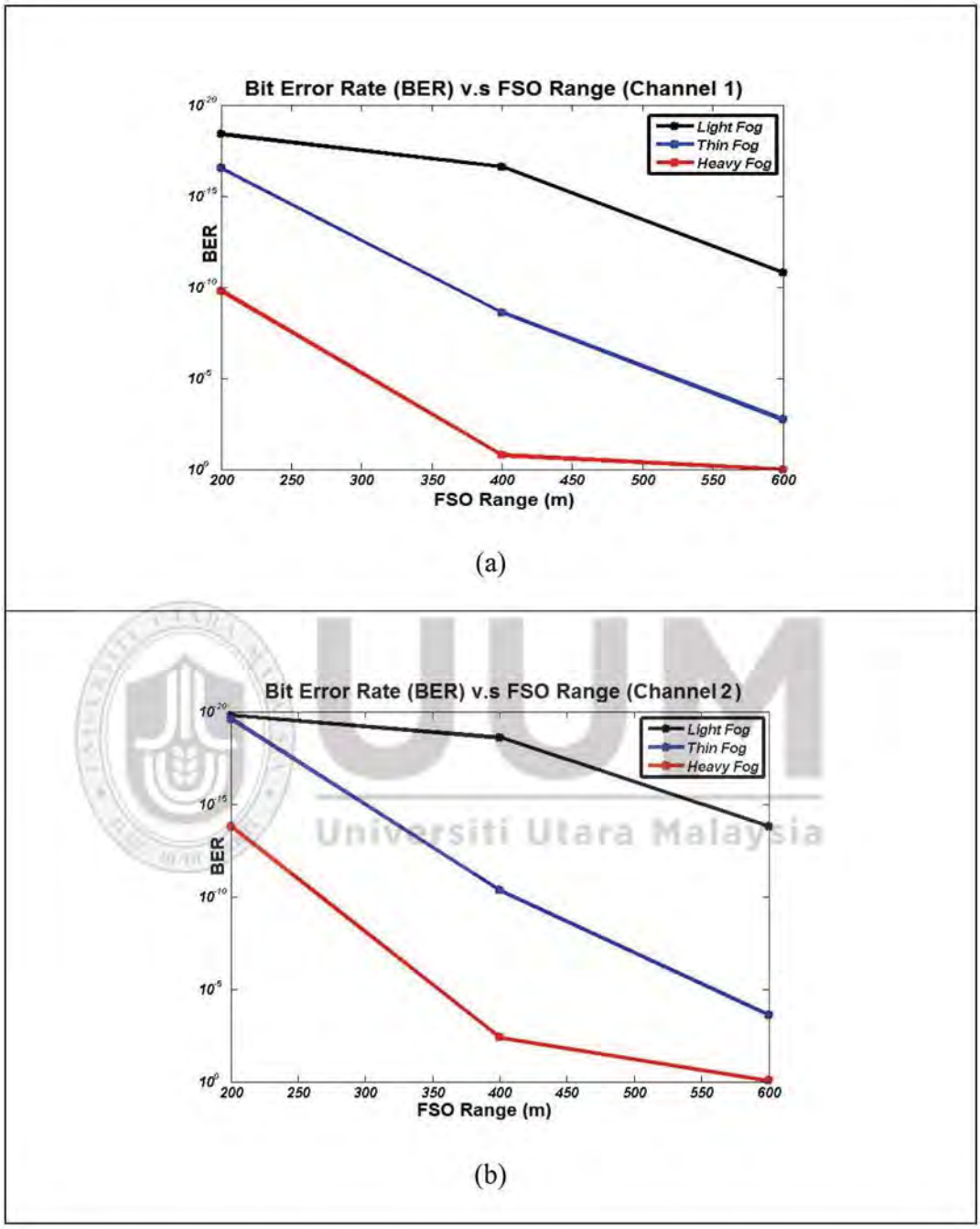

Figure 5.39. Measured BER under atmospheric turbulences (a) Channel 1 (b) Channel 2 and (c) Channel 3

Figure 5.39 continued.

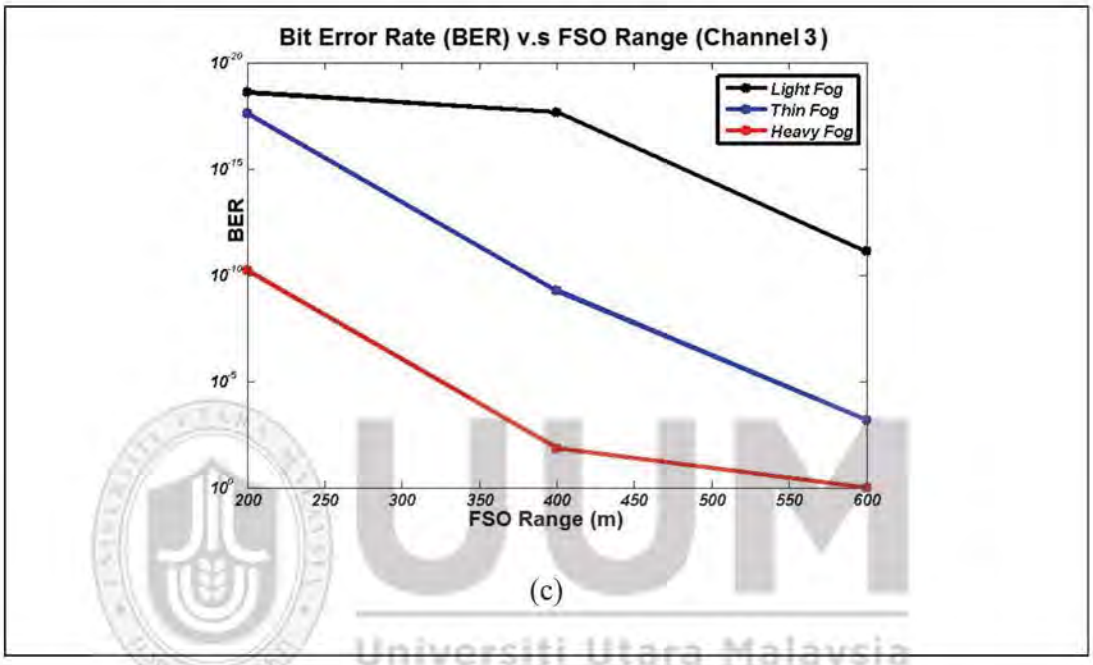

(c)

Figure 5.39 represents the measured BER at receiver side under the impact of atmospheric turbulences. It indicates that under influence of light fog the value of BER for Channel 1 is computed as 4.9878×10^{-19} and 1.5824×10^{-11}; under thin fog it is 2.8746×10^{-17} and 1.8598×10^{-3}; under heavy fog it is 1.6509×10^{-10} and 1; for Channel 2, under influence of light fog it is computed as 1.5845×10^{-20} and 1.5847×10^{-14}; under thin fog it is 2.5487×10^{-20} and 2.4768×10^{-4}; under heavy fog it is 1.5698×10^{-14} and 1 whereas for Channel 3, under the influence of light fog it is noted as 2.5846×10^{-19} and 7.8765×10^{-13}, under thin fog it is 2.4589×10^{-18} and 6.7865×10^{-5}, under heavy fog it is 5.8798×10^{-11} and 1 at FSO transmission link of 200 m and 600 m.

In this work, three independent channels, each carrying 2.5Gbps-5GHz NRZ encoded data, operated on LG 01 in conjunction with three core PCF A, with effective indexes of 1.50, 1.40 and 1.01, are transmitted over FSO link having span of 2 kms. The results are reported in terms of received spatial profiles of transmitted modes, mode spectrum at receiver side, BER and eye diagrams. It is concluded from the reported results that each channel is transmitted and received successfully over 2 km FSO link with acceptable BER and eye diagrams. The use of three core PCF at transmitter side as well as single core PCF at receiver side shows significant improvement in data transmission. Under clear weather conditions, the FSO link prolongs to 2 km with acceptable BER. When the atmosphere changes to light fog, FSO link prolongs to 600 m and when it changes to thin fog, the FSO link prolongs to 400 m whereas when atmosphere changes to heavy fog, FSO prolongs to only 200 m only with acceptable BER.

5.5 Summary

This chapter is focused on the design of a new equalization scheme for Ro-FSO transmission system in order to compensate for the losses and mode coupling introduced during transmission through FSO channel. The equalization scheme is based on the utilization of PCF at transmitter side as well as at receiver side. Moreover, PCF at receiver side is also used as mode selector. Further, this chapter is divided into four phases. Case 1 is based on the design of two SC-PCFs to transmit two Ro-FSO channels, each carrying 2.5Gbps-5GHz data, and two SC-PCFs at the receiver side to receive the Ro-FSO channels. The reported results indicate the significant improvement with the use of PCF in Ro-FSO transmission system. Under clear weather conditions, the FSO link prolongs to 2.5 km whereas under the influence of light fog, thin fog and heavy fog, the FSO link prolongs to 600 m, 400 m

and 200 m respectively with acceptable BER and eye diagrams. Case 2 is based on the design of three SC-PCFs to transmit three Ro-FSO channels, each carrying 2.5Gbps-5GHz data, and three SC-PCFs at the receiver side to receive three Ro-FSO channels. The reported results concluded that the FSO link prolongs to 2.5 km under clear weather conditions whereas under the influence of light fog, thin fog and heavy fog, the FSO link prolongs to 600 m, 400 m and 200 m respectively with acceptable BER and eye diagrams. Case 3 is based on the design of one dual-core PCF to transmit two Ro-FSO channels, each carrying 2.5Gbps-5GHz data, and two SC-PCFs at the receiver side to receive Ro-FSO channels. The reported results depicted that the FSO link prolongs to 2 km under clear weather conditions whereas under the influence of light fog, thin fog and heavy fog, the FSO link prolongs to 600 m, 400 m and 200 m respectively with acceptable BER and eye diagrams. Case 4 is based on the design of one three-core PCF to transmit three Ro-FSO channels, each carrying 2.5Gbps-5GHz data, and three SC-PCFs at the receiver side to receive Ro-FSO channels. The reported results show that the FSO link prolongs to 2 km under clear weather conditions whereas under the influence of light fog, thin fog and heavy fog, the FSO link prolongs to 600 m, 400 m and 200 m respectively with acceptable BER and eye diagrams.

CHAPTER SIX
CONCLUSION AND FUTURE WORK

This thesis focuses on the design and evaluation of OFDM-MDM and PCF-MDM scheme for integration with Ro-FSO transmission systems as a means for mitigating deep fading attenuation and mode coupling due to fog. The current chapter aims at describing an overall conclusion and future work of the thesis. Section 6.1 summarizes the thesis and Section 6.2 elaborates the overall research contribution of the thesis whereas Section 6.3 briefly discusses the future scope of this research.

6.1 Summary of Thesis

This thesis is focused on designing MDM-OFDM and PCF-based equalization schemes for Ro-FSO transmission systems. **Chapter 1** of this thesis has discussed the motivation for Ro-FSO systems along with the issues of inter-symbol interference and atmospheric turbulences in Ro-FSO systems affecting the transmission distance and capacity. The chapter has also discussed the scope and objectives of this research.

Chapter 2 has provided an extensive overview of optical communications, RoF, FSO and Ro-FSO communication systems while highlighting their current multiplexing and modulation technologies in the wavelength, code, subcarrier and intensity domains. Recent developments in MDM experiments and simulations have highlighted the importance of MDM in enhancing data capacity and spectral efficiency in optical communications and particularly in FSO and RoF systems. However, there is still potential room for research in the application of MDM in Ro-FSO systems for mitigation of atmospheric turbulence, increase in channel diversity and enhancement of spectral efficiency. This aims to fill this research gap.

Chapter 3 has described the extensive research methodology used in this thesis to ensure successful accomplishment of its research objectives. The research methodology contains four stages from DRM framework by Luicienne Blessing and Amaresh Chakrabarty. Stage 1 is focused on a comprehensive understanding of Ro-FSO systems while addressing the problem statement and an overall research plan. Stage 2 provides an extensive literature review of previous works in optical communication systems related to the existing solutions and directions of Ro-FSO systems. Stage 3 is focused on designing a hybrid MDM-OFDM scheme for Ro-FSO systems while evaluating its performance under atmospheric turbulences. It also describes the design of a new PCF-based equalization scheme for the developed Ro-FSO systems. Stage 4 aims at evaluating the performance of this PCF-based equalization scheme.

Chapter 4 describes the design, simulations and evaluation of an MDM-OFDM Ro-FSO MDM transmission system. There are three phases in this chapter: Phase 1 describes the design of 10Gbps-OFDM-FSO transmission system under atmospheric turbulences. The results have shown that the FSO link prolongs to 180 km under clear weather conditions and 2.5 km under heavy fog with acceptable SNR and total received power. Phase 2 describes the integration of 40 GHz radio carrier to 20Gbps-OFDM-FSO transmission system under atmospheric turbulences. It also investigates the LG modes for transmitting Ro-FSO channel. The results have shown that the FSO link prolongs to 100 km for LG 00 and LG 02 modes under clear weather conditions and 60 km for LG 04 mode with acceptable SNR and total received power. In the case of turbulent atmosphere, the FSO link prolongs to 9 km under haze, 4.9 km under thin fog, 3.4 km under thick fog and 2.8 km under heavy fog with acceptable SNR and total received power. Phase 3 describes the design of MDM-based OFDM-Ro-FSO transmission system where three cases are significant. Case 1 uses MDM of LG 01

and LG 10 modes for OFDM-Ro-FSO system while transmitting two channels, each carrying 20Gbps-40GHz data, over FSO link. The results have shown that the FSO link prolongs to 100 km under clear weather conditions and 65 km under atmospheric scintillations with acceptable SNR and total received power. Case 2 uses MDM of HG 00, HG 01 and HG 02 modes for OFDM-Ro-FSO transmission system while transmitting three channels, each carrying 20Gbps-40GHz data, over FSO link. The results have shown that the FSO link prolongs to 50 km for HG 00 mode under clear weather conditions and merely 25 km for HG 01 and HG 02 modes with acceptable SNR and total received power. Case 3 uses MDM of LG 02 mode with vortex lens m=2 and LG 03 mode with vortex lens m=5 as well as of HG 11 and HG 12 modes for Ro-FSO transmission systems while transmitting four channels, each carrying 20Gbps-40GHz data, over FSO link. The results have shown that the FSO link prolongs to 50 km under clear weather conditions, 4 km under thin fog, 3 km under thick fog and 2 km under heavy fog with acceptable SNR and total received power. The reported results show a significant 47 % power improvement in deep fades from multi-path propagation with the use of OFDM in MDM-Ro-FSO systems as compared to without OFDM.

Chapter 5 reports on the design, simulations and evaluation of a PCF-based equalization scheme for a Ro-FSO system. The PCF has been used both at the transmitter and receiver sides, as mode selector for the Ro-FSO transmission system and for compensating for mode coupling introduced during transmission through FSO channel. This chapter contains four cases. Case 1 is focused on the design of two SC-PCFs for transmitting two Ro-FSO channels, each carrying 2.5Gbps-5GHz data, and two SC-PCFs at receiver side for receiving the Ro-FSO channels. The reported results show 90.6% improvement in power in the dominant mode as compared to without PCF. The reported results have shown that the FSO link prolongs to

2.5 km under clear weather conditions, 600 m under light fog, 400 m under thin fog and 200 m under heavy fog with acceptable BER and eye diagrams. Case 2 is focused on the design of three SC-PCFs for transmitting three Ro-FSO channels, each carrying 2.5Gbps-5GHz data, and three SC-PCFs for receiving three Ro-FSO channels. The results have shown that the FSO link prolongs to 2.5 km under clear weather conditions, 600 m under light fog, 400 m under thin fog and 200 m under heavy fog with acceptable BER and eye diagrams. Case 3 is focused on the design of one dual-core PCF for transmitting two Ro-FSO channels, each carrying 2.5Gbps-5GHz data, and two SC-PCFs for receiving Ro-FSO channels. The results have shown that the FSO link prolongs to 2 km under clear weather conditions, 600 m under light fog, 400 m under thin fog and 200 m under heavy fog with acceptable BER and eye diagrams. Phase 4 is focused on the design of one three-core PCF for transmitting three Ro-FSO channels, each carrying 2.5Gbps-5GHz data, and three SC-PCFs for receiving Ro-FSO channels. The results have shown that the FSO link prolongs to 2 km under clear weather conditions, 600 m under light fog, 400 m under thin fog and 200 m under heavy fog with acceptable BER and eye diagrams.

6.2 Research Contributions

This thesis contains the following key research contributions:

1. This thesis has proposed a high-speed hybrid MDM-OFDM- Ro-FSO transmission system for clear weather conditions with longer distance. The results, as described in Chapter 4, have demonstrated significant improvement in transmission capacity and distance in the proposed Ro-FSO system under clear weather conditions as compared to previous systems.
2. This thesis has proposed a high-speed hybrid MDM-OFDM-Ro-FSO transmission system for various atmospheric turbulences, particularly for fog,

in order to increase the transmission distance. The results, as described in Chapter 4, have demonstrated significant improvement in transmission capacity and distance in the proposed Ro-FSO system under fog as compared to previous systems due to reduction in deep fading.

3. A new PCF-based equalization scheme for Ro-FSO transmission system for clear weather conditions has been designed and numerically simulated. The results, as described in Chapter 5, have demonstrated significant improvement in Ro-FSO transmission system under clear weather conditions as compared to previous Ro-FSO systems due to reduction in mode coupling.
4. A new PCF-based equalization scheme for Ro-FSO transmission system for atmospheric turbulences, particularly for fog has been designed and numerically simulated. The results, as described in Chapter 5, have demonstrated significant improvement in Ro-FSO transmission system under fog as compared to previous Ro-FSO systems due to reduction in mode coupling.
5. A new PCF-based mode selector for MDM in Ro-FSO transmission systems has been designed and numerically simulated.

6.3 Future Work

The following future work may be suggested:

1. This thesis has used QAM modulation scheme for MDM-OFDM-Ro-FSO transmission system. In addition to QAM, other digital modulations such as quadrature phase shift key (QPSK), differential phase shift key (DPSK), phase shift key (PSK) etc. can be used for evaluating the performance of MDM-OFDM-Ro-FSO transmission system.

2. This thesis has used direct detection scheme for MDM-OFDM-Ro-FSO transmission system. Apart from direction detection, coherent detection scheme may be used for evaluating the performance of MDM-OFDM-Ro-FSO transmission system.
3. This thesis has designed PCF-based equalization scheme for MDM-Ro-FSO transmission system. Other equalization schemes may be used for mitigation of mode coupling in a MDM-Ro-FSO transmission system.
4. This thesis has evaluated the performance of the proposed OFDM-MDM-Ro-FSO and PCF-MDM-Ro-FSO systems under fog. In addition to fog, the performance of these proposed systems may be evaluated under rainfall and snowfall.

List of Published/Accepted/Communicated Work

1. Angela Amphawan, Sushank Chaudhary, "Secure Hybrid MDM-OFDM-Ro-FSO System", International Journal of Sensors, Wireless Communications and Control, Vol. 5, Iss. 1, pp. 13-18, March 2015, (http://www.eurekaselect.com/131543)

2. Sushank Chaudhary, Angela Amphawan, Kashif Nisar, "Realization of free space optics with OFDM under atmospheric turbulence", Optik, 125, Iss. 18, pp. 5196-5198, September 2014 (http://www.sciencedirect.com/science/article/pii/S0030402614006214) **(Scopus) (Impact Factor 0.94)**

3. Sushank Chaudhary, Angela Amphawan, "The Role and Challenges of Free-space Optical Systems". Journal of Optical Communications, August 2014, ISSN (Online) 2191-6322, ISSN (Print) 0173-491 (DOI: 10.1515/joc-2014-0004) **(Scopus)**

4. Angela Amphawan, Sushank Chaudhary, Tarek Elfouly, Khalid Abualsaud, "Mode Division Multiplexing for Secure Ro-FSO WLANs ", Advanced Science Letters, November 2015, **(ISI Indexed) Impact Fact. 1.2.**

5. Angela Amphawan, Sushank Chaudhary, Tse-Kian Neo, "Hermite-Gaussian Mode Division Multiplexing for Free-Space Optical Interconnects", Advanced Science Letters, November 2015, **(ISI Indexed) Impact Fact. 1.2.**

6. Angela Amphawan, Sushank Chaudhary, Vincent W. S. Chan, "2 x 20 Gbps - 40GHz OFDM Ro-FSO transmission with mode division multiplexing", Journal of European Optical Society: Rap. Publications, Volume 9, 14041 (2014), DOI: October 2014, **(ISI Indexed) Impact Fact. 1.17** , (http://dx.doi.org/10.2971/jeos.2014.14041)

7. Angela Amphawan, Sushank Chaudhary, Hafiza Samad, Jihadah Ahmad, "Mode Division Multiplexing of LG and HG modes in Ro-FSO", Proceeding of the Electrical Engineering Computer Science and Informatics 2 (1), November, 2015 , DOI: 10.11591/eecsi.2.604 (Scopus)

8. Angela Amphawan, Sushank Chaudhary, "Free-Space Optical Mode Division Multiplexing for Switching Between Millimeter-Wave Picocells", International Conference on Optical and Photonic Engineering (icOPEN2015)", SPIE, 14-16 April 2015 **(Scopus)** (http://spie.org/Publications/Proceedings/Paper/10.1117/12.2189694)

9. Angela Amphawan, Sushank Chaudhary, Roshidi Din, Mohd Nizam Omar, "5Gbps HG 0,1 and HG 0,3 Optical Mode Division Multiplexing for RoFSO", IEEE International Colloquium on Signal Processing and its Applications (CSPA), 6-9th March 2015. (http://ieeexplore.ieee.org/stamp/stamp.jsp?tp=&arnumber=7225635) (Scopus)

10. Angela Amphawan and Sushank Chaudhary "4 X 2.5Gbps-10 GHz Ro-FSO Transmission Systems by Incorporating Hybrid WDM-MDM of Spiral Phased

LG-HG Modes" International Conference on Internet Applications, Protocols and Services **(NETAPPS2015)**, 1-3 December 2015.

11. Sushank Chaudhary and Angela Amphawan "High Speed MDM-Ro-FSO System by Incorporating Spiral Phased Hermite Gaussian Modes" Journal of Photonic Network Communication **(Accepted)**

12. Sushank Chuadhary and Angela Amphawan "Optimization of AMI-MDM-RoFSO Under Atmpshpheric Turbulences" INCAPE 2017 conference.

13. Sushank Chaudhary and Angela Amphawan "High Speed Millimeter Communication through Ro-FSO Network by Mode Division Multiplexing" Journal of Optical Engineering **(Communicated)**

14. Sushank Chaudhary and Angela Amphawan "Hybrid OFDM based Ro-FSO Transmission system by incorporating LG Modes" Journal of Optics Communication **(Communicated)**

15. Sushank Chaudhary and Angela Amphawan "2 x 2.5 Gbps-5 GHz Hybrid PCF-MDM-Ro-FSO Transmission System under Influence of Atmospheric Turbulences" Journal of Optical and Quantum Electronics **(Communicated)**

16. Sushank Chaudhary and Angela Amphawan "A Novel PCF based Mode Selector in MDM-Ro-FSO Systems" Journal of Optical Switching and Networking **(Communicated)**

17. Sushank Chaudhary and Angela Amphawan "2 X 2.5Gbps-10GHz Ro-FSO Transmission System by MDM of Spiral Phase HG Modes under Atmospheric Turbulences" Journal of modern optics **(Communicated)**

18. Sushank Chaudhary and Angela Amphawan "Empirical Evaluation of Digital Encoding Schemes in MDM based High Speed Ro-FSO Transmission Systems for Millimeter Applications" Journal of Photonic Network Communications **(Communicated)**

19. Sushank Chaudhary, Angela Amphawan and Abhishek Sharma "High Speed MDM-Ro-FSO Communication System by Incorporating AMI Scheme" Journal of Electronics **(Communicated)**

REFERENCES

[1] B. Sanou, "ICT Facts & Figures The world in 2015. *International Telecommunication Union Report* " retrieved from www.itu.int/en, 2016.

[2] B. Sanou, "The world in 2013: ICT facts and figures," *International Telecommunications Union Report,* retrieved from www.itu.int/en, 2013.

[3] J. Bohata, S. Zvanovec, P. Pesek, T. Korinek, M. M. Abadi, and Z. Ghassemlooy, "Experimental verification of long-term evolution radio transmissions over dual-polarization combined fiber and free-space optics optical infrastructures," *Applied Optics,* vol. 55, pp. 2109-2116, 2016.

[4] R. Kaur, R. Kaur, and R. Singh, "Performance Analysis of Radio over Free Space Optical Link under the Effect of different Attenuation Factors Using Advanced Modulation Formats, *International Journal of Engineering Development and Reseaech* ",vol.4, pp.176-182, 2016.

[5] S. Iezekiel, "Radio-over-fiber technology and devices for 5G: An overview," in *SPIE OPTO*, 2016, pp. 97720A-97720A.

[6] K. Prabu, D. S. Kumar, and R. Malekian, "BER analysis of BPSK-SIM-based SISO and MIMO FSO systems in strong turbulence with pointing errors," *Optik-International Journal for Light and Electron Optics,* vol. 125, pp. 6413-6417, 2014.

[7] X. Li, J. Xiao, and J. Yu, "Long-distance wireless mm-wave signal delivery at W-band," *Journal of Lightwave Technology,* vol. 34, pp. 661-668, 2016.

[8] Y. Xu, J. Yu, X. Li, J. Xiao, and Z. Zhang, "Experimental investigation on fiber-wireless MIMO system with different LO at W band," *IEEE Photonics Journal,* vol. 7, pp. 1-7, 2015.

[9] Y. Yan, G. Xie, M. P. Lavery, H. Huang, N. Ahmed, C. Bao, *et al.*, "High-capacity millimetre-wave communications with orbital angular momentum multiplexing," *Nature Communications,* vol. 5, 2014.

[10] H. Ahmad, M. Soltanian, I. Amiri, S. Alavi, A. Othman, and A. Supa'at, "Carriers generated by mode-locked laser to increase serviceable channels in radio over free space optical systems," *IEEE Photonics Journal,* vol. 7, pp. 1-12, 2015.

[11] A. Bekkali, C. Ben Naila, K. Kazaura, K. Wakamori, and M. Matsumoto, "Transmission analysis of OFDM-based wireless services over turbulent radio-on-FSO links modeled by Gamma--Gamma distribution," *Photonics Journal, IEEE,* vol. 2, pp. 510-520, 2010.

[12] P. Pesek, J. Bohata, S. Zvanovec, and J. Perez, "Analyses of dual polarization WDM and SCM Radio over Fiber and Radio over FSO for C-RAN architecture," in *Wireless and Optical Communication Conference (WOCC), 2016 25th*, 2016, pp. 1-4.

[13] X. Wu, K. Xu, D. Dai, and H. K. Tsang, "Mode division multiplexing switch for on-chip optical interconnects," in *OptoElectronics and Communications Conference (OECC) held jointly with 2016 International Conference on Photonics in Switching (PS), 2016 21st*, 2016, pp. 1-3.

[14] N. Ahmed, Z. Zhao, L. Li, H. Huang, M. P. Lavery, P. Liao, *et al.*, "Mode-division-multiplexing of multiple Bessel-Gaussian beams carrying orbital-angular-momentum for obstruction-tolerant free-space optical and millimetre-wave communication links," *Scientific Reports,* vol. 6, 2016.

[15] J. Zhang, F. Li, J. Li, Y. Feng, and Z. Li, "120 Gbit/s 2× 2 Vector-Modes-Division-Multiplexing DD-OFDM-32QAM Free-Space Transmission," *IEEE Photonics Journal,* vol. 8, pp. 1-8, 2016.

[16] F. Ren, J. Li, Z. Wu, T. Hu, J. Yu, Q. Mo, *et al.*, "Three-mode mode-division-multiplexing passive optical network over 12-km low mode-crosstalk FMF using all-fiber mode MUX/DEMUX," *Optics Communications,* vol. 383, pp. 525-530, 2017.

[17] X.-D. Bai, X.-L. Liang, Y.-T. Sun, P.-C. Hu, Y. Yao, K. Wang, *et al.*, "Experimental Array for Generating Dual Circularly-Polarized Dual-Mode OAM Radio Beams," *Scientific Reports,* vol. 7, p. 40099, 2017.

[18] S. Anees and M. R. Bhatnagar, "Performance evaluation of decode-and-forward dual-hop asymmetric radio frequency-free space optical communication system," *IET Optoelectronics,* vol. 9, pp. 232-240, 2015.

[19] K. Prabu, R. Rajendran, and D. S. Kumar, "Spectrum analysis of radio over free space optical communications systems through different channel models," *Optik-International Journal for Light and Electron Optics,* vol. 126, pp. 1142-1145, 2015.

[20] H. Al-Musawi, T. Cseh, J. Bohata, P. Pesek, W. P. Ng, Z. Ghassemlooy, *et al.*, "Fundamental investigation of extending 4G-LTE signal over MMF/SMF-FSO under controlled turbulence conditions," in *Communication Systems, Networks and Digital Signal Processing (CSNDSP), 2016 10th International Symposium on*, 2016, pp. 1-6.

[21] A. Nevo, J. L. Turner, and J. W. Williams, "Usage-Based Pricing and Demand for Residential Broadband," *Econometrica,* vol. 84, pp. 411-443, 2016.

[22] I. Facts, "Figures. 2015. The World in 2015.[cited 2016 Feb 15]," ed.

[23] A. de la Fuente, R. P. Leal, and A. G. Armada, "New Technologies and Trends for Next Generation Mobile Broadcasting Services," *IEEE Communications Magazine,* vol. 54, pp. 217-223, 2016.

[24] C. Liu, "Architectural Evolution and Novel Design of Fiber-Wireless Access Networks," in *Fiber-Wireless Convergence in Next-Generation Communication Networks*, ed: Springer, 2017, pp. 213-233.

[25] H. Henniger and O. Wilfert, "An introduction to free-space optical communications," *Radioengineering,* vol. 19, pp. 203-212, 2010.

[26] A. Malik and P. Singh, "Free space optics: current applications and future challenges," *International Journal of Optics,* vol. 2015, 2015.

[27] C. Lim, K. Wang, and A. Nirmalathas, "Optical wireless communications for high-speed in-building personal area networks," in *Transparent Optical Networks (ICTON), 2016 18th International Conference on*, 2016, pp. 1-4.

[28] A. K. Majumdar, "Fundamentals of Free-Space Optical (FSO) Communication System," in *Advanced Free Space Optics (FSO)*, ed: Springer, 2015, pp. 1-20.

[29] I. Alimi, A. Shahpari, V. y. Ribeiro, tor, N. Kumar, P. Monteiro, and A. y. Teixeira, nio, "Optical wireless communication for future broadband access networks," in *Networks and Optical Communications (NOC), 2016 21st European Conference on*, 2016, pp. 124-128.

[30] N. Dayal, P. Singh, and P. Kaur, "Performance Enhancement in WDM-FSO System Using Optical Amplifiers Under Different Rain Conditions," in *Proceeding of International Conference on Intelligent Communication, Control and Devices*, 2017, pp. 293-298.

[31] H. Hemmati and D. M. Boroson, "Free-Space Laser Communication and Atmospheric Propagation XXVI," in *Proc. of SPIE Vol*, 2014, pp. 897101-1.

[32] S. Khan, N. Gupta, and N. Parveen, "Comparative Analysis of Free Space Optical Communication Methodologies," *International Journal of Advanced Electronics and Communication Systems,* vol. 3, 2014.

[33] L. Andrews, R. Phillips, Z. Bagley, N. Plasson, and L. Stotts, "Hybrid Optical/Radio Frequency (RF) Communications," in *Advanced Free Space Optics (FSO)*, ed: Springer, 2015, pp. 295-342.

[34] A. Demeter and C.-Z. Kertesz, "Simulation of free-space communication using the Orbital Angular Momentum of radio waves," in *Optimization of Electrical and Electronic Equipment (OPTIM), 2014 International Conference on*, 2014, pp. 846-851.

[35] Thide, *et al.*, "Angular momentum radio," in *SPIE OPTO*, 2014, pp. 89990B-89990B.

[36] P. Yue, X. Yi, and Z. Liu, "A Novel Wireless Network Architecture for WLAN Based on Radio over Free Space Optics Technology and Its Spectrum Assignment Function," in *Recent Advances in Computer Science and Information Engineering*, ed: Springer, 2012, pp. 415-421.

[37] K.-H. Kim, H. Onodera, T. Higashino, K. Tsukamoto, S. Komaki, Y. Aburakawa, *et al.*, "A new statistical model of scintillation in RoFSO link and performance evaluation of WLAN system," in *Microwave Photonics,* 2008, pp. 193-196.

[38] A. S. Das and A. S. Patra, "Radio-over-fiber transport system employing free-space optical communication scheme with parabolic reflector," in *SPIE OPTO*, 2015, pp. 93870W-93870W-5.

[39] H. Al-Musawi, T. Cseh, M. M. Abadi, W. Ng, Z. Ghassemlooy, E. Udvary, *et al.*, "Experimental demonstration of transmitting LTE over FSO for in-building POF network s," in *Transparent Optical Networks (ICTON), 2015 17th International Conference on, Budapest, Hungry*, 2015, pp. 1-4.

[40] K. Kazaura, P. Dat, A. Bekkali, A. Shah, T. Suzuki, K. Wakamori, *et al.*, "Experimental evaluation of a radio-on-FSO communication system for multiple RF signal transmission," in *SPIE LASE: Lasers and Applications in Science and Engineering*, 2009, pp. 719907-719907.

[41] Q.-S. Hu, J.-B. Wang, J.-Y. Wang, M. Chen, and X. Song, "Outage probability analysis of multi-hop free space optical communications over strong turbulence channels," in *Wireless Communications and Signal Processing (WCSP), 2013 International Conference on*, 2013, pp. 1-6.

[42] M. A. Kashani, M. Uysal, and M. Kavehrad, "A novel statistical model for turbulence-induced fading in free-space optical systems," in *Transparent Optical Networks (ICTON), 2013 15th International Conference on*, 2013, pp. 1-5.

[43] S. Robinson and S. Jasmine, "Performance Analysis of Hybrid WDM-FSO System under Various Weather Conditions," *Frequenz,* vol. 70, pp. 433-441, 2016.

[44] A. Shahidinejad, I. S. Amiri, and T. Anwar, "Enhancement of indoor wavelength division multiplexing-based optical wireless communication using microring resonator," *Reviews in Theoretical Science,* vol. 2, pp. 201-210, 2014.

[45] H. Hu, F. Qian, X. Xie, T. Duan, and H. Feng, "Demonstration of flexible optical time-division multiplexing system for high-speed free-space optical communications," *Journal of Optics,* vol. 45, pp. 1-6, 2016.

[46] D. Wang, W. Zhou, Z. Li, Z. Chen, H. Yin, S. Zhu, *et al.*, "Research on free-space optical communication based on time-division multiplexing," in *SPIE/COS Photonics Asia*, 2016, pp. 100201F-100201F-9.

[47] F.-L. Jenq, T.-J. Liu, and F.-Y. Leu, "An AC LED smart lighting system with visible light time-division multiplexing free space optical communication," in *Innovative Mobile and Internet Services in Ubiquitous Computing (IMIS), 2011 Fifth International Conference on*, 2011, pp. 589-593.

[48] G. Xie, F. Wang, A. Dang, and H. Guo, "A novel polarization-multiplexing system for free-space optical links," *Photonics Technology Letters, IEEE,* vol. 23, pp. 1484-1486, 2011.

[49] F.-C. Qian, Y.-l. Ye, Y. Wen, T. Duan, and H. Feng, "Demonstration of 20Gb/s polarization-insensitive wavelength switching system for high-speed free-space optical network," in *Applied Optics and Photonics China (AOPC2015)*, 2015, pp. 967908-967908-5.

[50] J.-H. Lee and S.-H. Hwang, "Selection diversity-aided subcarrier intensity modulation/spatial modulation for free-space optical communication," *IET Optoelectronics,* vol. 9, pp. 116-124, 2015.

[51] V. Sharma and G. Kaur, "High speed, long reach OFDM-FSO transmission link incorporating OSSB and OTSB schemes," *Optik-International Journal for Light and Electron Optics,* vol. 124, pp. 6111-6114, 2013.

[52] M. H. Yeaseen, F. Azam, S. Saha, and A. Islam, "Free-space optical communication with BPSK subcarrier intensity modulation in presence of

atmospheric turbulence and pointing error," in *Computer and Information Technology (ICCIT), 2015 18th International Conference on*, 2015, pp. 516-521.

[53] P. Liu, X. Wu, K. Wakamori, T. D. Pham, M. S. Alam, and M. Matsumoto, "Bit error rate performance analysis of optical CDMA time-diversity links over gamma-gamma atmospheric turbulence channels," in *Wireless Communications and Networking Conference (WCNC), 2011 IEEE*, 2011, pp. 1932-1936.

[54] R. K. Z. Sahbudin, M. Kamarulzaman, S. Hitam, M. Mokhtar, and S. B. A. Anas, "Performance of SAC OCDMA-FSO communication systems," *Optik-International Journal for Light and Electron Optics,* vol. 124, pp. 2868-2870, 2013.

[55] A. Amphawan, "Binary encoded computer generated holograms for temporal phase shifting," *Optics Express,* vol. 19, pp. 23085-23096, 2011.

[56] A. Amphawan, "Holographic mode-selective launch for bandwidth enhancement in multimode fiber," *Optics Express,* vol. 19, pp. 9056-9065, 2011.

[57] A. Amphawan, "Binary spatial amplitude modulation of continuous transverse modal electric field using a single lens for mode selectivity in multimode fiber," *Journal of Modern Optics,* vol. 59, pp. 460-469, 2012.

[58] J. Carpenter and T. D. Wilkinson, "All optical mode-multiplexing using holography and multimode fiber couplers," *Journal of Lightwave Technology,* vol. 30, pp. 1978-1984, 2012.

[59] A. Amphawan, V. Mishra, K. Nisar, and B. Nedniyom, "Real-time holographic backlighting positioning sensor for enhanced power coupling

efficiency into selective launches in multimode fiber," *Journal of Modern Optics,* vol. 59, pp. 1745-1752, 2012.

[60] R. Ryf, S. Randel, A. H. Gnauck, C. Bolle, R.-J. Essiambre, P. Winzer, *et al.*, "Space-division multiplexing over 10 km of three-mode fiber using coherent 6 multiply 6 MIMO processing," in *Optical Fiber Communication Conference*, 2011, p. PDPB10.

[61] Y. Jung, *et al.*, "Dual mode fused optical fiber couplers suitable for mode division multiplexed transmission," *Optics express,* vol. 21, pp. 24326-24331, 2013.

[62] Y. Jung, *et al.*, "Low-loss 25.3 km few-mode ring-core fibre for mode-division multiplexed transmission," *Journal of Lightwave Technology,* pp.1363-1368, 2016.

[63] C. P. Tsekrekos and D. Syvridis, "All-fiber broadband mode converter for future wavelength and mode division multiplexing systems," *Photonics Technology Letters, IEEE,* vol. 24, pp. 1638-1641, 2012.

[64] A. Amphawan, B. Nedniyom, and N. M. Al Samman, "Selective excitation of LP01 mode in multimode fiber using solid-core photonic crystal fiber," *Journal of Modern Optics,* vol. 60, pp. 1675-1683, 2013.

[65] S. Cai, S. Yu, Y. Wang, M. Lan, L. Gao, and W. Gu, "Hybrid Dual-Core Photonic Crystal Fiber for Spatial Mode Conversion," *IEEE Photonics Technology Letters,* vol. 28, pp. 339-342, 2016.

[66] H. Zhang, W. Zhang, L. Xi, X. Tang, X. Zhang, and X. Zhang, "A New Type Circular Photonic Crystal Fiber for Orbital Angular Momentum Mode Transmission," *IEEE Photonics Technology Letters,* vol. 28, pp. 1426-1429, 2016.

[67] T. Kaiser, et al., "Complete modal decomposition for optical fibers using CGH-based correlation filters," *Optics Express,* vol. 17, pp. 9347-9356, 2009.

[68] J. Carpenter, B. C. Thomsen, and T. D. Wilkinson, "Degenerate mode-group division multiplexing," *Journal of Lightwave Technology,* vol. 30, pp. 3946-3952, 2012.

[69] J. Libich, J. Perez, S. Zvanovec, Z. Ghassemlooy, R. Nebuloni, and C. Capsoni, "Combined effect of turbulence and aerosol on free-space optical links," *Applied Optics,* vol. 56, pp. 336-341, 2017.

[70] M. S. Islam, M. S. Islam, A. B. Mohammad, and S. A. Al-Gailani, "Characteristics of free space optics communication link in an unusual haze," *Indian Journal of Pure & Applied Physics (IJPAP),* vol. 54, pp. 46-50, 2016.

[71] A. Cavanna, F. Just, X. Jiang, G. Leuchs, M. V. Chekhova, P. S. J. Russell, *et al.*, "Hybrid photonic-crystal fiber for single-mode phase matched generation of third harmonic and photon triplets," *Optica,* vol. 3, pp. 952-955, 2016.

[72] J. Mondal, A. H. Howlader, and M. S. Rahman, "Highly Birefringent Wideband Residual Dispersion Compensating Photonic Crystal Fiber," *International Journal of Innovation and Applied Studies,* vol. 20, p. 328, 2017.

[73] A. M. Haider, "The advantages of using photonic crystal fibers instead of the conventional fibers in optical gyroscope," *Восточно-Европейский журнал передовых технологий,* vol. 2, 2015.

[74] H. T. Huang, W. L. Liang, C. T. Lin, C. C. Wei, and S. Chi, "100 GHz DD OFDM RoF system over 150 km fiber transmission employing pilot aided phase noise suppression and bit loadingoading algorithm," *Optics express,* vol. 22, pp. 3938-3943, 2014.

[75] L. Tao, Z. Dong, J. Yu, N. Chi, J. Zhang, X. Li, *et al.*, "Experimental demonstration of 48 Gb/s PDM-QPSK radio-over-fiber system over 40GHz mm wave MIMO wireless transmission," *Photonics Technology Letters, IEEE,* vol. 24, pp. 2276-2279, 2012.

[76] G. Abdalla, "Orthogonal Frequency Division Multiplexing Theory and Challenges," *University of Khartoum Engineering Journal,* vol.1, pp.1-8, 2016.

[77] J. Kaur, H. Kaur, and M. Sandhu, "OFDM: Comparison with Multicarrier Techniques and Applications," *International Research Journal of Engineering and Technology,* vol. 03, Issue.04, 2016.

[78] J. S. Rose, "Communication Efficiencies: Utilizing Electromagnetic Spectrum for Wireless Broadband Services," *Georgetown University,* 2016.

[79] A. Kumar, A. Karandikar, G. Naik, M. Khaturia, S. Saha, M. Arora, *et al.*, "Towards Enabling Broadband for a Billon Plus Population with TV White Spaces," *arXiv preprint arXiv:1603.01999,* 2016.

[80] R. V. Jensen, N. Gru, Lars, N. H. Wong, Y. Sun, Y.-m. Jung, and D. J. Richardson, "Demonstration of a 9 LP-mode transmission fiber with low DMD and loss," in *Optical Fiber Communication Conference*, 2015, pp. W2A-34.

[81] J. M. Kahn, K.-P. Ho, and M. B. Shemirani, "Mode coupling effects in multi-mode fibers," in *Optical Fiber Communication Conference*, 2012, p. OW3D. 3.

[82] D. Richardson, J. Fini, and L. Nelson, "Space-division multiplexing in optical fibres," *Nature Photonics,* vol. 7, pp. 354-362, 2013.

[83] S. Attri, C. Narula, and S. Kumar, "Techniques to mitigate fading effect in FSO using OFDM," in *2015 2nd International Conference on Recent Advances in Engineering \& Computational Sciences (RAECS)*, 2015, pp. 1-5.

[84] D. Chen, "PAPR Reduction of Optical OFDM Systems with Exponential Companding Transform and Zero Padding," 2016.

[85] Y.-H. Jan, "Reduced-Overhead Channel Estimation for OFDM Systems in Multipath Fast Time-Varying Channels,"*Journal of Internet Technology,* vol. 16, pp. 1099-1108, 2015.

[86] Y.-H. Jan, "Transmission Efficient Channel Estimation for OFDM System Under Multi-path Fast Fading Channel," *Wireless Personal Communications,* vol. 84, pp. 1561-1575, 2015.

[87] N. Shibata, K. Watanabe, and M. Ohashi, "Chromatic Dispersion Diagnosis for the Two-Modes of Few-Mode Photonic Crystal Fiber," *IEEE Photonics Technology Letters,* vol. 28, pp. 437-440, 2016.

[88] F. Hamaoka, S. Okamoto, K. Horikoshi, K. Yonenaga, A. Hirano, and Y. Miyamoto, "Mode-selective coherent detection technique for low-complexity mode division multiplexing systems," *Electronics Letters,* vol. 51, pp. 1899-1900, 2015.

[89] B. Inan, B. Spinnler, F. Ferreira, A. P. L. Polo, S. Adhikari, V. Sleiffer, *et al.*, "Equalizer complexity of mode division multiplexed coherent receivers," in *Optical Fiber Communication Conference*, 2012, pp. OW3D-4.

[90] G. T. Reed, G. Mashanovich, F. Gardes, and D. Thomson, "Silicon optical modulators," *Nature photonics,* vol. 4, pp. 518-526, 2010.

[91] C. M. Watts, D. Shrekenhamer, J. Montoya, G. Lipworth, J. Hunt, T. Sleasman, *et al.*, "Terahertz compressive imaging with metamaterial spatial light modulators," *Nature Photonics,* 2014.

[92] F. Becerra, J. Fan, and A. Migdall, "Photon number resolution enables quantum receiver for realistic coherent optical communications," *Nature Photonics,* 2014.

[93] A. Pospischil, M. Humer, M. M. Furchi, D. Bachmann, R. Guider, T. Fromherz, *et al.*, "CMOS-compatible graphene photodetector covering all optical communication bands," *Nature Photonics,* vol. 7, pp. 892-896, 2013.

[94] O. Graydon, "Terahertz photonics: Quantum cascade amplifier," *Nature Photonics,* vol. 8, pp. 812-812, 2014.

[95] M. Nishikino and T. Kawachi, "Soft-X-ray sources: X-ray laser plasma amplifiers," *Nature Photonics,* vol. 8, pp. 352-354, 2014.

[96] A. B. Khanikaev and Alu, Andrea, "Silicon photonics: One-way photons in silicon," *Nature Photonics,* vol. 8, pp. 680-682, 2014.

[97] G. Keiser, *Optical fiber communications*: Wiley Online Library, 2003.

[98] C. G. Gavrincea, J. Baranda, and P. Henarejos, "Rapid prototyping of standard-compliant visible light communications system," *IEEE Communications Magazine,* vol. 52, pp. 80-87, 2014.

[99] J. Mitola, "Cognitive radio for flexible mobile multimedia communications," *IEEE International Workshop on Mobile Multimedia Communications, (MoMuC'99),* 1999, pp. 3-10.

[100] J. Wang, L. Pei, S. Weng, L. Wu, L. Huang, T. Ning, *et al.*, "A Tunable Polarization Beam Splitter Based on Magnetic Fluids-Filled Dual-Core Photonic Crystal Fiber," *IEEE Photonics Journal,* vol. 9, pp. 1-10, 2017.

[101] A. Emsia, et al., "1Tbps WDM OFDM PON Power Budget Extension Techniques," in *IEEE Photonics Conference (IPC),* , 2013, pp. 529-530.

[102] V. Sarup and A. Gupta, "Performance analysis of an ultra high capacity 1 Tbps DWDM-RoF system for very narrow channel spacing," in *Wireless and Optical Communications Networks (WOCN), 2014 Eleventh International Conference on*, 2014, pp. 1-5.

[103] T. Takahara, T. Tanaka, M. Nishihara, Y. Kai, L. Li, Z. Tao, *et al.*, "Discrete Multi-Tone for 100 Gb/s Optical Access Networks," in *Optical Fiber Communication Conference*, 2014, pp. M2I-1.

[104] D. K. Tripathi, P. Singh, N. Shukla, and H. Dixit, "Design and Transmission Performance Study of OpticalTDM up to 3Tb/s," *International Journal of Advanced Electronics and Communication Systems,* vol. 2, 2014.

[105] X. Wang, Q. Zhang, I. Kim, P. Palacharla, and M. Sekiya, "Support Statistical Sharing in Circuit Switching WDM Optical Networks," in *Optical Fiber Communication Conference*, 2013, pp. OTu3A-1.

[106] G. P. Agrawal, "Fiber-optic communication systems," *Wiley-Interscience,* vol. 1, 1997.

[107] A. M. Mbah, J. G. Walker, and A. J. Phillips, "Performance evaluation of digital pulse position modulation for wavelength division multiplexing FSO systems impaired by interchannel crosstalk," *IET Optoelectronics,* vol. 8, pp. 245-255, 2014.

[108] K.-i. Yoshino, M. Fujiwara, A. Tanaka, S. Takahashi, Y. Nambu, A. Tomita, *et al.*, "High-speed wavelength-division multiplexing quantum key distribution system," *Optics letters,* vol. 37, pp. 223-225, 2012.

[109] K. Patel, J. Dynes, M. Lucamarini, I. Choi, A. Sharpe, Z. Yuan, *et al.*, "Quantum key distribution for 10 Gb/s dense wavelength division multiplexing networks," *Applied Physics Letters,* vol. 104, p. 051123, 2014.

[110] G. Ji and Y. Sun, "Wavelength division multiplexing," ed: Google Patents, 2015.

[111] V. R. Balaji, M. Murugan, and S. Robinson, "Optimization of Dense Wavelength Division Multiplexing demultiplexer with 25GHz uniform channel spacing," *arXiv preprint arXiv:1608.00235,* 2016.

[112] I. a. Cano, n, X. Escayola, P. Schindler, M. i. Santos, a C, V. Polo, J. Leuthold, *et al.*, "Experimental Demonstration of Multi-band Upstream in Statistical OFDM-PONs and Comparison with Digital Subcarrier Assignment," in *Optical Fiber Communication Conference*, 2014, pp. Th3G-4.

[113] B. Ranjha and M. Kavehrad, "Hybrid Asymmetrically Clipped OFDM-Based IM/DD Optical Wireless System," *Journal of Optical Communications and Networking,* vol. 6, pp. 387-396, 2014.

[114] S. Shimizu, G. Cincotti, and N. Wada, "Chromatic dispersion monitoring and adaptive compensation using pilot symbols in an 8 x 12.5 Gbit/s all-optical OFDM system," *Optics Express,* vol. 22, pp. 8734-8741, 2014.

[115] J. Singh, V. Mishra Smieee, P. Patel, and P. Gilawat, "Simulation and analysis of dispersion compensation schemes for 100Gbps PDM--OFDM optical communication system," *Optik-International Journal for Light and Electron Optics,* vol. 125, pp. 2026-2030, 2014.

[116] C. Li, Y. Shao, Z. Wang, J. Zhou, Y. Zhou, and W. Ma, "Optical 64QAM-OFDM Transmission Systems with Different Sub-Carriers," *Optics and Photonics Journal,* vol. 6, p. 196, 2016.

[117] G. Milione, H. Huang, M. Lavery, A. Willner, R. R. Alfano, T. A. Nguyen, *et al.*, "Orbital-Angular-Momentum Mode (De) Multiplexer: A Single Optical Element for MIMO-based and non-MIMO-based Multimode Fiber Systems," in *Optical Fiber Communication Conference*, 2014, pp. M3K-6.

[118] Z. Cao, F. Li, Y. Liu, J. Yu, Q. Wang, C. Oh, *et al.*, "61.3 Gbps hybrid fiber-wireless in-home network enabled by optical heterodyne and polarization multiplexing," *Journal of Lightwave Technology,* vol. 32, pp. 3227-3233, 2014.

[119] M. Morant, et al., "Polarization Division Multiplexing of OFDM Radio-over-Fiber Signals in Passive Optical Networks," *Advances in Optical Technologies,* vol. 2014, 2014.

[120] H. Zhou, J. Yu, J. Tang, and L. Chen, "Polarization-insensitive wavelength conversion for polarization multiplexing non-return-to-zero quadrature phase shift keying signals based on four-wave mixing in a semiconductor optical amplifier using digital coherent detection," *Optical Engineering,* vol. 52, pp. 025001-025001, 2013.

[121] J. M. Buset, et al., "Experimental demonstration of a 10 Gb/s RSOA-based 16-QAM subcarrier multiplexed WDM PON," *Opt. Express,* pp. 1-8, 2014.

[122] C. Kottke, et al., "Coherent subcarrier-WDM-PON system with SSB modulation and wavelength reuse," in *Optical Fiber Communication Conference*, 2013, pp. OM2A-3.

[123] H. S. Mohammad, et al., "Generation of a new hybrid subcarrier multiplexign-SAC-OCDMA system based on FSO," *Journal of Theoretical and Applied Information Technology,* vol. 58, 2013.

[124] A. N. Z. Rashed, "Ultra Wide Wavelength Division Multiplexing Optical Code Division Multiple Access Communication Systems in Wide Area Optical Communication Networks," *International Journal of Basics and Applied Science,* vol. 1, pp. 650-663, 2013.

[125] M. A. Sedaghat, F. Marvasti, and others, "Performance analysis of asynchronous optical code division multiple access with spectral-amplitudecoding," *Communications, IET,* vol. 8, pp. 956-963, 2014.

[126] M. Hadi and M. R. Pakravan, "Analysis and Design of Adaptive OCDMA Passive Optical Networks," *arXiv preprint arXiv:1607.07707,* 2016.

[127] Y. Shao, S. Wang, Z. Tan, Y. Luo, and Y. Lai, "Seamless integration of RZ-DQPSK-DWDM optical links with MISO-OFDM-QPSK system for fourth generation wide-area coverage mobile communication," *Microwave and Optical Technology Letters,* vol. 56, pp. 797-801, 2014.

[128] M. Tan, et al., "Transmission comparison of ultra-long Raman fibre laser based amplification with first and dual order Raman amplification using 10 x 118 Gbit/s DP-QPSK," in *Transparent Optical Networks (ICTON), 2014 16th International Conference on*, 2014, pp. 1-4.

[129] J. Wei, Z. Huang, S. Su, and C. Liu, "Accurate and fast chromatic dispersion estimation for PDM-QPSK optical signals with multiple data rates," in *Australian Conference on Optical Fibre Technology*, 2016, p. AThlC. 3.

[130] D. O. Otuya, et al., "A Single-Channel 1.92 Tbit/s, 64 QAM Coherent Pulse OTDM Transmission over 150 km," in *OptoElectronics and Communications Conference and Photonics in Switching*, 2013.

[131] D. O. Otuya, K. Kasai, M. Yoshida, T. Hirooka, and M. Nakazawa, "Single-channel 1.92 Tbit/s, Pol-Mux-64 QAM coherent Nyquist pulse transmission over 150 km with a spectral efficiency of 7.5 bit/s/Hz," *Optics Express,* vol. 22, pp. 23776-23785, 2014.

[132] Y. Wang, K. Kasai, T. Omiya, and M. Nakazawa, "120 Gbit/s, polarization-multiplexed 10 Gsymbol/s, 64 QAM coherent transmission over 150 km using an optical voltage controlled oscillator," *Optics Express,* vol. 21, pp. 28290-28296, 2013.

[133] P. Luo, M. Zhang, Z. Ghassemlooy, H. Le Minh, H.-M. Tsai, X. Tang, *et al.*, "Experimental demonstration of a 1024-QAM optical camera communication system," *IEEE Photonics Technology Letters,* vol. 28, pp. 139-142, 2016.

[134] P. Wang, L. Zhang, L. Guo, F. Huang, T. Shang, R. Wang, *et al.*, "Average BER of subcarrier intensity modulated free space optical systems over the exponentiated Weibull fading channels," *Optics Express,* vol. 22, pp. 20828-20841, 2014.

[135] P. Wu and J. Ma, "BPSK optical mm-wave signal generation by septupling frequency via a single optical phase modulator," *Optics Communications,* vol. 374, pp. 69-74, 2016.

[136] F. c. Horlin, ,ois, J. Fickers, P. Emplit, A. e. Bourdoux, and J. e. Louveaux, rome, "Dual-polarization OFDM-OQAM for communications over optical fibers with coherent detection," *Optics Express,* vol. 21, pp. 6409-6421, 2013.

[137] K. Margariti and T. Kamalakis, "Performance of coherent detection in optical wireless systems for high speed indoor communications," *Optical and Quantum Electronics,* pp. 1-19, 2014.

[138] C. Xie, et al., "960-km SSMF transmission of 105.7-Gb/s PDM 3-PAM using directly modulated VCSELs and coherent detection," *Optics Express,* vol. 21, pp. 11585-11589, 2013.

[139] K. Byron, "Simultaneous amplification and pulse compression in a single-mode optical fibre," *Electronics Letters,* vol. 22, pp. 1275-1277, 1986.

[140] S. H. Chang, et al., "Mode division multiplexed optical transmission enabled by all--fiber mode multiplexer," *Optics Express,* vol. 22, pp. 14229-14236, 2014.

[141] C. Chow, C. Yeh, S. M. Lo, C. Li, and H. Tsang, "Long-reach radio-over-fiber signal distribution using single-sideband signal generated by a silicon-modulator," *Optics Express,* vol. 19, pp. 11312-11317, 2011.

[142] G. El-Howayek and M. M. Hayat, "Method for performance analysis and optimization of APD optical receivers operating under dynamic reverse bias," in *Photonics Conference (IPC), 2013 IEEE*, 2013, pp. 362-363.

[143] E. E. R. Vera, J. E. U. Restrepo, N. E. G. Cardona, and M. Varón, "Mode selective coupler based in a dual-core photonic crystal fiber with non-identical cores for spatial mode conversion," in *Latin America Optics and Photonics Conference*, 2016, p. LTu3C. 1.

[144] V. Sarup and A. Gupta, "A study of various trends and enabling technologies in Radio over Fiber (RoF) systems," *Optik-International Journal for Light and Electron Optics,* vol. 126, pp. 2606-2611, 2015.

[145] S. Iezekiel, "Radio-over-fiber technology and devices for 5G: An overview," in *SPIE OPTO*, 2016, pp. 97720A-97720A-7.

[146] D. Novak, R. B. Waterhouse, A. Nirmalathas, C. Lim, P. A. Gamage, T. R. Clark, *et al.*, "Radio-over-fiber technologies for emerging wireless systems," *IEEE Journal of Quantum Electronics,* vol. 52, pp. 1-11, 2016.

[147] B. Singh and D. Singh, "A Review on Advantages and Applications of Radio over Fiber System," *International Journal of Current Engineering and Technology,* pp.2277-4106, 2016.

[148] B. T. Binder, P. Yu, J. H. Shapiro, and J. K. Bounds, "An atmospheric optical ring network," *Communications, IEEE Transactions on,* vol. 38, pp. 74-81, 1990.

[149] V. Reddy and L. Jolly, "Simulation and Analysis of Radio over Fiber (RoF) Systems using Frequency Up-Conversion Technique," *Simulation,* vol. 133, 2016.

[150] D. Wake, A. Nkansah, and N. J. Gomes, "Radio over fiber link design for next generation wireless systems," *Lightwave Technology, Journal of,* vol. 28, pp. 2456-2464, 2010.

[151] M. S. Abdullah, M. A. Sarijari, A. H. F. A. Hamid, N. Fisal, A. Lo, R. A. Rashid, *et al.*, "Green Architecture for Dense Home Area Networks Based on Radio-over-Fiber with Data Aggregation Approach," *Journal of Electronic Science and Technology,* vol. 2, p. 008, 2016.

[152] M. Fabbri and P. Faccin, "Radio over fiber technologies and systems: New opportunities," in *Transparent Optical Networks, 2007. ICTON'07. 9th International Conference on*, 2007, pp. 230-233.

[153] J. e. Capmany, B. Ortega, D. Pastor, and S. Sales, "Discrete-time optical processing of microwave signals," *Journal of Lightwave Technology,* vol. 23, p. 702, 2005.

[154] J. Hecht, "Understanding fiber optics," *Laser Light Press, Massachusetts* 2015.

[155] A. Nain, S. Kumar, and S. Singla, "Performance Estimation of WDM Radio-over-Fiber Links Under the Influence of SRS Induced Crosstalk," in *Proceeding of International Conference on Intelligent Communication, Control and Devices*, 2017, pp. 279-284.

[156] M. Zhu, L. Zhang, J. Wang, L. Cheng, C. Liu, and G.-K. Chang, "Radio-over-fiber access architecture for integrated broadband wireless services," *Journal of Lightwave Technology,* vol. 31, pp. 3614-3620, 2013.

[157] H.-S. Kim, T. T. Pham, Y.-Y. Won, and S.-K. Han, "Simultaneous wired and wireless 1.25-Gb/s bidirectional WDM-RoF transmission using multiple optical carrier suppression in FP LD," *Journal of Lightwave Technology,* vol. 27, pp. 2744-2750, 2009.

[158] W.-J. Jiang, C.-T. Lin, A. Ng'oma, P.-T. Shih, J. Chen, M. Sauer, *et al.*, "Simple 14 Gb/s short-range radio-over-fiber system employing a single-electrode MZM for 60-GHz wireless applications," *Journal of Lightwave Technology,* vol. 28, pp. 2238-2246, 2010.

[159] C.-T. Lin, J. Chen, P.-T. Shih, W.-J. Jiang, and S. Chi, "Ultra-high data-rate 60 GHz radio-over-fiber systems employing optical frequency multiplication and OFDM formats," *Journal of Lightwave Technology,* vol. 28, pp. 2296-2306, 2010.

[160] A. Kanno, K. Inagaki, I. Morohashi, T. Sakamoto, T. Kuri, I. Hosako, *et al.*, "40 Gb/s W-band (75--110 GHz) 16-QAM radio-over-fiber signal generation and its wireless transmission," *Optics Express,* vol. 19, pp. B56-B63, 2011.

[161] C.-H. Ho, R. Sambaraju, W. Jiang Jr, T. H. Lu, C.-Y. Wang, H. Yang, *et al.*, "50 Gb/s radio-over-fiber system employing MIMO and OFDM modulation at 60 GHz," in *Optical Fiber Communication Conference*, 2012, pp. OM2B-3.

[162] J. Ma, Y. Zhan, M. Zhou, H. Liang, Y. Shao, and C. Yu, "Full-duplex radio over fiber with a centralized optical source for a 60 GHz millimeter-wave system with a 10 Gb/s 16-QAM downstream signal based on frequency quadrupling," *Journal of Optical Communications and Networking,* vol. 4, pp. 557-564, 2012.

[163] C.H. Ho, et al., "Performance Evaluation of a 60 GHz Radio-over-Fiber System Employing MIMO and OFDM Modulation," *IEEE Journal on Selected Areas in Communications,* vol. 31, pp. 780-787, 2013.

[164] H. T. Huang, W. L. Liang, C. T. Lin, C. C. Wei, and S. Chi, "100 GHz DD OFDM RoF system over 150 km fiber transmission employing pilot-aided phase noise suppression and bit loading algorithm," *Optics Express,* vol. 22, pp. 3938-3943, 2014.

[165] R. Zhang, et al., "Full-duplex fiber-wireless link with 40Gbit/s 16-QAM signals for alternative wired and wireless accesses based on homodyne/heterodyne coherent detection," *Optical Fiber Technology,* vol. 20, pp. 261-267, 2014.

[166] E. P. Martin, et al., "25-Gb/s OFDM 60-GHz radio over fiber system based on a gain switched laser," *Journal of Lightwave Technology,* vol. 33, pp. 1635-1643, 2015.

[167] S. Ahmad and M. Zafrullah, "40 Gb/s 4-QAM OFDM radio over fiber system at 60 GHz employing coherent detection," *Journal of Modern Optics,* vol. 62, pp. 296-301, 2015.

[168] Q. Mo, et al., "2× 2 MIMO OFDM/OQAM radio signals over an elliptical core few-mode fiber," *Optics Letters,* vol. 41, pp. 4546-4549, 2016.

[169] M. Rashid, F. Qamar, F. Rashid, and S. Ahmad, "Implementation of OFDM-RoF at 60 GHz with DCF for Long Haul Communication," *Nucleus,* vol. 53, pp. 195-199, 2016.

[170] S. You, Y. Wang, Z. Wang, M. Chen, X. Li, M. Luo, *et al.*, "Radio over WDM-PON by spatial multiplexing in few mode fiber," in *Communication Systems, Networks and Digital Signal Processing (CSNDSP), 2016 10th International Symposium on*, 2016, pp. 1-5.

[171] P. T. Dat, A. Kanno, N. Yamamoto, and T. Kawanishi, "Simultaneous transmission of 4G LTE-A and wideband MMW OFDM signals over fiber links," in *Microwave Photonics (MWP), 2016 IEEE International Topical Meeting on*, 2016, pp. 87-90.

[172] A. Kanno, K. Inagaki, I. Morohashi, T. Sakamoto, T. Kuri, I. Hosako, *et al.*, "20 Gb/s QPSK W-band (75-110GHz) wireless link in free space using radio-over-fiber technique," *IEICE Electronics Express,* vol. 8, pp. 612-617, 2011.

[173] C.-T. Lin, A. Ngoma, W.-Y. Lee, C.-C. Wei, C.-Y. Wang, T.-H. Lu, *et al.*, "2 multiply 2 MIMO radio-over-fiber system at 60 GHz employing frequency domain equalization," *Optics express,* vol. 20, pp. 562-567, 2012.

[174] N. Hamedazimi, Z. Qazi, H. Gupta, V. Sekar, S. R. Das, J. P. Longtin, *et al.*, "Firefly: A reconfigurable wireless data center fabric using free-space optics," *ACM SIGCOMM Computer Communication Review,* vol. 44, pp. 319-330, 2015.

[175] S. Hranilovic, *Wireless optical communication systems*: Springer, 2005.

[176] N. Cvijetic, D. Qian, J. Yu, Y.-K. Huang, and T. Wang, "Polarization-multiplexed optical wireless transmission with coherent detection," *Journal of Lightwave Technology,* vol. 28, pp. 1218-1227, 2010.

[177] J. Vitásek, J. Látal, S. Hejduk, J. Bocheza, P. Koudelka, J. Skapa, *et al.*, "Atmospheric turbulences in free space optics channel," in *Telecommunications and Signal Processing (TSP), 2011 34th International Conference on*, 2011, pp. 104-107.

[178] S. A. Zabidi, W. Khateeb, M. R. Islam, and A. W. Naji, "The effect of weather on free space optics communication (FSO) under tropical weather conditions and a proposed setup for measurement," in *Computer and Communication Engineering (ICCCE), 2010 International Conference on*, 2010, pp. 1-5.

[179] J. Perez, Z. Ghassemlooy, S. Rajbhandari, M. Ijaz, and H. Le Minh, "Ethernet FSO communications link performance study under a controlled fog environment," *IEEE Communications Letters,* vol. 16, pp. 408-410, 2012.

[180] J. Wang, J.-Y. Yang, I. M. Fazal, N. Ahmed, Y. Yan, H. Huang, *et al.*, "Terabit free-space data transmission employing orbital angular momentum multiplexing," *Nature Photonics,* vol. 6, pp. 488-496, 2012.

[181] Y. Ren, H. Huang, G. Xie, N. Ahmed, Y. Yan, B. I. Erkmen, *et al.*, "Atmospheric turbulence effects on the performance of a free space optical

link employing orbital angular momentum multiplexing," *Optics Letters,* vol. 38, pp. 4062-4065, 2013.

[182] B. T. Vu, N. T. Dang, T. C. Thang, and A. T. Pham, "Bit error rate analysis of rectangular QAM/FSO systems using an APD receiver over atmospheric turbulence channels," *Journal of Optical Communications and Networking,* vol. 5, pp. 437-446, 2013.

[183] N. Kumar and T. Singh, "2.50 Gbits optical CDMA over FSO communication system," *Optik-International Journal for Light and Electron Optics,* vol.125, p.p. 4538-4542, 2014.

[184] V. Sharma, "High speed CO-OFDM-FSO transmission system," *Optik-International Journal for Light and Electron Optics,* vol. 125, pp. 1761-1763, 2014.

[185] P. Patel, V. Mishra, and V. Singh, "Performance analysis of CO-OFDM FSO system under different weather conditions," in *Emerging Technology Trends in Electronics, Communication and Networking (ET2ECN), 2014 2nd International Conference on*, 2014, pp. 1-5.

[186] P. Kumar and A. Srivastava, "Enhanced performance of FSO link using OFDM and comparison with traditional TDM-FSO link," in *Broadband and Photonics Conference (IBP), 2015 IEEE International*, 2015, pp. 65-70.

[187] R. Singh and G. Soni, "Realization of OFDM based free space optics," in *Green Computing and Internet of Things (ICGCIoT), 2015 International Conference on*, 2015, pp. 32-35.

[188] N. Kumar and A. L. J. Teixeira, "10 Gbit/s OFDM based FSO communication system using M-QAM modulation with enhanced detection," *Optical and Quantum Electronics,* vol. 48, p. 9, 2016.

[189] Y. Su, F. Bai, and T. Sato, "Transmission analysis of CPolM-based OFDM FSO system in atmospheric turbulence," *Optics Communications,* vol. 369, pp. 111-119, 2016.

[190] S. Parkash, A. Sharma, H. Singh, and H. P. Singh, "Performance investigation of 40 Gbps DWDM over free space optical communication system using RZ modulation format," *Advances in Optical Technologies,* vol. 2016, 2016.

[191] F. Rashidi, J. He, and L. Chen, "Spectrum slicing WDM for FSO communication systems under the heavy rain weather," *Optics Communications,* vol. 387, pp. 296-302, 2017.

[192] G. Soni, "A Performance Analysis of Free-Space Optical Link at 1,550 nm, 850 nm, 650 nm and 532 nm Optical Wavelengths," *Journal of Optical Communications*.

[193] C. B. Naila, K. Wakamori, and M. Matsumoto, "Transmission analysis of M-ary phase shift keying multiple-subcarrier modulation signals over radio-on-free-space optical channel with aperture averaging," *Optical Engineering,* vol. 50, pp. 105006-105006-9, 2011.

[194] P. T. Dat, A. Bekkali, K. Kazaura, K. Wakamori, T. Suzuki, M. Matsumoto, *et al.*, "Performance evaluation of an advanced DWDM RoFSO system for heterogeneous wireless," in *Proceedings of the 28th IEEE conference on Global telecommunications*, 2009, pp. 808-813.

[195] K. Wang, A. Nirmalathas, C. Lim, and E. Skafidas, "4 x 12.5 Gb/s WDM Optical Wireless Communication System for Indoor Applications," *Journal of Lightwave Technology,* vol. 29, pp. 1988-1996, 2011.

[196] F.-M. Kuo, C.-B. Huang, J.-W. Shi, N.-W. Chen, H.-P. Chuang, J. E. Bowers, *et al.*, "Remotely up-converted 20-Gbit/s error-free wireless on--off-keying data transmission at W-band using an ultra-wideband photonic transmitter-mixer," *Photonics Journal, IEEE,* vol. 3, pp. 209-219, 2011.

[197] A. Khalid, G. Cossu, R. Corsini, P. Choudhury, and E. Ciaramella, "1 Gb/s transmission over a phosphorescent white LED by using rate-adaptive discrete multitone modulation," *Photonics Journal, IEEE,* vol. 4, pp. 1465-1473, 2012.

[198] L. Tao, Z. Dong, J. Yu, N. Chi, J. Zhang, X. Li, *et al.*, "Experimental demonstration of 48 Gbpss PDM QPSK radio-over-fiber system over 40GHz mm wave MIMO wireless transmission," *Photonics Technology Letters, IEEE,* vol. 24, pp. 2276-2279, 2012.

[199] L. Deng, D. Liu, X. Pang, X. Zhang, V. Arlunno, Y. Zhao, *et al.*, "42.13 Gbit/s 16qam OFDM photonics wireless transmission in 75 110 GHz band," *Progress In Electromagnetics Research,* vol. 126, pp. 449-461, 2012.

[200] C. Chow, C. Yeh, Y. Liu, and P. Huang, "Mitigation of optical background noise in light-emitting diode (LED) optical wireless communication systems," *Photonics Journal, IEEE,* vol. 5, pp. 7900307-7900307, 2013.

[201] F. Bai, Y. Su, and T. Sato, "Performance evaluation of a dual diversity reception base on OFDM RoFSO systems over correlated log-normal fading channel," in *ITU Kaleidoscope Academic Conference: Living in a converged world-Impossible without standards?, Proceedings of the 2014*, 2014, pp. 263-268.

[202] J. Bohata, S. Zvanovec, T. Korinek, M. M. Abadi, and Z. Ghassemlooy, "Characterization of dual-polarization LTE radio over a free-space optical turbulence channel," *Applied optics,* vol. 54, pp. 7082-7087, 2015.

[203] H. Nistazakis, A. Stassinakis, H. Sandalidis, and G. Tombras, "QAM and PSK OFDM RoFSO Over M Turbulence Induced Fading Channels," *IEEE Photonics Journal,* vol. 7, pp. 1-11, 2015.

[204] A. Stassinakis, M. Ninos, H. Nistazakis, S. S. Muhammad, A. Tsigopoulos, and G. Tombras, "BER Estimation of Dual Hop QAM OFDM ROFSO over Exponentially Modeled Turbulence and Optical Fiber with Nonlinear Clipping," *International Conference from Scientific Computing to Computational Engineering,* vol. 1, 2016.

[205] S. T. Liverman, Q. Wang, Y.-J. Chu, A. Natarajan, T. Nguyen, and A. X. Wang, "Hybrid Wireless Communication Networks: Integrating Free-Space Optics and WiFi," in *Frontiers in Optics*, 2016, p. JTh2A. 56.

[206] S. S. Muhammad, P. Kohldorfer, and E. Leitgeb, "Channel modeling for terrestrial free space optical links," in *Transparent Optical Networks, 2005, Proceedings of 2005 7th International Conference*, 2005, pp. 407-410.

[207] T. H. Carbonneau and D. R. Wisely, "Opportunities and challenges for optical wireless: the competitive advantage of free space telecommunications links in today's crowded marketplace," in *Voice, Video, and Data Communications*, 1998, pp. 119-128.

[208] A. Alkholidi and K. Altowij, "Effect of clear atmospheric turbulence on quality of free space optical communications in Western Asia," *Optical Communications Systems. Croatia: InTech,* 2012.

[209] L. C. Andrews and R. L. Phillips, *Laser beam propagation through random media* vol. 10: SPIE press Bellingham, 2005.

[210] H. Zhou, S. Mao, and P. Agrawal, "Optical power allocation for adaptive WDM transmissions in free space optical networks," in *Wireless Communications and Networking Conference (WCNC), 2014 IEEE*, 2014, pp. 2677-2682.

[211] C. B. Naila, K. Wakamori, and M. Matsumoto, "Transmission analysis of M-ary phase shift keying multiple-subcarrier modulation signals over radio-on-free-space optical channel with aperture averaging," *Optical Engineering,* vol. 50, pp. 105006-105006, 2011.

[212] J. Crisp, "Introduction to fiber optics," *Elsevier,* book, 2005.

[213] A. Ghatak and K. Thyagarajan, *An introduction to fiber optics*: Cambridge University Press, 1998.

[214] H. Huang, G. Xie, Y. Yan, N. Ahmed, Y. Ren, Y. Yue, *et al.*, "100 Tbit/s free-space data link using orbital angular momentum mode division multiplexing combined with wavelength division multiplexing," in *Optical Fiber Communication Conference*, 2013, p. OTh4G. 5.

[215] H. Huang, G. Xie, Y. Yan, N. Ahmed, Y. Ren, Y. Yue, *et al.*, "100 Tbit/s free-space data link enabled by three-dimensional multiplexing of orbital angular momentum, polarization, and wavelength," *Optics Letters,* vol. 39, pp. 197-200, 2014.

[216] M. Krenn, R. Fickler, M. Fink, J. Handsteiner, M. Malik, T. Scheidl, *et al.*, "Communication with spatially modulated light through turbulent air across Vienna," *New Journal of Physics,* vol. 16, p. 113028, 2014.

[217] S. O. Arik, J. M. Kahn, and K.-P. Ho, "MIMO signal processing for mode-division multiplexing: An overview of channel models and signal processing architectures," *Signal Processing Magazine, IEEE,* vol. 31, pp. 25-34, 2014.

[218] R. Ryf, S. Randel, A. H. Gnauck, C. Bolle, R.-J. Essiambre, P. Winzer, *et al.*, "Space-division multiplexing over 10 km of three-mode fiber using coherent 6× 6 MIMO processing," in *Optical Fiber Communication Conference*, 2011, p. PDPB10.

[219] A. Amphawan and D. O'Brien, "Modal decomposition of output field for holographic mode field generation in a multimode fiber channel," *International Conference on Photonics (ICP),* 2010, pp. 1-5.

[220] T. Kaiser, D. Flamm, S. Schröter, and M. Duparré, "Complete modal decomposition for optical fibers using CGH-based correlation filters," *Optics Express,* vol. 17, pp. 9347-9356, 2009.

[221] Y. Ren, Z. Wang, G. Xie, L. Li, Y. Cao, C. Liu, *et al.*, "Free-space optical communications using orbital-angular-momentum multiplexing combined with MIMO-based spatial multiplexing," *Optics Letters,* vol. 40, pp. 4210-4213, 2015.

[222] Y. Ren, Z. Wang, P. Liao, L. Li, G. Xie, H. Huang, *et al.*, "400-Gbit/s free space optical communications link over 120-meter using multiplexing of 4 collocated orbital-angular-momentum beams," in *Optical Fiber Communication Conference*, 2015, p. M2F. 1.

[223] Y. Ren, Z. Wang, P. Liao, L. Li, G. Xie, H. Huang, *et al.*, "Experimental characterization of a 400 Gbit/s orbital angular momentum multiplexed free-space optical link over 120 m," *Optics Letters,* vol. 41, pp. 622-625, 2016.

[224] Y. Zhao, J. Liu, J. Du, S. Li, Y. Luo, A. Wang, *et al.*, "Experimental Demonstration of 260-meter Security Free-Space Optical Data Transmission Using 16-QAM Carrying Orbital Angular Momentum (OAM) Beams Multiplexing," in *Optical Fiber Communication Conference*, 2016, p. Th1H. 3.

[225] G. Xie, Y. Ren, Y. Yan, H. Huang, N. Ahmed, L. Li, *et al.*, "Experimental demonstration of a 200-Gbit/s free-space optical link by multiplexing Laguerre–Gaussian beams with different radial indices," *Optics Letters,* vol. 41, pp. 3447-3450, 2016.

[226] A. Trichili, C. Rosales-Guzmán, A. Dudley, B. Ndagano, S. A. Ben, M. Zghal, *et al.*, "Optical communication beyond orbital angular momentum," *Scientific Reports,* vol. 6, p. 27674, 2016.

[227] V. Sharma and G. Kaur, "Modelling of ofdm-odsb-fso transmission system under different weather conditions," in *Advanced Computing and Communication Technologies (ACCT), 2013 Third International Conference on*, 2013, pp. 154-157.

[228] C.-Y. Lin, Y.-P. Lin, H.-H. Lu, C.-Y. Chen, T.-W. Jhang, and M.-C. Chen, "Optical free-space wavelength-division-multiplexing transport system," *Optics Letters,* vol. 39, pp. 315-318, 2014.

[229] C. Chen, W.-D. Zhong, X. Li, and D. Wu, "MDPSK-based nonequalization OFDM for coherent free-space optical communication," *IEEE Photonic Technology Letters,* vol. 26, pp. 1617-1620, 2014.

[230] K. Nakamura, I. Mizukoshi, and M. Hanawa, "Optical wireless transmission of 405 nm, 1.45 Gbit/s optical IM/DD-OFDM signals through a 4.8 m underwater channel," *Optics Express,* vol. 23, pp. 1558-1566, 2015.

[231] X. Huang, J. Shi, J. Li, Y. Wang, Y. Wang, and N. Chi, "750Mbit/s visible light communications employing 64QAM-OFDM based on amplitude equalization circuit," in *Optical Fiber Communication Conference*, 2015, p. Tu2G. 1.

[232] J. Zhou, Y. Shao, Z. Wang, C. Li, Y. Zhou, and W. Ma, "A 16PSK-OFDM-FSO Communication System under Complex Weather Conditions," *Optics and Photonics Journal,* vol. 6, p. 131, 2016.

[233] P. Kumar and A. Srivastava, "Performance improvement of OFDM-FSO multi-user communication system with combined transmit frequency diversity and receive space diversity," *Optics Communications,* vol. 366, pp. 410-418, 2016.

[234] F. Rashidi, J. He, and L. Chen, "Performance Investigation of FSO–OFDM Communication Systems under the Heavy Rain Weather," *Journal of Optical Communications*.

[235] http://www.rfwireless-world.com, 2016.

[236] Z. Guo, J. Yuan, C. Yu, X. Sang, K. Wang, B. Yan, *et al.*, "Highly Coherent Supercontinuum Generation in the Normal Dispersion Liquid-Core Photonic Crystal Fiber," *Progress In Electromagnetics Research M,* vol. 48, pp. 67-76, 2016.

[237] M. Hasan, M. S. Habib, M. S. Habib, and S. A. Razzak, "Highly nonlinear and highly birefringent dispersion compensating photonic crystal fiber," *Optical Fiber Technology,* vol. 20, pp. 32-38, 2014.

[238] P. Russell, "Photonic crystal fibers," *science,* vol. 299, pp. 358-362, 2003.

[239] A. M. Cubillas, S. Unterkofler, T. G. Euser, B. J. Etzold, A. C. Jones, P. J. Sadler, *et al.*, "Photonic crystal fibres for chemical sensing and photochemistry," *Chemical Society Reviews,* vol. 42, pp. 8629-8648, 2013.

[240] T. P. Hansen, J. Broeng, S. E. Libori, E. Knudsen, A. Bjarklev, J. R. Jensen, *et al.*, "Highly birefringent index-guiding photonic crystal fibers," *IEEE Photonics Technology Letters,* vol. 13, pp. 588-590, 2001.

[241] P. Lin, Y. Li, T. Cheng, T. Suzuki, and Y. Ohishi, "Coexistence of Photonic Bandgap Guidance and Total Internal Reflection in Photonic Crystal Fiber Based on a High-Index Array With Internal Air Holes," *IEEE Journal of Selected Topics in Quantum Electronics,* vol. 22, pp. 265-270, 2016.

[242] M. R. Hasan, M. A. Islam, A. A. Rifat, and M. I. Hasan, "A single-mode highly birefringent dispersion-compensating photonic crystal fiber using hybrid cladding," *Journal of Modern Optics,* vol. 64, pp. 218-225, 2017.

[243] R. Robledo-Fava, A. Castillo-Guzman, J. M. Sierra-Hernández, R. Selvas-Aguilar, J. M. Estudillo, and R. Rojas-Laguna, "L-Band Switchable Multiwavelength Fiber Laser Using a Novel Photonic Crystal Fiber," in *Optical Sensors*, 2016, p. SeTu2E. 5.

[244] F. Tani, J. C. Travers, and P. S. J. Russell, "Multimode ultrafast nonlinear optics in optical waveguides: numerical modeling and experiments in kagomé photonic-crystal fiber," *JOSA B,* vol. 31, pp. 311-320, 2014.

[245] W. Tian, H. Zhang, X. Zhang, L. Xi, W. Zhang, and X. Tang, "A circular photonic crystal fiber supporting 26 OAM modes," *Optical Fiber Technology,* vol. 30, pp. 184-189, 2016.

[246] C. Zhao, X. Gan, P. Li, L. Fang, L. Han, L. Tu, *et al.*, "Design of multicore photonic crystal fibers to generate cylindrical vector beams," *Journal of Lightwave Technology,* vol. 34, pp. 1206-1211, 2016.

[247] M. S. Habib, M. S. Habib, S. A. Razzak, and M. A. Hossain, "Proposal for highly birefringent broadband dispersion compensating octagonal photonic crystal fiber," *Optical Fiber Technology,* vol. 19, pp. 461-467, 2013.

[248] M. P. Tan, S. T. M. Fryslie, J. A. Lott, N. N. Ledentsov, D. Bimberg, and K. D. Choquette, "Error-free transmission over 1-km OM4 multimode fiber at 25 Gb/s using a single mode photonic crystal vertical-cavity surface-emitting laser," *IEEE Photonics Technology Letters,* vol. 25, pp. 1823-1825, 2013.

[249] M. I. Hasan, M. S. Habib, M. S. Habib, and S. A. Razzak, "Design of hybrid photonic crystal fiber: Polarization and dispersion properties," *Photonics and Nanostructures-Fundamentals and Applications,* vol. 12, pp. 205-211, 2014.

[250] H. Zhang, N. Kavanagh, Z. Li, J. Zhao, N. Ye, Y. Chen, *et al.*, "100 Gbit/s WDM transmission at 2 μm: transmission studies in both low-loss hollow core photonic bandgap fiber and solid core fiber," *Optics Express,* vol. 23, pp. 4946-4951, 2015.

[251] P. Kumar, A. K. Meher, S. Acharya, and P. S. Mund, "Novel design of PCF with zero dispersion with high birefringence," in *Electronics and Communication Systems (ICECS), 2015 2nd International Conference on*, 2015, pp. 1075-1077.

[252] J. Liao, T. Huang, Z. Xiong, F. Kuang, and Y. Xie, "Design and analysis of an ultrahigh birefringent nonlinear spiral photonic crystal fiber with large negative flattened dispersion," *Optik-International Journal for Light and Electron Optics,* vol. 135, pp. 42-49, 2017.

[253] L. T. Blessing, A. Chakrabarti, and K. Wallace, "A design research methodology," in *Proceedings of the 10th International Conference on Engineering Design (ICED'95)*, 1995, pp. 50-55.

[254] L. T. Blessing and A. Chakrabarti, *DRM, a design research methodology*: Springer Science and Business Media, 2009.

[255] M. Guizani, *Network modeling and simulation: a practical perspective*: John Wiley and Sons, 2010.

[256] N. N. Antoniades, G. Ellinas, and I. Roudas, *WDM Systems and Networks: Modeling, Simulation, Design and Engineering*: Springer Science & Business Media, 2011.

[257] A. M. Law, W. D. Kelton, and W. D. Kelton, *Simulation modeling and analysis* vol. 2: McGraw-Hill New York, 1991.

[258] R. Jain, *The art of computer systems performance analysis*: John Wiley \& Sons, 2008.

[259] K. Pawlikowski, H.-D. Jeong, and J.-S. Lee, "On credibility of simulation studies of telecommunication networks," *Communications Magazine, IEEE,* vol. 40, pp. 132-139, 2002.

[260] X. Yang and Y. Hechao, "The application of optiSystem in optical fiber communication experiments," in *Proceedings of the Third International Symposium on Computer Science and Computational Technology (ISCSCT'10)*, 2010, pp. 376-378.

[261] O. Design, "Optiwave Corporation 7 Capella Court Ottawa," *Report, Ontario, Canada*.

[262] B. U. s. Guide, "RSoft Inc., 200 Executive Blvd," *Ossining, NY, Report,* vol. 10562, 2001.

[263] J. Armstrong, "OFDM for optical communications," *Journal of Lightwave Technology,* vol. 27, pp. 189-204, 2009.

[264] E. J. McCartney, "Optics of the atmosphere: scattering by molecules and particles," *John Wiley and Sons, Inc., 1976. 421 p.,* vol. 1, 1976.

[265] I. I. Kim, B. McArthur, and E. J. Korevaar, "Comparison of laser beam propagation at 785 nm and 1550 nm in fog and haze for optical wireless communications," in *Information Technologies 2000*, 2001, pp. 26-37.

[266] A. K. Majumdar, "Free-space laser communication performance in the atmospheric channel," *Journal of Optical and Fiber Communications Reports,* vol. 2, pp. 345-396, 2005.

[267] L. C. Andrews, R. L. Phillips, and C. Y. Hopen, *Laser beam scintillation with applications* vol. 99: SPIE Press, 2001.

[268] A. A. Farid and S. Hranilovic, "Outage capacity optimization for free-space optical links with pointing errors," *Journal of Lightwave Technology,* vol. 25, pp. 1702-1710, 2007.

[269] J. W. Goodman, *Introduction to Fourier optics*: Roberts and Company Publishers, 2005.

[270] E. G. Johnson, J. Stack, and C. Koehler, "Light Coupling by a Vortex Lens intoGraded Index Fiber," *Journal of lightwave Technology,* vol. 19, p. 753, 2001.

[271] R. Soft, " Photonics Component Design Suite, version 8.2," Report, 2010.